Recent Advances in Splitting Methods Based on Robin-Robin Coupling Conditions

by

Rebecca F. Durst

B.A., Williams College; Williamstown, MA, 2017

M.Sc., Brown University; Providence, RI, 2019

A dissertation submitted in partial fulfillment of the

requirements for the degree of Doctor of Philosophy

in The Division of Applied Mathematics at Brown University

PROVIDENCE, RHODE ISLAND

May 2022

This dissertation by Rebecca F. Durst is accepted in its present form
by The Division of Applied Mathematics as satisfying the
dissertation requirement for the degree of Doctor of Philosophy.

Date________________ ____

Johnny Guzmán, Ph.D., Advisor

Recommended to the Graduate Council

Date________________ ____

Chi-Wang Shu, Ph.D., Reader

Date________________ ____

Erik Burman, Ph.D., Reader

Approved by the Graduate Council

Date________________ ____

Andrew G. Campbell, Dean of the Graduate School

Vita

Education

- Brown University, Providence, RI, 2017 – 2022

  Ph.D. in Applied Mathematics, expected May 2022

  M.Sc. in Applied Mathematics, 2019

- Williams College, Williamstown, MA, 2013 – 2017

  B.A. with Honors in Mathematics

Awards and Honors

- 2021, Simon-Ostrach Fellowship

- 2019 – 2022, National Science Foundation Graduate Research Fellow

- 2017, Associate Member of Sigma Xi, elected by the Williams College Chapter

- Summer 2016, Williams College Finnerty Fund

Teaching Experience

- Teaching Assistant, GirlsGetMath@ICERM, ICERM, Summer 2021

- Instructor, Applied Ordinary Differential Equations, Brown University, Summer 2020

- Graduate Teaching Assistant, Applied Ordinary Differential Equations, Brown University, Spring 2019
- Graduate Teaching Assistant, Introduction to Computational Linear Algebra, Brown University, Fall 2019

Service and Professional Activities

- Sheridan Center for Teaching and Learning, Brown University
  - Course Design Seminar, Spring 2020
  - Certificate I: Reflective Teaching, Fall 2019
- Invited Panelist, Nebraska Conference for Undergraduate Women in Mathematics 2022, University of Nebraska, Lincoln, January 2022 (Online)
- Faculty-Graduate Liaison, Division of Applied Mathematics, Brown University, 2020 – Present
- President, Brown University Association for Women in Mathematics Student Chapter, Fall 2020 – Present
- Treasurer, Brown University Association for Women in Mathematics Student Chapter, Fall 2019 – Spring 2020
- Mentor, Directed Reading Program, Division of Applied Mathematics, Brown University, Fall 2018 and Spring 2020
- Mentor, Applied Math Undergraduate Mentoring Program, Division of Applied Mathematics, Brown University, Fall 2017 - Spring 2021
- Vice President, American Mathematical Society Student Chapter, Department of Mathematics, Williams College, Fall 2016 – Spring 2017

- Head Teaching Fellow, Milham Planetarium, Astronomy Department, Williams College, June 2015 – June 2017
- Teaching Fellow, Milham Planetarium, Astronomy Department, Williams College, June 2014 – June 2015

Publications *Published*

- Erik Burman, Rebecca Durst, Johnny Guzmán 2021, "Stability and error analysis of a splitting method using Robin-Robin coupling applied to a fluid-structure interaction problem," *Numerical Methods for Partial Differential Equations*, 2021.
- Rebecca F. Durst, Chi Huynh, Adam Lott, Steven J. Miller, Eyvindur A. Palsson, E. A., Wouter Touw, and Gert Vriend 2020, "The Inverse Gamma Distribution and Benford's Law," *The PUMP Journal of Undergraduate Research* **3** (2020), 95–109.
- Sam Alterman, Jaeho Choi, Rebecca Durst, Sarah Flemming, and William K. Wootters, 2018, "The Boltzmann distribution and the quantum-classical correspondence," *J. Phys. A* **51** 345 – 301 (2018).
- Pasachoff, Jay M., Bryce A. Babcock, Rebecca F. Durst, Christina H. Seeger, Stephen E. Levine, Amanda S. Bosh, Michael J. Person, Amanda A. Sickafoose, Carlos A. Zuluaga, Molly R. Kosiarek , Fumio Abe, Masayuki Nagakane, Daisuke Suzuki, Paul J. Tristram, 2016, "Pluto Occultation on 2015 June 29 UTC With Central Flash and Atmospheric Spikes Just Before the New Horizons Flyby," *Icarus*, **296** (2017), 305–314.
- Amanda S. Bosh, Michael J. Person, Carlos A. Zuluaga, Amanda A. Sickafoose, Stephen E. Levine, Jay M. Pasachoff, Bryce A. Babcock, Edward W.

Dunham, Ian S. McLean, Jürgen Wolf,Fumio Abe, Eric E. Becklin, Thomas A. Bida, Len P. Bright, Tim Brothers, Grant Christie, Peter L.Collins, Rebecca F. Durst, Alan C. Gilmore, Ryan T. Hamilton, Hugh C. Harris, Chris Johnson,Pamela M. Kilmartin, Molly Kosiarek, Karina Leppik, Sarah E. Logsdon, Robert Lucas, ShevillMathers, C. J. K. Morley, Peter Nelson, Haydn Ngan, Enrico Pfüller, Tim Natusch, Hans-PeterRöser, Stephanie Sallum, Maureen L. Savage, Christina H. Seeger, Ho Chit Siu, Chris Stockdale,Daisuke Suzuki, Thanawuth Thanathibodee, Trudy Tilleman, Paul J. Tristram, Jeffrey Van Cleve,Carolle Varughese, Luke W. Weisenbach, Elizabeth Widen, Manuel Wiedemann, 2016, "Haze inPluto's atmosphere: Results from SOFIA and ground- based observations of the 2015 June 29Pluto occultation," *Icarus*, **365** (2021).

Preprints

- *Loosely coupled, non-iterative time-splitting scheme based on Robin-Robin coupling: unified analysis for parabolic/parabolic and parabolic/hyperbolic problems* (with Erik Burman, Johnny Guzmán, and Miguel Fernández) arXiv: 2110.08181 [math.NA]

- *Fully discrete loosely coupled Robin-Robin scheme for incompressible fluid-structure interaction: stability and error analysis* (with Erik Burman, Johnny Guzmán, and Miguel Fernández) arXiv: 2007.03846 [math.NA]

Presentations

- Finite Element Circus, Pennsylvania State University, *Nearly optimal splitting method based on Robin-Robin coupling conditions: some surprising results!*

November 5, 2021

- 26th International Domain Decomposition Conference, The Chinese University of Hong Kong, *Fully discrete loosely coupled Robin-Robin scheme for incompressible fluid-structure interaction: stability and error analysis*, December 11, 2020 (online)

- 50th Anniversary Finite Element Circus, *Fluid-Structure Interactions: Stability and error analysis for a loosely coupled Robin-Robin scheme*, November 7, 2020 (Online)

- WIMIN 2020, Smith College, *Fluid-Structure Interactions: Stability and error analysis for a loosely coupled scheme*, October 17, 2020 (Online)

Professional Organizations

- American Mathematical Society (AMS)

- Association for Women in Mathematics (AWM)

- Society for Industrial and Applied Mathematics (SIAM)

Dedication

This thesis is dedicated to my grandmothers Alice Berman Durst (1926 – 2015) and Rose Chetta Emig, who taught me the value of education and self-confidence.

I learned my unrelenting optimism and assertiveness from you, and I am so proud to be your granddaughter.

Preface and Acknowledgments

To my adviser Johnny Guzmán, thank you so much. You have been a truly excellent adviser, and I am so thankful to have been guided by you throughout my Ph.D. You have always been incredibly supportive and have believed in me and my abilities. You provided honest and constructive feedback, and you took the time to explain your reasoning to me so that I always knew you had my best interests at heart. I have always appreciated your enthusiasm, your honesty and your patience, and I hope to one day follow your example and provide the same to my own students. So, thank you, again, Johnny! Your confidence in me has been infectious, and I have gained valuable confidence in myself as a result. Thanks to you, I feel ready to take the next steps in my academic journey.

I have also had the incredible opportunity to work with two wonderful collaborators, Erik Burman and Miguel Fernández, while completing the work on this thesis. Thank you to both of you for all of your help and incredible knowledge of the field. Your feedback and advice were my lifeline while I took on my first research projects as a graduate student. Thank you also to Erik for serving on my thesis committee. Your and Miguel's guidance and advice helped give life to these projects, so I am delighted and honored to have you as a reader. And thank you to Chi-Wang Shu for also serving on my committee. Your classes were some of my favorite at Brown, and I am so appreciative of all of your teaching and guidance. It is an honor to have you on my committee.

To my academic siblings, Anna Lischke, Sining Gong, and Ernesto Caceres-Valenzuela, you were my friends, mentors, teachers, and conference buddies. Thank you for joining me on this journey!

Thank you to my office mates, Anna Grim and Patrick Liscio. Your presence brought joy, puzzles, and an incredible number of Cheerios to my life both in and out of the office every day.[1] Thank you also to my other fellow Ph.D. students and friends, Rebecca Santorella (the "Other Rebecca"), Justin Dong, Emily Winn, Angelina Grosso, Tim Roberts, Kevin Hu, Gabriel Provencher Langlois, Teressa Chambers, and many others. I am grateful for the laughs, the baked goods, the donuts (Justin), and the games of pool at the GCB.

Thank you to my fellow astronauts Tim, Angelina, and Meg Wilson, and thank you to my wonderful and amazing friends Kari, Jackie, Carlo, Joaquin, Jordan (JMann), Jamar, Dylan, and the rest of this wonderful family. The time spent with you all exercising, playing games, reading Brandon Sanderson books, meeting up on Tuesday nights, and drinking boba tea made the city of Providence feel like home to me, and I wish I could take you all with me to Pittsburgh. To my friends from Williams, thank you for shaping me into the person I am now. And to my cousin Jay, thank you for reading your way through the Cosmere with me.

Thank you also to the incredible teachers I have had who guided me to where I am today. Thank you especially to my high school teachers Chris Orlando and Matthew Jacobs. So much of my passion and confidence in math started in your classes. And thank you to the Williams College math department where I found my first math home. Professor Mihai Stoiciu, I'm so glad you convinced me to take your

[1] Except when you hid plastic cockroaches around my apartment, Anna! Check the mugs on your desk...

Math 151 class[2] during that first Math/Stat dinner of Fall 2013!

To my wonderful partner, Dvivid Trivedi, thank you for being such an amazing and solid presence in my life these past eight years. Even when we are many miles apart, I have always felt your incredible support and belief in me. Knowing that I have you in my corner is both comforting and empowering, and I look forward to all of our future adventures.

Finally, thank you to my amazing family. Thank you to my grandmothers, to whom I have dedicated this thesis. To my parents Carol Emig and Michael Durst, thank you for your unconditional love and support. You have always encouraged my love of science and been incredible role models for me. Thank you for always reminding me to be strong and confident in my presence. To my sister, Claire, the great recommender of audiobooks, I love you dearly. Thank you to Jonathan Coventry and Leah Plave. To Mireya Malespin, te quiero mucho. And to all of my uncles, aunts, and cousins, thank you so much for your love and support.

Last but not least, thank you to the dogs in my life, although I am not their full-time human. To Davey, the 60lbs ball of chaos, you were a major distraction when I was working, but I love you. And to Rhett of the giant ears, you're very cute.

[2]And the 4 other courses I took with you!

Contents

Vita iv

Dedication ix

Preface and Acknowledgments x

1 Introduction 1

1.1 Background and Motivation . . . 5

1.1.1 The origins of Robin-Robin coupling conditions . . . 5

1.1.2 Explicit couplings for the FSI problem . . . 7

1.2 Overview of the thesis . . . 18

1.2.1 Organization of the thesis . . . 20

2 Preliminaries 22

2.1 Norms and Inequalities . . . 23

2.1.1 Norms and spaces . . . 23

2.1.2 Inequalities . . . 25

2.2 Finite elements . . . 29

2.2.1 The interpolants . . . 33

3 Robin-Robin coupling for parabolic-parabolic and parabolic-hyperbolic problems 43

3.1 The Parabolic-Parabolic and the Parabolic-Hyperbolic Model Problems . . . 44

3.1.1 The Parabolic-Parabolic problem . . . 44

3.1.2 The Parabolic-Hyperbolic problem . . . 47

3.1.3 The generalized system . . . 48

3.1.4 Variational form of the generalized system . . . 49

3.2 Robin-Robin coupling . . . 50

3.2.1 The time discrete method . . . 51

3.3 Stability . . . 55

3.4 Error Analysis . . . 59

3.4.1 The Error Equations . . . 60

3.4.2 Step 1: Preliminary Estimates . . . 63

3.4.3 Step 2: Estimate for $\frac{\Delta t}{\alpha}\langle g_3^{n+1}, \Lambda^{n+1}\rangle$ using a lifting-residual argument . . . 71
3.4.4 Step 3: Main Result . . . 79
3.5 Final Discussion . . . 84
3.5.1 Special Case . . . 84
3.5.2 Example: Constructing ϕ . . . 86
3.5.3 Sub-optimal error estimate . . . 88
3.5.4 Comments on regularity . . . 89
3.5.5 Concluding remarks . . . 90
3.6 Numerical Experiments . . . 91
3.6.1 Numerical experiments for simple case with uniform mesh . . . 91
3.6.2 Numerical experiments for less simple case with non-uniform mesh . . . 92

4 Robin-Robin coupling for fluid-structure interaction, Part I: the time-semi-discrete framework 95
4.1 Robin-Robin coupling for the fluid-structure interaction problem . . . 96
4.1.1 The FSI problem . . . 97
4.1.2 The time-discrete Robin-Robin method . . . 100
4.2 Stability . . . 102
4.3 Error Analysis . . . 104
4.3.1 FSI vs. parabolic-hyperbolic: pressures and parameters . . . 104
4.3.2 The Error Equations . . . 106
4.3.3 Step 1: Preliminary Estimates . . . 108
4.3.4 Step 2: Estimate for $\frac{\Delta t}{\alpha}\langle \boldsymbol{g}_3^{n+1}, \boldsymbol{e_\lambda}^n\rangle$ . . . 113
4.3.5 Step 3: Main Result . . . 122
4.4 Final Discussion . . . 128
4.4.1 Parameter sensitivity . . . 128
4.4.2 Concluding remarks . . . 135
4.5 Numerical Experiements . . . 136
4.6 Numerical Experiments for Stokes-Elastic . . . 136

5 Robin-Robin coupling for fluid-structure interaction, Part II: the fully discrete framework 139
5.1 Robin-Robin coupling for fluid-structure interaction, fully discrete formulation . . . 140
5.1.1 The fully-discrete Robin-Robin method for FSI . . . 140
5.1.2 Stability . . . 144
5.2 Error Analysis . . . 145
5.2.1 Time-semi-discrete vs. fully discrete: linear interpolants and L^2-projections . . . 146
5.2.2 The error equations . . . 148
5.2.3 Step 1: Preliminary Estimates . . . 153

5.2.4 Step 2: Estimate for $\frac{\Delta t}{\alpha}\langle \boldsymbol{g}_{3,h}^{n+1}, \boldsymbol{e}_{\boldsymbol{\lambda},h}^{n}\rangle$ 161
5.2.5 Step 3: Main Result 169
5.3 Final Discussion 182
5.3.1 A comment about the numerical experiments 182
5.3.2 Concluding remarks 183

6 Conclusion **185**
6.1 Summary of results 186
6.2 Future work 186
6.2.1 Parameter sensitivity questions 186
6.2.2 Static interface vs. moving interface 190
6.2.3 Second order and beyond! 191

List of Tables

3.1 Convergence rates and errors for the parabolic-parabolic problem in the special case where Σ is perpendicular to $\partial\Omega$. 92
3.2 Convergence rates and errors for the parabolic-parabolic problem for a more general case. 94
3.3 More convergence rates and errors for the parabolic-parabolic problem for a more general case. 94

4.1 Convergence rates for select values of α when $\mu = L_1 = L_2 = 1$. 134
4.2 Convergence rates for select values of α when $\mu = L_1 = L_2 = 100$. 134
4.3 Convergence rates for select values of α when $\mu = L_1 = 100$ and $L_2 = 1000$. 134
4.4 Convergence rates for the FSI system. 137
4.5 Errors for the FSI system, part 1. 137
4.6 Errors for the FSI system, part 2. 138

List of Figures

1.1 An example of a domain for a problem in which two systems are coupled across an interface Σ. 3
1.2 Two examples of FSI domains. 8

2.1 A $\mathcal{P}^1$ Lagrange element in $\mathbb{R}^2$. 32

3.1 An example of the domains Ω_s and Ω_f with interface Σ. 45
3.2 Schematic of our special case 84
3.3 $\Omega_f = [0,1]^2$ with the regions $\{K_i\}_{i=1}^5$. 87
3.4 An example of the non-uniform mesh for $n = 1$. 93

4.1 Numerical experiments demonstrating the effect of parameters on convergence of the Robin-Robin method. 132

5.1 An example of a polygonal domain as described above. 141

Chapter One

Introduction

In this thesis, we develop and analyze loosely coupled splitting methods for coupled, time-dependent problems based on Robin-type interface conditions. In the context of this work, a *coupled* problem refers to the case in which two or more systems interact across an interface via *interface coupling conditions* (also referred to as *transmission conditions*).

Coupled problems arise in many different contexts, and have a wide variety of applications. In particular, a coupled problem will arise whenever two physical media interact across an interface. The coupled problem of particular interest to us in this thesis will be the *fluid-structure interaction (FSI) problem*, describing the flow of a fluid past an elastic, non-porous solid. Other examples of coupled problems include the Stokes-Darcy model of a fluid flowing past a porous medium, and heat transfer between two materials.

The interface coupling conditions will often take the form of two boundary conditions applied at the interface: one Dirichlet-type condition that may, for example, prescribe some conformity of the solutions at the interface, and one Neumann-type condition, perhaps governing a flux across the interface. For example, for two parabolic systems with solutions u and w on subdomains Ω_f and Ω_s, respectively, coupled across an interface, Σ, the coupling conditions may be defined

$$u = w \quad \text{on } \Sigma, \tag{1.0.1a}$$

$$\nabla u \cdot \boldsymbol{n}_u + \nabla w \cdot \boldsymbol{n}_w = 0 \quad \text{on } \Sigma, \tag{1.0.1b}$$

Where Σ represents the interface as shown in Figure **??**, and $\boldsymbol{n}_w$ and $\boldsymbol{n}_u$ are the outward facing unit normal vectors at said interface. In this case, (1.0.1a) enforces continuity across Σ, while (1.0.1b) enforces a net-zero flux across Σ.

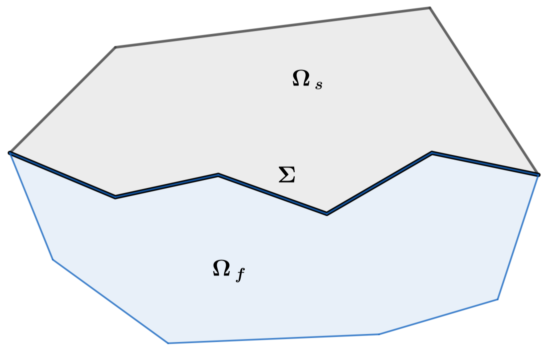

Figure 1.1: An example of a domain for a problem in which two systems are coupled across an interface Σ.

Traditionally, there are two methods to approach the numerical solution of a coupled problem. The first is to solve the system using a *monolithic* method, meaning the coupled subproblems are solved simultaneously through the use of one all-inclusive solver. These methods are generally stable, as the transmission conditions do not have to be altered in any way. However, this approach is problem-specific, so the solver may have to be redesigned for each new problem. Additionally, solving two systems and coupling conditions together at each time step can be computationally expensive.

The other approach is to solve the system using a *partitioned* or *splitting method* in which we decouple the subproblems and solve them using separate solvers. These methods have the advantage of allowing us to use existing solvers to compute multiple, smaller systems at each time step, making them generally more efficient than the monolithic methods. However, they may suffer from stability and accuracy issues depending on how the coupling conditions are addressed.

The interface coupling conditions govern how the subproblems interact with each other in space and time. Therefore, they represent a critical feature when designing numerical methods for coupled problems. If a method satisfies the coupling conditions exactly at each time step, we say that it is *strongly coupled*. Otherwise, if the coupling conditions are not exactly satisfied at each time step, we say that the method is *loosely coupled*. Monolithic methods will be strongly coupled by construction, but many splitting methods will require inexact coupling conditions to decouple the subproblems. However, we will still consider some partitioned procedures to be strongly coupled, provided that sufficient subiterations are performed in each time step to ensure that the inexact coupling conditions converge to the exact conditions within a reasonable tolerance.

For this thesis we will focus on *explicit coupling schemes*, which we define as loosely coupled splitting methods in which the subproblems are solved sequentially at each time step by passing information across the interface via a time-explicit treatment of the interface coupling conditions. We will accomplish this by replacing the exact coupling conditions with Robin-type conditions relating the solutions across the current and previous time steps. For the parabolic-parabolic coupling mentioned previously, these Robin conditions will take the form

$$\begin{aligned} \nabla w^{n+1} \cdot \boldsymbol{n}_w + \alpha w^{n+1} =& \alpha u^n - \nabla u^n \cdot \boldsymbol{n}_u, \\ \nabla u^{n+1} \cdot \boldsymbol{n}_u + \alpha u^{n+1} =& \alpha w^{n+1} + \nabla u^n \cdot \boldsymbol{n}_u. \end{aligned}$$

for $\alpha > 0$. We may think of these conditions as linear combinations of (1.0.1a) and (1.0.1b), split between times t_n and t_{n+1}. In the following section, we will discuss the origins of this method and how it came to be applied to splitting methods.

1.1 Background and Motivation

1.1.1 The origins of Robin-Robin coupling conditions

Robin-Robin coupling conditions were first proposed by Lions in [39] in the context of iterative domain decomposition methods. Lions proposed the Robin-Robin domain decomposition method as a variation of the Schwarz alternating method for non-overlapping domains. More specifically, he proposed an iterative method to solve the Poisson equation

$$\begin{aligned} -\Delta u =& f, \quad \text{in } \Omega \\ u =& 0 \quad \text{on } \Gamma = \partial\Omega, \end{aligned}$$

where $f \in L^2(\Omega)$.

For this method, Lions decomposes the domain Ω into m non-overlapping subdomains, $\Omega = \cup_{1\leq i \leq m}\Omega_i$. He then defines the subdomain interfaces $\gamma_{ij} = \gamma_{ji} = \partial\Omega_i \cap \partial\Omega_j$, for $(i \neq j)$. Lions further assumes γ_{ij} intersects Γ orthogonally for each $i \neq j$. Then, given an arbitrary initial guess on each subdomain, $\{u_i\}_{i=1}^m$, the method iteratively solves

$$\begin{aligned} -\Delta u_i^{n+1} =& f && \text{in } \Omega_\mathrm{i}, \\ u_i^{n+1} =& 0 && \text{on } \partial\Omega_i \cap \Gamma, \\ \frac{\partial u_i^{n+1}}{\partial n_{ij}} + \lambda_{ij} u_i^{n+1} =& \frac{\partial u_j^n}{\partial n_{ij}} + \lambda_{ij} u_j^n, && \text{on } \gamma_{ij},\ \forall 1 \leq j \leq m,\ j \neq i, \end{aligned}$$

where $n_{ij} = -n_{ji}$ is the outward normal to $\partial\Omega_i$ on the interface γ_{ij}, and $\lambda_{ij} = \lambda_{ji} > 0$ is the Robin parameter.

Here we see possible the first example of *decoupling* via the use of Robin interface conditions. More specifically, we note that the solution in Ω_i at iteration $n+1$ is solved completely independently from the solutions in the other subdomains at that iteration. The only information received from adjoining subdomains comes from the previous iteration, n. Thus, we may say that the subproblems are decoupled.

Lions' method has since motivated the use of Robin interface couple conditions for a wide variety of domain decomposition problems. For example, Deng in [24] proposes a variation in which the normal derivative does not have to be computed at any point. In [25], the authors propose a Robin-based iterative domain decomposition procedure for mixed finite element approximations of second-order elliptic problems. The method has also given rise to the field of *optimized Schwarz methods* in which the aim is to optimize the transmission conditions proposed by Lions (see e.g. [35, 41, 25]). For coupled problems, the Robin-Robin domain decomposition method has been applied to a variety of systems. Notably, the Stokes-Darcy problem (see [20] and the references therein), advection-diffusion problems (e.g. [19] for sand transport modeling), and the FSI system (e.g. [1, 22, 36, 2], among others).

It should be emphasized that, although the authors of [25] mention the possible extension to time-stepping, the Robin couplings in these problems are not used to move the system forward in time by solving the subproblems in sequence, as they would in an explicit coupling scheme. Rather, in the both the stationary and time-dependent examples mentioned here, the Robin methods allow the subproblems to be solved in parallel. Furthermore, although explicit time-stepping methods are mentioned in [43], the use of Robin interface conditions is only discussed in the contexts of iterative methods, which we consider to be strong couplings when considered for time-dependent problems.

1.1.2 Explicit couplings for the FSI problem

In this thesis, we will present the Robin-Robin coupling conditions as a general and effective method for defining explicit coupling methods for time-dependent problems. However, this work was originally motivated by a problem arising in the development of splitting methods for the FSI problem known as the *added-mass instability* which we describe below.

1.1.2.1 Fluid-structure interaction

We will begin by defining the FSI system as it will appear in this thesis. A full FSI model represents a coupled, nonlinear problem that presents significant challenges for numerical approximation.[1] As the structure is elastic, the fluid-structure interface will be deformed as the system evolves, so the numerical approximation must track and repeatedly update the interface for each time step. We refer the reader to [1] for a description of how such an evolving system may be written using a purely Lagrangian representation for the structure and an ALE (arbitrary Lagrangian-Eulerian) representation for the fluid.

However, to simplify the analyses in this thesis, we will consider a low Reynolds regime so that the fluid may be described by the Stokes equations. Furthermore, we will assume that the interface only undergoes infinitesimal displacements. In other words, *the interface does not move.* This assumption is incredibly common when analyzing FSI coupling methods (see e.g. [13, 48, 32, 1, 17, 14, 18, 16], and many others), as it removes the added complication introduced by updating the domain at each step via a *geometry subproblem.*

[1]Observation: If a fluid is involved, you should never assume that the problem will be easy!

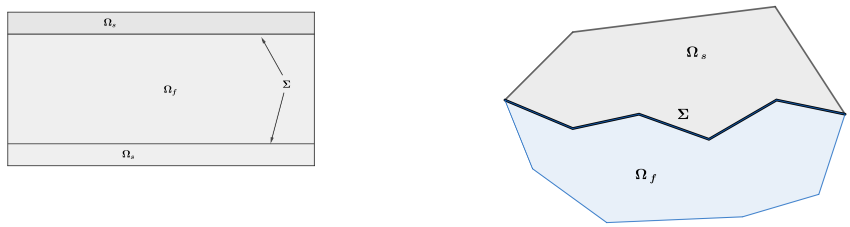

(a) (b)

Figure 1.2: Two examples of FSI domains.

The authors of [48] demonstrate that the FSI problem coupled with Robin-Robin interface conditions remains stable in the case of a moving interface. However, they employ the "static interface" assumption to derive their convergence results. Essentially, the analysis becomes more complex in the case of moving interface because the subproblems are not solved on the same domains, so steps must be added in order to compare terms on the interface (see e.g. [48]). We will further discuss these assumptions and consequences in 6.2.2.

With this established, our FSI system is defined as follows. Consider a domain $\Omega \subset \mathbb{R}^2$ consisting of a fluid domain, Ω_f, interacting with a structure domain, Ω_s, separated by interface Σ. This domain could take several forms, with two examples provided in Figure 1.2.

Let $\mathbf{u}$, p, and $\mathbf{e}$ be the fluid velocity, fluid pressure, and structural displacement, respectively. Then the FSI system is described by

$$\rho_f \partial_t \mathbf{u} - \operatorname{div} \sigma_f(\mathbf{u}, \mathsf{p}) = 0 \quad \text{in } (0,T) \times \Omega_f, \tag{1.1.1a}$$

$$\operatorname{div} \mathbf{u} = 0 \quad \text{in } (0,T) \times \Omega_f, \tag{1.1.1b}$$

$$\mathbf{u} = 0 \quad \text{on } (0,T) \times \Sigma_f, \tag{1.1.1c}$$

$$\begin{aligned}
\rho_s \partial_t \mathbf{q} - \operatorname{div} \sigma_s(\mathbf{e}) =& 0 \quad \text{in } (0,T)\times\Omega_s, && (1.1.2a)\\
\boldsymbol{q} - \partial_t \mathbf{e} =& 0 \quad \text{in } (0,T)\times\Omega_s, && (1.1.2b)\\
\mathbf{e} =& 0 \quad \text{on } (0,T)\times\Sigma_s, && (1.1.2c)
\end{aligned}$$

$$\begin{aligned}
\mathbf{u} =& \mathbf{q} \quad \text{on } (0,T)\times\Sigma, && (1.1.3a)\\
\sigma_f(\mathbf{u},\mathsf{p})\boldsymbol{n}_f + \sigma_s(\mathbf{e})\boldsymbol{n}_s =& 0 \quad \text{on } (0,T)\times\Sigma, && (1.1.3b)
\end{aligned}$$

where $\Sigma_f := \partial\Omega_f \setminus \Sigma$ and $\Sigma_s := \partial\Omega_s \setminus \Sigma$.

Here, $\boldsymbol{n}_i$ is the outward pointing normal to $\partial\Omega_i$ for $i = s, f$, and ρ_f and ρ_s are the fluid and solid velocities, respectively.

We define the stress tensors for the fluid and solid by the equations

$$\begin{aligned}
\sigma_f(\mathbf{u},\mathsf{p}) :=& 2\mu\epsilon(\mathbf{u}) - \mathsf{p}\mathbf{I},\\
\sigma_s(\mathbf{e}) :=& 2L_1\epsilon(\mathbf{e}) + L_2(\operatorname{div}\mathbf{e})\mathbf{I},
\end{aligned}$$

where μ is the viscosity of the fluid and $L_1, L_2 > 0$ are the Lamé parameters governing the elasticity of the solid.

The interface condition (1.1.3a) is known as the *kinematic condition*, and it forces the fluid and solid to remain flush at the interface by requiring the velocities to match. The condition (1.1.3b) is known as the *dynamic condition*, and it is an enforcement of Newton's second law of motion: *for every action, there is an equal and opposite* *reaction*. In other words, the force applied to the solid by the fluid, $\sigma_f(\mathbf{u}, \mathsf{p})\boldsymbol{n}_f$ (we assume there is no tangential force because the movement of the interface is negligible) must be equal and opposite to the force applied to the fluid by the solid, $\sigma_s(\mathbf{e})\boldsymbol{n}_s$.

Remark 1. Note that we have applied Dirichlet boundary conditions to $\partial\Omega$, which may not be appropriate for all problems. However, we do this for the sake of simplification, and we refer the reader to [17, 18] for less simplified boundary conditions. The results of this thesis would not change in any meaningful way if these less simple conditions were used.

1.1.2.2 Added-mass

The FSI system is very stiff, and monolithic and other strongly coupled methods (typically implemented as iterative partitioned procedures) can have prohibitive computational costs, especially on large models. Unfortunately, loose couplings are known to suffer from severe stability issues related to a phenomenon present in FSI systems known as the *added-mass effect*. As we will see, the added-mass effect is not a special result of the interaction between a solid and a fluid. Rather, it is a way of interpreting the interaction using Newton's laws of motion and the law of conservation of energy that allow us to prescribe a concept of *mass* to the fluid

It is a simple fact of life that two objects cannot occupy the same space (this is also very easy to test). So, when a non-porous solid body moves through a fluid (as in an FSI system), it necessarily displaces the fluid as it moves. If the solid is moving at a constant speed, then the fluid will be displaced at a constant rate. However, if the solid is *accelerating*, then the fluid around the solid is no longer being displaced at a constant rate. Thus, the velocity of the fluid at the fluid-solid interface is no longer constant, thereby changing the fluid's *kinetic energy*.

In [7], the author describes the added-mass effect as a means to determine "the necessary work done to change the kinetic energy associated with the motion of the fluid." From the perspective of Newton's first law of motion, this would be the work required to overcome the fluid's *inertia*, or its resistance to change of motion brought on by the acceleration of the solid. In physics, *work*, W, refers to the amount of energy , ΔE, transferred between two objects via the application of a force, F. Heuristically, the relationship between work, energy, and force may be written

$$\Delta E \propto W \propto F.$$

In the FSI problem, this means that, since the energy of the fluid is changing, the fluid is doing work on the solid. Thus, by resisting the displacement by the solid, *the fluid is exerting a drag force on the solid proportional to the change in the fluid velocity at the fluid-solid interface.* We call this the *added-mass force* and include it in the total force applied to solid by the fluid [7].

1.1.2.3 So what is the *added-mass*?

In the context of this problem, the idea of a fluid mass does not make sense as it is a flowing medium through which the solid is moving. However, we may use the added-mass force to prescribe a concept of mass to the fluid at the interface by Newton's second law of motion. More specifically, if u_Σ is the fluid velocity at the interface, then the drag force on the solid may be written

$$F_a = m_a \frac{d}{dt} u_\Sigma,$$

where m_a is a quantity that will have the units of a mass and is related to the inertia of the fluid. Thus, we call m_a the *added-mass* of the system.

1.1.2.4 Why is this concept relevant for numerical methods?

In high velocity flows, the added-mass force will likely be effectively negligible (see [38]). However, there are many cases in which it will be a dominating component of the fluid force acting on the solid which can have catastrophic effects on loosely coupled schemes. To see this, we consider a seemingly natural explicit coupling of the FSI method (1.1.1)-(1.1.3) defined by prescribing the interface conditions

$$\mathbf{u}^{n+1} = \mathbf{q}^{n+1} \quad \text{on } (0,T)\times\Sigma, \tag{1.1.4a}$$

$$\sigma_f(\mathbf{u}^n, \mathsf{p}^n)\boldsymbol{n}_f + \sigma_s(\mathbf{e}^{n+1})\boldsymbol{n}_s = 0 \quad \text{on } (0,T)\times\Sigma. \tag{1.1.4b}$$

To define a loose coupling with these interface conditions, we assume the solutions at time step n, namely $\mathbf{u}^n$, p^n, $\mathbf{e}^n$, and $\mathbf{q}^n$ are known. We then begin by solving for $\mathbf{e}^{n+1}$ and $\mathbf{q}^{n+1}$ using the solid system (1.1.2). To do so, we apply (1.1.4b) as a Neumann condition on the interface so that the only information needed from the fluid is known from the previous time step. Once the solid system has been solved, we use the now known value of $\mathbf{q}^{n+1}$ at the interface to set (1.1.4b) as a Dirichlet condition on the interface to solve for the fluid system (1.1.1). In this way, we may solve the FSI system in sequence, passing the information from the solid to the fluid within one time step.

However, in defining these interface conditions, we have broken (1.1.3b) across two time steps. In doing so, we are breaking Newton's law because we are no longer guaranteed to have an equal and opposite force pairing at each time step. Because force and energy go hand-in-hand, as we have previously established, this means that our method now violates the golden rule of physics; it does not conserve energy.

We note that this is different from what is typically referred to as energy conservation of a numerical method, although the concepts are very much related. Here, when we say that the method does not conserve energy, we mean in a *physical* sense. As Le Tallec writes in [38], "the variation of the sum of the kinetic energy of the system and of the elastic energy of the structure must be equal to the difference between the energy introduced by the external boundary conditions and the energy dissipated by viscous effects inside the fluid." In other words, physics requires that any change in *kinetic* and *elastic* energy must be equal to the energy added to or lost by the system.

On the other hand, when we refer to an energy conserving *numerical scheme*, we refer to a scheme for which the *energy norm* remains constant with each time step. This is however, not always required for a scheme to perform well, as many dissipative numerical methods exist. And yet, as Le Tallec points out, the bound on the (physical) energy provides a critical tool in the numerical analysis of the FSI system. In other words, it may shed light on when and *why* a numerical scheme performs well or performs poorly. Conveniently, this brings us back to the concept of added-mass.

To see how the added-mass factors in to all of this, recall that the fluid applies a drag force known as the *added-mass force* to the solid when it is displaced. Consequently, the force applied to the solid by the fluid at the interface, namely $\sigma_f(\mathbf{u}, \mathsf{p})\boldsymbol{n}_f$, may be decomposed into the added-mass force, F_a and any additional force, F_{ext}. In this case, we may write (4.1.4a) as

$$\rho_s(\partial_t \mathbf{q}, \boldsymbol{\xi})_s + a_s(\mathbf{e}, \boldsymbol{\xi}) + \left\langle F_a, \boldsymbol{\xi} \right\rangle + \left\langle F_{ext}, \boldsymbol{\xi} \right\rangle = 0.$$

If we were to then construct a loose coupling using (1.1.4), we would necessarily prescribe the added-mass force from the previous time-step, rather than the added-mass force from the current time step. This violates the conservation of energy of the system.

If $F_a << F_{ext}$, there is a chance that the lack of energy conservation will not have a major effect on the system. However, if the added-mass, m_a is large enough, the discrepancy in time-steps will lead to unconditional instability. Indeed, in [22], the authors derive the *added-mass operator*, $\mathscr{M}_A$– analogous to m_a in (1.1.2.2)– for the FSI system in the special case of an incompressible, inviscid fluid and a thin solid of thickness h_s. They subsequently prove (see Propisition 3 in [22]) that a loosely coupled scheme using the equivalent of (1.1.4) above will be unconditionally unstable if

$$\frac{\rho_s h_s}{\rho_f \mu_{max}} < 1,$$

where μ_{max} is the largest eigenvalue of $\mathscr{M}_A$. In other words, if the added-mass is large enough relative to the density of the solid, then the scheme is unconditionally unstable. A similar result is also derived in [34] for a more general fluid by deriving a discrete added-mass operator.

1.1.2.5 Previous attempts to address added-mass instability

Efforts to decouple the FSI problem began with the introduction of *semi-implicit* coupling schemes. These methods were first introduced by Fernández, Gerbeau, and Grandmont in [30], and they employ a method based on Chorin and Temam's projection method for decomposing the Navier-Stokes equations [23, 49]. In this approach, the fluid velocity is decoupled from the fluid pressure using Chorin and Temam's projection technique. The fluid velocity system is then loosely coupled to the structure system via an *explicit* treatment of the interface conditions. This solution is then passed to the fluid pressure system that is strongly coupled to the structure system via an *implicit* treatment of the interface conditions. We thus have one system that is loosely coupled to a related, strongly coupled system.

A similar approach in which the fluid velocity is explicitly coupled while the pressure is implicitly coupled is taken in [42, 3]. However, in this case the decoupling is entirely algebraic to avoid the complications that arise from the Chorin and Temam method when prescribing boundary conditions to the decoupled pressure system. By leaving the pressure strongly coupled to the structure, these semi-implicit coupling schemes avoid the traditional stability issues suffered by explicit couplings from the added-mass.

A third, very different semi-implicit method based on Lie splitting is introduced in [11]. In this method, the fluid and the structure are decoupled, and the instabilities are avoided by redefining the fluid subproblem as a simpler, monolithic coupled problem in which the fluid is coupled with the structural intertial problem. Like the other two semi-implicit schemes described, this method successfully breaks the coupled system up into smaller subproblems without introducing catastrophic instability. However, all three methods are not fully explicit, as one of the subproblems involves an implicit coupling, and they may have conditions on the time stepping in one or both subproblems. Thus they are more computationally expensive than completely explicit methods.

1.1.2.6 Successful loose couplings and motivation for the current work

A fully explicit coupling for the FSI system with *provable stability* was first proposed by Burman and Fernández in [17], however it is very similar to a single iteration of the Robin iterative procedure introduced by Badia et. al. in [1]. Burman and Fernández's method was based on Nitsche's method, inspired by the work in [37], that allows the Dirichlet-type interface coupling condition to be incorporated into the weak formulation of the problem. To ensure stability of the explicit coupling, an *artificial compressibility* is applied at the interface in the form of a temporal pressure jump of the form $c\frac{\partial \mathsf{p}}{\partial t}$.

This stabilization method is analogous to the artificial incompressibility method proposed by Chorin in [23] to decouple the momentum and continuity equations for an incompressible fluid. The idea originates from an alternative explanation for the added-mass instability; namely, that loosely coupled FSI splitting methods violate conservation of *mass*.[2] More specifically, the mismatching time steps when using Dirichlet-Neumann interface conditions such as (1.1.4) may result in a fluid velocity applied as a boundary condition that does not satisfy the incompressibility condition, $\operatorname{div} \mathbf{u} = 0$. As this condition is a consequence of conservation of mass for physical systems, this indicates yet another way in which these broken interface conditions violate the physical laws of the FSI system [44].

As explained in [23, 44], a natural way to counteract this problem (assuming the structure is governed by the linear elasticity equations) is to replace the incompress-

[2] Again, this refers to a violation of the physical law of conservation of mass in classical mechanics. Mass is really just a form of energy (thanks, Einstein), so is this *really* an alternative explanation in the grand scheme of things?

ibility condition with an artificial compressibility condition, specifically

$$\operatorname{div} \mathbf{u} + c\frac{\partial \mathsf{p}}{\partial t} = 0.$$

This may be interpreted as allowing the fluid density to vary proportionally to the pressure. Furthermore, the artificial compressibility may be applied locally, restricting it to a region close to the interface, as seen in [17, 44]. Although the inclusion of an artificial compressibility term allows for provable stability, the implementation of this stabilization method results in a loss in accuracy. In [17], the authors analyze the terms in the (formal) error bound of their FSI solver and demonstrate that this stabilization term limits the convergence of the method to $\mathcal{O}(\frac{\Delta t}{h})$. Thus, the scheme requires $\Delta t = \mathcal{O}(h^k)$, $k > 1$, in order to achieve suboptimal, $\mathcal{O}(\sqrt{\Delta t})$, convergence.

The main motivation for the work presented in this thesis came from a subsequent paper by Burman and Fernández, [18]. In this paper, Burman and Fernández compare their Nitsche-based explicit coupling to a related explicit coupling, named the *genuine Robin-Robin method*, based on Robin-type interface coupling conditions given by

$$\sigma_s(\mathbf{e}^{n+1})\boldsymbol{n}_s + \frac{\gamma\mu}{h}\partial_t\mathbf{e}^{n+1} = \frac{\gamma\mu}{h}\mathbf{u}^n - \sigma_f(\mathbf{u}^n, \mathsf{p}^n)\boldsymbol{n}_f \quad \text{on } \Sigma, \tag{1.1.5a}$$

$$\sigma_f(\mathbf{u}^{n+1}, \mathsf{p}^{n+1})\boldsymbol{n}_f + \frac{\gamma\mu}{h}\mathbf{u}^{n+1} = \frac{\gamma\mu}{h}\partial_t\mathbf{e}^{n+1} + \sigma(\mathbf{u}^n, \mathsf{p}^n)\boldsymbol{n}_f \quad \text{on } \Sigma. \tag{1.1.5b}$$

Here, γ is the Nitsche parameter introduced in [17], and h is the spacial discretization parameter. Their numerical experiments showed that this hence-forth named *Robin-Robin* method was *unconditionally* stable without the need for the pressure stabilization time used previously. The method was observed to be $\mathcal{O}(\sqrt{\Delta t})$, however a rigorous analysis was not achieved. Unlike the domain decomposition methods based on Robin-type interface conditions, Burman and Fernández's method uses the

Robin interface conditions to solve the subproblems sequentially. As mentioned before, a similar Robin-Robin method is proposed as an iterative method by Badia et. al. in [1] that similarly allows the subproblems to be solved in sequence. However, this method is proposed as an iterative method, and it is not considered as an explicit time-stepping scheme. Thus Burman and Fernández are likely the first to use the Robin-Robin coditions to generate an explicit coupling method.[3]

In general, rigorous error analyses of explicit coupling methods for the FSI problem with thick walled structure have proven difficult. A notable example that may be the first rigorously analyzed explicit coupling for FSI is the Robin-Neumann method of [29, 32] in which the fluid is treated with a Robin interface condition and the solid is treated with a Neumann condition consistent with one of the traditional FSI interface conditions. Considerably more success has been made with regards to rigorous analyses of loosely coupled methods for FSI with *thin walled structures*, and we refer the reader to works such as [28, 31, 12].

1.2 Overview of the thesis

Motivated by the results of [18], our work for this thesis has primarily been focused on developing a rigorous analysis of the Robin-Robin coupling method for FSI. In our work, we seek to show that the Robin-Robin method is unconditionally stable without the addition of a stabilization term (as applied in [17]). Furthermore, this stability is independent of the Robin parameter and the discretization parameters, as we replace the original Robin conditions of [18] (which had a Robin parameter

[3] An explicit coupling related to Robin conditions was proposed in [6]. However, the authors do not provide a full theoretical justification.

dependent on h and μ) with the more general conditions

$$\sigma_s(\mathbf{e}^{n+1})\boldsymbol{n}_s + \alpha\partial_t\mathbf{e}^{n+1} = \alpha\mathbf{u}^n - \sigma_f(\mathbf{u}^n, \mathsf{p}^n)\boldsymbol{n}_f \quad \text{on } \Sigma, \tag{1.2.1a}$$

$$\sigma_f(\mathbf{u}^{n+1}, \mathsf{p}^{n+1})\boldsymbol{n}_f + \alpha\mathbf{u}^{n+1} = \alpha\partial_t\mathbf{e}^{n+1} + \sigma(\mathbf{u}^n, \mathsf{p}^n)\boldsymbol{n}_f \quad \text{on } \Sigma, \tag{1.2.1b}$$

where $\alpha > 0$. We believe our method is the first rigorously proven, *unconditionally stable* explicit coupling for the FSI system. Additionally, it is the first *non-iterative* method proven to have nearly first order accuracy in time.[4] Additionally, through the use of a method introduced by Baker in [4], our stability and error estimates have no exponential growth in time of perturbations.

The *key to stability* of the Robin-Robin method is in the ability to rewrite the conditions (1.2.1) as the following identities.

$$\sigma_s(\mathbf{e}^{n+1})\boldsymbol{n}_s + \sigma_f(\mathbf{u}^{n+1}, \mathsf{p}^{n+1})\boldsymbol{n}_f = \alpha(\mathbf{u}^n - \mathbf{u}^{n+1}) \quad \text{on } \Sigma, \tag{1.2.2a}$$

$$\alpha(\mathbf{u}^{n+1} - \partial_t\mathbf{e}^{n+1}) = \sigma_f(\mathbf{u}^n, \mathsf{p}^n)\boldsymbol{n}_f - \sigma_f(\mathbf{u}^{n+1}, \mathsf{p}^{n+1})\boldsymbol{n}_f, \quad \text{on } \Sigma. \tag{1.2.2b}$$

With these identities, we are able to equate the traditional coupling conditions, (1.1.3) with time differences of the fluid velocities and stresses. Thus, given sufficient regularity in time, the splitting error will be equivalent to these time differences and will decay as $\Delta t \to 0$.

However, we note that these identities may not hold at the spacially discrete

[4] We would also like to acknowledge the very impressive results in the recent works [48, 13, 10]. These papers were completed separately and in parallel to the works presented in this thesis. Although their Robin-Robin loosely coupled scheme in these works is comparable to our own, we employ some key differences to set our results apart. Namely, we employ residual lifting for the stress terms at the interface. Furthermore, our estimates do not feature exponential growth, and we achieve nearly first order accuracy for all schemes presented in this thesis.

level if standard finite elements are used. Indeed, the spacial derivatives in the stress terms will likely not have the same continuity across element boundaries as the velocities. Thus, we will employ the methods in [38] to formulate a variationally consistent representation of the fluid stress on which we can impose the requisite inter-element continuity. This will be explained in more detail in the chapters that follow, particularly in Chapter 5.

1.2.1 Organization of the thesis

The remainder of this thesis proceeds as described. Following a chapter on mathematical background and preliminaries, we introduce in Chapter 3 the Robin-Robin coupling method as applied to two model cases: a parabolic-parabolic coupled problem, and a parabolic-hyperbolic coupled problem. We analyze these two model systems before the FSI system because they provide valuable insight into the behavior and applicability of the Robin-Robin method in a simpler, less stiff formulation. We carry out a unified stability and error analysis of these two model systems and show that the method is unconditionally stable and nearly first-order accurate. Note that we only discretize our system in time in order to focus on the time convergence properties of the splitting method. For the parabolic system (and later for the Stokes system) we use a backward Euler method, and for the hyperbolic (and elasticity) system, we use a Newmark method. The results presented in this chapter have been submitted for publication, see [15] for the preprint.

To the best of our knowledge, the Robin-Robin conditions have not previously been explored in a unified framework. However, the success of our analysis indicates that the Robin-Robin coupling is particularly amenable to the generalization offered by the unified framework. Thus, given that the parabolic and hyperbolic equations may be viewed as general/simplified settings of many well-known partial differential equations,[5] *we hope Chapter 3 will serve as useful reference for the application of the Robin-Robin method to a variety of systems.*

Following the analysis of the Robin-Robin method for the parabolic/hyperbolic couplings, in Chapter 4 we introduce the problem of interest: the Robin-Robin method for the FSI system. As in the previous chapter, we continue to restrict our analysis to the time-semi-discrete system, and we use the methods established for the parabolic/hyperbolic model problems to carry out a successful analysis of the FSI system (with some important adjustments to accommodate for added terms and conditions). We show that the method is unconditionally stable in time and nearly first-order accurate, just as in the previous chapter.

Finally, in Chapter 5, we extend the FSI results to the fully discrete case. We apply a linear finite element discretization to the FSI problem and prove that the Robin-Robin method remains unconditionally stable. Furthermore, provided $h \leq C\Delta t$, we prove that the method remains optimally convergent in space and nearly optimal in time.

Note that all numerical experiments were run using the FEniCS automated finite element solver [40] and the library Multiphenics [5].

[5] Stokes, linear elasticity, advection-diffusion, the list goes on...

Chapter Two

Preliminaries

Before we begin the content of the thesis, we introduce some important concepts, notations, and results that will be used throughout the work that follows.

2.1 Norms and Inequalities

2.1.1 Norms and spaces

In this thesis, we will use the standard definitions of the L^p and Sobolev spaces, H^k. In the definitions and results that follow, we assume a domain, Ω is a (Lebesgue) measurable subset of $\mathbb{R}^n$ [1]

Definition 2.1.1 (L^p-space (see e.g. [33, 8]))**.** Consider a domain $\Omega \subset \mathbb{R}^n$. Then for p an integer such that $1 \leq p \leq \infty$, we define

$$L^p(\Omega) := \{v : \Omega \to \mathbb{R},\ \|v\|_{L^p(\Omega)} < \infty\},$$

where

$$\|v\|_{L^p(\Omega)} := \begin{cases} \left(\int_\Omega |v|^p dx \right)^{1/p}, & p < \infty, \\ \text{ess sup}\{|v(x)|,\ x \in \Omega\}, & p = \infty. \end{cases}$$

To define Sobolev spaces, we first define the concept *locally integrable functions* and *weak derivatives.*

Definition 2.1.2 (Locally integrable functions, $L^1_{loc}(\Omega)$ (see e.g. Definition 1.2.3 [8]))**.** Let Ω be defined as above. Then the set of **locally integrable fuctions** is

[1] n will most often be 2 in this thesis, but it is left unspecified for the sake of full generality in the preliminary results in this chapter.

defined as

$$L^1_{loc}(\Omega) := \{f,\ f \in L^1(K)\ \forall \text{ compact } K \subset \text{interior}(\Omega)\}.$$

In other words, $L^1_{loc}(\Omega)$ contains functions that are *almost* in $L^1(\Omega)$, but may behave badly near the boundary.

Definition 2.1.3 (Weak derivative (see e.g. Definition 1.2.4 of [8] or Chapter 5 of [27])). Suppose $u, v \in L^1_{loc}(\Omega)$, and let α be a **multi-index**, or an n-tuple of non-negative integers, α_i. Then we say v is the α^{th}-weak partial derivative of u, or

$$v = D^\alpha u,$$

if

$$\int_\Omega u D^\alpha \phi dx = (-1)^{|\alpha|} \int_\Omega v \phi dx,$$

for all $\phi \in C_c^\infty(\Omega)$.

Here, $|\alpha| := \sum_i \alpha_i$, and $C_c^\infty(\Omega)$ is the set of infinitely differentiable functions with compact support on Ω.

Finally, we may define the Sobolev spaces.

Definition 2.1.4 (The Sobolev spaces, $W_p^k(\Omega)$ and $H^k(\Omega)$ (see e.g. [8, 27])). Assume Ω is defined as above. Let k be a non-negative integer, and let $f \in L^1_{loc}(\Omega)$ such that the weak derivativesD^α exist for all $|\alpha| \leq k$. Then we define the **Sobolev norm**

$$\|f\|_{W_p^k(\Omega)} := \left(\sum_{|\alpha| \leq k} \|D^\alpha f\|^p_{L^p(\Omega)} \right)^{1/p},$$

if $1 \le p < \infty$. In the case $p = \infty$, we define

$$\|f\|_{W^k_\infty(\Omega)} := \max_{|\alpha| \le k} \|D^\alpha f\|_{L^\infty(\Omega)}.$$

Consequently, we define the **Sobolev space**

$$W^k_p(\Omega) := \{f \in L^1_{loc}(\Omega),\ \|f\|_{W^k_p(\Omega)} < \infty\}.$$

When $p = 2$, we recognize that the Sobolev space is a Hilbert space, and we will use the alternative notation

$$H^k(\Omega) := W^k_2(\Omega).$$

In addition to the L^p and Sobolev spaces, we will frequently make use of the Bochner norms defined as follows.

Definition 2.1.5 (Bochner norms)**.** Let X be a Hilbert space. Then we define the Bochner norms

$$\|v\|_{L^2(a,b;X)} := \Big(\int_a^b \|v(\cdot,s)\|_X^2 ds \Big)^{1/2}, \tag{2.1.1a}$$

$$\|v\|_{L^\infty(a,b;X)} := \text{ess sup}_{a \le s \le b} \|v(\cdot,s)\|_X. \tag{2.1.1b}$$

2.1.2 Inequalities

We will also use some standard inequalities related to the norms and inner products on a domain Ω. The first inequality holds for any normed vector space, X. We will use this identity several times in the proofs of this thesis, and it relates the inner product of a difference of functions with the difference of the norms of the functions.

Lemma 2.1.6. *Let $(\cdot, \cdot)$ be an inner product on a normed vector space X, and let $\|\cdot\|$ be the corresponding norm. Then for $\phi, \psi, \theta \in X$, we have*

$$(\phi - \psi, \theta) = \frac{1}{2}(\|\phi\|^2 - \|\psi\|^2 + \|\theta - \psi\|^2 - \|\theta - \phi\|^2). \tag{2.1.2}$$

Proof. To prove this identity, we note that for $u, v \in X$, we have

$$\|u - v\|^2 = \|u\|^2 - 2(u, v) + \|v\|^2.$$

Thus we may write

$$\begin{aligned}(\phi - \psi, \theta) =& (\phi, \theta) - (\psi, \theta)\\ =& \frac{1}{2}(\|\phi\|^2 + \|\theta\|^2 - \|\theta - \phi\|^2) - \frac{1}{2}(\|\psi\|^2 + \|\theta\|^2 - \|\theta - \psi\|^2).\end{aligned}$$

The result subsequently follows by combining terms. □

The next result is a standard result for products that goes by several different names[2] Here, we will refer to it as *Young's inequality*.

Lemma 2.1.7 (Young's inequality for products)**.** *Let $\epsilon > 0$. Then for $a, b \in \mathbb{R}$,*

$$ab \leq \frac{\epsilon a^2}{2} + \frac{b^2}{2\epsilon}$$

[2]For example, some refer to it as the Peter-Paul inequality.

Proof. To begin, we write

$$ab = ((\sqrt{\epsilon})a)\big(\frac{b}{\sqrt{\epsilon}}\big) = -\frac{1}{2}(((\sqrt{\epsilon})a) - \frac{b}{\sqrt{\epsilon}})^2 + \frac{\epsilon a^2}{2} + \frac{b^2}{2\epsilon}.$$

The result follows from recognizing that $-\frac{1}{2}(((\sqrt{\epsilon})a) - \frac{b}{\sqrt{\epsilon}})^2 \leq 0$. □

The subsequent inequalities are standard results, so we will provide references in lieu of proofs.

Lemma 2.1.8 (Cauchy-Schwarz Inequality, 5.19 in [33])**.** *Let $(\cdot,\cdot)$ be an inner product on the space X, and let $\|\cdot\|$ be the induced norm. Then for all $u, v \in X$, we have*

$$|(u,v)| \leq \|u\|\|v\|,$$

with equality if and only if $u = v$.

We will often combine Lemma 2.1.8 and Lemma 2.1.7 for the following result.

Corollary 2.1.9 (Consequence of Lemmas 2.1.7 and 2.1.8)**.** *Let u, v be as defined in Lemma 2.1.8. Then*

$$(u,v) \leq \frac{\epsilon}{2}\|u\|^2 + \frac{1}{2\epsilon}\|v\|^2.$$

Proposition 2.1.10 (A variation of Poincaré's inequality, see e.g. Proposition 5.3.4 of [8])**.** *Let Ω be a bounded, connected subset of $\mathbb{R}^2$ with Lipschitz boundary,*[3] *$\partial\Omega$ and let $\Gamma \subset \partial\Omega$ be closed with meas$(\Gamma) > 0$. Define*

$$V = \{v \in H^1(\Omega) : v|_\Gamma = 0\}.$$

[3] In [8] the requirement for this result is that Ω is the finite union of star-shaped domains with respect to a ball. However, by Proposition 2.5.4 of [21], a Lipschitz boundary should be more than sufficient to satisfy this requirement.

Then there exists a constant C_P depending only on Ω and Γ such that

$$\|v\|_{L^2(\Omega_f)} \leq C_P \|\nabla v\|_{L^2(\Omega)} \quad \forall v \in V. \tag{2.1.3}$$

Proposition 2.1.11 (Trace inequality, Theorm 1.6.6 of [8])**.** *Let Ω be a domain in $\mathbb{R}^n$ with Lipschitz boundary. Then there exists a constant C_{tr} such that*

$$\|\boldsymbol{v}\|_{L^2(\Sigma)} \leq C\|\boldsymbol{v}\|_{H^1(\Omega)}. \tag{2.1.4}$$

Corollary 2.1.12 (Consequence of Proposition 2.1.10 and Proposition 2.1.11)**.**

$$\|v\|_{L^2(\Sigma)} \leq C_{tr} \|\nabla v\|_{L^2(\Omega)} \quad \forall v \in V. \tag{2.1.5}$$

Finally, we complete this section with a relation between the H^1-norm and the ***symmetric gradient***, $\varepsilon(v)$, defined by

$$\epsilon(v) = \frac{1}{2}(\nabla v + (\nabla v)^T).$$

Lemma 2.1.13 (Corollary of Korn's Inequality, see Corollary 11.2.22 in [8])**.** *There exists a positive constant C such that*

$$\|\epsilon(v)\|_{L^2(\Omega)} \geq C\|v\|_{H^1(\Omega)} \quad \forall v \in V,$$

where $V = \{v \in H^1(\Omega), v|_\Gamma = 0\}$, and $\Gamma \subset \partial\Omega$, meas$(\Gamma) > 0$.

2.2 Finite elements

In Chapter 5 we will pose our problem in a fully discrete formulation using linear finite elements. The *finite element method* (see [8]) is a method for approximating the solution to the variational problem

$$a(u,v) = F(v),\ \forall v \in V, \tag{2.2.1}$$

on our domain Ω. Here $a(\cdot,\cdot)$ is a bilinear form, and V is an infinite dimensional function space containing the solution.

To approximate the solution to (2.2.1), we first define a ***mesh***, $\mathcal{T}_h$, on Ω.

Definition 2.2.1 (Mesh and elements (Definition 1.49 of [26]))**.** A **mesh** is a union of a finite number N_E of compact, connected, Lipschitz[4] sets K_i with non-empty interiors, known as ***elements***, such that $\{K_i\}_{i=1}^{N_E}$ form a partition of Ω.

We require these elements to be disjoint, so that we have

$$\bigcup_{i=1}^{N_E} K_i = \bar{\Omega}, \qquad \mathrm{int} K_i \cap\ \mathrm{int} K_j = \emptyset,\ i \neq j.$$

For this thesis, we will consider meshes (in $\mathbb{R}^2$) defined by a ***simplical triangulation*** of a domain Ω.

Definition 2.2.2 (Simplex and simplical triangulation (see [26]))**.** Consider a set of points $\{a_1, \ldots, a_d\} \in \mathbb{R}^n$ such that the vectors $\{a_2 - a_1, \ldots, a_d - a_{d-1}\}$ are linearly independent. Then we define a **simplex** with **vertices** $\{a_1, \ldots, a_d\}$ to be the convex hull of $\{a_1, \ldots, a_d\}$. Furthermore, when the elements forming a mesh $\mathcal{T}_h$ are all

[4] A domain is Lipschitz if it has a Lipschitz boundary.

simplices, we say $\mathcal{T}_h$ is a **simplical triangulation**.[5]

For each element $K \in \mathcal{T}_h$ we define

$$\operatorname{diam}(K) = h_K := \max_{x_1, x_2 \in K} |x_1 - x_2|.$$

Then, we define the ***mesh parameter*** or ***spatial discretization parameter***, h to be [26]

$$h := \max_{K \in \mathcal{T}_h} h_K.$$

Consequently, we may refine the mesh $\mathcal{T}_h$ by decreasing the size of h. However, we do not want the elements to become to flat as we refine the mesh, as this will result in a poorly conditioned transformation between K and a *reference element* $\hat{K}$. This could subsequently prevent us from computing global error estimates of our finite element approximation (see [26] for more details). To avoid this issue, we define a concept of ***shape regularity***.

Definition 2.2.3 (Shape regularity, Definition 1.107 in [26])**.** A family of meshes $\{\mathcal{T}_h\}_{h>0}$ is said to be **shape regular** if there exists σ_0 such that

$$\forall h,\ \forall K \in \mathcal{T}_h, \quad \sigma_K = \frac{h_K}{\rho_K} \le \sigma_0,$$

where ρ_K is the diameter of the largest ball that can be inscribed in K.

From this point on, when we refer to a mesh $\mathcal{T}_h$ as shape regular, we mean the family of mesh refinements take as $h \to 0$.

[5]Thankfully, in this thesis, our meshes will always be made up of triangular meshes, so the term "triangulation" will be less misleading.

Now that a mesh has been defined, we may establish the definition of a ***finite element***.

Definition 2.2.4 (Finite element, Definition 3.1.1 of [8]). A **finite element** is defined as $(K, \mathcal{P}, \mathcal{N})$, where

1. $K \subset \mathbb{R}^n$ be a bounded closed set with nonempty interior and piecewise smooth boundary (the **element domain**),
2. $\mathcal{P}$ be a finite-dimensional space of functions on K (the space of **shape functions**), and
3. $\mathcal{N} = \{N_1, N_2, \ldots, N_k\}$ be a basis for the dual space of $\mathcal{P}$, $\mathcal{P}'$ (the set of **nodal variables**).

Critically, the nodal variables determine the ***degrees of freedom*** that uniquely determine the functions in $\mathcal{P}$ on K. As we will see below, we will consider the case where N_i returns the value of a function v at the $i-th$ element node. However, for more complicated finite elements, N_i could return something else, such as the value of a derivative. The important thing is that the values returned by each N_i *uniquely determine a function in* $\mathcal{P}$. Consequently, on each element we will be able to assign a ***nodal basis*** with which we may interpolate functions.

Definition 2.2.5 (Nodal basis of P, Definition 3.1.2 in [8]). Let $(K, \mathcal{P}, \mathcal{N})$ be a finite element. The basis $\{\phi_1, \phi_2, \ldots, \phi_k\}$ of $\mathcal{P}$ dual to $\mathcal{N}$ (i.e. $N_i(\phi_j) = \delta_{ij}$) is called the ***nodal basis*** of $\mathcal{P}$.

Thus, for any function in $u \in \mathcal{P}$ defined in K, we may write

$$u(x) = \sum_{i=1}^{k} N_i(u)\phi_i(x).$$

In this thesis, we will only consider ***linear Lagrange finite elements***.

Definition 2.2.6 (Linear Lagrange finite element in $\mathbb{R}^2$ (see [8]))**.** The ***linear Lagrange finite element*** in $\mathbb{R}^2$ is a finite element $(K, \mathcal{P}, \mathcal{N})$ defined such that

1. K is a triangle with vertices z_1, z_2, z_3, (see Figure 2.1)
2. $\mathcal{P} = \mathcal{P}^1(K)$, the space of linear functions defined on the element K,
3. $\mathcal{N} = (N_1, N_2, N_3)$ where $N_i(v) = v(z_i)$ (note that $\mathcal{N}$ determines $\mathcal{P}^1(K)$, since a linear polynomial in $\mathbb{R}^2$ is uniquely determined by its value at three points. See [8]).

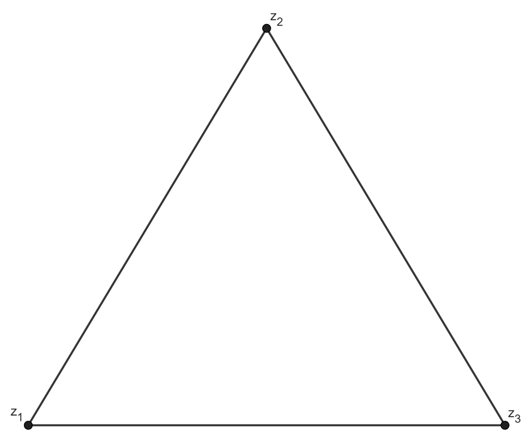

Figure 2.1: A $\mathcal{P}^1$ Lagrange element in $\mathbb{R}^2$.

Consequently, the ***finite element approximation*** of (2.2.1) on the mesh $\mathcal{T}_h$ is the solution $u_h \in V_h$ that satisfies

$$a(u_h, v) = F(v), \quad \forall v \in V_h,$$

where $V_h = \{v \in V,\ v|_K \in \mathcal{P}^1(K), \forall K \in \mathcal{T}_h\}$.

2.2.1 The interpolants

Note that the finite element space V_h is a finite dimensional subset of the space V. However, we will rarely be lucky enough to have $V = V_h$. Thus, if we want to compare the finite element approximation $u_h \in V_h$ to the *exact solution* $u \in V$ of (2.2.1), we will need some way to *project* u into V_h.

First, however, we consider how to accomplish this task *locally*. As such, we define an interpolant on the element K using the nodal basis functions defined above.

Definition 2.2.7 (Local interpolant, Definition 3.3.1 in [8])**.** Given a finite element $(K, \mathcal{P}, \mathcal{N})$, let the set $\{\phi_i,\ 1 \le i \le k\} \subset \mathcal{P}$ be the basis dual to $\mathcal{N}$. If v is a function for which all $N_i \in \mathcal{N}$, $i = 1, \ldots, k$ are defined, then we define the ***local interpolant*** on K by

$$\mathcal{I}_K v := \sum_{i=1}^{k} N_i(v)\phi_i.$$

For a more global perspective, we have more options to play with, but for this thesis we will use only two methods. The first is the standard L^2 projection. The second is the ***Scott-Zhang interpolant***, introduced by Scott and Zhang in [47]. We begin by defining the L^2 projection.

Definition 2.2.8 (L^2 Orthogonal Projection)**.** Let V_h be a finite dimensional subspace of V. Then we define the L^2 ***orthogonal projection***, $\mathbb{P}_h : V \to V_h$, to be such that

$$\left\langle \mathbb{P}_h u, v_h \right\rangle = \left\langle u, v_h \right\rangle \quad \forall v_h \in V_h. \tag{2.2.2}$$

We will not use any stability or error results for this projection.

2.2.1.1 The Scott-Zhang interpolant

To define the Scott-Zhang interpolant, we will loosely follow the derivation in [8]. Therefore, we first define the concept of a ***nodal basis function***.

Definition 2.2.9 (Nodal basis of $\mathcal{P}$, Definition 3.1.2 of [8])**.** Let $(K, \mathcal{P}, \mathcal{N})$ be a finite elemen with k degrees of freedom. The set of basis functions $\{\phi_1, \ldots, \phi_k\}$ of $\mathcal{P}$ dual to $\mathcal{N}$ (i.e. $N_i(\phi_j) = \delta_{ij}$) is called the ***nodal basis*** of $\mathcal{P}$.

Thus for an element K with nodes z_1, z_2, z_3 the nodal basis function $\phi_i(z_j)$ returns 1 when $i = j$ and 0 when $i \neq j$.

However, this basis is local on the element K, and we will need to consider problems *globally*, or at each point on the mesh $\mathcal{T}_h$. As $\mathcal{T}_h$ is a finite element mesh, it is clear that for each node z of $\mathcal{T}_h$ we may assign a corresponding nodal variable N_z that comes from the finite elements with element domains that make up the mesh $\mathcal{T}_h$ (the mesh is made up of the same type of element, so it is not hard to convince ourselves that if two elements share a node, then the nodal variables from each element corresponding to this node will match). Therefore, for a smooth function, we may define the ***global interpolating function***

$$\mathcal{I}^h u := \sum_z N_z(u)\Phi_z, \tag{2.2.3}$$

where Φ_z is a ***global basis function*** defined element-by-element.

Definition 2.2.10 (Global Basis Function)**.** We define the ***global basis functions*** Φ_z to be functions $\Phi_z \in V_h$, each corresponding to a particular node, z, of $\mathcal{T}_h$, such that if y is also a node of $\mathcal{T}_h$, we have

$$\Phi_z(y) = \begin{cases} 1 & y = z, \\ 0 & \text{else.} \end{cases}$$

Furthermore, we define Φ_z element-wise such that if z is a node associated with the element K, and ϕ_z^K is the *nodal* basis function associated to that node on the element K (see Definition 2.2.9), then we define

$$\Phi_z|_K = \phi_z^K.$$

Note that the global interpolating function function interpolates a function u at the nodes of $\mathcal{T}_h$ in such a way that $\mathcal{I}^h u|_K \in \mathcal{P}(K)$. In other words, the global interpolant is defined so that it matches the local interpolant when restricted to the element K. Recall that for the case of linear Lagrange finite elements, $N_z(u) = u(z)$.

Assume now that Ω is a Lipschitz bounded domain and $\mathcal{T}_h$ is a shape regular mesh. Without loss of generality, we can *assign* an element domain to each node, so that for each z we associate a single $K_z \in \mathcal{T}_h$ with $z \in K_z$. We may then further define a subset $\tilde{K}_z \subset K_z$ so that $z \in \tilde{K}_z$. We note that this step represents one of the most useful features of the Scott-Zhang interpolant, as there is incredible flexibility in choosing $\tilde{K}_z$ as long as the restriction of functions in the element K_z to the "sub-element" $\tilde{K}_z$ is appropriate (see [47] for more details). A more precise way to state this is to let $(K_z, \mathcal{P}_z, \mathcal{N}_z)$ be the finite element with element domain K_z. Then we define the restriction of functions in $\mathcal{P}_z$ to $\tilde{K}_z$ by

$$\tilde{\mathcal{P}}_z := \{f|_{\tilde{K}_z},\ f \in \mathcal{P}_z\}.$$

Then we require $\tilde{K}_z$ to be chosen such that $(\tilde{K}_z, \tilde{\mathcal{P}}_z, \tilde{\mathcal{N}}_z)$ is a well defined finite element for some $\tilde{\mathcal{N}}_z \subset \mathcal{N}_z$.

Instead of working with this very general framework, however, we will define the remainder of the Scott-Zhang interpolant for the specific case where we choose $\tilde{K}_z$ to be the edge of the element K_z containing the node z. Furthermore, *we will assume for the remainder of this section that* Ω *is a polygonal domain so that mesh conforms to the boundary.* Thus, if z is on the boundary, **we may choose K_z such that $\tilde{K}_z$ lies along the boundary.**

Although not always necessary, we may assume that all Scott-Zhang interpolants in this thesis are defined in this way, and we will assume that our original finite elements $(K, \mathcal{P}, \mathcal{N})$ are all linear Lagrange finite elements. We do so to make sure that we can achieve the desired stability and error results for the interpolant on both the interior domains *and* the interface Σ. For a fully general derivation of the Scott-Zhang interpolant, we refer the reader to the paper by Scott and Zhang, [47].

Consequently, we have $(\tilde{K}_z, \tilde{\mathcal{P}}_z, \tilde{\mathcal{N}}_z)$ defined such that $\tilde{K}_z = e_z$, where e_z is an edge of K containing z. Then $\tilde{\mathcal{P}}_z = \{f|_{e_z}, f \in \mathcal{P}^1(K)\}$, and $\tilde{\mathcal{N}}_z = (N_1, N_2)$ map functions to their values at the endpoints of e_z.

We will now let x be the other node of K contained in e_z. In other words, $e_z = [x, z]$. Then, we define a local nodal basis for $\tilde{\mathcal{P}}_z$,

$$\{\phi_i,\ i = x, z\},$$

such that ϕ_x and ϕ_z are the restrictions of the local nodal basis functions on K to the edge e_z. Note that this means ϕ_x and ϕ_z are linear functions such that

$$\phi_x(x) = 1,\ \phi_x(z) = 0, \quad \text{and} \quad \phi_z(x) = 0,\ \phi_z(z) = 1.$$

For linear Lagrange elements, we can define ϕ_x and ϕ_z, as they are the unique linear functions satisfying the properties above. Thus, if we let $x = (x_1, x_2)$ and $z = (z_1, z_2)$, and we define $s = (s_1, s_2)$ to be any point on the edge e_z, we have

$$\begin{aligned}\phi_x(s) :=& \frac{s_1 z_2 - s_2 z_1}{x_1 z_2 - x_2 z_1},\\ \phi_z(s) :=& \frac{x_1 s_2 - x_2 z_1}{x_1 z_2 - x_2 z_1}.\end{aligned}$$

Recall that for any $u_h \in \tilde{\mathcal{P}}$, we can write

$$u_h(s) = u_h(x)\phi_x(s) + u_h(z)\phi_z(s),\ \ s \in e_z.$$

We next define

$$\{\psi_x, \psi_y\}$$

be the $L^2(\tilde{K}_z)$-dual basis for $\tilde{\mathcal{P}}_z$, so that

$$\int_{\tilde{K}_z} \phi_i(s)\psi_j(s)ds = \delta_{ij}.$$

Thus, for $u_h \in \tilde{\mathcal{P}}$, as before, we have

$$\begin{aligned}\int_{e_z} \psi_x(s)u_h(s)ds =& \int_{e_z} \psi_x(s)(u_h(x)\phi_x(s) + u_h(z)\phi_z(s))ds\\ =& u_h(x),\end{aligned}$$

Then, the ***Scott-Zhang interpolant*** may finally be defined.

Definition 2.2.11 (Scott-Zhang interpolant (see [47, 8])). The ***Scott-Zhang interpolant*** (as we will use it in this thesis) of a function u is the (global) interpolant defined

$$\tilde{\mathcal{I}}^h u = \sum_z \left(\int_{e_z} \psi_z(s) u(s) ds \right) \Phi_z. \tag{2.2.4}$$

From this, we see that ψ_z allows us to ensure that $\tilde{\mathcal{I}}^h$ is a projection into V_h, as whenever we have $u \in V_h$, we know $u|_K \in \mathcal{P}(K)$ and therefore $u|_{e_z} \in \tilde{\mathcal{P}}$. Thus we find

$$\tilde{\mathcal{I}}^h u = \sum_z u(z) \Phi_z = u,$$

for the case of linear Lagrange elements.

These interpolants come with useful stability results. The first two results, (2.2.5) and (2.2.6), are well-known, see [8, 47]. We provide a proof for the third result, (2.2.7), for the specific choice of Scott-Zhange interpolant that we have defined above.

Lemma 2.2.12 (A variant of Corollary 4.8.15 in [8]). *Assume Ω is a polygonal domain and each finite element $(K, \mathcal{P}_K, \mathcal{N}_K)$ is a linear Lagrange element. Let $u \in W_p^1(\Omega)$ for $1 \le p \le \infty$. Then for $1 \le p < \infty$, we have*

$$\|\tilde{\mathcal{I}}^h u\|_{W_p^1(\Omega)} \le \left(\sum_{K \in \mathcal{T}^h} \|\tilde{\mathcal{I}}^h u\|^p_{W_p^1(K)} \right)^{1/p} \le C \|u\|_{W_p^1(\Omega)}, \tag{2.2.5}$$

and for $p = \infty$,

$$\|\tilde{\mathcal{I}}^h u\|_{W_\infty^1(\Omega)} \le \sum_{K \in \mathcal{T}^h} \|\tilde{\mathcal{I}}^h u\|_{W_\infty^1(K)} \le C \|u\|_{W_\infty^1(\Omega)}. \tag{2.2.6}$$

Furthermore, let $\Gamma = \partial\Omega$*, and assume* $u \in L^2(\Gamma)$*. Then we have*

$$\|\tilde{\mathfrak{I}}^h u\|_{L^2(\Gamma)} \leq C\|u\|_{L^2(\Gamma)}. \tag{2.2.7}$$

Proof of (2.2.7). Let Z_Γ be the set of mesh nodes on Γ. We begin by writing

$$\begin{aligned}
\|\tilde{\mathfrak{I}}^h u\|^2_{L^2(\Gamma)} =& \int_\Gamma \left(\sum_{z \in Z_\Gamma} \int_{e_z} \psi_z(s)u(s)ds \right) \Phi_z(x) \Bigg)^2 dx \\
\leq& C \sum_{z \in Z_\Gamma} \int_\Gamma \left(\int_{e_z} \psi_z(s)u(s)ds \right)^2 |\Phi_z(x)|^2 dx \\
\leq& C \sum_{z \in Z_\Gamma} \left(\int_{e_z} \psi_z(s)u(s)ds \right)^2 \|\Phi_z(x)\|^2_{L^2(e_z)}.
\end{aligned}$$

Recall that for each $z \in Z_\Gamma$, we choose K_z (the element containing z) such that one of the edges containing z lies along Γ. This would then be the "subelement" $\tilde{K}_z$, which we call e_z.

We note that $0 \leq \Phi_z \leq 1$ on K_z, so we have

$$\|\Phi_z(x)\|^2_{L^2(K_z)} = \int_{K_z} |\Phi_z(x)|^2 dx \leq \int_{e_z} dx = |e_z|.$$

As a result, we are left with

$$\|\tilde{\mathfrak{I}}^h u\|^2_{L^2(\Gamma)} \leq C \sum_{z \in \Gamma} |e_z| \left(\int_{e_z} \psi_z(s)u(s)ds \right)^2,$$

on which we apply Hölder's inequality to determine

$$\|\tilde{\mathfrak{I}}^h u\|^2_{L^2(\Gamma)} \leq C \sum_{z \in Z_\Gamma} |e_z| \|\psi_z\|^2_{L^2(e_z)} \|u\|^2_{L^2(e_z)}.$$

From [47] (see Lemma 3.1 of this paper) we have

$$\|\psi_z\|_{L^\infty(e_z)} \leq C|e_z|^{-1}.$$

Thus we have

$$\begin{aligned}\|\psi_z\|^2_{L^2(e_z)} \leq & \|\psi_z\|^2_{L^\infty(e_z)} \int_{e_z} ds \\ \leq & C|e_z|^{-2}|e_z| = C|e_z|^{-1}.\end{aligned}$$

From this we may write

$$\|\tilde{\mathfrak{I}}^h u\|^2_{L^2(\Gamma)} \leq C \sum_{z\in Z_\Gamma} \|u\|^2_{L^2(e_z)} \leq C\|u\|^2_{L^2(\Gamma)}.$$

□

We also have error bounds for the interpolation error. For these, we will need a definition of the H^k norm on the boundary $\Gamma = \partial\Omega$.

Recall that Ω is a polygonal domain, so we assume it has M sides, and we may write $\Gamma = \bigcup_{i=1}^M \Gamma_i$, where Γ_i is a straight line segment representing a side of Γ. We let τ_i denote the tangent vector along the line segment Γ_i. Then we define the H^k norm on Γ, $k \geq 1$ an integer, in the following way.

Definition 2.2.13 ($H^k(\Gamma)$-norm)**.** We define

$$\|u\|^2_{H^k(\Gamma)} := \sum_{|\alpha|\leq k} \|D^\alpha_\Gamma\|_{L^2(\Gamma)} = \sum_{|\alpha|\leq k} \big(\sum_{i=1}^M \|D^\alpha_{\tau_i}\|^2_{L^2(\Gamma_i)}\big),$$

where $D^\alpha_{\tau_i}$ indicates the weak directional derivative along τ_i of order α.

We may now state the error bounds. We note that the result for (2.2.8) is well known and refer to [8, 47] for details.

Lemma 2.2.14 (A variant of Theorem 4.8.12 in [8])**.** *Under the conditions of Lemma 2.2.12, we have*

$$\|u - \tilde{\mathfrak{I}}^h u\|_{L^p(\Omega)} + h\|u - \tilde{\mathfrak{I}}^h u\|_{W_p^1(\Omega)} \leq Ch^2 \|u\|_{W_p^2(\Omega)}, \tag{2.2.8}$$

for $1 \leq p \leq \infty$*.*

Furthermore, let $\Gamma = \partial\Omega$*, and assume* $u \in L^2(\Gamma)$*. Then we have*

$$\|u - \tilde{\mathfrak{I}}^h u\|_{L^2(\Gamma)} \leq C\|u\|_{L^2(\Gamma)}, \tag{2.2.9a}$$

$$\|u - \tilde{\mathfrak{I}}^h u\|_{L^2(\Gamma)} \leq Ch\|u\|_{H^1(\Gamma)}, \tag{2.2.9b}$$

$$\|u - \tilde{\mathfrak{I}}^h u\|_{L^2(\Gamma)} \leq Ch^2\|u\|_{H^3(\Omega)}. \tag{2.2.9c}$$

The error result (2.2.9a) follows from applying the triangle inequality to (2.2.7), so we only prove (2.2.9b) and (2.2.9c).

Proof of (2.2.9b) *and* (2.2.9c). To prove (2.2.9b), we consider

$$\|u - \tilde{\mathfrak{I}}^h u\|_{L^2(\Gamma)} \leq \|u - \pi_h u\|_{L^2(\Gamma)} + \|\pi_h u - \tilde{\mathfrak{I}}^h u\|_{L^2(\Gamma)},$$

where π_h is the (linear) Lagrange interpolant at the nodes of Σ.

It is a well-known result that

$$\|u - \pi_h u\|_{L^2(\Gamma)} \leq Ch\|D_\Gamma u\|_{L^2(\Gamma)},$$

where D_Γ denotes the derivative along the tangent vector at boundary Γ, in the sense of directional derivatives. For example, if Ω is a rectangle with sides Γ_i, $i = 1, 2, 3, 4$, then

$$\|D_\Gamma u\|^2_{L^2(\Gamma)} = \sum_{i=1}^{4} \|D_{\tau_i} u\|^2_{L^2(\Gamma_i)},$$

where τ_i is the tangent vector along Γ_i (see Definition 2.2.13).

For the second term, we use the fact that $\pi_h u \in V_h$, and $\mathcal{I}_h$ is a projection. Thus $\pi_h u = \mathcal{I}_h \pi_h u$, and we may use the stability result (2.2.7). Thus we have

$$\begin{aligned} \|\pi_h u - \tilde{\mathcal{I}}^h u\|_{L^2(\Gamma)} =& \|\tilde{\mathcal{I}}^h(\pi_h u - u)\|_{L^2(\Gamma)} \\ \leq& C\|u - \pi_h u\|_{L^2(\Gamma)} \\ \leq& h\|D_\Gamma u\|_{L^2(\Gamma)}. \end{aligned}$$

The result then follows immediately.

The proof of (2.2.9c) follows in the same manner. However, we now use the result

$$\|u - \pi_h u\|_{L^2(\Gamma)} \leq Ch^2 \|D^2_\Gamma u\|_{L^2(\Gamma)},$$

where $D^2_\Gamma u$ now denotes the *Hessian* of u along Γ in the sense of directional derivatives.

We then similarly bound $\|\pi_h u - \tilde{\mathcal{I}}^h u\|_{L^2(\Gamma)}$ and apply Proposition 2.1.11 to complete the result. □

Chapter Three

Robin-Robin coupling for parabolic-parabolic and parabolic-hyperbolic problems

3.1 The Parabolic-Parabolic and the Parabolic-Hyperbolic Model Problems

In this chapter, we introduce a loosely coupled scheme based on Robin-Robin type coupling conditions applied to two model problems: a parabolic-parabolic coupled interface problem and a parabolic-hyperbolic coupled interface problem. We analyze these problems in the time-semi-discrete framework, using a novel unified approach to the two model problems. The main goal of this chapter is to provide rigorous proofs of stability and nearly optimal error estimates for this loosely coupled scheme.

This chapter is organized as follows. In this section, we introduce the two model problems in their separate and unified forms. Then, in Section 3.2 we introduce the Robin-Robin coupling and the time-semi-discrete formulation. Subsequently, in Section 3.3 we prove stability of the Robin-Robin method before proceeding to the error analysis in Section 3.4. We then discuss some key concluding points and provide numerical experiments in Sections 3.5 and 3.6.1.

3.1.1 The Parabolic-Parabolic problem

For the two systems that we will consider, let Ω be a bounded, connected subset of $\mathbb{R}^2$ with Lipschitz boundary that can be decomposed as $\Omega = \Omega_f \cup \Omega_s$ where the common interface $\Sigma = \partial\Omega_f \cap \partial\Omega_s$, like that shown in Figure 3.1. Below, we define the two interface problems separately before presenting them in their unified form.

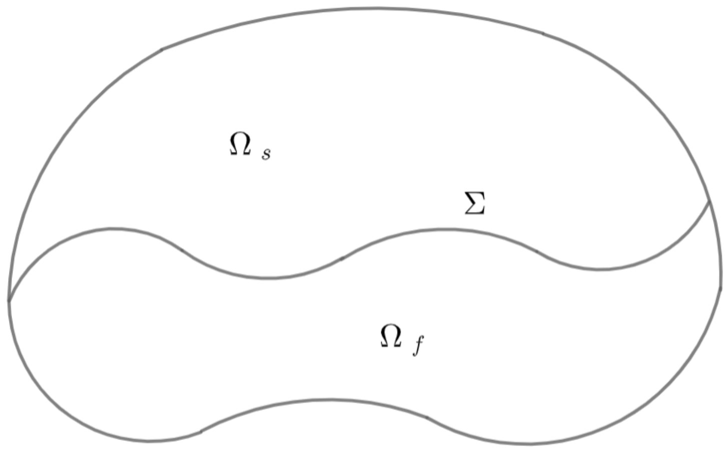

Figure 3.1: An example of the domains Ω_s and Ω_f with interface Σ.

We first consider the standard parabolic problem,

$$\partial_t y - \operatorname{div}(\nu \nabla y) = 0, \qquad \text{in } (0,T)\times\Omega, \tag{3.1.1a}$$

$$y(0,x) = y_0(x), \qquad \text{in } \Omega, \tag{3.1.1b}$$

$$y = 0, \qquad \text{on } (0,T)\times\partial\Omega, \tag{3.1.1c}$$

where ν is a piece-wise constant function given by

$$\nu(x) := \begin{cases} \nu_f, & x \in \Omega_f, \\ \nu_s, & x \in \Omega_s. \end{cases} \tag{3.1.2}$$

We may then write (3.1.1) as an interface problem, where $\mathsf{u} := y|_{\Omega_f}$ and $\mathsf{w} := y|_{\Omega_s}$, since this is the form we will use for the analysis of the method:

$$\partial_t \mathsf{u} - \nu_f \Delta \mathsf{u} = 0, \qquad \text{in } (0,T)\times\Omega_f, \tag{3.1.3a}$$

$$\mathsf{u}(0,x) = \mathsf{u}_0(x), \quad \text{in } \Omega_f, \tag{3.1.3b}$$

$$\mathsf{u} = 0, \quad \text{on } (0,T)\times\partial\Omega_f \setminus \Sigma, \tag{3.1.3c}$$

$$\partial_t \mathsf{w} - \nu_s \Delta \mathsf{w} = 0, \quad \text{in } (0,T)\times\Omega_s, \tag{3.1.4a}$$

$$\mathsf{w}(0,x) = \mathsf{w}_0(x), \quad \text{in } \Omega_s, \tag{3.1.4b}$$

$$\mathsf{w} = 0, \quad \text{on } (0,T)\times\partial\Omega_s \setminus \Sigma, \tag{3.1.4c}$$

and

$$\mathsf{w} - \mathsf{u} = 0, \quad \text{in } (0,T)\times\Sigma, \tag{3.1.5a}$$

$$\nu_s \nabla \mathsf{w} \cdot \boldsymbol{n}_s + \nu_f \nabla \mathsf{u} \cdot \boldsymbol{n}_f = 0 \quad \text{in } (0,T)\times\Sigma. \tag{3.1.5b}$$

where $\boldsymbol{n}_f$ and $\boldsymbol{n}_s$ are the outward facing normal vectors for Ω_f and Ω_s, respectively.

The interface coupling conditions (3.1.5) were chosen to resemble the interface conditions of the FSI problem (1.1.3). However, in the case that $\nu_f = \nu_s$, they are also the standard Dirichlet-Neumann interface conditions that would be applied to the domain decomposition of the parabolic problem (see Section 1.2 of [43])

A parabolic/parabolic coupled problem such as this one parallels the well-known Stokes-Darcy problem. However, unlike in the Stokes-Darcy problem, we do not consider the case of a penetrable interface. Thus, we will have first-order terms (specifically $\nabla \mathsf{u} \cdot \boldsymbol{n}_f$ and $\nabla \mathsf{w} \cdot \boldsymbol{n}_s$) on the interface Σ that must be treated with care. This is distinct from the work in [20], in which the authors are able to avoid a gradient term on the interface.

3.1.2 The Parabolic-Hyperbolic problem

Similarly, we consider the standard parabolic and hyperbolic problems in Ω_f and Ω_s, respectively as an interface problem, where ν_f and ν_s are defined as in (3.1.2).

$$
\begin{aligned}
\partial_t \mathsf{u} - \nu_f \Delta \mathsf{u} =& 0, && \text{in } (0,T) \times \Omega_f, && (3.1.6a)\\
\mathsf{u}(0,x) =& \mathsf{u}_0(x), && \text{on } \Omega_f, && (3.1.6b)\\
\mathsf{u} =& 0, && \text{on } (0,T) \times \partial\Omega_f \setminus \Sigma, && (3.1.6c)
\end{aligned}
$$

$$
\begin{aligned}
\partial_t \mathsf{q} - \nu_s \Delta \mathsf{w} =& 0, && \text{in } (0,T) \times \Omega_s, && (3.1.7a)\\
\mathsf{q} =& \partial_t \mathsf{w}, && \text{in } (0,T) \times \Omega_s, && (3.1.7b)\\
\mathsf{q}(0,x) =& \mathsf{q}_0(x), && \text{on } \Omega_s, && (3.1.7c)\\
\mathsf{w}(0,x) =& \mathsf{w}_0(x), && \text{on } \Omega_s, && (3.1.7d)\\
\mathsf{w} =& 0, && \text{on } (0,T) \times \partial\Omega_s \setminus \Sigma, && (3.1.7e)
\end{aligned}
$$

and

$$
\begin{aligned}
\mathsf{q} - \mathsf{u} =& 0, && \text{in } (0,T) \times \Sigma, && (3.1.8a)\\
\nu_s \nabla \mathsf{w} \cdot \boldsymbol{n}_s + \nu_f \nabla \mathsf{u} \cdot \boldsymbol{n}_f =& 0, && \text{in } (0,T) \times \Sigma, && (3.1.8b)
\end{aligned}
$$

where $\boldsymbol{n}_f$ and $\boldsymbol{n}_s$ are defined as before.

The parabolic-hyperbolic coupled problem may be seen as a less-constrained version of the fluid-structure interaction problem with a linear elastic solid. However, we will see in Chapter 4 that the pressure term in the Stokes equation requires a careful handling when conducting the error analysis.

3.1.3 The generalized system

To avoid redundancy in the analyses, we will work instead with a unified version that can represent either the parabolic-parabolic system described in (3.1.1)-(3.1.5), or the parabolic-hyperbolic system described in (3.1.6)-(3.1.8), depending on the choice of integer, k. More specifically, when $k = 1$, we recover (3.1.3)-(3.1.5), and when $k = 2$, we recover (3.1.6)-(3.1.8). We will carry out the stability and error analyses of both model problems using this unified framework.

Remark 2. The success of this unified analysis suggests some interesting implications with regard to the Robin-Robin coupling method described below. In particular, it is indicative of the wide applicability of the Robin-Robin method.

The generalized system may be written for $k = 1, 2$,

$$\partial_t \mathsf{u} - \nu_f \Delta \mathsf{u} = 0, \qquad \text{in } (0,T) \times \Omega_f, \tag{3.1.9a}$$

$$\mathsf{u}(0,x) = \mathsf{u}_0(x), \qquad \text{on } \Omega_f, \tag{3.1.9b}$$

$$\mathsf{u} = 0, \qquad \text{on } [0,T] \times \partial\Omega_f \setminus \Sigma, \tag{3.1.9c}$$

$$\partial_t \mathsf{q} - \nu_s \Delta \mathsf{w} = 0, \qquad \text{in } (0,T) \times \Omega_s, \tag{3.1.10a}$$

$$\mathsf{q} = \partial_t^{k-1} \mathsf{w}, \qquad \text{in } (0,T) \times \Omega_s, \tag{3.1.10b}$$

$$\mathsf{w}(0,x) = \mathsf{w}_0(x), \qquad \text{on } \Omega_s, \tag{3.1.10c}$$

$$\mathsf{q}(0,x) = \mathsf{q}_0(x), \qquad \text{on } \Omega_s, \tag{3.1.10d}$$

$$\mathsf{w} = 0, \qquad \text{on } (0,T)\times\partial\Omega_s\setminus\Sigma, \tag{3.1.10e}$$

and

$$\mathsf{q}-\mathsf{u} = 0, \quad \text{on } (0,T)\times\Sigma, \tag{3.1.11a}$$

$$\nu_s\nabla\mathsf{w}\cdot\boldsymbol{n}_s+\nu_f\nabla\mathsf{u}\cdot\boldsymbol{n}_f = 0, \quad \text{on } (0,T)\times\Sigma. \tag{3.1.11b}$$

When $k=1$, we assume that $\mathsf{q}_0=\mathsf{w}_0$ and, hence, (3.1.10d) is redundant in that case.

3.1.4 Variational form of the generalized system

Let $(\cdot,\cdot)_i$ be the L^2-inner product on Ω_i for $i=f,s$. Moreover, let $\langle\cdot,\cdot\rangle$ be the L^2-inner product on Σ. Let $N>0$ be an integer, and define $\Delta t=\frac{T}{N}$, and let $\mathsf{u}^n=\mathsf{u}(t_n,\cdot)$, where $t_n=n\Delta t$ for $n\in\{0,1,2,\dots,N\}$. We consider the spaces

$$\begin{aligned}
V_f &= \{v\in H^1(\Omega_f) : v=0 \text{ on } \partial\Omega_f\backslash\Sigma\},\\
V_s &= \{v\in H^1(\Omega_s) : v=0 \text{ on } \partial\Omega_s\backslash\Sigma\},\\
V_g &= L^2(\Sigma).
\end{aligned}$$

Define $\mathsf{l}^{n+1}=\nu_f\nabla\mathsf{u}^{n+1}\cdot\boldsymbol{n}_f$ and assuming that $\mathsf{l}^{n+1}\in L^2(\Sigma)$ for all n, the solutions to (3.1.9)-(3.1.11) at time t_{n+1} also satisfy the following problem: Find $\mathsf{u}^{n+1}\in V_f$, $\mathsf{q}^{n+1},\mathsf{w}^{n+1}\in V_s$, and $\mathsf{l}^{n+1}\in V_g$ such that

$$(\partial_t\mathsf{q}^{n+1},z)_s+\nu_s(\nabla\mathsf{w}^{n+1},\nabla z)_s+\left\langle\mathsf{l}^{n+1},z\right\rangle = 0, \quad z\in V_s \tag{3.1.12a}$$

$$(\partial_t\mathsf{u}^{n+1},v)_f+\nu_f(\nabla\mathsf{u}^{n+1},\nabla v)_f-\left\langle\mathsf{l}^{n+1},v\right\rangle = 0, \quad v\in V_f \tag{3.1.12b}$$

$$(\mathsf{q}^{n+1}-\partial_t^{k-1}\mathsf{w}^{n+1},r)_s = 0, \quad r\in V_s \tag{3.1.12c}$$

$$\left\langle \mathsf{q}^{n+1} - \mathsf{u}^{n+1}, \mu \right\rangle = 0, \quad \mu \in V_g \tag{3.1.12d}$$

Remark 3. As we will see in Section 3.2, the inclusion of the space V_g will be useful when we formulate the Robin-Robin splitting method. Defining $\mathsf{l}^{n+1} := \nu_f \nabla \mathsf{u}^{n+1} \cdot \boldsymbol{n}_f$ will make it easier to compare (3.1.12) to the Robin-Robin time-splitting method.

3.2 Robin-Robin coupling

We note that if we were to discretize (3.1.12) in time, the method would *not* be loosely coupled because the systems on Ω_s and Ω_f must be solved together at each time-step. The seemingly most natural way to make this a loose coupling would be to split one of the interface conditions in (3.1.11) across time-steps. For example, we might apply

$$\begin{aligned} \mathsf{q}^{n+1} - \mathsf{u}^{n+1} &= 0 \quad \text{on } \Sigma, \\ \nu_s \nabla \mathsf{w}^{n+1} \cdot \boldsymbol{n}_s + \nu_f \nabla \mathsf{u}^{n} \cdot \boldsymbol{n}_f &= 0 \quad \text{on } \Sigma. \end{aligned}$$

In this case, the term $\left\langle \mathsf{l}^{n+1}, z \right\rangle$ in (3.1.12a) would be replaced with $\left\langle \mathsf{l}^{n}, z \right\rangle$, which becomes a known quantity, assuming that the solutions at the previous time-step are known. Consequently, we would be able to solve for q^{n+1} and w^{n+1} independently from u^{n+1} and l^{n+1}, using $\nu_f \nabla \mathsf{u} \cdot \boldsymbol{n}_f$ as Neumann data. We would then be able to use this solution and the other interface condition to solve for u^{n+1} on Σ, which in turn becomes Dirichlet data for solving u^{n+1} and l^{n+1} on the whole domain.

However, in many applications the act of breaking one of the interface conditions in (3.1.11) requires us to break the physical laws of the system that these conditions represent. This can cause significant issues, as the system no longer conserves energy, affecting the scheme's overall accuracy [38]. Thus, the most natural loose coupling is, in fact, completely unnatural from a physical perspective.

To off-set the consequences of broken physics, we apply the Robin-Robin coupling method to (3.1.12). We recall from Chapter 1 that the Robin-Robin splitting method takes linear combinations of the exact interface conditions (3.1.11) split across time-steps n and $n+1$, namely

$$\nu_s \nabla \mathsf{w} \cdot \boldsymbol{n}_s + \alpha \mathsf{q}^{n+1} = \alpha \mathsf{u}^n - \mathsf{l}^n \qquad \text{on } \Sigma, \tag{3.2.1a}$$

$$\mathsf{l}^{n+1} + \alpha \mathsf{u}^{n+1} = \alpha \mathsf{q}^{n+1} + \mathsf{l}^n \qquad \text{on } \Sigma, \tag{3.2.1b}$$

where $\alpha > 0$. As we will see, applying these conditions instead of (3.1.11) results in a loose coupling that maintains stability.

3.2.1 The time discrete method

The main focus of this chapter is to gain an understanding of the time-splitting method introduced by the Robin-Robin coupling conditions. Thus, we choose to not discretize our problem in space and limit ourselves to the time-semi-discrete framework.

However, it should be noted that the Robin-Robin coupling conditions may present some difficulties if we were to discretize in space using standard finite elements. More specifically, the gradient terms present in the Robin-Robin coupling will present an issue with continuity across element boundaries on the interface. As this poses a significant concern, we choose to accommodate this issue in our time-semi-discrete problem by casting our scheme as a Lagrange multiplier method using a variationally consistent representation of the gradient term $\nu_f \nabla \mathsf{u}^{n+1}\boldsymbol{n}_f$ on Σ. This method is fully described in 5.1.1 in the context of a fluid-structure interaction.

For the time discrete Robin-Robin method, we use a backward-Euler method for the parabolic system on Ω_f. When $k=1$, we also use a backward-Euler method for the resulting parabolic system on Ω_s, and when $k=2$, we use a Newmark method for the resulting hyperbolic system on Ω_s. Thus, we define the discrete derivative in time

$$\partial_{\Delta t} v^{n+1} = \frac{v^{n+1}-v^n}{\Delta t},$$

and the discrete average in time

$$v^{n+1/2} = \frac{v^{n+1}+v^n}{2}.$$

We will also use the notation

$$\partial_{\Delta t}^j v = \begin{cases} v, & j=0, \\ \partial_{\Delta t} v, & j=1, \end{cases}$$

The Robin-Robin splitting method is as follows.

Find $q^{n+1}, w^{n+1} \in V_s$, $u^{n+1} \in V_f$, and $\lambda^{n+1} \in V_g$ such that, for $k=1,2$ and $n \geq 0$,

$$(\partial_{\Delta t} q^{n+1}, z)_s + \nu_s(\nabla w^{n+1/k}, \nabla z)_s + \alpha\left\langle \partial_{\Delta t}^{k-1} w^{n+1} - u^n, z\right\rangle + \left\langle \lambda^n, z\right\rangle = 0, \quad \forall z \in V_s, \tag{3.2.2a}$$

$$(q^{n+1/k} - \partial_{\Delta t}^{k-1} w^{n+1}, r)_s = 0, \quad \forall r \in V_s, \tag{3.2.2b}$$

$$(\partial_{\Delta t} u^{n+1}, v)_f + \nu_f (\nabla u^{n+1}, \nabla v)_f - \left\langle \lambda^{n+1}, v \right\rangle = 0, \quad \forall v \in V_f, \tag{3.2.2c}$$

$$\left\langle \alpha(u^{n+1} - \partial_{\Delta t}^{k-1} w^{n+1}) + (\lambda^{n+1} - \lambda^n), \mu \right\rangle = 0, \quad \forall \mu \in V_g, \tag{3.2.2d}$$

Here, we assume that the two sub-problems in (3.2.2) are well-posed. We also set $\lambda^0 = \mathsf{l}^0 = \nu_f \nabla \mathsf{u}(0, x) \cdot \boldsymbol{n}_f$

To derive (3.2.2), we assumed q, w, u, and λ satisfied (3.2.1). The condition (3.2.1b) is then enforced on the system using (3.2.2d). We then use (3.2.1a) to replace the interface term $\left\langle \nu_s \nabla w^{n+1} \cdot \boldsymbol{n}_s, z \right\rangle$ that results from taking the inner product of (3.1.10) with z.

We also point out some important consequences of (3.2.2) that will be important for proving our main results.

First, from (3.2.2b) we see that the relation (3.1.10b) is still strongly enforced in a time discrete setting. Indeed, if we set $r = q^{n+1/k} = \partial_{\Delta t}^{k-1} w^{n+1}$ we can show

$$q^{n+1/k} = \partial_{\Delta t}^{k-1} w^{n+1}, \qquad \text{on } \Omega_s. \tag{3.2.3}$$

Additionally, by setting $\mu = \alpha(u^{n+1} - \partial_{\Delta t}^{k-1} w^{n+1}) - (\lambda^n - \lambda^{n+1})$ in (3.2.2d), we acquire the identity

$$\alpha(u^{n+1} - \partial_{\Delta t}^{k-1} w^{n+1}) = \lambda^n - \lambda^{n+1}, \qquad \text{on } \Sigma. \tag{3.2.4}$$

Using (3.2.3), this may be rewritten as

$$\alpha(u^{n+1} - q^{n+1/k}) = \lambda^n - \lambda^{n+1}, \quad \text{on } \Sigma. \tag{3.2.5}$$

As mentioned for the FSI problem in (1.2.2) in Chapter 1, (3.2.4) and (3.2.5) reveal that applying the Robin condition (3.2.1b) is equivalent to setting the difference in (3.1.11a) equal to a time difference in λ instead of zero. In the analysis that follows, we will see that this time difference is a term that we are able to control.

Remark 4. The equivalent to other "key to stability" mentioned in Chapter 1, namely

$$\nu_s \nabla w^{n+1} \cdot \boldsymbol{n}_s + \lambda^{n+1} = \alpha(u^n - u^{n+1}) \quad \text{on } \Sigma,$$

is also a critical feature of the Robin-Robin splitting method. However, we cannot directly recover it like (3.2.5) because the relation is derived by adding (3.2.1a) and (3.2.1b), and (3.2.1a) is only weakly imposed on the system through (3.2.2a). Thus, it is not strongly imposed on the system like (3.2.5) (which is just a rearrangement of (3.2.1b)).

In practice, this splitting method would be implemented sequentially. We assume that solutions from the previous time-step are known. Therefore, q^{n+1} and w^{n+1} may be solved using (3.2.2a) and (3.2.2b) with q^n, w^n, u^n, and λ^n applied as data. The solutions on Ω_s at time-step $n+1$ is then applied as data in (3.2.2d), which serves as an interface coupling equation, we may then solve for λ^{n+1} on Σ and for u^{n+1} in Ω_f together using (3.2.2c) and (3.2.2d).

In this way, the Robin-Robin splitting method is a loosely coupled scheme for the numerical time semi-discrete approximation of (3.1.9)-(3.1.11). We may also observe one of the strong advantages of loosely coupled schemes from this method. Namely, the loosely coupled scheme allows us to use separate solvers for the subsystems on Ω_f and Ω_s. Thus, loosely coupled schemes are appealing when it comes to implementation, as it is a more manageable task to develop a solver for an isolated system than for a two coupled systems. Additionally, for many coupled problems, robust and efficient solvers may already exist for the separate subsystems.

3.3 Stability

In this section we prove stability of the method (3.2.2). More specifically, we will prove the following lemma that states that the energy of the Robin-Robin system at time-step $T = \Delta t N$ is less than or equal to the energy at time $t = 0$.

Lemma 3.3.1. *Let*

$$
\begin{aligned}
Z^{n+1} :=& \frac{1}{2}\|q^{n+1}\|^2_{L^2(\Omega_s)} + \frac{1}{2}\|u^{n+1}\|^2_{L^2(\Omega_f)} + \frac{(k-1)\nu_s}{2}\|\nabla w^{n+1}\|^2_{L^2(\Omega_s)} + \frac{\Delta t\alpha}{2}\|u^{n+1}\|^2_{L^2(\Sigma)} \\
&+ \frac{\Delta t}{2\alpha}\|\lambda^{n+1}\|^2_{L^2(\Sigma)} \\
S^{n+1} :=& \nu_f \Delta t\|\nabla u^{n+1}\|^2_{L^2(\Omega_f)} + (2-k)\nu_s\Delta t\|\nabla w^{n+1}\|^2_{L^2(\Omega_s)} + \frac{(2-k)}{2}\|q^{n+1} - q^n\|^2_{L^2(\Omega_s)} \\
&+ \frac{1}{2}\|u^{n+1} - u^n\|^2_{L^2(\Omega_f)} + \frac{\Delta t\alpha}{2}\|q^{n+1/k} - u^n\|^2_{L^2(\Sigma)}.
\end{aligned}
$$

Then it holds,

$$
Z^N + \sum_{n=0}^{N-1} S^{n+1} = Z^0.
$$

Proof. We will use the identity from Lemma 2.1.6, namely

$$
(\phi - \psi, \theta) = \frac{1}{2}(\|\phi\|^2 - \|\psi\|^2 + \|\theta - \psi\|^2 - \|\theta - \phi\|^2).
$$

To begin, we set $z = \Delta t q^{n+1/k}$ and $v = \Delta t u^{n+1}$ in (3.2.2a) and (3.2.2c), respectively. We also apply (3.2.3) to replace all $\partial_{\Delta t}^{k-1} w^{n+1}$ with $q^{n+1/k}$. Note that we do not do this in the problem formulation (3.2.2) as a stylistic choice.

In the case $k = 1$, we note that setting $z = \Delta t q^{n+1/k}$ in (3.2.2a) is equivalent to setting $z = \Delta t w^{n+1}$, by (3.2.3). In this case, (3.2.2a) yields

$$\begin{aligned}
0 =& (w^{n+1} - w^n, w^{n+1})_s + \nu_s \Delta t (\nabla w^{n+1}, \nabla w^{n+1})_s \\
&+ \alpha \Delta t \big\langle w^{n+1} - u^n, w^{n+1} \big\rangle + \Delta t \big\langle \lambda^n, w^{n+1} \big\rangle \\
=& \frac{1}{2}(\|w^{n+1}\|^2_{L^2(\Omega_s)} - \|w^n\|^2_{L^2(\Omega_s)} + \|w^{n+1} - w^n\|^2_{L^2(\Omega_s)}) + \nu_s \Delta t \|\nabla w^{n+1}\|^2_{L^2(\Omega_s)} \\
&+ \alpha \Delta t \big\langle w^{n+1} - u^n, w^{n+1} \big\rangle + \Delta t \big\langle \lambda^n, w^{n+1} \big\rangle,
\end{aligned}$$

where Lemma 2.1.6 was used to determine

$$(w^{n+1} - w^n, w^{n+1})_s = \frac{1}{2}(\|w^{n+1}\|^2_{L^2(\Omega_s)} - \|w^n\|^2_{L^2(\Omega_s)} + \|w^{n+1} - w^n\|^2_{L^2(\Omega_s)}).$$

Note that the same methods for (3.2.2a) in the $k = 1$ case may be applied to (3.2.2c) by setting $v = \Delta t u^{n+1}$. This yields

$$\begin{aligned}
0 =& \frac{1}{2}(\|u^{n+1}\|^2_{L^2(\Omega_s)} - \|u^n\|^2_{L^2(\Omega_f)} + \|u^{n+1} - u^n\|^2_{L^2(\Omega_f)}) + \nu_f \Delta t \|\nabla u^{n+1}\|^2_{L^2(\Omega_f)} \\
&+ \Delta t \big\langle \lambda^{n+1}, u^{n+1} \big\rangle,
\end{aligned}$$

For the case $k = 2$, we set $z = q^{n+1/2}$ and have more cancellation. Indeed, if we recall that (3.2.3) implies $q^{n+1/2} = \partial_{\Delta t} w^{n+1}$ when $k = 2$, we find that (3.2.2a) yields

$$\begin{aligned}
0 =& \frac{1}{2}(q^{n+1} - q^n, q^{n+1} + q^n)_s + \frac{\nu_s}{2}(\nabla w^{n+1} + \nabla w^n, \nabla w^{n+1} - \nabla w^n)_s \\
&+ \alpha \Delta t \big\langle q^{n+1/2} - u^n, q^{n+1/2} \big\rangle + \Delta t \big\langle \lambda^n, q^{n+1/2} \big\rangle
\end{aligned}$$

$$
\begin{aligned}
=&\frac{1}{2}(\|q^{n+1}\|^2_{L^2(\Omega_s)} - \|q^n\|^2_{L^2(\Omega_s)}) - \frac{\nu_s}{2}\left(\|\nabla w^{n+1}\|^2_{L^2(\Omega_s)} - \|\nabla w^n\|^2_{L^2(\Omega_s)}\right)\\
&+ \alpha\Delta t\left\langle q^{n+1/2} - u^n, q^{n+1/2}\right\rangle + \Delta t\left\langle \lambda^n, q^{n+1/2}\right\rangle.
\end{aligned}
$$

We now write this in a unified setting and take the sum with the corresponding result for (3.2.2c). For $n \geq 0$, we find

$$
\begin{aligned}
&\frac{1}{2}\|q^{n+1}\|^2_{L^2(\Omega_s)} + \frac{1}{2}\|u^{n+1}\|^2_{L^2(\Omega_f)} + \frac{(2-k)}{2}\|q^{n+1} - q^n\|^2_{L^2(\Omega_s)} + \frac{1}{2}\|u^{n+1} - u^n\|^2_{L^2(\Omega_f)}\\
&+ \frac{(k-1)\nu_s}{2}\|\nabla w^{n+1}\|^2_{L^2(\Omega_s)} + (2-k)\nu_s\Delta t\|\nabla w^{n+1}\|^2_{L^2(\Omega_s)} + \nu_f\Delta t\|\nabla u^{n+1}\|^2_{L^2(\Omega_f)}\\
&= \frac{1}{2}\|q^n\|^2_{L^2(\Omega_s)} + \frac{1}{2}\|u^n\|^2_{L^2(\Omega_f)} + \frac{(k-1)\nu_s}{2}\|\nabla w^n\|^2_{L^2(\Omega_s)} + \Delta t J^{n+1},
\end{aligned}
\tag{3.3.1}
$$

where

$$
J^{n+1} := -\alpha\left\langle q^{n+1/k} - u^n, q^{n+1/k}\right\rangle - \left\langle \lambda^n, q^{n+1/k}\right\rangle + \left\langle \lambda^{n+1}, u^{n+1}\right\rangle.
$$

Using (3.2.5) we have

$$
\begin{aligned}
J^{n+1} =& -\alpha\left\langle q^{n+1/k} - u^{n+1} + u^{n+1} - u^n, q^{n+1/k}\right\rangle - \left\langle \lambda^n, q^{n+1/k}\right\rangle\\
&+ \left\langle \lambda^{n+1}, u^{n+1} - q^{n+1/k} + q^{n+1/k}\right\rangle\\
=& -\alpha\left\langle q^{n+1/k} - u^{n+1}, q^{n+1/k}\right\rangle + \alpha\left\langle u^n - u^{n+1}, q^{n+1/k}\right\rangle\\
&- \left\langle \lambda^n - \lambda^{n+1}, q^{n+1/k}\right\rangle + \left\langle \lambda^{n+1}, u^{n+1} - q^{n+1/k}\right\rangle\\
=&\left\langle \lambda^n - \lambda^{n+1}, q^{n+1/k}\right\rangle + \alpha\left\langle u^n - u^{n+1}, q^{n+1/k} - u^{n+1} + u^{n+1}\right\rangle\\
&- \left\langle \lambda^n - \lambda^{n+1}, q^{n+1/k}\right\rangle + \frac{1}{\alpha}\left\langle \lambda^{n+1}, \lambda^n - \lambda^{n+1}\right\rangle\\
=&\alpha\left\langle u^n - u^{n+1}, q^{n+1/k} - u^{n+1}\right\rangle + \alpha\left\langle u^n - u^{n+1}, u^{n+1}\right\rangle + \frac{1}{\alpha}\left\langle \lambda^{n+1}, \lambda^n - \lambda^{n+1}\right\rangle\\
=&\alpha\left\langle u^n - u^{n+1}, u^{n+1}\right\rangle + \frac{1}{\alpha}\left\langle \lambda^n - \lambda^{n+1}, \lambda^{n+1}\right\rangle - \left\langle u^n - u^{n+1}, \lambda^n - \lambda^{n+1}\right\rangle.
\end{aligned}
$$

If we use we (2.1.2) on the first two terms we obtain

$$\alpha\langle u^n - u^{n+1}, u^{n+1}\rangle = \frac{\alpha}{2}(\|u^n\|^2_{L^2(\Sigma)} - \|u^{n+1}\|^2_{L^2(\Sigma)} - \|u^{n+1} - u^n\|^2_{L^2(\Sigma)}),$$
$$\frac{1}{\alpha}\langle \lambda^n - \lambda^{n+1}, \lambda^{n+1}\rangle = \frac{1}{2\alpha}(\|\lambda^n\|^2_{L^2(\Sigma)} - \|\lambda^{n+1}\|^2_{L^2(\Sigma)} - \|\lambda^{n+1} - \lambda^n\|^2_{L^2(\Sigma)}).$$

Thus we have

$$\begin{aligned} J^{n+1} =& \frac{\alpha}{2}(\|u^n\|^2_{L^2(\Sigma)} - \|u^{n+1}\|^2_{L^2(\Sigma)}) + \frac{1}{2\alpha}(\|\lambda^n\|^2_{L^2(\Sigma)} - \|\lambda^{n+1}\|^2_{L^2(\Sigma)}) \\ & - \frac{\alpha}{2}\|u^n - u^{n+1}\|^2_{L^2(\Sigma)} - \frac{1}{2\alpha}\|\lambda^n - \lambda^{n+1}\|^2_{L^2(\Sigma)} - \langle u^n - u^{n+1}, \lambda^n - \lambda^{n+1}\rangle. \end{aligned}$$

We now note that using (3.2.5) we have $u^n - u^{n+1} + \frac{1}{\alpha}(\lambda^n - \lambda^{n+1}) = u^n - q^{n+1/k}$. Thus, applying this along with a simple identity to the last three terms above, we observe

$$\begin{aligned} & - \frac{\alpha}{2}\|u^n - u^{n+1}\|^2_{L^2(\Sigma)} - \frac{1}{2\alpha}\|\lambda^n - \lambda^{n+1}\|^2_{L^2(\Sigma)} - \langle u^n - u^{n+1}, \lambda^n - \lambda^{n+1}\rangle \\ =& - \frac{\alpha}{2}\|(u^n - u^{n+1}) + \frac{1}{\alpha}(\lambda^n - \lambda^{n+1})\|^2_{L^2(\Sigma)} \\ =& \frac{-\alpha}{2}\|u^n - q^{n+1/k}\|^2_{L^2(\Sigma)} \\ =& \frac{-\alpha}{2}\|u^n - u^{n+1} + (u^{n+1} - q^{n+1/k})\|^2_{L^2(\Sigma)} \\ =& \frac{-\alpha}{2}\|(u^n - u^{n+1}) + \frac{1}{\alpha}(\lambda^n - \lambda^{n+1})\|^2_{L^2(\Sigma)}. \end{aligned}$$

Consequently, we find

$$\begin{aligned} J^{n+1} =& \frac{\alpha}{2}(\|u^n\|^2_{L^2(\Sigma)} - \|u^{n+1}\|^2_{L^2(\Sigma)}) + \frac{1}{2\alpha}(\|\lambda^n\|^2_{L^2(\Sigma)} - \|\lambda^{n+1}\|^2_{L^2(\Sigma)}) \\ & - \frac{\alpha}{2}\|(u^n - u^{n+1}) + \frac{1}{\alpha}(\lambda^n - \lambda^{n+1})\|^2_{L^2(\Sigma)}. \end{aligned} \tag{3.3.2}$$

Plugging this result into (3.3.1), we arrive at

$$Z^{n+1} + S^{n+1} = Z^n.$$

Taking the sum over n yields the final result. □

3.4 Error Analysis

We now wish to prove the main, a priori error estimate by comparing the Robin-Robin splitting method in (3.2.2) with the fully coupled method in (3.1.12), which is satisfied by the exact solutions (note that this is a strong coupling because the exact coupling conditions are satisfied, rather than the Robin conditions).

The proof in this section will proceed in three parts. First, we will prove a preliminary estimate in which we use techniques from the proof of Lemma 3.3.1 to bound all but one term in the error analysis. We will then bound this remaining term before finally stating the main result and completing the proof.

We choose to split the error analysis up in this way because the term that remains unbounded in the preliminary estimates requires special treatment to derive the strictest bound involving a lifting-residual argument. We also wait until the end to bound all of the residual terms that arise from the time discretization and splitting method, as this allows us to present a much cleaner set of estimates at each stage.

At the end of this chapter, we include a discussion of the delicacy of the term that remains unbounded after the first stage of the proof. We show that if we were to bound it using the same techniques as the other terms in the error equations, we would derive a sub-optimal error estimate. We also discuss a special case in which we may relax some of the assumptions necessary in our error analysis.

3.4.1 The Error Equations

To begin the analysis, we denote the error variables

$$\begin{aligned} U^n &= \mathsf{u}^n - u^n, \quad Q^n = \mathsf{q}^n - q^n, \\ W^n &= \mathsf{w}^n - w^n, \quad \Lambda^n = \mathsf{l}^n - \lambda^n. \end{aligned}$$

We assume that we chose the initial conditions of the splitting method to be exactly the initial conditions of the coupled problem and so these quantities vanish when $n = 0$. Then using (3.2.2a)-(3.2.2d) and (3.1.12a)-(3.1.12d), we recover the error equations by taking the differences. However, in order to ensure that the time-steps match up as nicely as possible, we take the average of (3.1.12a)-(3.1.12d) at time steps n and $n+1$. More specifically, we use the following form of (3.1.12a)

$$(\partial_t \mathsf{q}^{n+1/k}, z)_s + \nu_s(\nabla \mathsf{w}^{n+1/k}, \nabla z)_s + \langle \mathsf{l}^{n+1/k}, z \rangle = 0, \quad \forall z \in V_s.$$

We thus have

$$(\partial_{\Delta t} Q^{n+1}, z)_s + \nu_s(\nabla W^{n+1/k}, \nabla z)_s + \alpha\langle (\partial_{\Delta t}^{k-1} W^{n+1} - U^n), z\rangle + \langle \Lambda^n, z\rangle = L_1(z) - L_4(z), \tag{3.4.1a}$$

$$(Q^{n+1/k} - \partial_{\Delta t}^{k-1} W^{n+1}, r)_s = L_2(r), \tag{3.4.1b}$$

$$(\partial_{\Delta t} U^{n+1}, v)_f + \nu_f (\nabla U^{n+1}, \nabla v)_f - \langle \Lambda^{n+1}, v \rangle = L_3(v), \tag{3.4.1c}$$

$$\alpha \langle U^{n+1} - \partial_{\Delta t}^{k-1} W^{n+1}, \mu \rangle + \langle \Lambda^{n+1} - \Lambda^n, \mu \rangle = L_4(\mu). \tag{3.4.1d}$$

where

$$\begin{aligned}
L_1(z) :=& \frac{(k-1)}{2} \langle g_2^{n+1}, z \rangle + \alpha \langle g_1^{n+1}, z \rangle - (h_1^{n+1}, z)_s, \\
L_2(r) :=& (h_3^{n+1}, r)_s, \\
L_3(v) :=& -(h_2^{n+1}, v)_f, \\
L_4(\mu) :=& \alpha \langle h_4^{n+1}, \mu \rangle + \langle g_2^{n+1}, \mu \rangle,
\end{aligned}$$

and

$$\begin{aligned}
h_1^{n+1} &:= \partial_t \mathsf{q}^{n+1/k} - \partial_{\Delta t} \mathsf{q}^{n+1}, \qquad & g_1^{n+1} &:= \mathsf{u}^{n+1} - \mathsf{u}^n, \\
h_2^{n+1} &:= \partial_t \mathsf{u}^{n+1} - \partial_{\Delta t} \mathsf{u}^{n+1}, \qquad & g_2^{n+1} &:= \mathsf{l}^{n+1} - \mathsf{l}^n, \\
h_3^{n+1} &:= \partial_t^{k-1} \mathsf{w}^{n+1/k} - \partial_{\Delta t}^{k-1} \mathsf{w}^{n+1}, \\
h_4^{n+1} &:= \partial_t^{k-1} \mathsf{w}^{n+1} - \partial_{\Delta t}^{k-1} \mathsf{w}^{n+1}.
\end{aligned}$$

Here the terms $\{h_i^{n+1}\}_{i=1}^4$ represent the error we acquire by discretizing in time. For example, the term h_1^{n+1} arises when we subtract the first term in (3.2.2a) from the first term in (3.1.12a), as we have

$$\begin{aligned}
(\partial_t \mathsf{q}^{n+1/k} - \partial_{\Delta t} q^{n+1}, z)_s =& (\partial_t \mathsf{q}^{n+1/k} - \partial_{\Delta t} \mathsf{q}^{n+1}, z)_s + (\partial_{\Delta t} \mathsf{q}^{n+1} - \partial_{\Delta t} q^{n+1}, z)_s \\
=& (h_1^{n+1}, z)_s + (\partial_{\Delta t} Q^{n+1}, z)_s
\end{aligned}$$

The terms $\{g_i^{n+1}\}_{i=1}^2$, on the other hand, represent the residual error that arises from the Robin-Robin splitting method, or the *splitting error*. We note that these residual terms only appear on the interface and are exactly the quantities that appear in the "key to stability" elements previously mentioned. It therefore seems reasonable to suggest that the residual terms g_1^{n+1} and g_2^{n+1} represent the error we acquire at each time-step when we replace the exact coupling conditions (3.1.11) with the Robin-Robin coupling conditions (3.2.1).

Note that each g_i^{n+1} and h_i^{n+1} here depends only on the solutions to (3.2.2). Assuming appropriate regularity, we will show in 3.4.4 that these are terms that we can control.

The error equations (3.4.1) also have consequences that are directly analogous to (3.2.3), (3.2.4), and (3.2.5) that we derived from (3.2.2).

First, as a direct consequence of (3.4.1b), we may write

$$Q^{n+1/k} = \partial_{\Delta t}^{k-1} W^{n+1} + h_3^{n+1}, \quad \text{on } \Omega_s. \tag{3.4.2}$$

It also follows from (3.4.1d) that

$$\alpha(U^{n+1} - \partial_{\Delta t}^{k-1} W^{n+1}) = \Lambda^n - \Lambda^{n+1} + \alpha h_4^{n+1} + g_2^{n+1}, \quad \text{on } \Sigma. \tag{3.4.3}$$

Then, (3.4.2) and (4.3.3) combine so that we may write

$$\begin{aligned} 0 =& \alpha(U^{n+1} - \partial_{\Delta t}^{k-1} W^{n+1}) - (\Lambda^n - \Lambda^{n+1}) - \alpha h_4^{n+1} - g_2^{n+1} \\ =& \alpha(U^{n+1} - Q^{k+1/k}) + \alpha h_3^{n+1} - (\Lambda^n - \Lambda^{n+1}) - \alpha h_4^{n+1} - g_2^{n+1}, \quad \text{on } \Sigma. \end{aligned}$$

It is then straightforward to show, using the fact that $\partial_t^{k-1}\mathsf{w}^n = \mathsf{u}^n$ on Σ, that $(h_3^{n+1} - h_4^{n+1})|_\Sigma = \frac{(k-1)}{2} g_1^{n+1}$. Therefore we have

$$\alpha\big(U^{n+1} - Q^{n+1/k}\big) = \Lambda^n - \Lambda^{n+1} + g_3^{n+1}, \quad \text{on } \Sigma, \tag{3.4.4}$$

where

$$g_3^{n+1} := \alpha\frac{(k-1)}{2} g_1^{n+1} + g_2^{n+1}.$$

Note that g_3^{n+1} is not a splitting error, but, rather, a linear combination of the splitting errors. In the case $k = 1$, $g_3^{n+1} = g_2^{n+1}$.

Finally, we define the quantities that will allow to perform the error analysis. As in Section 3.3, we use the parameter k to control which terms are only included for the parabolic-parabolic problem and which are only included for the parabolic-hyperbolic problem.

$$\begin{aligned}
\mathsf{Z}^{n+1} :=& \frac{1}{2}\|Q^{n+1}\|^2_{L^2(\Omega_s)} + \frac{1}{2}\|U^{n+1}\|^2_{L^2(\Omega_f)} + \frac{(k-1)\nu_s}{2}\|\nabla W^{n+1}\|^2_{L^2(\Omega_s)} \\
&+ \frac{\Delta t\alpha}{2}\|U^{n+1}\|^2_{L^2(\Sigma)} + \frac{\Delta t}{2\alpha}\|\Lambda^{n+1}\|^2_{L^2(\Sigma)}, \\
\mathsf{S}^{n+1} :=& \nu_f\Delta t\|\nabla U^{n+1}\|^2_{L^2(\Omega_f)} + (2-k)\nu_s\Delta t\|\nabla W^{n+1}\|^2_{L^2(\Omega_s)} \\
&+ \frac{(2-k)}{2}\|Q^{n+1} - Q^n\|^2_{L^2(\Omega_s)} + \frac{1}{2}\|U^{n+1} - U^n\|^2_{L^2(\Omega_f)} \\
&+ \frac{\Delta t\alpha}{2}\|U^n - Q^{n+1/k}\|^2_{L^2(\Sigma)} + \frac{\Delta t}{2\alpha}\|g_3^{n+1}\|^2_{L^2(\Sigma)}.
\end{aligned}$$

3.4.2 Step 1: Preliminary Estimates

We now proceed with the first step of the error analysis and prove a preliminary result. To this end, we start by proving the following lemma.

Lemma 3.4.1. *It holds,*

$$\mathsf{Z}^{n+1} + \mathsf{S}^{n+1} = \mathsf{Z}^n + \Delta t F^{n+1} + \frac{\Delta t}{\alpha}\big\langle g_3^{n+1}, \Lambda^{n+1}\big\rangle, \tag{3.4.5}$$

where

$$\begin{aligned} F^{n+1} :=& -(h_1^{n+1}, Q^{n+1/k})_s - (h_2^{n+1}, U^{n+1})_f - \nu_s(\nabla W^{n+1/k}, \nabla h_3^{n+1})_s \\ &+ \big\langle g_4^{n+1}, Q^{n+1/k}\big\rangle + \big\langle U^{n+1} - U^n, g_3^{n+1}\big\rangle - \big\langle g_3^{n+1}, Q^{n+1/k} - U^n\big\rangle, \end{aligned}$$

and

$$g_4^{n+1} := \alpha g_1^{n+1} + \frac{k-1}{2} g_2^{n+1}.$$

Proof. We begin as in the proof of Lemma 3.3.1 and set $z = \Delta t Q^{n+1/k}$ in (3.4.1a) and $v = \Delta t U^{n+1}$ in (3.4.1c).

We also apply (3.4.2) to replace all $\partial_{\Delta t}^{k-1} W^{n+1}$ with $Q^{n+1/k}$ to address the interior gradient term in (3.4.1a). However this requires special care, as this now generates error from the time discretization.

More specifically, the term $\alpha\big\langle h_3^{n+1}, Q^{n+1/k}\big\rangle$ now appears on the interface because we have

$$\begin{aligned} &\alpha\big\langle \partial_{\Delta t}^{k-1} W^{n+1} - U^n, Q^{n+1/k}\big\rangle \\ =&\alpha\big\langle Q^{n+1/k} - U^n, Q^{n+1/k}\big\rangle - \alpha\big\langle h_3^{n+1}, Q^{n+1/k}\big\rangle. \end{aligned}$$

Thus, (3.4.1a) yields

$$\Delta t(\partial_{\Delta t} Q^{n+1}, Q^{n+1/k})_s + \Delta t \nu_s(\nabla W^{n+1/k}, \nabla Q^{n+1/k})_s$$

$$+ \Delta t\alpha\big\langle (Q^{n+1/k} - U^n), Q^{n+1/k}\big\rangle + \Delta t\big\langle \Lambda^n, Q^{n+1/k}\big\rangle$$
$$= \Delta t\alpha\big\langle h_3^{n+1}, Q^{n+1/k}\big\rangle + \Delta t L_1(Q^{n+1/k}) - \Delta t L_4(Q^{n+1/k})$$

Additionally, the term $\nu_s(\nabla W^{n+1/k}, \nabla h_3^{n+1})_s$ now appears when we apply (3.4.2) such that

$$\nu_s(\nabla W^{n+1/k}, \Delta t Q^{n+1/2})_s = \nu_s(\nabla W^{n+1/k}, \nabla(W^{n+1} - W^n) + \nabla h_3^{n+1})_s.$$

Thus, we further have

$$\begin{aligned}
&\Delta t(\partial_{\Delta t}Q^{n+1}, Q^{n+1/k})_s + \Delta t\nu_s(\nabla W^{n+1/k}, \nabla(W^{n+1} - W^n) \\
&\quad + \Delta t\alpha\big\langle (Q^{n+1/k} - U^n), Q^{n+1/k}\big\rangle + \Delta t\big\langle \Lambda^n, Q^{n+1/k}\big\rangle \\
&\quad\quad = -\Delta t\nu_s(\nabla W^{n+1/k}, \nabla h_3^{n+1})_s + \Delta t\alpha\big\langle h_3^{n+1}, Q^{n+1/k}\big\rangle \\
&\quad\quad\quad + \Delta t L_1(Q^{n+1/k}) - \Delta t L_4(Q^{n+1/k})
\end{aligned}$$

Consequently, we find

$$\begin{aligned}
&\frac{1}{2}\|Q^{n+1}\|^2_{L^2(\Omega_s)} + \frac{1}{2}\|U^{n+1}\|^2_{L^2(\Omega_f)} + \frac{(2-k)}{2}\|Q^{n+1} - Q^n\|^2_{L^2(\Omega_s)} + \frac{1}{2}\|U^{n+1} - U^n\|^2_{L^2(\Omega_f)} \\
&+ \frac{(k-1)\nu_s}{2}\|\nabla W^{n+1}\|_{L^2(\Omega_s)} + (2-k)\nu_s\Delta t\|\nabla W^{n+1}\|^2_{L^2(\Omega_s)} + \nu_f\Delta t\|\nabla U^{n+1}\|^2_{L^2(\Omega_f)} \\
&= \frac{1}{2}\|Q^n\|^2_{L^2(\Omega_s)} + \frac{1}{2}\|U^n\|^2_{L^2(\Omega_f)} + \frac{(k-1)\nu_s}{2}\|\nabla W^n\|^2_{L^2(\Omega_s)} + \Delta t \mathsf{J}^{n+1}.
\end{aligned} \tag{3.4.6}$$

where

$$\begin{aligned}
\mathsf{J}^{n+1} :=& -\alpha\big\langle Q^{n+1/k} - U^n, Q^{n+1/k}\big\rangle - \big\langle \Lambda^n, Q^{n+1/k}\big\rangle + \big\langle \Lambda^{n+1}, U^{n+1}\big\rangle \\
&+ \alpha\big\langle h_3^{n+1}, Q^{n+1/k}\big\rangle - \nu_s(\nabla W^{n+1/k}, \nabla h_3^{n+1})_s \\
&+ L_1(Q^{n+1/k}) - L_4(Q^{n+1/k}) + L_3(U^{n+1}).
\end{aligned}$$

Manipulating the first three terms above and using (4.3.4), we mirror the stability argument (while collecting residual terms) to obtain

$$
\begin{aligned}
&-\alpha\big\langle Q^{n+1/k}-U^{n},Q^{n+1/k}\big\rangle-\big\langle \Lambda^{n},Q^{n+1/k}\big\rangle+\big\langle \Lambda^{n+1},U^{n+1}\big\rangle\\
=&-\alpha\big\langle Q^{n+1/k}-U^{n+1},Q^{n+1/k}\big\rangle-\alpha\big\langle U^{n+1}-U^{n},Q^{n+1/k}\big\rangle-\big\langle \Lambda^{n},Q^{n+1/k}\big\rangle\\
&+\big\langle \Lambda^{n+1},U^{n+1}-Q^{n+1/k}+Q^{n+1/k}\big\rangle\\
=&\big\langle \Lambda^{n}-\Lambda^{n+1},Q^{n+1/k}\big\rangle+\big\langle g_3^{n+1},Q^{n+1/k}\big\rangle+\alpha\big\langle U^{n}-U^{n+1},Q^{n+1/k}\big\rangle\\
&-\big\langle \Lambda^{n}-\Lambda^{n+1},Q^{n+1/k}\big\rangle+\big\langle \Lambda^{n+1},U^{n+1}-Q^{n+1/k}\big\rangle\\
=&\alpha\big\langle U^{n}-U^{n+1},Q^{n+1/k}-U^{n+1}+U^{n+1}\big\rangle\\
&+\big\langle \Lambda^{n+1},U^{n+1}-Q^{n+1/k}\big\rangle+\big\langle g_3^{n+1},Q^{n+1/k}\big\rangle\\
=&-\big\langle U^{n}-U^{n+1},\Lambda^{n}-\Lambda^{n+1}\big\rangle+\alpha\big\langle U^{n}-U^{n+1},U^{n+1}\big\rangle\\
&+\frac{1}{\alpha}\big\langle \Lambda^{n+1},\Lambda^{n}-\Lambda^{n+1}\big\rangle+\frac{1}{\alpha}\big\langle g_3^{n+1},\Lambda^{n+1}\big\rangle\\
&-\big\langle U^{n}-U^{n+1},g_3^{n+1}\big\rangle+\big\langle g_3^{n+1},Q^{n+1/k}\big\rangle.
\end{aligned}
$$

Thus,

$$
\begin{aligned}
&-\alpha\big\langle Q^{n+1/k}-U^{n},Q^{n+1/k}\big\rangle-\big\langle \Lambda^{n},Q^{n+1/k}\big\rangle+\big\langle \Lambda^{n+1},U^{n+1}\big\rangle\\
=&\mathbb{J}^{n+1}+\frac{1}{\alpha}\big\langle g_3^{n+1},\Lambda^{n+1}\big\rangle+\big\langle g_3^{n+1},Q^{n+1/k}\big\rangle-\big\langle U^{n}-U^{n+1},g_3^{n+1}\big\rangle,
\end{aligned}
$$

where

$$
\mathbb{J}^{n+1}:=\alpha\big\langle U^{n}-U^{n+1},U^{n+1}\big\rangle+\frac{1}{\alpha}\big\langle \Lambda^{n}-\Lambda^{n+1},\Lambda^{n+1}\big\rangle-\big\langle U^{n}-U^{n+1},\Lambda^{n}-\Lambda^{n+1}\big\rangle.
$$

Finally, as we did in the stability analysis (see (3.3.2)) we get

$$
\begin{aligned}
\mathbb{J}^{n+1}=&\frac{\alpha}{2}(\|U^{n}\|^2_{L^2(\Sigma)}-\|U^{n+1}\|^2_{L^2(\Sigma)})+\frac{1}{2\alpha}(\|\Lambda^{n}\|^2_{L^2(\Sigma)}-\|\Lambda^{n+1}\|^2_{L^2(\Sigma)})\\
&-\frac{\alpha}{2}\|(U^{n}-U^{n+1})+\frac{1}{\alpha}(\Lambda^{n}-\Lambda^{n+1})\|^2_{L^2(\Sigma)}.
\end{aligned}
$$

Using (4.3.4) we can re-write the last term

$$
\begin{aligned}
&\|(U^n - U^{n+1}) + \frac{1}{\alpha}(\Lambda^n - \Lambda^{n+1})\|^2_{L^2(\Sigma)} \\
=&\|U^n - Q^{n+1/k} - \frac{1}{\alpha} g_3^{n+1}\|^2_{L^2(\Sigma)} \\
=&\|U^n - Q^{n+1/k}\|^2_{L^2(\Sigma)} + \frac{1}{\alpha^2}\|g_3^{n+1}\|^2_{L^2(\Sigma)} + \frac{2}{\alpha}\big\langle Q^{n+1/k} - U^n, g_3^{n+1}\big\rangle.
\end{aligned}
$$

Plugging this back into J^{n+1} we arrive at

$$
\begin{aligned}
\mathsf{J}^{n+1} =& \frac{\alpha}{2}\big(\|U^n\|^2_{L^2(\Sigma)} - \|U^{n+1}\|^2_{L^2(\Sigma)}\big) + \frac{1}{2\alpha}\big(\|\Lambda^n\|^2_{L^2(\Sigma)} - \|\Lambda^{n+1}\|^2_{L^2(\Sigma)}\big) \\
&- \frac{\alpha}{2}\|U^n - Q^{n+1/k}\|^2_{L^2(\Sigma)} - \frac{1}{2\alpha}\|g_3^{n+1}\|^2_{L^2(\Sigma)} \\
&- \big\langle g_3^{n+1}, Q^{n+1/k} - U^n\big\rangle - \nu_s(\nabla W^{n+1/k}, \nabla h_3^{n+1})_s \\
&+ L_1(Q^{n+1/k}) - L_4(Q^{n+1/k}) + L_3(U^{n+1}) \\
&+ \alpha\big\langle h_3^{n+1}, Q^{n+1/k}\big\rangle + \frac{1}{\alpha}\big\langle g_3^{n+1}, \Lambda^{n+1}\big\rangle + \big\langle g_3^{n+1}, Q^{n+1/k}\big\rangle \\
&- \big\langle g_3^{n+1}, U^n - U^{n+1}\big\rangle.
\end{aligned}
$$

We now note, using (3.4.2), (4.3.3), and (4.3.4), that

$$
\begin{aligned}
-L_4(Q^{n+1/k}) + \alpha\big\langle h_3^{n+1}, Q^{n+1/k}\big\rangle &= -\big\langle \alpha h_4^{n+1} + g_2^{n+1} - \alpha h_3^{n+1}, Q^{n+1/k}\big\rangle \\
&= -\big\langle \alpha(U^{n+1} - Q^{n+1/k}) - (\Lambda^n - \Lambda^{n+1}), Q^{n+1/k}\big\rangle \\
&= -\big\langle g_3^{n+1}, Q^{n+1/k}\big\rangle.
\end{aligned}
$$

Thus we have

$$
\begin{aligned}
\mathsf{J}^{n+1} =& \frac{\alpha}{2}\big(\|U^n\|^2_{L^2(\Sigma)} - \|U^{n+1}\|^2_{L^2(\Sigma)}\big) + \frac{1}{2\alpha}\big(\|\Lambda^n\|^2_{L^2(\Sigma)} - \|\Lambda^{n+1}\|^2_{L^2(\Sigma)}\big) \\
&- \frac{\alpha}{2}\|U^n - Q^{n+1/k}\|^2_{L^2(\Sigma)} - \frac{1}{2\alpha}\|g_3^{n+1}\|^2_{L^2(\Sigma)} + F^{n+1} + \frac{1}{\alpha}\big\langle g_3^{n+1}, \Lambda^{n+1}\big\rangle.
\end{aligned}
$$

If we plug in these results to (3.4.6) we arrive at the identity. Note that the term

$\frac{1}{2\alpha}\|g_3^{n+1}\|^2_{L^2(\Sigma)}$ is incorporated in S^{n+1}. $\square$

3.4.2.1 Estimate for F^{n+1}

At this stage, we have successfully isolated the term that, as stated, requires special care in our error analysis, $\frac{\Delta t}{\alpha}\langle g_3^{n+1}, \Lambda^{n+1}\rangle$. However, before we address this term, we would like to bound the terms in F^{n+1}. Fortunately, we will see that these terms may be bounded using reasonably direct techniques.

In order to derive a final, a priori error estimate for the Robin-Robin method, we will need to compare the error norms at time-step N to those at time-step 0 (which should be equal to 0 by the selection of our initial conditions). Consequently, we now bound the quantity $\Delta t \sum_{n=0}^{M-1} F^{n+1}$, for an integer $0 < M \leq N+1$. Note that we will need the Poincare-Friedrichs type inequality from Proposition 2.1.10 and the trace inequality from Proposition 2.1.11 in Chapter 2.

Lemma 3.4.2. *Let $1 \leq M \leq N$, then*

$$\Delta t \sum_{n=0}^{M-1} F^{n+1} \leq \frac{1}{4} \max_{1\leq n\leq M} \mathsf{Z}^n + \frac{1}{4}\sum_{n=0}^{M-1} \mathsf{S}^{n+1} + CD(M), \tag{3.4.7}$$

where

$$\begin{aligned} D(M) :=& \Delta t T \sum_{n=0}^{M-1} \left(\|h_1^{n+1}\|^2_{L^2(\Omega_s)} + \|h_2^{n+1}\|^2_{L^2(\Omega_f)} + (k-1)\nu_s \|\nabla h_3^{n+1}\|^2_{L^2(\Omega_s)} \right) \\ &+ \Delta t \sum_{n=0}^{M-1} \left(\frac{1}{\alpha} + \frac{C_{tr}^2}{\nu_f} \right) \left(\|g_4^{n+1}\|^2_{L^2(\Sigma)} + \|g_3^{n+1}\|^2_{L^2(\Sigma)} \right). \end{aligned}$$

Proof. To begin, we consider the first three terms of F^{n+1}, taking the sum from $n = 0$ to $N = M-1$. For each term, we apply the Cauchy-Schwarz inequality, followed by Young's inequality as explained in Corollary (2.1.9). For example, for the term $-\Delta t(h_1^{n+1}, Q^{n+1/k})_s$ we have

$$\begin{aligned}\Delta t(h_1^{n+1}, Q^{n+1/k})_s \leq & \Delta t\|h_1^{n+1}\|_{L^2(\Omega_s)}\|Q^{n+1/k}\|_{L^2(\Omega_s)} \\ \leq & \Delta t\left(2T\|h_1^{n+1}\|^2_{L^2(\Omega_s)} + \frac{1}{8T}\|Q^{n+1/k}\|^2_{L^2(\Omega_s)}\right).\end{aligned}$$

We also use the fact that $h_3^{n+1} = 0$ when $k = 1$, so the term $\nu_s(\nabla W^{n+1/k}, \nabla h_3^{n+1})_s$ is only present when $k = 2$. We indicate this by the factor $(k-1)$.

With this approach, we see that

$$\begin{aligned}& -\Delta t\sum_{n=0}^{M-1}\left((h_1^{n+1}, Q^{n+1/k})_s + (h_2^{n+1}, U^{n+1})_f + \nu_s(\nabla W^{n+1/k}, \nabla h_3^{n+1})_s\right) \\ \leq & \frac{\Delta t}{8T}\sum_{n=0}^{M-1}\left(\|Q^{n+1/k}\|^2_{L^2(\Omega_s)} + \|U^{n+1}\|^2_{L^2(\Omega_f)} + (k-1)\nu_s\|\nabla W^{n+1/k}\|^2_{L^2(\Omega_s)}\right) \\ & + C\Delta tT\sum_{n=0}^{M-1}\left(\|h_1^{n+1}\|^2_{L^2(\Omega_s)} + \|h_2^{n+1}\|^2_{L^2(\Omega_f)} + (k-1)\nu_s\|\nabla h_3^{n+1}\|^2_{L^2(\Omega_s)}\right).\end{aligned}$$

Referring to the definition of Z^{n+1}, we see that

$$\begin{aligned}& \frac{\Delta t}{8T}\sum_{n=0}^{M-1}\left(\|Q^{n+1/k}\|^2_{L^2(\Omega_s)} + \|U^{n+1}\|^2_{L^2(\Omega_f)} + (k-1)\nu_s\|\nabla W^{n+1/k}\|^2_{L^2(\Omega_s)}\right) \\ \leq & \frac{\Delta t}{4T}\sum_{n=0}^{M-1}\mathsf{Z}^{n+1} \\ \leq & \frac{\Delta t}{4T}\sum_{n=0}^{M-1}\max_{1\leq n\leq M}\mathsf{Z}^{n} \\ \leq & \frac{N\Delta t}{4T}\max_{1\leq n\leq M}\mathsf{Z}^{n}.\end{aligned}$$

Using $N\Delta t = T$, we therefore have

$$-\Delta t\sum_{n=0}^{M-1}\left((h_1^{n+1}, Q^{n+1/k})_s + (h_2^{n+1}, U^{n+1})_f + \nu_s(\nabla W^{n+1/k}, \nabla h_3^{n+1})_s\right)$$

$$\leq \frac{1}{4}\max_{1\leq n\leq M}\mathsf{Z}^n + C\Delta t T\sum_{n=0}^{M-1}\Big(\|h_1^{n+1}\|^2_{L^2(\Omega_s)} + \|h_2^{n+1}\|^2_{L^2(\Omega_f)} + (k-1)\nu_s\|\nabla h_3^{n+1}\|^2_{L^2(\Omega_s)}\Big).$$

For the remaining three terms, we have

$$\begin{aligned}
&\Delta t\sum_{n=0}^{M-1}\Big(\big\langle g_4^{n+1}, Q^{n+1/k}\big\rangle + \big\langle g_3^{n+1}, U^{n+1}-U^n\big\rangle - \big\langle g_3^{n+1}, Q^{n+1/k}-U^n\big\rangle\Big)\\
=&\Delta t\sum_{n=0}^{M-1}\Big(\big\langle g_4^{n+1}, Q^{n+1/k}-U^n\big\rangle + \big\langle g_4^{n+1}, U^n\big\rangle\\
&\qquad + \big\langle g_3^{n+1}, U^{n+1}-U^n\big\rangle - \big\langle g_3^{n+1}, Q^{n+1/k}-U^n\big\rangle\Big)\\
\leq&\Delta t\sum_{n=0}^{M-1}\bigg(\|g_4^{n+1}\|_{L^2(\Sigma)}\Big(\|Q^{n+1/k}-U^n\|_{L^2(\Sigma)} + \|U^{n+1}\|_{L^2(\Sigma)}\Big)\\
&\qquad + \|g_3^{n+1}\|_{L^2(\Sigma)}\Big(\|U^{n+1}-U^n\|_{L^2(\Sigma)} + \|Q^{n+1/k}-U^n\|_{L^2(\Sigma)}\Big).
\end{aligned}$$

Now using (2.1.5) and Young's inequality, we have

$$\begin{aligned}
&\Delta t\sum_{n=0}^{M-1}\bigg(\|g_4^{n+1}\|_{L^2(\Sigma)}\Big(\|Q^{n+1/k}-U^n\|_{L^2(\Sigma)} + \|U^{n+1}\|_{L^2(\Sigma)}\Big)\\
&\qquad + \|g_3^{n+1}\|_{L^2(\Sigma)}\Big(\|U^{n+1}-U^n\|_{L^2(\Sigma)} + \|Q^{n+1/k}-U^n\|_{L^2(\Sigma)}\Big)\\
\leq&\Delta t\sum_{n=0}^{M-1}\bigg(\|g_4^{n+1}\|_{L^2(\Sigma)}\Big(\|Q^{n+1/k}-U^n\|_{L^2(\Sigma)} + C_{\mathrm{tr}}\|\nabla U^{n+1}\|_{L^2(\Omega_f)}\Big)\\
&\qquad + \|g_3^{n+1}\|_{L^2(\Sigma)}\Big(C_{tr}\|\nabla U^{n+1}\|_{L^2(\Omega_f)} + C_{tr}\|\nabla U^n\|_{L^2(\Omega_f)}\\
&\qquad\qquad + \|Q^{n+1/k}-U^n\|_{L^2(\Sigma)}\Big)\\
\leq& C\Delta t\sum_{n=0}^{M-1}\left(\frac{1}{\alpha}+\frac{C_{\mathrm{tr}}^2}{\nu_f}\right)\bigg(\|g_4^{n+1}\|^2_{L^2(\Sigma)} + \|g_3^{n+1}\|^2_{L^2(\Sigma)}\bigg)\\
&\qquad + \Delta t\sum_{n=0}^{M-1}\Big(\frac{\alpha}{8}\|Q^{n+1/k}-U^n\|^2_{L^2(\Sigma)} + \frac{\nu_f}{8}\|\nabla U^{n+1}\|^2_{L^2(\Omega_f)}\Big).
\end{aligned}$$

Thus, recalling the definition of S and repeating the reasoning above, we have

$$\begin{aligned}&\Delta t \sum_{n=0}^{M-1} \Big(\big\langle g_4^{n+1}, Q^{n+1/k} \big\rangle + \big\langle g_3^{n+1}, U^{n+1} - U^n \big\rangle - \big\langle g_3^{n+1}, Q^{n+1/k} - U^n \big\rangle \Big) \\ \leq & \frac{1}{4} \sum_{n=0}^{M-1} \mathsf{S}^{n+1} + C\Delta t \sum_{n=0}^{M-1} \left(\frac{1}{\alpha} + \frac{C_{\mathrm{tr}}^2}{\nu_f} \right) \left(\|g_4^{n+1}\|_{L^2(\Sigma)}^2 + \|g_3^{n+1}\|_{L^2(\Sigma)}^2 \right).\end{aligned}$$

Combining this with the bound for the first three terms of F^{n+1} proves the result. □

3.4.3 Step 2: Estimate for $\frac{\Delta t}{\alpha}\big\langle g_3^{n+1}, \Lambda^{n+1} \big\rangle$ using a lifting-residual argument

We now show how to estimate the term

$$\sum_{n=0}^{M-1} \frac{\Delta t}{\alpha} \big\langle g_3^{n+1}, \Lambda^{n+1} \big\rangle.$$

We need to either bound this term by residual terms that we can control (g_i^{n+1} or h_i^{n+1}) or balance it using the left-hand side of (3.4.5). However, we will see in 3.5.3 that if we want to balance Λ^{n+1} in this way, we must sacrifice a factor of $(\Delta t)^{1/2}$ from the convergence of the residual term g_2^{n+1}. This is due to the extra factor of Δt that appears on all interface norms in the quantity Z^{n+1}. Therefore, the difficulty with this term is that it resides on the interface Σ, so, in order to avoid this loss of accuracy, we must find some way to avoid the interface Σ as much as possible.

Our solution to this obstacle is to utilize (3.4.1c) to pull the term Λ^{n+1} from the interface Σ into the interior domain Ω_f. However, this requires the second argument in the inner product–in this case g_3^{n+1}– to be in V_f when extended into

Ω_f. Critically, this means that the extension needs to vanish on $\partial\Omega_f \backslash \Sigma$. As it is defined now, $g_3^{n+1} = \alpha\frac{(k-1)}{2} g_1^{n+1} + g_2^{n+1}$ depends, in part, on $\mathsf{l} = \nabla \mathsf{u} \cdot \boldsymbol{n}_f$ which is only defined on Σ and will not, in general, satisfy this criterion. Therefore, we will utilize a cut-off function technique to continuously lift the residual g_3^{n+1} from V_g into V_f.

To do this, we will make two assumptions. The first is that the normal $\boldsymbol{n}$ can be extended from Σ to Ω_f in such a way that the extension has a bounded gradient.

Assumption 3.4.3. There exists $\tilde{\boldsymbol{n}} \in [W^{1,\infty}(\Omega_f)]^2$ such that $\tilde{\boldsymbol{n}}|_\Sigma = \boldsymbol{n}$.

We know that this extension can be done if the interface Σ is smooth. Furthermore, if Σ is a straight line, this extension is trivial because $\boldsymbol{n}$ will be constant. In the case that Σ is more complex, however, the existence of such a $\tilde{\boldsymbol{n}}$ may not be as trivial.[1]

The second assumption regards the existence of a cut-off function, dependent on Δt, that is equal to 1 on *most* of Σ such that the gradient can be controlled appropriately in the L^2 norm. In 3.5.2, we show how to construct such a function in a simple case.

Assumption 3.4.4. Assume that the time step is given and satisfies $\Delta t < \frac{1}{2}$. There exists a function $\phi : \Omega_f \to \mathbb{R}$ satisfying:

(i) $0 \leq \phi \leq 1$,

(ii) $\phi \in V_f$,

(iii) $|\{x \in \Sigma : \phi(x) \neq 1\}| = C\Delta t$,

(iv) $\|\nabla\phi\|^2_{L^2(\Omega_f)} \leq C(1 + \log\frac{1}{\Delta t})$,

[1] This result may be known, but we would need to check the literature. Thus it is presently beyond the scope of this thesis, so we state the existence of $\tilde{\boldsymbol{n}}$ as an assumption.

where each C represents a general constant independent of Δt and the physical parameters.

Remark 5. It is interesting to note that Condition (iv) above allows the gradient to grow with Δt. As we will see in 3.5.2, this value governs how quickly ϕ decays in the neighborhood around the boundary, which means we are allowing this decay rate to grow as $\Delta t \to 0$. However, as we will see in the following analysis, Condition (iv) also restricts how fast this decay rate grows so that a polynomial decay from factors of Δt will still dominate. In other words, we need ϕ to remain equal to 1 for as long as possible on Σ, yet still go to 0 on the boundary. This will necessitate a very fast decay rate and a large $\nabla\phi$ that grows with Δt. Thus, Condition (iv) permits this behavior while ensuring that $\nabla\phi$ does not grow uncontrollably fast.

Given the above two assumption we will define the following quantities:

$$\begin{aligned}
\tilde{\mathsf{l}}(x,t) :=& \nabla \mathsf{u}(x,t)\cdot \tilde{\boldsymbol{n}}, \quad && \text{on } \Omega_f,\\
\mathcal{L}(x,t) :=& \phi(x)\tilde{\mathsf{l}}(x,t), && \text{on } \Omega_f,\\
\tilde{g}_2^{n+1} :=& \mathcal{L}^{n+1} - \mathcal{L}^n, && \text{on } \Omega_f.
\end{aligned}$$

These three quantities demonstrate, step-by-step, how we utilize $\tilde{\boldsymbol{n}}$ and ϕ to appropriately lift g_2^{n+1} from V_g into V_f. Indeed, we see that $\tilde{\mathsf{l}}$ is an extension of l from Σ into Ω_f via the extended normal vector from Assumption 3.4.3. Clearly, $\tilde{\mathsf{l}}|_\Sigma = \mathsf{l}$.

Once l has been lifted into Ω_f, the function ϕ is applied to enforce the conditions needed so that the resulting function $\mathcal{L}$ is in V_f. Unfortunately, this means that it is no longer the case that $\mathcal{L}|_\Sigma = \mathsf{l}$. However, by condition (iii) of Assumption 3.4.4, we see that we may control the size of the region for which the two functions differ on Σ. More specifically, it holds that

$$|\{x \in \Sigma : \mathcal{L}(x,t)|_{\Sigma} \neq \mathsf{l}(x,t)\}| = C\Delta t.$$

Consequently, we may then use the function $\mathcal{L}$ to construct a lifted version of g_2^{n+1}, namely $\tilde{g}_2^{n+1}$.

Note that $\tilde{g}_2^{n+1} \in V_f$ for all n and thus we can prove the following result.

Lemma 3.4.5. *Under Assumptions 3.4.3 and 3.4.4 we have*

$$\|\tilde{g}_2^{n+1} - g_2^{n+1}\|^2_{L^2(\Sigma)} \leq C\Delta t \|g_2^{n+1}\|^2_{L^\infty(\Sigma)}. \tag{3.4.8}$$

Proof. If we use Assumptions 3.4.3 and the definition of $\tilde{g}_2^{n+1}$ we see that, on Σ, we can write $\tilde{g}_2^{n+1} = \phi g_2^{n+1}$. Thus, we obtain

$$\begin{aligned}
\|\tilde{g}_2^{n+1} - g_2^{n+1}\|^2_{L^2(\Sigma)} =& \|(1-\phi) g_2^{n+1}\|^2_{L^2(\Sigma)} \\
\leq& \|g_2^{n+1}\|^2_{L^\infty(\Sigma)} \|1-\phi\|^2_{L^2(\Sigma)} \\
\leq& C\Delta t \|g_2^{n+1}\|^2_{L^\infty(\Sigma)},
\end{aligned}$$

where in the last inequality we used conditions (i) and (iii) of Assumption 3.4.4. □

We will also need the definition of the second-order difference operator:

$$\partial^2_{\Delta t} v^n = \frac{v^{n+1} - 2v^n + v^{n-1}}{(\Delta t)^2},$$

which is a discrete approximation of the second order time derivative.

We may now state the error bound for $\frac{\Delta t}{\alpha}\left\langle g_3^{n+1}, \Lambda^{n+1}\right\rangle$.

Lemma 3.4.6. *Under Assumptions 3.4.3, 3.4.4 we have*

$$\frac{\Delta t}{\alpha}\sum_{n=0}^{M-1}\left\langle g_3^{n+1}, \Lambda^{n+1}\right\rangle \leq \frac{1}{4}\sum_{n=0}^{M-1}\mathsf{S}^{n+1} + \frac{1}{4}\max_{1\leq n\leq M}\mathsf{Z}^n + C\Psi(M).$$

where

$$\begin{aligned}
\Psi(M) :=& \Psi_1(M) + \Psi_2(M),\\
\Psi_1(M) :=& \Delta t\sum_{n=0}^{M-1}\left((1+\nu_f)\|g_1^{n+1}\|^2_{H^1(\Omega_f)} + \|h_2^{n+1}\|^2_{L^2(\Omega_f)}\right)\\
&+ T(\Delta t)^3\sum_{n=1}^{M-1}\|\partial^2_{\Delta t}\mathsf{u}^n\|^2_{L^2(\Omega_f)} + \|g_1^M\|^2_{L^2(\Omega_f)},\\
\Psi_2(M) :=& \Delta t\sum_{n=0}^{M-1}\left(\left(\frac{1+\nu_f}{\alpha^2}\right)\|\tilde{g}_2^{n+1}\|^2_{H^1(\Omega_f)} + \|h_2^{n+1}\|^2_{L^2(\Omega_f)}\right),\\
&+ \frac{T(\Delta t)^3}{\alpha^2}\sum_{n=1}^{M-1}\|\partial^2_{\Delta t}\mathcal{L}^n\|^2_{L^2(\Omega_f)} + \frac{1}{\alpha^2}\|\tilde{g}_2^M\|^2_{L^2(\Omega_f)} + \frac{T\Delta t}{\alpha}\sum_{n=0}^{M-1}\|g_2^{n+1}\|^2_{L^\infty(\Sigma)}.
\end{aligned}$$

Proof. Using the definition of g_3^{n+1} we write

$$\frac{\Delta t}{\alpha}\sum_{n=0}^{M-1}\left\langle g_3^{n+1}, \Lambda^{n+1}\right\rangle = \frac{\Delta t}{\alpha}\sum_{n=0}^{M-1}\left\langle g_2^{n+1}, \Lambda^{n+1}\right\rangle + \frac{\Delta t(k-1)}{2}\sum_{n=0}^{M-1}\left\langle g_1^{n+1}, \Lambda^{n+1}\right\rangle. \tag{3.4.9}$$

Unlike g_2^{n+1}, the residual g_1^{n+1} has a very natural extension into Ω_f from Σ, as there is no $\boldsymbol{n}$. Thus, we can see that the first term in (3.4.9) above will be more difficult to handle, so we address it first. To this end, we have

$$\frac{\Delta t}{\alpha}\sum_{n=0}^{M-1}\left\langle g_2^{n+1}, \Lambda^{n+1}\right\rangle = \frac{\Delta t}{\alpha}\sum_{n=0}^{M-1}\left\langle g_2^{n+1} - \tilde{g}_2^{n+1}, \Lambda^{n+1}\right\rangle + \frac{\Delta t}{\alpha}\sum_{n=0}^{M-1}\left\langle \tilde{g}_2^{n+1}, \Lambda^{n+1}\right\rangle.$$

We then see that if we use Lemma 3.4.5 and our old friends Cauchy-Schwarz and

Young's inequalities, we determine

$$\begin{aligned}\frac{\Delta t}{\alpha}\sum_{n=0}^{M-1}\big\langle g_2^{n+1}-\tilde{g}_2^{n+1},\Lambda^{n+1}\big\rangle \leq & \frac{CT}{\alpha}\sum_{n=0}^{M-1}\|g_2^{n+1}-\tilde{g}_2^{n+1}\|^2_{L^2(\Sigma)}+\frac{(\Delta t)^2}{32T\alpha}\sum_{n=0}^{M-1}\|\Lambda^{n+1}\|^2_{L^2(\Sigma)}\\ \leq & \frac{CT\Delta t}{\alpha}\sum_{n=0}^{M-1}\|g_2^{n+1}\|^2_{L^\infty(\Sigma)}+\frac{(\Delta t)^2}{32T\alpha}\sum_{n=0}^{M-1}\|\Lambda^{n+1}\|^2_{L^2(\Sigma)}.\end{aligned}$$

Note here that the residual term $g_2^{n+1}-\tilde{g}_2^{n+1}$ initially gives up a factor of Δt to the error term Λ^{n+1} when we apply Young's inequality. However, because we are comparing the residual to the lifted residual on Σ, we are able to recover this lost Δt, avoiding a potential loss of accuracy.

To estimate $\frac{\Delta t}{\alpha}\sum_{n=0}^{M-1}\big\langle \tilde{g}_2^{n+1},\Lambda^{n+1}\big\rangle$, we cannot recover the lost Δt in this way, so, instead, we use (3.4.1c) to write everything in terms of inner products on Ω_f. More precisely, we have

$$\Delta t\big\langle \tilde{g}_2^{n+1},\Lambda^{n+1}\big\rangle=(U^{n+1}-U^n,\tilde{g}_2^{n+1})_f+\Delta t\nu_f(\nabla U^{n+1},\nabla\tilde{g}_2^{n+1})_f+\Delta t(h_2^{n+1},\tilde{g}_2^{n+1})_f.$$

From here, we use Cauchy-Schwarz and Young's inequalities on the last two inner products, yielding

$$\begin{aligned}\frac{\Delta t}{\alpha}\sum_{n=0}^{M-1}\big\langle \tilde{g}_2^{n+1},\Lambda^{n+1}\big\rangle \leq & \frac{1}{\alpha}\sum_{n=0}^{M-1}(U^{n+1}-U^n,\tilde{g}_2^{n+1})_f+\frac{\Delta t\nu_f}{8}\sum_{n=0}^{M-1}\|\nabla U^{n+1}\|^2_{L^2(\Omega_f)}\\ & +C\Delta t\sum_{n=0}^{M-1}\left(\left(\frac{1+\nu_f}{\alpha^2}\right)\|\tilde{g}_2^{n+1}\|^2_{H^1(\Omega_f)}+\|h_2^{n+1}\|^2_{L^2(\Omega_f)}\right).\end{aligned}$$

It now remains for us to bound $\frac{1}{\alpha}\sum_{n=0}^{M-1}(U^{n+1}-U^n,\tilde{g}_2^{n+1})_f$. To do so, we apply a summation by parts formula so that we may write

$$\frac{1}{\alpha}\sum_{n=0}^{M-1}(U^{n+1}-U^n,\tilde{g}_2^{n+1})_f$$

$$=\frac{1}{\alpha}\sum_{n=1}^{M-1}(U^n, \tilde{g}_2^n - \tilde{g}_2^{n+1})_f + \frac{1}{\alpha}(U^M, \tilde{g}_2^M)_f,$$

where we use the fact that $U^0 = 0$.

Next, we recall the definition of $\tilde{g}_2^{n+1}$, and observe

$$\tilde{g}_2^n - \tilde{g}_2^{n+1} = -(\Delta t)^2 \partial_{\Delta t}^2 \mathcal{L}^n.$$

Applying this new observation, we may finally return to our favorite inequalities. Thus, we have

$$\begin{aligned}
&\frac{1}{\alpha}\sum_{n=0}^{M-1}(U^{n+1} - U^n, \tilde{g}_2^{n+1})_f \\
=& -\frac{(\Delta t)^2}{\alpha}\sum_{n=1}^{M-1}(U^n, \partial_{\Delta t}^2 \mathcal{L}^n)_f + \frac{1}{\alpha}(U^M, \tilde{g}_2^M)_f \\
\leq& \frac{\Delta t}{32T}\sum_{n=0}^{M-1}\|U^n\|_{L^2(\Omega_f)}^2 + \frac{CT(\Delta t)^3}{\alpha^2}\sum_{n=1}^{M-1}\|\partial_{\Delta t}^2 \mathcal{L}^n\|_{L^2(\Omega_f)}^2 \\
&+ \frac{1}{32}\|U^M\|_{L^2(\Omega_f)}^2 + \frac{C}{\alpha^2}\|\tilde{g}_2^M\|_{L^2(\Omega_f)}^2.
\end{aligned}$$

Combining everything from above, we have

$$\begin{aligned}
\frac{\Delta t}{\alpha}\sum_{n=0}^{M-1}\left\langle g_2^{n+1}, \Lambda^{n+1}\right\rangle \leq& \frac{\Delta t \nu_f}{8}\sum_{n=0}^{M-1}\|\nabla U^{n+1}\|_{L^2(\Omega_f)}^2 \\
&+ \frac{\Delta t}{16T}\sum_{n=1}^{M}\left(\frac{1}{2}\|U^n\|_{L^2(\Omega_f)}^2 + \frac{\Delta t}{2\alpha}\|\Lambda^n\|_{L^2(\Sigma)}^2\right) \\
&+ \frac{1}{32}\|U^M\|_{L^2(\Omega_f)}^2 + C\Psi_2(M) \\
\leq& \frac{1}{8}\sum_{n=0}^{M-1}\mathsf{S}^{n+1} + \frac{1}{8}\max_{1\leq n\leq M}\mathsf{Z}^n + C\Psi_2(M).
\end{aligned}$$

Here, the final step follows from the definitions of S^{n+1} and Z^{n+1} and the fact that

$\Delta t N = T$. A similar technique is detailed in the previous step of the error analysis.

Thus we have successfully bounded the first term in (3.4.9), so it just remains to bound the second, $\frac{\Delta t(k-1)}{2}\sum_{n=0}^{M-1}\langle g_1^{n+1}, \Lambda^{n+1}\rangle$.

As stated above, bounding this term is much easier since g_1^{n+1} already belongs to V_f and we do not have to use a cut-off function technique. Instead, we can immediately use (3.4.1c) to move everything into Ω_f so that

$$\begin{aligned}\frac{\Delta t(k-1)}{2}\langle g_1^{n+1}, \Lambda^{n+1}\rangle =&\frac{(k-1)}{2}\Big((U^{n+1}-U^n, g_1^{n+1})_f\\ &+\Delta t\nu_f(\nabla U^{n+1}, \nabla g_1 2^{n+1})_f - \Delta t(h_2^{n+1}, g_1^{n+1})_f\Big).\end{aligned}$$

We may then complete the bound using the same method as above. Thus, we may conclude

$$\begin{aligned}\frac{\Delta t(k-1)}{2}\sum_{n=0}^{M-1}\langle g_1^{n+1}, \Lambda^{n+1}\rangle \leq&\frac{(k-1)}{2}\Bigg(\sum_{n=0}^{M-1}(U^{n+1}-U^n, g_1^{n+1})_f\\ &+\frac{\Delta t\nu_f}{8}\sum_{n=0}^{M-1}\|\nabla U^{n+1}\|^2_{L^2(\Omega_f)}\\ &+C\Delta t\sum_{n=0}^{M-1}\left(\Big((1+\nu_f)\Big)\|g_1^{n+1}\|^2_{H^1(\Omega_f)}+\|h_2^{n+1}\|^2_{L^2(\Omega_f)}\right)\Bigg)\\ \leq&\frac{(k-1)}{8}\sum_{n=0}^{M-1}\mathsf{S}^{n+1}+\frac{(k-1)}{8}\max_{1\leq n\leq M}\mathsf{Z}^n\\ &+C(k-1)\Psi_1(M).\end{aligned}$$

Plugging this in to (3.4.9) completes the proof. □

With the completion of this proof, we finally see the error estimate begin to take shape. Indeed, summing both sides of Lemma 3.4.1 from $n=0$ to $n=M-1\leq N-1$

and combining this with the results of Lemmas 3.4.2 and 3.4.6 yields

$$\mathsf{Z}^M + \frac{1}{2}\sum_{n=0}^{M-1} \mathsf{S}^{n+1} \leq \frac{1}{2}\max_{1\leq n\leq N} \mathsf{Z}^n + C\big(D(M) + \Psi(M)\big).$$

Note that we again used the fact that $\mathsf{Z}^0 = 0$.

We may further note that this is true for *all* $M \leq N$. Therefore, we may write our error estimate in its penultimate form, namely

$$\frac{1}{2}\max_{1\leq M\leq N} \mathsf{Z}^M + \frac{1}{2}\sum_{n=0}^{N-1} \mathsf{S}^{n+1} \leq C\max_{0\leq M\leq N} \big(D(M) + \Psi(M)\big). \tag{3.4.10}$$

3.4.4 Step 3: Main Result

For the final step of the error analysis, we need to estimate $D(M)$ and $\Psi(M)$. We consider these as catch-all quantities that we have employed to collect error terms that depend only on the solutions to (3.2.2). As stated above, these terms represent the error that results from either the time discretization or the splitting method. In this section, we will show that all of these terms may be estimated by a bounded norm of the solutions of (3.2.2), assuming sufficient regularity, times a convergence factor $\gamma(\Delta t) \leq (1 + \log\frac{1}{\Delta t})(\Delta t)^2$.

We use the following results.

Lemma 3.4.7. *Let $X = H^\ell$ for some $\ell \geq 0$ or $X = L^\infty$, and let $v \in X$. It follows*

$$\int_a^b \|v(\cdot,s)\|_X^2 ds \leq (b-a)\|v\|_{L^\infty(a,b;X)}^2, \tag{3.4.11a}$$

$$\|v^{n+1} - v^n\|_X^2 \leq C\Delta t\int_{t_n}^{t_{n+1}} \|\partial_t v(\cdot,s)\|_X^2 ds, \tag{3.4.11b}$$

$$\|\partial_{\Delta t}v^{n+1} - \partial_t v^{n+1}\|_X^2 \leq C\Delta t \int_{t_n}^{t_{n+1}} \|\partial_t^2 v(\cdot,s)\|_X^2 ds, \tag{3.4.11c}$$

$$\|\partial_{\Delta t}v^{n+1} - \partial_t v^{n+1/2}\|_X^2 \leq C(\Delta t)^3 \int_{t_n}^{t_{n+1}} \|\partial_t^3 v(\cdot,s)\|_X^2 ds, \tag{3.4.11d}$$

$$\|\partial_{\Delta t}^2 v^n\|_X^2 \leq \frac{C}{\Delta t} \int_{t_{n-1}}^{t_{n+1}} \|\partial_t^2 v(\cdot,s)\|_X^2 ds. \tag{3.4.11e}$$

Proof. The proof for each inequality in this lemma is very straightforward. Indeed, (3.4.11a) is a direct result of bounding the left-hand integrand by the Bochner norm $\|v\|_{L^\infty(a,b;X)}$ and proceeding with the integration.

For the remaining inequalities (3.4.11b)-(3.4.11e), we rewrite the left-hand terms using standard methods from calculus. It is thus straightforward to show

$$\begin{aligned}
\|v^{n+1} - v^n\|_X^2 &= \|\int_{t_n}^{t_{n+1}} \partial_t v(\cdot,s)ds\|_X^2, \\
\|\partial_{\Delta t}v^{n+1} - \partial_t v^{n+1}\|_X^2 &= \|\frac{-1}{\Delta t}\int_{t_n}^{t_{n+1}} (s-t_n)\partial_t^2 v(\cdot,s)ds\|_X^2, \\
\|\partial_{\Delta t}v^{n+1} - \partial_t v^{n+1/2}\|_X^2 &= \|\frac{1}{2\Delta t}\int_{t_n}^{t_{n+1}} (t_{n+1}-s)(s-t_n)\partial_t^3 v(\cdot,s)ds\|_X^2, \\
\|\partial_{\Delta t}^2 v^n\|_X &= \|\frac{1}{(\Delta t)^2}\int_{-\Delta t}^{\Delta t} \partial_t^2 v(\cdot,t_n+s)ds\|_X^2.
\end{aligned}$$

From here, the proof is completed by applying the following identity: For any H^ℓ-norm $\|\cdot\|$ it holds that

$$\|\int_{t_n}^{t_{n+1}} w(\cdot,s)ds\|^2 \leq \Delta t \int_{t_n}^{t_{n+1}} \|w(\cdot,s)\|^2 ds. \tag{3.4.12}$$

Note that this indentity is a direct result of Minkowski's integral inequality and Jensen's inequality. $\square$

Finally, using Lemma 3.4.7 we can prove the following approximation lemma.

Lemma 3.4.8. *For all* $1 \le M \le N$, *it holds,*

$$
\begin{aligned}
D(M) \le & CT(\Delta t)^{2k}\Big(\|\partial_t^{k+1}\mathsf{q}\|^2_{L^2(0,T;L^2(\Omega_s))} + (k-1)\nu_s\|\partial_t^{k+1}\nabla\mathsf{w}\|^2_{L^2(0,T;L^2(\Omega_s))}\Big) \\
& + CT(\Delta t)^2\|\partial_t^2\mathsf{u}\|^2_{L^2(0,T;L^2(\Omega_f))} + (\Delta t)^2\Big((\alpha + \frac{\alpha^2}{\nu_f})\|\partial_t\mathsf{u}\|^2_{L^2(0,T;L^2(\Sigma))} \\
& + (\frac{1}{\alpha} + \frac{1}{\nu_f})\|\partial_t\mathsf{l}\|^2_{L^2(0,T;L^2(\Sigma))}\Big), \\
\Psi_1(M) \le & C(\Delta t)^2\Bigg((1+\nu_f)\|\partial_t\mathsf{u}\|^2_{L^2(0,T;H^1(\Omega_f))} + (1+T)\|\partial_t^2\mathsf{u}\|^2_{L^2(0,T;L^2(\Omega_f))} \\
& + \|\partial_t\mathsf{u}\|^2_{L^\infty(0,T;L^2(\Omega_f))}\Bigg), \\
\Psi_2(M) \le & C(\Delta t)^2\Bigg(\frac{\nu_f^2(1+\nu_f)}{\alpha^2}\|\partial_t\mathsf{u}\|^2_{L^2(0,T;H^2(\Omega_f))} \\
& + (1+\log(\frac{1}{\Delta t}))\frac{\nu_f^2(1+\nu_f)}{\alpha^2}\|\nabla\partial_t\mathsf{u}\|^2_{L^2(0,T;L^\infty(\Omega_f))} \\
& + \left(1 + \frac{\nu_f^2 T}{\alpha^2}\right)\|\partial_t^2\mathsf{u}\|^2_{L^2(0,T;H^1(\Omega_f))} + \frac{\nu_f^2}{\alpha^2}\|\nabla\partial_t\mathsf{u}\|^2_{L^\infty(0,T;L^2(\Omega_f))} \\
& + \frac{T}{\alpha}\|\partial_t\mathsf{l}\|^2_{L^2(0,T;L^\infty(\Sigma))}\Bigg).
\end{aligned}
$$

Proof. The estimates for $D(M)$ and $\Psi_1(M)$ follow immediately from (3.4.11). The same may be said for the terms in $\Psi_2(M)$ with the exception of the terms $\frac{T(\Delta t)^3}{\alpha^2}\sum_{n=0}^{M-1}\|\partial^2_{\Delta t}\mathcal{L}^n\|^2_{L^2(\Omega_f)}$, $(\frac{1+\nu_f}{\alpha^2})\sum_{n=0}^{M-1}\|\tilde{g}_2^{n+1}\|^2_{H^1(\Omega_f)}$ and $\frac{1}{\alpha^2}\|\tilde{g}_2^M\|^2_{L^2(\Omega_f)}$.

The term $\frac{T(\Delta t)^3}{\alpha^2}\sum_{n=0}^{M-1}\|\partial^2_{\Delta t}\mathcal{L}^n\|^2_{L^2(\Omega_f)}$ follows from the definition of $\mathcal{L}$, Assumptions 3.4.3 nad 3.4.4, and (3.4.11e). More specifically, we have

$$
\begin{aligned}
\frac{T(\Delta t)^3}{\alpha^2}\sum_{n=0}^{M-1}\|\partial^2_{\Delta t}\mathcal{L}^n\|^2_{L^2(\Omega_f)} = & \frac{T\nu_f^2(\Delta t)^3}{\alpha^2}\sum_{n=0}^{M-1}\|\partial^2_{\Delta t}(\phi\nabla u^n\tilde{\boldsymbol{n}}_f)\|^2_{L^2(\Omega_f)} \\
\le & \frac{T\nu_f^2(\Delta t)^3}{\alpha^2}\sum_{n=0}^{M-1}\|\phi\|^2_{L^\infty(\Omega_f)}\|\partial^2_{\Delta t}\nabla^n\|^2_{L^2(\Omega_f)}\|\tilde{\boldsymbol{n}}_f\|^2_{L^\infty(\Omega_f)} \\
\le & \frac{CT\nu_f^2(\Delta t)^3}{\alpha^2}\sum_{n=0}^{M-1}\|\partial^2_{\Delta t}\nabla u^n\|^2_{L^2(\Omega_f)}
\end{aligned}
$$

$$
\begin{aligned}
&\leq \frac{CT\nu_f^2(\Delta t)^2}{\alpha^2} \sum_{n=0}^{M-1} \int_{t_{n-1}}^{t_{n+1}} \|\partial_t^2 \nabla u^n\|^2_{L^2(\Omega_f)} \\
&\leq \frac{CT\nu_f^2(\Delta t)^2}{\alpha^2} \|\partial_t^2 \nabla u^n\|^2_{L^2(0,T;H^1(\Omega_f))}.
\end{aligned}
$$

For the last term, we begin by recalling $0 \leq \phi \leq q$, so we may write

$$
|\tilde{g}_2^{n+1}| = |\phi \nu_f \nabla(\mathsf{u}^{n+1} - \mathsf{u}^n) \cdot \tilde{\boldsymbol{n}}| \leq \nu_f |\nabla(\mathsf{u}^{n+1} - \mathsf{u}^n)||\tilde{\boldsymbol{n}}|.
$$

Then it clearly follows from Assumption 3.4.3, (3.4.11b), and (3.4.11c)

$$
\begin{aligned}
\frac{1}{\alpha^2}\|\tilde{g}_2^M\|^2_{L^2(\Omega_f)} &\leq \frac{\nu_f^2}{\alpha^2}\|\nabla(\mathsf{u}^M - \mathsf{u}^{M-1})\|^2_{L^2(\Omega_f)}\|\tilde{\boldsymbol{n}}\|^2_{L^\infty(\Omega_f)} \\
&\leq \frac{C\Delta t \nu_f^2}{\alpha^2} \int_{t_{M-1}}^{t_M} \|\nabla \partial_t \mathsf{u}(\cdot, s)\|^2_{L^2(\Omega_f)} ds \\
&\leq \frac{C(\Delta t)^2 \nu_f^2}{\alpha^2} \|\nabla \partial_t \mathsf{u}\|^2_{L^\infty(0,T;L^2(\Omega_f))}.
\end{aligned}
$$

To bound $\left(\frac{1+\nu_f}{\alpha^2}\right) \sum_{n=0}^{M-1} \|\tilde{g}_2^{n+1}\|^2_{H^1(\Omega_f)}$ is slightly more difficult. We begin by recalling the definition of $\tilde{g}_2^{n+1}$ and applying the product rule. After further applying Assumption 3.4.3 and (i) and (iv) of Assumption 3.4.4, we obtain

$$
\begin{aligned}
&\Delta t \left(\frac{1+\nu_f}{\alpha^2}\right) \sum_{n=0}^{M-1} \|\nabla \tilde{g}_2^{n+1}\|^2_{L^2(\Omega_f)} \\
\leq& C\Delta t \left(\frac{\nu_f^2(1+\nu_f)}{\alpha^2}\right) \sum_{n=0}^{M-1} \Big(\|\nabla \phi\|^2_{L^2(\Omega_f)} \|\nabla(\mathsf{u}^{n+1} - u^n)\|^2_{L^\infty(\Omega_f)} \\
&\qquad + \|\nabla \tilde{\boldsymbol{n}}\|^2_{L^\infty(\Omega_f)} \|\nabla(\mathsf{u}^{n+1} - u^n)\|^2_{L^2(\Omega_f)} \\
&\qquad + \|D^2(\mathsf{u}^{n+1} - \mathsf{u}^n)\|^2_{L^2(\Omega_f)} \Big) \\
\leq& C\Delta t \left(\frac{\nu_f^2(1+\nu_f)}{\alpha^2}\right) \sum_{n=0}^{M-1} \Big(\big(1 + \log(\frac{1}{\Delta t})\big) \|\nabla(\mathsf{u}^{n+1} - \mathsf{u}^n)\|^2_{L^\infty(\Omega_f)} \\
&\qquad + \|D^2(\mathsf{u}^{n+1} - \mathsf{u}^n)\|^2_{L^2(\Omega_f)} \Big),
\end{aligned}
$$

where $D^2\mathsf{u}$ denotes the Hessian of u.

Consequently, it follows from (3.4.11b) that

$$\Delta t\Big(\frac{1+\nu_f}{\alpha}\Big)\sum_{n=0}^{M-1}\|\nabla\tilde{g}_2^{n+1}\|^2_{L^2(\Omega_f)} \le C(\Delta t)^2\Big(\frac{\nu_f^2(1+\nu_f)}{\alpha^2}\Big)\Bigg(\|\partial_t\mathsf{u}\|^2_{L^2(0,T;H^2(\Omega_f))} + (1+\log(\frac{1}{\Delta t}))\|\nabla\partial_t\mathsf{u}\|^2_{L^2(0,T;L^\infty(\Omega_f))}\Bigg).$$

□

We may now provide the main result of this section: the complete error estimate.

Theorem 3.4.9. *Under Assumptions 3.4.3, 3.4.4, and assuming that the solution is smooth enough so that* Y *defined below and* $\|\nabla\partial_t\mathsf{u}\|^2_{L^2(0,T;L^\infty(\Omega_f))}$ *are bounded we have*

$$\max_{1\le M\le N}\mathsf{Z}^M + \sum_{n=0}^{N-1}\mathsf{S}^{n+1} \le C(\Delta t)^2\Big(\mathsf{Y} + \frac{\nu_f^2(1+\nu_f)}{\alpha^2}\big(1+\log(\frac{1}{\Delta t})\big)\|\nabla\partial_t\mathsf{u}\|^2_{L^2(0,T;L^\infty(\Omega_f))}\Big),$$

where

$$\begin{aligned}\mathsf{Y} :=&(\Delta t)^{2k-2}\Big(\|\partial_t^{k+1}\mathsf{q}\|^2_{L^2(0,T;L^2(\Omega_s))} + (k-1)\nu_s\|\partial_t^{k+1}\nabla\mathsf{w}\|^2_{L^2(0,T;L^2(\Omega_s))}\Big)\\ &+\Big(1+(1+\frac{\nu_f^2}{\alpha^2})T\Big)\|\partial_t^2\mathsf{u}\|^2_{L^2(0,T;H^1(\Omega_f))} + \big(\alpha+\frac{\alpha^2}{\nu_f}\big)\|\partial_t\mathsf{u}\|^2_{L^2(0,T;L^2(\Sigma))}\\ &+\big(\frac{1}{\alpha}+\frac{1}{\nu_f}\big)\|\partial_t\mathsf{l}\|^2_{L^2(0,T;L^2(\Sigma))} + (1+\nu_f)\big(1+\frac{\nu_f^2}{\alpha^2}\big)\|\partial_t\mathsf{u}\|^2_{L^2(0,T;H^2(\Omega_f))}\\ &+\big(1+\frac{\nu_f^2}{\alpha^2}\big)\|\partial_t\mathsf{u}\|^2_{L^\infty(0,T;H^1(\Omega_f))} + \frac{T}{\alpha}\|\partial_t\mathsf{l}\|^2_{L^2(0,T;L^\infty(\Sigma))}.\end{aligned}$$

Proof. The result follows immediately from (3.4.10) and Lemma 3.4.8. □

3.5 Final Discussion

In this section, we comment on some final points that follow from the analysis above.

3.5.1 Special Case

We begin by outlining a special case in which we may prove an optimal error estimate of $\mathcal{O}(\Delta t)$, which is *slightly* better than $\mathcal{O}(\Delta t\sqrt{1+\log\frac{1}{\Delta t}})$.

We assume that $\Omega = [0,1]^2$ and that $\Omega_f = [0,1]\times[0,a]$ and $\Omega_s = [0,1]\times[a,1]$. Note that $\Sigma = [0,1]\times\{a\}$, as shown in Figure 3.2. We note that the outward facing normal vector on Σ, $\boldsymbol{n}_f$, is constant. In this case, $\boldsymbol{n}_f = [0,1]'$.

Let $\partial\Omega_f\backslash\Sigma = \Gamma_p \cup \Gamma_g$, where Γ_p consists of the sides of $\partial\Omega_f$ that are perpendicular to Σ. Consequently, this means that at the endpoints of Σ–where it meets Γ_p–$\boldsymbol{n}_f$ is parallel to Γ_p.

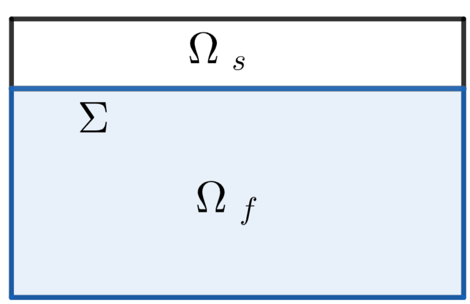

Figure 3.2: Schematic of our special case

From (3.1.9c), we know that $\mathsf{u}|_{\Gamma_p} = 0$. Therefore, at the endpoints of Σ we have

$$\mathsf{l} = \nu_f \nabla \mathsf{u}\cdot\boldsymbol{n}_f = \nu_f\nabla\mathsf{u}\cdot\tau_\Gamma = 0.$$

Consequently, Assumptions 3.4.3 and 3.4.4 are not required in this case to bound the term $\frac{\Delta t}{\alpha}\langle g_3^{n+1}, \Lambda^{n+1}\rangle$. Instead, we may define a cut-off function $\phi_c : \Omega_f \to \mathbb{R}$ that is any continuous function satisfying the following conditions:

(i) $\phi_c|_\Sigma = 1$,

(ii) $\phi_c|_{\Gamma_g} = 0$,

(iii) ϕ_c and $\nabla\phi_c$ are uniformly bounded.

Clearly, the conditions for ϕ_c are much less restrictive than those listed in Assumption 3.4.4. Indeed, a very simple construction of ϕ_c that satisfies these conditions would be a function that is equal to 1 on Σ and then decays linearly to 0 at Γ_a. We may use these looser restrictions because $\boldsymbol{n}_f$ is constant and may therefore be trivially extended into Ω_f, while the perpendicularity of Σ and Γ_p ensures that $\phi_c \nabla \mathsf{u} \cdot \boldsymbol{n}_f = 0$ on $\partial\Omega_f \setminus \Sigma$. Consequently, we may define

$$\tilde{g}_2^{n+1} := \mathcal{L}^{n+1} - \mathcal{L}^n,$$

where $\mathcal{L}(x,t) := \phi_c \nabla \mathsf{u}(x,t) \cdot \boldsymbol{n}$.

We may then follow the proofs of Lemmas 3.4.6 and 3.4.8. However, in this case, it follows from the uniform boundedness of ϕ_c and $\nabla\phi_c$ and Lemma 3.4.7 that we have

$$\begin{aligned}
\|\tilde{g}_2^{n+1}\|^2_{L^2(\Omega_f)} \leq & C\Delta t \int_{t_n}^{t_{n+1}} \|\partial_t \mathsf{u}(\cdot, s)\|^2_{H^1(\Omega_f)} ds, \\
\|\nabla\tilde{g}_2^{n+1}\|^2_{L^2(\Omega_f)} \leq & C\Delta t \int_{t_n}^{t_{n+1}} \|\partial_t \mathsf{u}(\cdot, s)\|^2_{H^2(\Omega_f)} ds.
\end{aligned}$$

Therefore, unlike in the proof of Lemma 3.4.8, we now have

$$\Delta t\left(\frac{1+\nu_f}{\alpha^2}\right)\sum_{n=0}^{M-1}\|\nabla\tilde{g}_2^{n+1}\|^2_{L^2(\Omega_f)} \leq C(\Delta t)^2\left(\frac{1+\nu_f}{\alpha^2}\right)\|\partial_t \mathsf{u}(\cdot,s)\|^2_{L^2(0,T;H^2(\Omega_f))}.$$

As a result, the final error estimate defined in Theorem 3.4.4 now becomes

$$\max_{1\leq M\leq N}\mathsf{Z}^M+\sum_{n=0}^{N-1}\mathsf{S}^{n+1}\leq C(\Delta t)^2\Big(\mathsf{Y}+\frac{\nu_f^2(1+\nu_f)}{\alpha^2}\|\nabla\partial_t\mathsf{u}\|^2_{L^2(0,T;L^\infty(\Omega_f))}\Big),$$

losing the factor $\big(1+\log(\frac{1}{\Delta t})\big)$.

3.5.2 Example: Constructing ϕ

Unfortunately, not all cases are as accommodating as the special case described above, so constructing an appropriate function ϕ is critical. For the purposes of this example construction, however, we do allow Σ to be perpendicular to $\partial\Omega\setminus\Sigma$, but we note that adjusting the angle of Σ with respect to the rest of the boundary will not drastically change the construction of this ϕ, as long as Σ remains a straight line.

The aim for this example is to provide proof that, in this base case, a ϕ exists satisfying the assumptions. We also suggest that it may be useful when constructing ϕ on more complex domains, as it can provide a valuable starting point for addressing more complicated Σ.

To begin the construction of our example, let $\Omega_f = [0,1]\times[0,1]$. Note that $\Sigma = [0,1]\times\{1\}$ marks the top boundary of Ω_f. We then divide Ω_f into five regions, $\{K_i\}_{i=1}^5$ as shown in Figure 3.3 for $x=(x_1,x_2)$. From here, we may define $\phi(x) =$

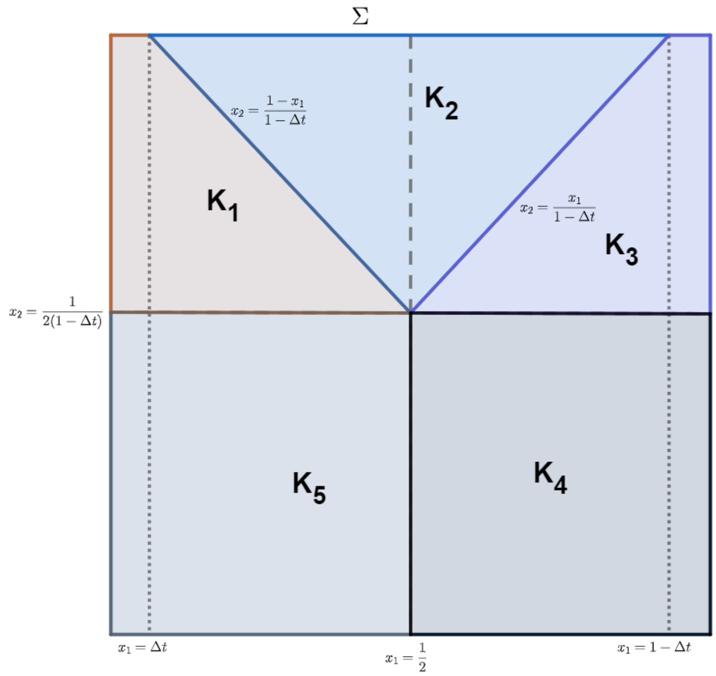

Figure 3.3: $\Omega_f = [0,1]^2$ with the regions $\{K_i\}_{i=1}^5$.

$\phi(x_1, x_2)$ by the following.

$$\phi(x) := \begin{cases} \frac{x_1}{1-(1-\Delta t)x_2}, & x \in K_1, \\ 1, & x \in K_2, \\ \frac{1-x_1}{1-(1-\Delta t)x_2}, & x \in K_3, \\ 4x_2(1-x_1)(1-\Delta t), & x \in K_4, \\ 4x_1x_2(1-\Delta t), & x \in K_5. \end{cases} \tag{3.5.1}$$

It is straightforward to check that this ϕ is globally continuous and piecewise differentiable, and it satisfies conditions (i)-(iii) in Assumption 3.4.4. For condition (iv), we note

$$\int_{\Omega_f} |\nabla\phi|^2 = \big(\frac{2}{1-\Delta t} + \frac{2(1-\Delta t)}{3}\big) \log\frac{1}{2\Delta t} + \frac{2(1-\Delta t)}{3} + \frac{2}{3(1-\Delta t)}.$$

Thus, if $\Delta t < \frac{1}{2}$, we have

$$\int_{\Omega_f} |\nabla \phi|^2 \leq C(1 + \log \frac{1}{\Delta t})$$

3.5.3 Sub-optimal error estimate

As mentioned above, if we do not treat the term $\frac{\Delta t}{\alpha}\langle g_3^{n+1}, \Lambda^{n+1}\rangle$ with enough care, we are likely to end up with a sub-optimal error estimate that does not match the nearly optimal behavior of numerical experiments (see Section 3.6.1).

In fact, if we were to include $\frac{\Delta t}{\alpha}\langle g_3^{n+1}, \Lambda^{n+1}\rangle$ in the terms of F^{n+1} from Lemma 3.4.1, we would then proceed to bound the term as in the proof of Lemma 3.4.2. In this case, we find

$$\begin{aligned}\frac{\Delta t}{\alpha}\sum_{n=0}^{M-1}\langle g_3^{n+1}, \Lambda^{n+1}\rangle &\leq \sum_{n=0}^{M-1}\Big(\frac{CT}{\alpha}\|g_3^{n+1}\|^2_{L^2(\Sigma)} + \frac{(\Delta t)^2}{8T}\|\Lambda^{n+1}\|^2_{L^2(\Sigma)}\Big)\\ &\leq \sum_{n=0}^{M-1}\frac{CT}{\alpha}\|g_3^{n+1}\|^2_{L^2(\Sigma)} + \frac{1}{4}\max_{1\leq m\leq N}\mathsf{Z}^m.\end{aligned}$$

As a result, (3.4.7) becomes

$$\Delta t\sum_{n=0}^{M-1}F^{n+1} \leq \frac{1}{2}\max_{1\leq n\leq M}\mathsf{Z}^n + \frac{1}{4}\sum_{n=0}^{M-1}\mathsf{S}^{n+1} + CD(M),$$

where $D(M)$ now acquires the term $\sum_{n=0}^{M-1}\frac{CT}{\alpha}\|g_3^{n+1}\|^2_{L^2(\Sigma)}$.

Unfortunately, the results of Lemma 3.4.7 indicate that this new term will not yield an optimal error estimate. Instead,

$$\sum_{n=0}^{M-1} \frac{CT}{\alpha} \|g_3^{n+1}\|_{L^2(\Sigma)}^2 \leq \frac{C\Delta t T}{\alpha} \big(\|\partial_t \mathsf{u}\|_{L^2(0,T;L^2(\Sigma))}^2 + \|\partial_t \mathsf{l}\|_{L^2(0,T;L^2(\Sigma))}^2 \big),$$

which forces the final error estimate (after taking the square root) to be $\mathcal{O}(\sqrt{\Delta t})$. Earlier stability proofs of the Robin-Robin method for FSI problems followed this approach and yielded suboptimal results that were later improved, as we will see in Chapters 4 and 5. For the suboptimal results, see [16, 14].

3.5.4 Comments on regularity

We note that the error estimate proven in this chapter requires sufficient regularity of the exact solutions, u and w. In particular, we require sufficient regularity to ensure that the norms in the main result in Theorem 3.4.4 are all bounded.

For most of these norms, it would be sufficient to require $\mathsf{u} \in H^2(\Omega_f)$ and $\mathsf{w} \in H^1(\Omega_s)$ with sufficient smoothness in time. However, this is not sufficient for the term $\|\partial_t \mathsf{l}\|_{L^2(0,T;L^2(\Sigma)}^2$, as this requires $\mathbf{u} \in H^1(\Sigma)$. Instead, we require $\mathsf{u} \in H^{3/2}(\Omega_f)$ in order to have sufficient regularity to ensure that this term is bounded. We then have to consider the kinematic coupling condition and what this will imply about the regularity of $\mathbf{q}$.

However, it is beyond the scope of this thesis to prove whether or not it is reasonable to expect this amount of regularity in the solutions to the parabolic-parabolic and parabolic-hyperbolic coupled problems. Therefore all results are stated under the assumption of sufficient regularity. We will further make the same assumption for all subsequent problems.

3.5.5 Concluding remarks

In this chapter we developed a loosely-coupled splitting method for parabolic-parabolic and parabolic-hyperbolic coupled problems based on Robin-type interface conditions, which we call the Robin-Robin splitting method. Working in a semi-discrete framework, we proved stability and nearly optimal accuracy in time. We further demonstrated that the analyses for the two coupled problems may be carried out together in a unified framework, potentially highlighting the versatility of the splitting method.

The main challenge in the analysis of the Robin-Robin splitting method was to bound the stress term $\nabla u \cdot \boldsymbol{n}$ on the interface. Indeed, we showed that if this term is not handled carefully we may lose a half order of accuracy. Consequently, a function must be constructed to appropriately lift the stress term from the interface into the interior domain.

So far, we have only seen the Robin-Robin method applied to two model problems. However, as stated in Chapter 1, similar methods have been applied to a wide variety of problems. In the following chapters, we will investigate the use Robin-Robin splitting method as a loosely-coupled splitting method for the FSI problem that does not suffer from the added-mass effect. We will see that the analysis suffers from the same challenges with the stress terms at the interface. However, the problem now includes a pressure term and incompressibility condition in the fluid, along with several physical constants related to viscosity, density, and elasticity, all of which add an interesting degree of complexity to the error analysis.

3.6 Numerical Experiments

To conclude this chapter, we seek to verify our theoretical results through numerical experiments. As our analysis above is carried out in a time-semi-discrete framework, the spacial discretization may be done with any appropriate numerical method. For simplicity, we choose to use linear finite elements with mesh parameters defined below for each case. To accommodate our Lagrange multiplier method, we require that the meshes on Ω_s and Ω_f match at the interface Σ. In all cases below, we set the coefficients $\nu_f = \nu_s = \alpha = 1$.

3.6.1 Numerical experiments for simple case with uniform mesh

For our first case, we take $\Omega = [0,1]^2$ and $\Omega_f = [0,1]\times[0,3/4]$ and $\Omega_s = [0,1]\times[3/4,1]$ and of course $\Sigma = \overline{\Omega_f} \cap \overline{\Omega_s}$. On each subdomain, we use a uniform mesh with $h = \Delta t$. We run the system to time $T = 0.25$.

For the Parabolic-Parabolic ($k = 1$) coupling, we take the exact solution to be

$$\begin{aligned}
u(t,x) &= e^{-2\pi^2 t}\sin(\pi x_1)\sin(\pi x_2),\\
w(t,x) &= e^{-2\pi^2 t}\sin(\pi x_1)\sin(\pi x_2),\\
\mathsf{l}(t,x) &= \pi e^{-2\pi^2 t}\sin(\pi x_1)\cos(\pi x_2).
\end{aligned}$$

For the Parabolic-Hyperbolic ($k = 2$) coupling, we take the exact solution to be

$$u(t,x) = (10^{-3})e^{t}x_1(1-x_1)x_2(1-x_2),$$

$$w(t,x) = (10^{-3})e^t x_1(1-x_1)x_2(1-x_2),$$

$$\mathsf{l}(t,x) = (10^{-3})e^t x_1(1-x_1)(1-2x_2).$$

In Table 3.1 below, we measure the error in the L^2-norm at the final time $T = 0.25$.

	$k=1$				$k=2$			
	Rates		Errors		Rates		Errors	
Δt	U	W	U	W	U	Q	U	Q
$(\frac{1}{2})^2$	–	–	0.04	0.09	–	–	4.48e-06	9.48e-06
$(\frac{1}{2})^3$	-0.30	0.59	0.05	0.06	2.16	1.94	1.01e-06	2.45e-06
$(\frac{1}{2})^4$	0.22	0.93	0.04	0.03	0.96	1.02	5.19e-07	1.22e-06
$(\frac{1}{2})^5$	1.08	1.67	0.02	9.6e-03	0.47	0.89	3.76e-07	6.67e-07
$(\frac{1}{2})^6$	2.43	3.71	3.5e-03	7.3e-04	0.74	0.88	2.25e-07	3.62e-07
$(\frac{1}{2})^7$	2.89	1.17	4.8e-04	3.3e-04	0.88	0.93	1.22e-07	1.89e-07
$(\frac{1}{2})^8$	1.77	0.85	1.4e-04	1.8e-04	0.94	0.97	6.36e-08	9.69e-08
$(\frac{1}{2})^9$	1.37	0.97	5.4e-05	9.6e-05	0.97	0.98	3.24e-08	4.91e-08

Table 3.1: Convergence rates and errors for the parabolic-parabolic problem in the special case where Σ is perpendicular to $\partial\Omega$.

Clearly, we can see that all the error terms behave as $O(\Delta t)$ as $\Delta t \to 0$, which agrees well with our theoretical results.

3.6.2 Numerical experiments for less simple case with non-uniform mesh

For our next set of numerical experiments, we investigate the case where Σ is not perpendicular to $\partial\Omega$. We again take $\Omega = [0,1]^2$, however Σ is now represented by the line $x_2 = \frac{x_1}{2} + \frac{1}{4}$. Furthermore, we generate a non-uniform mesh such that the interface Σ is aligned with the nodes of the mesh (See Figure 3.4).

We run our method on this grid for $\Delta t = \{(\frac{1}{2})^{n+2}\}_{n=0}^{8}$. For each n, the maximum

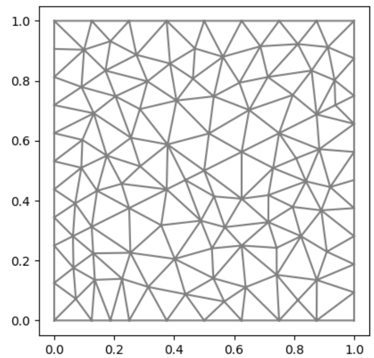

Figure 3.4: An example of the non-uniform mesh for $n = 1$.

element diameter, h_{max}, is given (to 4 significant digits) in the list below. From this we can see that h is roughly $O(\Delta t)$. Additionally, as before, we run to time $T = 0.25$.

$$(n, h_{max}) = \{(0, 0.3125),\ (1, 0.1574),\ (2, 0.0794),\ (3, 0.0398),\ (4, 0.0199),$$
$$(5, 0.0099),\ (6, 0.0050),\ (7, 0.0025),\ (8, 0.0012)\}.$$

We take the exact solution to be

$$\begin{aligned}
\mathsf{u}(t,x) &= (10^{-3})e^t x_1(1-x_1)x_2(1-x_2)\\
\mathsf{w}(t,x) &= (10^{-3})e^t x_1(1-x_1)x_2(1-x_2)\\
\mathsf{l}(t,x) &= \left(\frac{10^{-3}}{\sqrt{5}}\right) e^t \left(2x_1(1-x_1)(1-2x_2) - (1-2x_1)x_2(1-x_2)\right),
\end{aligned}$$

and we note that $\mathsf{l} = \nabla \mathsf{u} \cdot \boldsymbol{n}$ no longer vanishes on $\partial\Omega$.

In Tables 3.2 and 3.3 below, we again measure the L^2-norm of U and W at the final time $T = 0.25$. However, we also measure $\left(\Delta t \sum_{n=1}^{N} \|\nabla U^n\|^2_{L^2(\Omega_f)}\right)^{1/2}$ and $\left(\Delta t \sum_{n=1}^{N} \|\nabla W^n\|^2_{L^2(\Omega_s)}\right)^{1/2}$, where $N = \frac{T}{\Delta t}$.

As before, we see first order convergence in U and W. For ∇U and ∇W, the

	Rates		Errors	
Δt	Rate U	Rate W	U	W
$(\frac{1}{2})^2$	–	–	4.92e-07	1.27e-06
$(\frac{1}{2})^3$	1.28	1.87	2.02e-07	3.48e-07
$(\frac{1}{2})^4$	0.59	0.83	1.35e-07	1.95e-07
$(\frac{1}{2})^5$	0.45	0.87	9.85e-08	1.07e-07
$(\frac{1}{2})^6$	0.71	0.81	6.01e-08	6.09e-08
$(\frac{1}{2})^7$	0.89	0.89	3.26e-08	3.28e-08
$(\frac{1}{2})^8$	0.94	0.95	1.69e-08	1.70e-08
$(\frac{1}{2})^9$	0.97	0.98	8.62e-09	8.63e-09
$(\frac{1}{2})^{10}$	0.99	0.99	4.35e-09	4.36e-09

Table 3.2: Convergence rates and errors for the parabolic-parabolic problem for a more general case.

	Rates		Errors	
Δt	Rate ∇U	Rate ∇W	∇U	∇W
$(\frac{1}{2})^2$	–	–	4.60e-06	5.28e-06
$(\frac{1}{2})^3$	0.99	1.45	2.33e-06	1.93e-06
$(\frac{1}{2})^4$	1.12	0.78	1.07e-06	1.13e-06
$(\frac{1}{2})^5$	0.77	0.81	6.26e-07	6.43e-07
$(\frac{1}{2})^6$	0.66	0.69	3.96e-07	4.00e-07
$(\frac{1}{2})^7$	0.69	0.69	2.45e-07	2.47e-07
$(\frac{1}{2})^8$	0.74	0.75	1.46e-07	1.47e-07
$(\frac{1}{2})^9$	0.79	0.80	8.44e-08	8.45e-08
$(\frac{1}{2})^{10}$	0.83	0.83	4.74e-08	4.74e-08

Table 3.3: More convergence rates and errors for the parabolic-parabolic problem for a more general case.

convergence is slower, however it seems it will eventually approach first order.

Chapter Four

Robin-Robin coupling for fluid-structure interaction, Part I: the time-semi-discrete framework

4.1 Robin-Robin coupling for the fluid-structure interaction problem

In this chapter, we present the Robin-Robin splitting method for the FSI problem introduced in Chapter 1. As we will see below, the FSI problem strongly resembles the parabolic-hyperbolic coupling introduced in (3.1.6)-(3.1.8). Thus, it would be ideal if we could mirror the analysis done in Chapter 3 (in the case $k = 2$) for the FSI problem.

As it turns out, a large part of the FSI analysis can be done using the methods of Chapter 3, and we will make use of this advantage in the analysis that follows. However, unlike the parabolic problem presented in (3.1.6), the Stokes problem includes an additional pressure term, p, and an incompressibility condition, $\operatorname{div} u = 0$. Additionally, the stress terms for the Stokes and linear elasticity equations are significantly more complex than those in (3.1.6)-(3.1.8), and the system includes several physical parameters (such as density and the Lamé parameters) that may influence the splitting method in some way. Consequently, the FSI system presents a much stiffer problem than the parabolic-hyperbolic coupling. Thus, although we will mirror the techniques of Chapter 3 as much as possible, we will need to take special care to address the aspects stated above.

The chapter is organized as follows. We begin by introducing the FSI system and the time-discrete Robin-Robin method as applied in this context. We then prove stability and accuracy, as in Chapter 3. Finally, we discuss the behavior of the Robin-Robin method with respect to the parameters of the FSI system and verify our results with numerical experiments.

4.1.1 The FSI problem

As in Chapter 3, we work with a domain Ω that is split into two sub-domains, Ω_f and Ω_s, such that $\Omega = \Omega_f \cup \Omega_s$, with common interface $\Sigma = \partial\Omega_f \cap \partial\Omega_s$ (see Figure 3.2). Also as in Chapter 3, we assume Ω is a bounded, connected subset of $\mathbb{R}^2$ with Lipschitz boundary.

Unlike in the previous chapter, however, our solutions are now the vector-valued quantities, with the exception of the pressure, p, which is a scalar (see 1.1.2.1 for more detail). Let $\mathbf{u}$, p, $\mathbf{e}$, and $\mathbf{q}$ be the fluid velocity, fluid pressure, structural displacement, and structural velocity, respectively. Thus, the FSI system is as follows.

$$\rho_f \partial_t \mathbf{u} - \operatorname{div} \sigma_f(\mathbf{u}, \mathsf{p}) = 0 \quad \text{in } (0,T) \times \Omega_f, \tag{4.1.1a}$$

$$\operatorname{div} \mathbf{u} = 0 \quad \text{in } (0,T) \times \Omega_f, \tag{4.1.1b}$$

$$\mathbf{u} = 0 \quad \text{on } (0,T) \times \Sigma_f, \tag{4.1.1c}$$

$$\rho_s \partial_t \mathbf{q} - \operatorname{div} \sigma_s(\mathbf{e}) = 0 \quad \text{in } (0,T) \times \Omega_s, \tag{4.1.2a}$$

$$\mathbf{q} - \partial_t \mathbf{e} = 0 \quad \text{in } (0,T) \times \Omega_s, \tag{4.1.2b}$$

$$\mathbf{e} = 0 \quad \text{on } (0,T) \times \Sigma_s, \tag{4.1.2c}$$

$$\mathbf{u} = \mathbf{q} \quad \text{on } (0,T) \times \Sigma, \tag{4.1.3a}$$

$$\sigma_f(\mathbf{u}, \mathsf{p}) \boldsymbol{n}_f + \sigma_s(\mathbf{e}) \boldsymbol{n}_s = 0 \quad \text{on } (0,T) \times \Sigma, \tag{4.1.3b}$$

equipped with initial conditions:

$$\begin{aligned}
\mathbf{e}(0,\cdot) =& \mathbf{e}_0 \qquad \text{in } \Omega_s,\\
\mathbf{q}(0,\cdot) =& \mathbf{q}_0 \qquad \text{in } \Omega_s,\\
\mathbf{u}(0,\cdot) =& \mathbf{u}_0 \qquad \text{in } \Omega_f.
\end{aligned}$$

As before, $\boldsymbol{n}_i$ is the outward pointing normal to $\partial\Omega_i$ for $i = s, f$. The stress tensors are given as stated in 1.1.2.1,

$$\begin{aligned}
\sigma_f(\mathbf{u}, \mathsf{p}) :=& 2\mu\epsilon(\mathbf{u}) - \mathsf{p}\mathbf{I},\\
\sigma_s(\mathbf{e}) :=& 2L_1\epsilon(\mathbf{e}) + L_2(\operatorname{div}\mathbf{e})\mathbf{I},
\end{aligned}$$

where $\epsilon(\boldsymbol{v}) = \frac{1}{2}(\nabla\boldsymbol{v} + \nabla\boldsymbol{v}^T)$ is the symmetric gradient.

Here μ is the viscosity of the fluid and L_1, L_2 are the Lamé constants of the solid, with $L_1 > 0$ and $L_2 \geq 0$. The solid and fluid densities are denoted ρ_s, ρ_f, respectively.

Remark 6. As stated in the introduction, we apply Dirichlet conditions to the boundary of Ω. This was done for the sake of simplicity and may not be appropriate for all problems. However, changing the conditions on $\partial\Omega$ to those used in [17, 18], for example, will not change the applicability of the Robin-Robin method described in this chapter.

We will work primarily with the weak form of (4.1.1)-(4.1.3), and, just as in Chapter 3, we will represent the interfacial stress from Ω_f as a separate variable. More specifically, we define

$$\mathbf{l} := \sigma_f(\mathbf{u}, \mathsf{p})\boldsymbol{n}_f.$$

As with the parabolic-hyperbolic coupling, we do this to be able to match the terms of the true FSI system, (4.1.1)-(4.1.3), with the terms of the Robin-Robin system that we will define below. As such, we must also define the following spaces

$$\begin{aligned}
\boldsymbol{V}^s :=& \{\boldsymbol{v} \in \boldsymbol{H}^1(\Omega_s) : \boldsymbol{v} = 0 \text{ on } \partial\Omega_s \setminus \Sigma\}, \\
\boldsymbol{V}^f :=& \{\boldsymbol{v} \in \boldsymbol{H}^1(\Omega_f) : \boldsymbol{v} = 0 \text{ on } \partial\Omega_f \setminus \Sigma\}, \\
\boldsymbol{V}^g :=& L^2(\Sigma), \\
M^f :=& L^2_0(\Omega_f).
\end{aligned}$$

Then if we assume that $\mathsf{l}(t) \in [L^2(\Sigma)]^2$ we have that the solution of (4.1.1)-(4.1.3) satisfies the weak formulation: For $t > 0$, find $\mathbf{q}(t), \mathbf{e}(t) \in \boldsymbol{V}^s$, $\mathbf{u}(t) \in \boldsymbol{V}^f$, $\mathsf{l}(t) \in \boldsymbol{V}^g$, and $\mathsf{p}(t) \in M^f$ satisfying

$$\rho_s(\partial_t \mathbf{q}, \boldsymbol{\xi})_s + a_s(\mathbf{e}, \boldsymbol{\xi}) + \big\langle \mathsf{l}, \boldsymbol{\xi} \big\rangle = 0 \quad \forall \boldsymbol{\xi} \in \boldsymbol{V}^s \tag{4.1.4a}$$

$$(\mathbf{q}, \boldsymbol{\tau})_s - (\partial_t \mathbf{e}, \boldsymbol{\tau})_s = 0 \quad \forall \boldsymbol{\tau} \in \boldsymbol{V}^s \tag{4.1.4b}$$

$$\rho_f(\partial_t \mathbf{u}, \boldsymbol{v})_f + a_f\big((\mathbf{u}, \mathsf{p}), (\boldsymbol{v}, \theta)\big) - \big\langle \mathsf{l}, \boldsymbol{v} \big\rangle = 0 \quad \forall (\boldsymbol{v}, \theta) \in \boldsymbol{V}^f \times M^f \tag{4.1.4c}$$

$$\big\langle \mathbf{u} - \mathbf{q}, \boldsymbol{\mu} \big\rangle = 0 \quad \forall \boldsymbol{\mu} \in \boldsymbol{V}^g. \tag{4.1.4d}$$

Here, the bilinear forms $a_f(\cdot,\cdot)$ and $a_s(\cdot,\cdot)$ are respectively given by

$$\begin{aligned}
a_f\big((\mathbf{u}, \mathsf{p}), (\boldsymbol{v}, \theta)\big) :=& 2\mu(\epsilon(\mathbf{u}), \epsilon(\boldsymbol{v}))_f - (\mathsf{p}, \operatorname{div} \boldsymbol{v})_f + (\operatorname{div} \mathbf{u}, \theta), \\
a_s(\mathbf{e}, \boldsymbol{\xi}) :=& 2L_1(\epsilon(\mathbf{e}), \epsilon(\boldsymbol{\xi}))_s + L_2(\operatorname{div} \mathbf{e}, \operatorname{div} \boldsymbol{\xi})_s,
\end{aligned}$$

where $a_s(\cdot,\cdot)$ induces the elastic energy norm

$$\|\mathbf{e}\|_S^2 := a_s(\mathbf{e}, \mathbf{e}) = 2L_1\|\epsilon(\mathbf{e})\|^2_{L_2(\Omega_s)} + L_2\|\operatorname{div} \mathbf{e}\|^2_{L_2(\Omega_s)}.$$

The Lamé parameters govern the elasticity of the solid in Ω_s, and their values can vary depending on the problem. For blood vessels, the Lamé parameters can be on the order of 10^6 (see e.g. [46, 18, 1]) which, in a numerical simulation, may be comparable to $(\Delta t)^{-1}$. Thus, we must be careful in our analysis to keep track of the physical parameters.

4.1.2 The time-discrete Robin-Robin method

In this section, we will introduce the Robin-Robin scheme in a time-semi-discrete framework and prove that it is unconditionally stable and nearly first-order accurate. As mentioned in Chapter 1, the loosely coupled scheme based on the Robin-Robin interface conditions was originally proposed for the FSI system in response to the added-mass instability problem. This method replaces the problematic coupling conditions (1.1.4) with Robin-type interface conditions of the form

$$\sigma_s(\mathbf{e}^{n+1})\boldsymbol{n}_s + \alpha\partial_t\mathbf{e}^{n+1} = \alpha\mathbf{u}^n - \sigma_f(\mathbf{u}^n, p^n)\boldsymbol{n}_f \quad \text{on } \Sigma, \tag{4.1.5a}$$

$$\sigma_f(\mathbf{u}^{n+1}, p^{n+1})\boldsymbol{n}_f + \alpha\mathbf{u}^{n+1} = \alpha\partial_t\mathbf{e}^{n+1} + \sigma_f(\mathbf{u}^n, p^n)\boldsymbol{n}_f \quad \text{on } \Sigma, \tag{4.1.5b}$$

for $\alpha > 0$.

Just as in Chapter 3, we only address the time-semi-discrete form of the Robin-Robin splitting method, as our main concern is the stability and convergence in time of the splitting method. However, just as in Chapter 3, we acknowledge that the Robin-Robin interface conditions (4.1.5) may present continuity issues for spacial discretizations. Indeed, just as we saw before, (4.1.5) yields the identities

$$\sigma_s(\mathbf{e}^{n+1})\boldsymbol{n}_s + \sigma_f(\mathbf{u}^{n+1}, \mathsf{p}^{n+1})\boldsymbol{n}_f = \alpha(\mathbf{u}^n - \mathbf{u}^{n+1}) \quad \text{on } \Sigma,$$

$$\sigma_f(\mathbf{u}^n, \mathsf{p}^n)\boldsymbol{n}_f - \sigma_f(\mathbf{u}^{n+1}, \mathsf{p}^{n+1})\boldsymbol{n}_f = \alpha(\mathbf{u}^{n+1} - \partial_t\mathbf{e}^{n+1}) \quad \text{on } \Sigma,$$

which require the continuities of the stresses and velocities to match along Σ. Unfortunately, If standard finite elements are used to discretize in space, the stress terms will not be continuous across element boundaries, and the identities will not hold.

Thus, we use the same Lagrange Multiplier method as in Chapter 3. In doing so, we introduce $\boldsymbol{\lambda}$ as a variationally consistent representation of $\sigma_f(\mathbf{u}, \partial)\boldsymbol{n}_f$. This will allow us impose continuity across element boundaries on the stress term in the finite element formulation and recover identities similar to the ones above (for a full explanation of the Lagrange multiplier method, see 5.1.1). Furthermore, we apply a backward Euler method for the time discretization for the fluid and a Newmark method for the time discretization of the solid, just as we chose for the parabolic and hyperbolic systems in Chapter 3.

The Robin-Robin splitting method is as follows. Find $\boldsymbol{q}^{n+1}$, $\boldsymbol{\eta}^{n+1} \in \boldsymbol{V}_s$, $\boldsymbol{u}^{n+1} \in \boldsymbol{V}_f$, $p \in M_f$, and $\boldsymbol{\lambda}^{n+1} \in \boldsymbol{V}_g$ such that

$$\rho_s(\partial_{\Delta t}\boldsymbol{q}^{n+1}, \boldsymbol{\xi})_s + a_s(\boldsymbol{\eta}^{n+1/2}, \boldsymbol{\xi}) + \alpha\big\langle(\partial_{\Delta t}\boldsymbol{\eta}^{n+1} - \boldsymbol{u}^n), \boldsymbol{\xi}\big\rangle + \big\langle \boldsymbol{\lambda}^n, \boldsymbol{\xi}\big\rangle = 0 \quad \forall \boldsymbol{\xi} \in \boldsymbol{V}_s. \tag{4.1.6a}$$

$$(\boldsymbol{q}^{n+1/2} - \partial_{\Delta t}\boldsymbol{\eta}^{n+1}, \boldsymbol{\psi})_s = 0 \quad \forall \boldsymbol{\psi} \in \boldsymbol{V}_s. \tag{4.1.6b}$$

$$\rho_f(\partial_{\Delta t}\boldsymbol{u}^{n+1}, \boldsymbol{v})_f + a_f\big((\boldsymbol{u}^{n+1}, p^{n+1}), (\boldsymbol{v}, \theta)\big) - \big\langle \boldsymbol{\lambda}^{n+1}, \boldsymbol{v}\big\rangle = 0 \quad \forall (\boldsymbol{v}, \theta) \in \boldsymbol{V}_f \times M_f. \tag{4.1.6c}$$

$$\alpha\big\langle \boldsymbol{u}^{n+1} - \partial_{\Delta t}\boldsymbol{\eta}^{n+1}, \boldsymbol{\mu}\big\rangle = \big\langle \boldsymbol{\lambda}^n - \boldsymbol{\lambda}^{n+1}, \boldsymbol{\mu}\big\rangle \quad \forall \boldsymbol{\mu} \in \boldsymbol{V}_g. \tag{4.1.6d}$$

In this method, the Robin-Robin interface conditions are imposed just as in Chapter 3. Specifically, in (4.1.6a), we weakly impose the condition

$$\sigma_s(\boldsymbol{\eta}^{n+1})\boldsymbol{n}_s + \alpha\partial_{\Delta t}\boldsymbol{\eta}^{n+1} = \alpha\boldsymbol{u}^n - \boldsymbol{\lambda}^n, \quad \text{on } \Sigma,$$

and in (4.1.6d), we strongly impose

$$\boldsymbol{\lambda}^{n+1} + \alpha\boldsymbol{u}^{n+1} = \alpha\partial_{\Delta t}\boldsymbol{\eta}^{n+1} + \boldsymbol{\lambda}^n \quad \text{on } \Sigma.$$

We also note that we have identities analogous to (3.2.3) and (3.2.5). Namely, using the same approach as in Chapter 3, we find

$$\boldsymbol{q}^{n+1/2} = \partial_{\Delta t}\boldsymbol{\eta}^{n+1}, \quad \text{in } \Omega_s, \tag{4.1.7}$$

and

$$\alpha(\boldsymbol{u}^{n+1} - \boldsymbol{q}^{n+1/2}) = \boldsymbol{\lambda}^n - \boldsymbol{\lambda}^{n+1}, \quad \text{on } \Sigma. \tag{4.1.8}$$

4.2 Stability

In this section we will prove stability of the Robin-Robin splitting method for FSI problems, (4.1.6). However, as mentioned previously, the FSI problem is very similar the the parabolic-hyperbolic coupling, or (3.2.2) with $k = 2$. As a result, the proof of stability is nearly identical to the proof of Lemma 3.3.1. Therefore we will only provide a sketch of the proof for the FSI case, commenting primarily on how to address the pressure term.

As before, the goal for this section is to prove that the energy of the splitting method (4.1.6) at time-step $N = \Delta t T$ is less than the energy at the initial time, $t = 0$.

Lemma 4.2.1. *Let*

$$\begin{aligned}
\mathbf{Z}^{n+1} :=& \frac{\rho_s}{2}\|\boldsymbol{q}^{n+1}\|^2_{L^2(\Omega_s)} + \frac{\rho_f}{2}\|\boldsymbol{u}^{n+1}\|^2_{L^2(\Omega_f)} + \frac{1}{2}\|\boldsymbol{\eta}^{n+1}\|^2_S + \frac{\Delta t\alpha}{2}\|\boldsymbol{u}^{n+1}\|^2_{L^2(\Sigma)} \\
&+ \frac{\Delta t}{2\alpha}\|\boldsymbol{\lambda}^{n+1}\|^2_{L^2(\Sigma)} \\
\mathbf{S}^{n+1} :=& 2\mu\Delta t\|\epsilon(\boldsymbol{u})^{n+1}\|^2_{L^2(\Omega_f)} + \frac{\rho_f}{2}\|\boldsymbol{u}^{n+1} - \boldsymbol{u}^n\|^2_{L^2(\Omega_f)} + \frac{\Delta t\alpha}{2}\|\boldsymbol{q}^{n+1/2} - \boldsymbol{u}^n\|^2_{L^2(\Sigma)}.
\end{aligned}$$

Then it holds,

$$\mathbf{Z}^N + \sum_{n=0}^{N-1}\mathbf{S}^{n+1} = \mathbf{Z}^0.$$

Proof. We begin by mirroring the proof of Lemma 3.3.1, setting $\boldsymbol{\xi} = \Delta t\boldsymbol{q}^{n+1/2}$ and $\boldsymbol{v} = \Delta t\boldsymbol{u}^{n+1}$ in (4.1.6a) and (4.1.6c), respectively. We also apply (4.1.7) to replace all $\partial_{\Delta t}\boldsymbol{\eta}^{n+1}$ with $\boldsymbol{q}^{n+1/2}$.

We also set $\theta = \Delta t p^{n+1}$ in (4.1.6c). In doing so, we encounter a very convenient cancellation of terms in the bilinear form $a_f((\boldsymbol{u}, \partial), (\boldsymbol{v}, \theta))$. Specifically, the terms $-\Delta t(p^{n+1}, \operatorname{div}\boldsymbol{u}^{n+1})_f$ and $\Delta t(\operatorname{div}\boldsymbol{u}^{n+1}, p^{n+1})_f$ will cancel, removing the pressure terms entirely (at least on the interior, as $\boldsymbol{\lambda}$ still technically depends on p).

Consequently, we may add (4.1.6a) and (4.1.6c) together to determine, for $n \geq 0$,

$$\begin{aligned}
&\frac{\rho_s}{2}\|\boldsymbol{q}^{n+1}\|^2_{L^2(\Omega_s)} + \frac{\rho_f}{2}\|\boldsymbol{u}^{n+1}\|^2_{L^2(\Omega_f)} + \frac{\rho_f}{2}\|\boldsymbol{u}^{n+1} - \boldsymbol{u}^n\|^2_{L^2(\Omega_f)} \\
&+ \frac{1}{2}\|\boldsymbol{\eta}^{n+1}\|^2_S + \mu\Delta t\|\epsilon(\boldsymbol{u}^{n+1})\|^2_{L^2(\Omega_f)} \\
&= \frac{1}{2}\|\boldsymbol{q}^n\|^2_{L^2(\Omega_s)} + \frac{1}{2}\|\boldsymbol{u}^n\|^2_{L^2(\Omega_f)} + \frac{1}{2}\|\boldsymbol{\eta}^n\|^2_S + \Delta t\mathbf{J}^{n+1}. \qquad (4.2.1)
\end{aligned}$$

where

$$\mathbf{J}^{n+1} := -\,\alpha\big\langle \boldsymbol{q}^{n+1/2} - \boldsymbol{u}^n, \boldsymbol{q}^{n+1/k}\big\rangle - \big\langle \boldsymbol{\lambda}^n, \boldsymbol{q}^{n+1/2}\big\rangle + \big\langle \boldsymbol{\lambda}^{n+1}, \boldsymbol{u}^{n+1}\big\rangle.$$

Clearly, this is analogous to (3.3.1) in the proof of Lemma 3.3.1, with $\mu\Delta t\|\epsilon(\boldsymbol{u})\|^2_{L^2(\Omega_f)}$ replacing $\frac{\nu_f\Delta t}{2}\|\nabla u\|^2_{L^2(\Omega_f)}$, and $\frac{1}{2}\|\boldsymbol{\eta}\|^2_S$ replacing $\frac{\nu_s}{2}\|\nabla w^{n+1}\|^2_{L^2(\Omega_s)}$.

With these two substitutions, the remainder of this proof follows the proof of Lemma 3.3.1 in the case $k = 2$. $\square$

4.3 Error Analysis

The main result of this chapter is an a priori error estimate of the Robin-Robin splitting method, (4.1.6). Just like in the previous chapter, the proof of this result will proceed in three parts. In the first part, we will bound all but one term in the error analysis. This term will be analogous to the isolated term in Chapter 3, $\frac{\Delta t}{\alpha}\big\langle \Lambda^{n+1}, g_3^{n+1}\big\rangle$. In the second part of the error analysis, we will bound this remaining term as it requires special care, just like in the previous chapter. In the final part, we will state and prove the complete error result.

4.3.1 FSI vs. parabolic-hyperbolic: pressures and parameters

As we saw with the stability result, the similarities between the FSI problem and the parabolic-hyperbolic system mean that the proofs in this chapter will very closely resemble the proofs in Chapter 3. Thus, some of the analysis that follows will resemble the proofs of the previous chapter. However, we will still find that the significant differences between the FSI and parabolic-hyperbolic systems–namely the addition of a pressure term and the presence of physical parameters–add significant complexity to the FSI problem. To accommodate these differences, we will often take a different approach than we used for the parabolic-hyperbolic system.

4.3.1.1 The pressure term

We have already seen that previous methods for stabilizing loosely coupled FSI schemes focused on the pressure term by applying its time derivative as an artificial compressibility in the fluid. Unfortunately, this additional pressure derivative caused a notable loss in accuracy for these schemes. Fortunately, Robin-Robin method does not require artificial compressibility to ensure stability. However, this does not mean that the pressure term won't present us with some difficulties.

Arguably the main challenge when proving the error estimate of (4.1.6) is addressing the pressure term. Indeed, we will see in the second part of the error analysis that the pressure term prevents us from extending fluid stress on the interface into the fluid interior. Instead, any extension from the interface must be into the solid domain, to avoid introducing any pressure errors.

4.3.1.2 The physical parameters

Another important feature of the FSI problem is the presence of physical parameters. We have already seen in the case of the added-mass instability that the solid-fluid density ratio can determine the significance of the added-mass force. Therefore, it is not unreasonable to be concerned about how the values of the physical parameters may impact the convergence of our splitting method. Furthermore, as the values of these quantities will be entirely problem dependent, we run the risk of our splitting method under-performing for certain parameter ranges (as is the case with added-mass instability).

In fact, as mentioned in Chapter 1, when the Robin-Robin method was first introduced, the numerical experiments indicated that the method was sub-optimal, $\mathcal{O}(\sqrt{\Delta t})$. However, results that we will prove in this chapter and supporting numerical experiments (see Section 4.5) will show that this assumption was not correct. The Robin-Robin method is nearly optimal, and the incorrect assumption was caused by the scheme's sensitivity to physical parameters. We will discuss this in detail in 4.4.1.

In response to this concern, we will take special care to account for all physical parameters as we conduct our error analysis.

4.3.2 The Error Equations

We begin the error analysis as in the previous chapter. Recall that we wish to compare the solution to the continuous problem (4.1.4) with the solution to the Robin-Robin method (4.1.6). Thus, We define the error terms

$$\begin{aligned} \boldsymbol{e_u}^n &= \mathbf{u}^n - \boldsymbol{u}^n, \quad e_p^n = \mathsf{p}^n - p^n, \\ \boldsymbol{e}_\eta^n &= \mathbf{e}^n - \boldsymbol{\eta}^n, \quad \boldsymbol{e_q}^n = \mathbf{q}^n - \boldsymbol{q}^n, \\ \boldsymbol{e_\lambda}^n &= \mathbf{l}^n - \boldsymbol{\lambda}^n. \end{aligned}$$

We assume that the initial condition are the same for both the continuous and Robin-Robin problems, so the errors vanish at $t = 0$. Then, using the same approach as in Section 3.4.1, we derive the error equations.

$$\rho_s(\partial_{\Delta t}\boldsymbol{e_q}^{n+1}, \boldsymbol{\xi})_s + a_s(\boldsymbol{e}_\eta^{n+1}, \boldsymbol{\xi}) + \alpha\big\langle(\partial_{\Delta t}\boldsymbol{e}_\eta^{n+1} - \boldsymbol{e_u}^n), \boldsymbol{\xi}\big\rangle + \big\langle \boldsymbol{e_\lambda}^n, \boldsymbol{\xi}\big\rangle = \boldsymbol{L}_1(\boldsymbol{\xi}) - \boldsymbol{L}_4(\boldsymbol{\xi}), \tag{4.3.1a}$$

$$(\boldsymbol{e_q}^{n+1/2} - \partial_{\Delta t}\boldsymbol{e}_\eta^{n+1}, \boldsymbol{\psi})_s = \boldsymbol{L}_2(\boldsymbol{\psi}), \tag{4.3.1b}$$

$$\rho_f(\partial_{\Delta t}\boldsymbol{e_u}^{n+1}, \boldsymbol{v})_f + a_f((\boldsymbol{e_u}^{n+1}, e_p^{n+1})(\boldsymbol{v}, \theta)) - \big\langle \boldsymbol{e_\lambda}^{n+1}, \boldsymbol{v}\big\rangle = \boldsymbol{L}_3(\boldsymbol{v}), \tag{4.3.1c}$$

$$\alpha\big\langle \boldsymbol{e_u}^{n+1} - \partial_{\Delta t}\boldsymbol{e}_\eta^{n+1}, \boldsymbol{\mu}\big\rangle + \big\langle \boldsymbol{e_\lambda}^{n+1} - \boldsymbol{e_\lambda}^n, \boldsymbol{\mu}\big\rangle = \boldsymbol{L}_4(\boldsymbol{\mu}). \tag{4.3.1d}$$

where

$$\begin{aligned}
\boldsymbol{L}_1(\boldsymbol{\xi}) :=& \frac{1}{2}\big\langle \boldsymbol{g}_2^{n+1}, \boldsymbol{\xi}\big\rangle + \alpha\big\langle \boldsymbol{g}_1^{n+1}, \boldsymbol{\xi}\big\rangle - \rho_s(\boldsymbol{h}_1^{n+1}, \boldsymbol{\xi})_s,\\
\boldsymbol{L}_2(\boldsymbol{\psi}) :=& (\boldsymbol{h}_3^{n+1}, \boldsymbol{\psi})_s,\\
\boldsymbol{L}_3(\boldsymbol{v}) :=& -\rho_f(\boldsymbol{h}_2^{n+1}, \boldsymbol{v})_f,\\
\boldsymbol{L}_4(\mu) :=& \alpha\big\langle \boldsymbol{h}_4^{n+1}, \boldsymbol{\mu}\big\rangle + \big\langle \boldsymbol{g}_2^{n+1}, \boldsymbol{\mu}\big\rangle,
\end{aligned}$$

and

$$\begin{aligned}
\boldsymbol{h}_1^{n+1} &:= \partial_t \mathbf{q}^{n+1/2} - \partial_{\Delta t}\mathbf{q}^{n+1}, \quad \boldsymbol{g}_1^{n+1} := \mathbf{u}^{n+1} - \mathbf{u}^n,\\
\boldsymbol{h}_2^{n+1} &:= \partial_t \mathbf{u}^{n+1} - \partial_{\Delta t}\mathbf{u}^{n+1}, \qquad \boldsymbol{g}_2^{n+1} := \mathbf{l}^{n+1} - \mathbf{l}^n,\\
\boldsymbol{h}_3^{n+1} &:= \partial_t \mathbf{e}^{n+1/2} - \partial_{\Delta t}\mathbf{e}^{n+1},\\
\boldsymbol{h}_4^{n+1} &:= \partial_t \mathbf{e}^{n+1} - \partial_{\Delta t}\mathbf{e}^{n+1}.
\end{aligned}$$

Just as in Chapter 3, the $\{\boldsymbol{h}_i\}_{i=1}^4$ represent the error acquired from the time discretization, and the $\{\boldsymbol{g}_i\}_{i=1}^2$ represent the residual error produced by the Robin-Robin splitting method. We also have the following results as consequences of (4.3.1). They are derived in the same manner as (3.4.2)-(4.3.4).

$$
\begin{aligned}
\boldsymbol{e_q}^{n+1/2} =& \partial_{\Delta t}\boldsymbol{e}_\eta^{n+1} + \boldsymbol{h}_3^{n+1} && \text{on } \Omega_s, && (4.3.2)\\
\alpha(\boldsymbol{e_u}^{n+1} - \partial_{\Delta t}\boldsymbol{e}_\eta^{n+1}) =& \boldsymbol{e_\lambda}^n - \boldsymbol{e_\lambda}^{n+1} + \alpha\boldsymbol{h}_4^{n+1} + \boldsymbol{g}_2^{n+1} && \text{on } \Sigma, && (4.3.3)\\
\alpha\big(\boldsymbol{e_u}^{n+1} - \boldsymbol{e_q}^{n+1/2}\big) =& \boldsymbol{e_\lambda}^n - \boldsymbol{e_\lambda}^{n+1} + \boldsymbol{g}_3^{n+1} && \text{on } \Sigma, && (4.3.4)
\end{aligned}
$$

where

$$
\boldsymbol{g}_3^{n+1} := \frac{\alpha}{2}\boldsymbol{g}_1^{n+1} + \boldsymbol{g}_2^{n+1}.
$$

Finally, we define the following quantities that will make up our error estimates.

$$
\begin{aligned}
\mathsf{Z}^{n+1} :=& \frac{\rho_s}{2}\|\boldsymbol{e_q}^{n+1}\|^2_{L^2(\Omega_s)} + \frac{\rho_f}{2}\|\boldsymbol{e_u}^{n+1}\|^2_{L^2(\Omega_f)} + \frac{1}{2}\|\boldsymbol{e}_\eta^{n+1}\|_S \\
&+ \frac{\Delta t\alpha}{2}\|\boldsymbol{e_u}^{n+1}\|^2_{L^2(\Sigma)} + \frac{\Delta t}{2\alpha}\|\boldsymbol{e_\lambda}^{n+1}\|^2_{L^2(\Sigma)},\\
\mathsf{S}^{n+1} :=& 2\mu\Delta t\|\varepsilon(\boldsymbol{e_u}^{n+1})\|^2_{L^2(\Omega_f)} + \frac{\rho_f}{2}\|\boldsymbol{e_u}^{n+1} - \boldsymbol{e_u}^n\|^2_{L^2(\Omega_f)}\\
&+ \frac{\Delta t\alpha}{2}\|\boldsymbol{e_u}^n - \boldsymbol{e_q}^{n+1/2}\|^2_{L^2(\Sigma)}.
\end{aligned}
$$

4.3.3 Step 1: Preliminary Estimates

As before, we begin the first step of the error analysis with a preliminary bound analogous to Lemma 3.4.1.

Lemma 4.3.1. *It holds,*

$$
\mathsf{Z}^{n+1} + \mathsf{S}^{n+1} = \mathsf{Z}^n + \Delta t\mathbf{F}^{n+1} + \frac{\Delta t}{\alpha}\big\langle \boldsymbol{g}_3^{n+1}, \boldsymbol{e_\lambda}^n\big\rangle, \qquad (4.3.5)
$$

where

$$\begin{aligned}\mathbf{F}^{n+1} :=& \frac{1}{2\alpha}\|\boldsymbol{g}_3^{n+1}\|^2_{L^2(\Sigma)} + \left\langle \boldsymbol{g}_4^{n+1}, \boldsymbol{e_q}^{n+1/2}\right\rangle - a_s(\boldsymbol{e}_\eta^{n+1/2}, \boldsymbol{h}_3^{n+1/2}) \\ & - \rho_s(\boldsymbol{h}_1^{n+1}, \boldsymbol{e_q}^{n+1/2})_s - \rho_f(\boldsymbol{h}_2^{n+1}, \boldsymbol{e_u}^{n+1})_f,\end{aligned}$$

and

$$\boldsymbol{g}_4^{n+1} := \alpha \boldsymbol{g}_1^{n+1} + \frac{1}{2}\boldsymbol{g}_2^{n+1}.$$

Proof. To begin, we set $\boldsymbol{\xi} = \Delta t \boldsymbol{e_q}^{n+1/2}$ in (4.3.1a) and $\boldsymbol{v} = \Delta t \boldsymbol{e_u}^{n+1}$ and $\theta = \Delta t e_p^{n+1}$ in (4.3.1c). As in the proof of Lemma 4.2.1, this leads to a cancellation of the pressure terms in (4.3.1c).

We also use (4.3.2) to address the terms in the solid bilinear form $a_s(\cdot,\cdot)$. Consequently, this yields

$$\begin{aligned}&\frac{\rho_s}{2}\|\boldsymbol{e_q}^{n+1}\|^2_{L^2(\Omega_s)} + \frac{\rho_f}{2}\|\boldsymbol{e_u}^{n+1}\|^2_{L^2(\Omega_f)} + \frac{\rho_f}{2}\|\boldsymbol{e_u}^{n+1} - \boldsymbol{e_u}^{n}\|^2_{L^2(\Omega_f)} \\ &+ \frac{1}{2}\|\boldsymbol{e}_\eta^{n+1}\|_S + 2\mu\Delta t\|\varepsilon(\boldsymbol{e_u}^{n+1})\|^2_{L^2(\Omega_f)} \\ &= \frac{\rho_s}{2}\|\boldsymbol{e_q}^{n}\|^2_{L^2(\Omega_s)} + \frac{\rho_f}{2}\|\boldsymbol{e_u}^{n}\|^2_{L^2(\Omega_f)} + \frac{1}{2}\|\boldsymbol{e}_\eta^{n}\|^2_S + \Delta t \mathbf{J}^{n+1}.\end{aligned} \tag{4.3.6}$$

where

$$\begin{aligned}\mathbf{J}^{n+1} :=& \alpha\left\langle \boldsymbol{e_u}^{n} - \partial_{\Delta t}\boldsymbol{e}_\eta^{n+1}, \boldsymbol{e_q}^{n+1/2}\right\rangle - \left\langle \boldsymbol{e_\lambda}^{n}, \boldsymbol{e_q}^{n+1/2}\right\rangle + \left\langle \boldsymbol{e_\lambda}^{n+1}, \boldsymbol{e_u}^{n+1}\right\rangle \\ & - a_s(\boldsymbol{e}_\eta^{n+1/2}, \boldsymbol{h}_3^{n+1}) + \boldsymbol{L}_1(\boldsymbol{e_q}^{n+1/2}) - \boldsymbol{L}_4(\boldsymbol{e_q}^{n+1/2}) + \boldsymbol{L}_3(\boldsymbol{e_u}^{n+1/2})\end{aligned}$$

At this point, we note that the value $\mathbf{J}^{n+1}$ is analogous to the value J^{n+1} used in the proof of Lemma 3.4.1 for $k = 2$. However, in order to accommodate the later steps of the analysis (see Section 4.3.4), we will manipulate the terms of $\mathbf{J}^{n+1}$ slightly differently.

Thus, we write

$$\begin{aligned}\mathbf{J}^{n+1} :=& \alpha\left\langle \boldsymbol{e_u}^{n} - \boldsymbol{e_u}^{n+1}, \boldsymbol{e_q}^{n+1/2}\right\rangle + \left\langle \boldsymbol{e_\lambda}^{n+1}, \boldsymbol{e_u}^{n+1}\right\rangle \\ &+ \alpha\left\langle \boldsymbol{e_u}^{n+1} - \partial_{\Delta t}\boldsymbol{e}_\eta^{n+1} - \boldsymbol{h}_4^{n+1} - \frac{1}{\alpha}\boldsymbol{e_\lambda}^{n} - \frac{1}{\alpha}\boldsymbol{g}_2^{n+1}, \boldsymbol{e_q}^{n+1/2}\right\rangle \\ &+ \frac{1}{2}\left\langle \boldsymbol{g}_2^{n+1}, \boldsymbol{e_q}^{n+1/2}\right\rangle + \alpha\left\langle \boldsymbol{g}_1^{n+1}, \boldsymbol{e_q}^{n+1/2}\right\rangle + \mathbf{G}^{n+1},\end{aligned}$$

where

$$\mathbf{G}^{n+1} := -\rho_s(\boldsymbol{h}_1^{n+1}, \boldsymbol{e_q}^{n+1/2})_s - \rho_f(\boldsymbol{h}_2^{n+1}, \boldsymbol{e_u}^{n+1})_f - a_s(\boldsymbol{e}_\eta^{n+1/2}, \boldsymbol{h}_3^{n+1/2}).$$

Using (4.3.3) and (4.3.4), we may then write

$$\begin{aligned}\mathbf{J}^{n+1} :=& \alpha\left\langle \boldsymbol{e_u}^{n} - \boldsymbol{e_u}^{n+1}, \boldsymbol{e_q}^{n+1/2}\right\rangle + \left\langle \boldsymbol{e_\lambda}^{n+1}, \boldsymbol{e_u}^{n+1} - \boldsymbol{e_q}^{n+1/2}\right\rangle \\ &+ \left\langle \boldsymbol{g}_4^{n+1}, \boldsymbol{e_q}^{n+1/2}\right\rangle + \mathbf{G}^{n+1} \\ =& \alpha\left\langle \boldsymbol{e_u}^{n} - \boldsymbol{e_u}^{n+1}, \boldsymbol{e_q}^{n+1/2}\right\rangle + \frac{1}{\alpha}\left\langle \boldsymbol{e_\lambda}^{n+1}, \boldsymbol{e_\lambda}^{n} - \boldsymbol{e_\lambda}^{n+1}\right\rangle \\ &+ \frac{1}{\alpha}\left\langle \boldsymbol{e_\lambda}^{n+1}, \boldsymbol{g}_3^{n+1}\right\rangle + \left\langle \boldsymbol{g}_4^{n+1}, \boldsymbol{e_q}^{n+1/2}\right\rangle + \mathbf{G}^{n+1}.\end{aligned}$$

It therefore follows from Lemma 2.1.6 that we have

$$\begin{aligned}\mathbf{J}^{n+1} =& \frac{\alpha}{2}(\|\boldsymbol{e_u}^{n}\|^2_{L^2(\Sigma)} - \|\boldsymbol{e_u}^{n+1}\|^2_{L^2(\Sigma)} - \|\boldsymbol{e_u}^{n} - \boldsymbol{e_q}^{n+1/2}\|^2_{L^2(\Sigma)} + \|\boldsymbol{e_u}^{n+1} - \boldsymbol{e_q}^{n+1/2}\|^2_{L^2(\Sigma)}) \\ &+ \frac{1}{2\alpha}(\|\boldsymbol{e_\lambda}^{n}\|^2_{L^2(\Sigma)} - \|\boldsymbol{e_\lambda}^{n+1}\|^2_{L^2(\Sigma)} - \|\boldsymbol{e_\lambda}^{n+1} - \boldsymbol{e_\lambda}^{n}\|^2_{L^2(\Sigma)}) \\ &+ \frac{1}{\alpha}\left\langle \boldsymbol{e_\lambda}^{n+1}, \boldsymbol{g}_3^{n+1}\right\rangle + \left\langle \boldsymbol{g}_4^{n+1}, \boldsymbol{e_q}^{n+1/2}\right\rangle + \mathbf{G}^{n+1}.\end{aligned}$$

We now note

$$\frac{-1}{2\alpha}\|\boldsymbol{e_\lambda}^{n+1} - \boldsymbol{e_\lambda}^{n}\|^2_{L^2(\Sigma)} = \frac{-\alpha}{2}\|\boldsymbol{e_u}^{n+1} - \boldsymbol{e_q}^{n+1/2}\|^2_{L^2(\Sigma)} + \frac{1}{\alpha}\big\langle \boldsymbol{e_\lambda}^{n} - \boldsymbol{e_\lambda}^{n+1}, \boldsymbol{g}_3^{n+1}\big\rangle + \frac{1}{2\alpha}\|\boldsymbol{g}_3^{n+1}\|^2_{L^2(\Sigma)}.$$

Consequently, we have

$$\begin{aligned}\mathbf{J}^{n+1} =& \frac{\alpha}{2}(\|\boldsymbol{e_u}^{n}\|^2_{L^2(\Sigma)} - \|\boldsymbol{e_u}^{n+1}\|^2_{L^2(\Sigma)} - \|\boldsymbol{e_u}^{n} - \boldsymbol{e_q}^{n+1/2}\|^2_{L^2(\Sigma)}) \\ &+ \frac{1}{2\alpha}(\|\boldsymbol{e_\lambda}^{n}\|^2_{L^2(\Sigma)} - \|\boldsymbol{e_\lambda}^{n+1}\|^2_{L^2(\Sigma)}) + \frac{1}{\alpha}\big\langle \boldsymbol{e_\lambda}^{n}, \boldsymbol{g}_3^{n+1}\big\rangle \\ &+ \frac{1}{2\alpha}\|\boldsymbol{g}_3^{n+1}\|^2_{L^2(\Sigma)} + \big\langle \boldsymbol{g}_4^{n+1}, \boldsymbol{e_q}^{n+1/2}\big\rangle + \mathbf{G}^{n+1}.\end{aligned}$$

Plugging these results into (4.3.6) completes the proof. □

4.3.3.1 Estimate for $\mathbf{F}^{n+1}$

As in the previous chapter, we have successfully isolated the term that will require special care in the error analysis. In this case, the term is $\frac{\Delta t}{\alpha}\big\langle \boldsymbol{g}_3^{n+1}, \boldsymbol{e_\lambda}^{n}\big\rangle$. We note that, unlike in Chapter 3, the error term is at the previous time-step. However, because the pressure terms are completely eliminated in the first step of the proof, it would have been be very straightforward for us to mirror the proof of Lemma 3.4.1 above. This would have instead left the isolated term $\frac{\Delta t}{\alpha}\big\langle \boldsymbol{g}_3^{n+1}, \boldsymbol{e_\lambda}^{n+1}\big\rangle$.

The reason that we chose *not* to mirror the proof of Lemma 3.4.1 will become clear in the next section. However, first we will bound the terms in $\mathbf{F}^{n+1}$ using the same approach we used in Lemma 3.4.2.

Lemma 4.3.2. *Let $1 \leq M \leq N$, then*

$$\Delta t \sum_{n=0}^{M-1} \mathbf{F}^{n+1} \leq \frac{1}{4} \max_{1\leq n\leq M} \mathsf{Z}^n + \frac{1}{4} \sum_{n=0}^{M-1} \mathsf{S}^{n+1} + C\mathbf{D}(M), \tag{4.3.7}$$

where

$$\begin{aligned}\mathbf{D}(M) :=& \Delta t T \sum_{n=0}^{M-1} \Big(\rho_s \|\boldsymbol{h}_1^{n+1}\|^2_{L^2(\Omega_s)} + \rho_f \|\boldsymbol{h}_2^{n+1}\|^2_{L^2(\Omega_f)} + \|\boldsymbol{h}_3^{n+1}\|^2_S \Big) \\ &+ \Delta t \sum_{n=0}^{M-1} \left(\Big(\frac{1}{\alpha} + \frac{1}{\mu} \Big) \|\boldsymbol{g}_4^{n+1}\|^2_{L^2(\Sigma)} + \frac{1}{2\alpha} \|\boldsymbol{g}_3^{n+1}\|^2_{L^2(\Sigma)} \right).\end{aligned}$$

Proof. All of the methods in this proof will mirror the methods in the proof of Lemma 3.4.2 with the appropriate substitutions. Specifically, the terms $a_s(\boldsymbol{e}_\eta^{n+1/2}, \boldsymbol{h}_3^{n+1/2})$, $\rho_s(\boldsymbol{h}_1^{n+1}, \boldsymbol{e_q}^{n+1/2})_s$, and $\rho_f(\boldsymbol{h}_2^{n+1}, \boldsymbol{e_u}^{n+1})_f$ may be bounded in the same way as the terms $\langle g_4^{n+1}, Q^{n+1/k} \rangle$, $\nu_s(\nabla W^{n+1/k}, \nabla h_3^{n+1})_s$, $(h_1^{n+1}, Q^{n+1/k})_s$, and $(h_2^{n+1}, U^{n+1})_f$, respectively.

This gives us the bound

$$\begin{aligned}&- \Delta t \sum_{n=0}^{M-1} \Big(\rho_s(\boldsymbol{h}_1^{n+1}, \boldsymbol{e_q}^{n+1/2})_s + \rho_f(\boldsymbol{h}_2^{n+1}, \boldsymbol{e_u}^{n+1})_f + a_s(\boldsymbol{e}_\eta^{n+1/2}, \boldsymbol{h}_3^{n+1}) \Big) \\ \leq& \frac{1}{4} \max_{1\leq n\leq M} \mathsf{Z}^n + C\Delta t T \sum_{n=0}^{M-1} \Big(\rho_s \|\boldsymbol{h}_1^{n+1}\|^2_{L^2(\Omega_s)} + \rho_f \|\boldsymbol{h}_2^{n+1}\|^2_{L^2(\Omega_f)} + \|\boldsymbol{h}_3^{n+1}\|^2_S \Big).\end{aligned}$$

The term $\frac{1}{2\alpha}\|\boldsymbol{g}_3^{n+1}\|_{L^2(\Sigma)}$ is already in the form we need, so we are left with one remaining term to bound, $\langle \boldsymbol{g}_4^{n+1}, \boldsymbol{e_q}^{n+1/2} \rangle$. For this, we write

$$\begin{aligned}\Delta t \sum_{n=0}^{M-1} \langle \boldsymbol{g}_4^{n+1}, \boldsymbol{e_q}^{n+1/2} \rangle =& \Delta t \sum_{n=0}^{M-1} \big(\langle \boldsymbol{g}_4^{n+1}, \boldsymbol{e_q}^{n+1/2} - \boldsymbol{e_u}^n \rangle + \langle \boldsymbol{g}_4^{n+1}, \boldsymbol{e_u}^n \rangle \big) \\ \leq& \sum_{n=0}^{M-1} \|\boldsymbol{g}_4^{n+1}\|_{L^2(\Sigma)} \big(\|\boldsymbol{e_q}^{n+1/2} - \boldsymbol{e_u}^n\|^2_{L^2(\Sigma)} + \|\boldsymbol{e_u}^n\|^2_{L^2(\Sigma)} \big).\end{aligned}$$

Then, applying (2.1.5) and Korn's inequality (see Lemma 2.1.13), followed by Young's inequality, we find

$$\begin{aligned}
\Delta t \sum_{n=0}^{M-1} \left\langle \boldsymbol{g}_4^{n+1}, \boldsymbol{e_q}^{n+1/2} \right\rangle \leq & C \Delta t \sum_{n=0}^{M-1} \left(\frac{1}{\alpha} + \frac{1}{\mu} \right) \| \boldsymbol{g}_4^{n+1} \|^2_{L^2(\Sigma)} \\
& + \Delta t \sum_{n=0}^{M-1} \left(\frac{\alpha}{8} \| \boldsymbol{e_q}^{n+1/2} - \boldsymbol{e_u}^n \|^2_{L^2(\Sigma)} + \frac{\mu}{4} \| \varepsilon(\boldsymbol{e_u}^n) \|^2_{L^2(\Omega_f)} \right) \\
\leq & \frac{1}{4} \sum_{n=0}^{M-1} \mathsf{S}^{n+1} + C \Delta t \sum_{n=0}^{M-1} \left(\frac{1}{\alpha} + \frac{1}{\mu} \right) \| \boldsymbol{g}_4^{n+1} \|^2_{L^2(\Sigma)},
\end{aligned}$$

where we use that $\boldsymbol{e_u}^0 = 0$.

Combining these bounds completes the results. □

4.3.4 Step 2: Estimate for $\frac{\Delta t}{\alpha} \left\langle \boldsymbol{g}_3^{n+1}, \boldsymbol{e_\lambda}^n \right\rangle$

We now wish to bound the remaining term in our error analysis,

$$\frac{\Delta t}{\alpha} \sum_{n=0}^{M-1} \left\langle \boldsymbol{g}_3^{n+1}, \boldsymbol{e_\lambda}^n \right\rangle.$$

Up until this point, the proofs in this chapter have loosely followed the methods used for the parabolic-hyperbolic system in Chapter 3. This has been possible because, so far, the pressure terms have cancelled out of our error analysis. However, we can only be so lucky for so long.

We need to approach this term carefully or we risk finding a sub-optimal bound, as demonstrated in 3.5.3. Thus, the most obvious approach seems to be to continue following the method of Chapter 3. We have a residual term, g_3^{n+1} and the error term corresponding to the fluid stress tensor, so it seems reasonable to use (4.3.1c) to move the term from the interface Σ into the interior Ω_f.

However, unlike in Chapter 3, we will now pick up a pressure term, even if we assume $\theta = 0$. More specifically, if $\tilde{\boldsymbol{g}}_3^{n+1}$ is an appropriate extension of $\boldsymbol{g}_3^{n+1}$, we find

$$\begin{aligned}\frac{\Delta t}{\alpha}\langle \tilde{\boldsymbol{g}}_3^{n+1}, \boldsymbol{e_\lambda}^n \rangle =& \frac{\rho_f}{\alpha}(\partial_{\Delta t}\boldsymbol{e_u}^n, \tilde{\boldsymbol{g}}_3^{n+1})_f + \frac{2\mu\Delta t}{\alpha}(\varepsilon(\boldsymbol{e_u}^n), \varepsilon(\tilde{\boldsymbol{g}}_3^{n+1}))_f \\ &- \frac{\Delta t}{\alpha}(e_p^n, \operatorname{div}\tilde{\boldsymbol{g}}_3^{n+1})_f - \boldsymbol{L}_3(\tilde{\boldsymbol{g}}_3^{n+1}).\end{aligned}$$

Proceeding with the method in Chapter 3 will then lead to a term of the form $\Delta t\|e_p^n\|^2_{L^2(\Omega_f)}$ on the right-hand side of our error estimate that cannot be balanced or absorbed by any term on the left-hand side. Attempting to address this issue using an inf-sup argument will also present difficulties as we will pick up a factor of $(\Delta t)^{-1}$ from the time discretization.

Thus it seems that our luck has run out! We can no longer rely on the techniques of Chapter 3 to see us through this error analysis, and we may finally appreciate the warnings provided earlier in the chapter regarding the pressure term.

The solution, however, is deceptively straightforward: *pull* $\boldsymbol{e_\lambda}^n$ *from* Σ *into* Ω_s *instead of* Ω_f.

Initially, this seems like a very counter-intuitive approach; the term $\boldsymbol{e_\lambda}^n$ represents the *fluid* stress at the interface, and $\boldsymbol{g}_3^{n+1}$ represents a *fluid* residual term. However, recall that terms at the interface interact with both domains, so we do not necessarily have to restrict ourselves to Ω_f or Ω_s.

This is also why we chose to manipulate the terms in our error analysis so that we isolate ${\boldsymbol{e}_{\boldsymbol{\lambda}}}^n$ rather than ${\boldsymbol{e}_{\boldsymbol{\lambda}}}^{n+1}$ in Lemma 4.3.1. Indeed, we note that ${\boldsymbol{e}_{\boldsymbol{\lambda}}}^n$ shows up in (4.3.1a), so we may use this in the same way we use (3.4.1c) in Section 3.4.3. Furthermore, we may utilize the exact interface conditions (4.1.3) to rewrite the residual term $\boldsymbol{g}_3^{n+1}$ in terms of values defined on Ω_s. More specifically, on Σ we may write

$$\begin{aligned}
\boldsymbol{g}_3^{n+1} =& \frac{\alpha}{2}\boldsymbol{g}_1^{n+1} + \boldsymbol{g}_2^{n+1} \\
=& \frac{\alpha}{2}(\mathbf{u}^{n+1} - \mathbf{u}^n) + \mathbf{l}^{n+1} - \mathbf{l}^n \\
=& \frac{\alpha}{2}(\mathbf{q}^{n+1} - \mathbf{q}^n) - \sigma_s(\mathbf{e}^{n+1} - \mathbf{e}^n)\boldsymbol{n}_s \\
=& \frac{\alpha}{2}(\mathbf{q}^{n+1} - \mathbf{q}^n) - (\mathbf{l}_s^{n+1} - \mathbf{l}^n), \quad \text{on } \Sigma,
\end{aligned}$$

where $\mathbf{l}^n := \sigma_s(\mathbf{e}^n)\boldsymbol{n}_s$.

We may now extend $\boldsymbol{g}_3^{n+1}$ from $\boldsymbol{V}^g$ into $\boldsymbol{V}^s$ in much the same way that we moved from V_g tp V_f in Section 3.4.3. Thus we make two assumptions. First, we assume that the normal $\boldsymbol{n}_s$ (now to Ω_s, rather than Ω_f) can be extended from Σ into Ω_s in such a way that its gradient is bounded.

Assumption 4.3.3. There exists $\tilde{\boldsymbol{n}}_s \in [\mathbf{W}^{1,\infty}(\Omega_s)]^2$ such that $\tilde{\boldsymbol{n}}_s|_\Sigma = \boldsymbol{n}_s$.

As before, this assumption is only a concern when the interface is non-smooth.

The second assumption is the existence of a function $\tilde{\phi} : \Omega_s \to \mathbb{R}$ that serves the same purpose as ϕ in Chapter 3.

Assumption 4.3.4. Assume that the time step is given and satisfies $\Delta t < \frac{1}{2}$. There exists a function $\tilde{\phi} : \Omega_s \to \mathbb{R}$ satisfying:

(i) $0 \leq \tilde{\phi} \leq 1$,

(ii) $\tilde{\phi} \in \boldsymbol{V}^s$,

(iii) $|\{x \in \Sigma : \tilde{\phi}(x) \neq 1\}| = C\Delta t$,

(iv) $\|\nabla\tilde{\phi}\|^2_{L^2(\Omega_s)} \leq C(1 + \log \frac{1}{\Delta t})$,

where each C represents a general constant independent of Δt and the physical parameters.

We are now back in familiar territory for the time being, so we proceed in the same manner as Chapter 3. Recall that we defined ϕ in Section 3.4.3 because we needed to lift g_2^{n+1} from Σ into V_f, since the term is only defined on Σ and will not, in general, vanish on $\partial\Omega_f \setminus \Sigma$. We now have the same situation for the FSI problem. The residual $\boldsymbol{g}_2^{n+1} = -\sigma_s(\mathbf{e}^{n+1} - \mathbf{e}^n)\boldsymbol{n}_s$ is only defined on Σ, and will not necessarily vanish on $\partial\Omega_s \setminus \Sigma$. Thus, in order to extend this term into $\boldsymbol{V}^s$ appropriately, we use the assumptions above to define

$$\begin{aligned}
\tilde{\mathbf{l}}_s(x,t) :=& \sigma_s(\mathbf{e}(x,t))\tilde{\boldsymbol{n}}_s, \\
\mathcal{L}_s(x,t) :=& \tilde{\phi}(x)\tilde{\mathbf{l}}_s(x,t), \\
\tilde{\boldsymbol{g}}_2^{n+2} :=& -(\mathcal{L}_s^{n+1} - \mathcal{L}_s^n).
\end{aligned}$$

Note that we used (4.1.3b) to rewrite the terms of $\boldsymbol{g}_2^{n+1}$ so that we may extend it into Ω_s, as explained above. We now have $\tilde{\boldsymbol{g}}_2^{n+1} \in \boldsymbol{V}^s$ such that we may prove the following result, analogous to Lemma 3.4.5.

Lemma 4.3.5. *Under Assumptions 4.3.3 and 4.3.4 we have*

$$\|\tilde{\boldsymbol{g}}_2^{n+1} - \boldsymbol{g}_2^{n+1}\|^2_{L^2(\Sigma)} \leq C\Delta t\|\boldsymbol{g}_2^{n+1}\|^2_{L^\infty(\Sigma)}. \tag{4.3.8}$$

Proof. See the proof of Lemma 3.4.5. □

We may now state the error bound.

Lemma 4.3.6. *Under Assumptions 3.4.3, 3.4.4 we have*

$$\frac{\Delta t}{\alpha}\sum_{n=0}^{M-1}\left\langle \boldsymbol{g}_3^{n+1}, \boldsymbol{e_\lambda}^n\right\rangle \leq \frac{1}{4}\max_{0\leq m\leq M}\mathsf{Z}^m + \frac{1}{4}\sum_{n=0}^{M-1}\mathsf{S}^{n+1} + C\boldsymbol{\Psi}(M),$$

where

$$\begin{aligned}
\boldsymbol{\Psi}(M) :=& \boldsymbol{\Psi}_1(M) + \boldsymbol{\Psi}_2(M)\\
\boldsymbol{\Psi}_1(M) :=& T(\Delta t)^3\rho_s\sum_{n=0}^{M-1}\|\partial_{\Delta t}^2\mathsf{q}^n\|_{L^2(\Omega_s)}^2 + \rho_s\|\boldsymbol{g}_1^M\|_{L^2(\Omega_s)}^2\\
&+ \Delta t\sum_{n=0}^{M-1}\Big(T\|\boldsymbol{g}_1^{n+1}\|_S^2 + \big(1+\alpha\big)\|\boldsymbol{g}_1^{n+1}\|_{L^2(\Sigma)}^2 + \|\boldsymbol{g}_2^{n+1}\|_{L^2(\Sigma)}^2\\
&\qquad + \rho_s\|\boldsymbol{h}_1^{n+1}\|_{L^2(\Omega_s)}^2 + \rho_s\|\boldsymbol{g}_1^{n+1}\|_{L^2(\Omega_s)}^2\Big)\\
\boldsymbol{\Psi}_2(M) :=& \frac{T(\Delta t)^3\rho_s}{\alpha^2}\sum_{n=0}^{M-1}\|\partial_{\Delta t}^2\mathcal{L}_s^n\|_{L^2(\Omega_s)}^2 + \frac{\rho_s}{\alpha^2}\|\tilde{\boldsymbol{g}}_2^M\|_{L^2(\Omega_s)}^2\\
&+ \Delta t\sum_{n=0}^{M-1}\Big(\frac{T}{\alpha^2}\|\tilde{\boldsymbol{g}}_2^{n+1}\|_S^2 + \big(1+\frac{1}{\alpha}\big)\|\boldsymbol{g}_2^{n+1}\|_{L^2(\Sigma)}^2 + \|\boldsymbol{g}_1^{n+1}\|_{L^2(\Sigma)}^2\\
&\qquad + \rho_s\|\boldsymbol{h}_1^{n+1}\|_{L^2(\Omega_s)}^2 + \frac{\rho_s}{\alpha^2}\|\tilde{\boldsymbol{g}}_2^{n+1}\|_{L^2(\Omega_s)}^2 + \frac{T}{\alpha}\|\boldsymbol{g}_2^{n+1}\|_{L^\infty(\Sigma)}^2\Big).
\end{aligned}$$

Proof. We begin in the same manner as Lemma 3.4.6, using the definition of $\boldsymbol{g}_3^{n+1}$ to write

$$\frac{\Delta t}{\alpha}\sum_{n=0}^{M-1}\left\langle \boldsymbol{g}_3^{n+1}, \boldsymbol{e_\lambda}^n\right\rangle = \frac{\Delta t}{\alpha}\sum_{n=0}^{M-1}\left\langle \boldsymbol{g}_2^{n+1}, \boldsymbol{e_\lambda}^n\right\rangle + \frac{\Delta t}{2}\sum_{n=0}^{M-1}\left\langle \boldsymbol{g}_1^{n+1}, \boldsymbol{e_\lambda}^n\right\rangle. \tag{4.3.9}$$

Recall that when we are on Σ we may use (4.1.3a) to write $\boldsymbol{g}_1^{n+1} = \mathbf{q}^{n+1} - \mathbf{q}^n$ on Σ. Thus, unlike $\boldsymbol{g}_2^{n+1}$, it has a natural extension into Ω_s. This will not be the case for

$\boldsymbol{g}_2^{n+1}$, so we address this more difficult term first using the extension $\tilde{\boldsymbol{g}}_2^{n+1}$ we defined above. Thus, we have

$$\frac{\Delta t}{\alpha}\sum_{n=0}^{M-1}\big\langle \boldsymbol{g}_2^{n+1}, \boldsymbol{e_\lambda}^n\big\rangle = \frac{\Delta t}{\alpha}\sum_{n=0}^{M-1}\big\langle \boldsymbol{g}_2^{n+1} - \tilde{\boldsymbol{g}}_2^{n+1}, \boldsymbol{e_\lambda}^n\big\rangle + \frac{\Delta t}{\alpha}\sum_{n=0}^{M-1}\big\langle \tilde{\boldsymbol{g}}_2^{n+1}, \boldsymbol{e_\lambda}^n\big\rangle.$$

Then, using (4.3.5) and following the method of Lemma 3.4.6, we have

$$\begin{aligned}
\frac{\Delta t}{\alpha}\sum_{n=0}^{M-1}\big\langle \boldsymbol{g}_2^{n+1} - \tilde{\boldsymbol{g}}_2^{n+1}, \boldsymbol{e_\lambda}^n\big\rangle \leq& \frac{CT}{\alpha}\sum_{n=0}^{M-1}\|\boldsymbol{g}_2^{n+1} - \tilde{\boldsymbol{g}}_2^{n+1}\|_{L^2(\Sigma)}^2 + \frac{(\Delta t)^2}{32T\alpha}\sum_{n=0}^{M-1}\|\boldsymbol{e_\lambda}^n\|_{L^2(\Sigma)}^2 \\
\leq& \frac{CT\Delta t}{\alpha}\sum_{n=0}^{M-1}\|\boldsymbol{g}_2^{n+1}\|_{L^\infty(\Sigma)}^2 + \frac{(\Delta t)^2}{32T\alpha}\sum_{n=0}^{M-1}\|\boldsymbol{e_\lambda}^n\|_{L^2(\Sigma)}^2.
\end{aligned}$$

Now to estimate $\frac{\Delta t}{\alpha}\sum_{n=0}^{M-1}\big\langle \tilde{\boldsymbol{g}}_2^{n+1}, \boldsymbol{e_\lambda}^n\big\rangle$, we use (4.3.1a) to move as many terms as possible into Ω_s. To do so, we also note that $\boldsymbol{h}_4^{n+1} - \boldsymbol{h}_3^{n+1} = \frac{1}{2}\boldsymbol{g}_1^{n+1}$ on Σ. Thus we have

$$\begin{aligned}
\frac{\Delta t}{\alpha}\sum_{n=0}^{M-1}\big\langle \tilde{\boldsymbol{g}}_2^{n+1}, \boldsymbol{e_\lambda}^n\big\rangle =& \sum_{n=0}^{M-1}\Bigg(-\frac{\rho_s}{\alpha}(\boldsymbol{e_q}^{n+1} - \boldsymbol{e_q}^n, \tilde{\boldsymbol{g}}_2^{n+1})_s - \frac{\Delta t}{\alpha}a_s(\boldsymbol{e}_\eta^{n+1/2}, \tilde{\boldsymbol{g}}_2^{n+1}) \\
&- \Delta t\big\langle \boldsymbol{e_q}^{n+1/2} - \boldsymbol{e_u}^n, \tilde{\boldsymbol{g}}_2^{n+1}\big\rangle + L_1(\tilde{\boldsymbol{g}}_2^{n+1}) - L_4(\tilde{\boldsymbol{g}}_2^{n+1})\Bigg) \\
=& \sum_{n=0}^{M-1}\Bigg(-\frac{\rho_s}{\alpha}(\boldsymbol{e_q}^{n+1} - \boldsymbol{e_q}^n, \tilde{\boldsymbol{g}}_2^{n+1})_s - \frac{\Delta t}{\alpha}a_s(\boldsymbol{e}_\eta^{n+1/2}, \tilde{\boldsymbol{g}}_2^{n+1}) \\
&- \Delta t\big\langle \boldsymbol{e_q}^{n+1/2} - \boldsymbol{e_u}^n, \tilde{\boldsymbol{g}}_2^{n+1}\big\rangle + \Delta t\big\langle \boldsymbol{h}_3^{n+1}, \tilde{\boldsymbol{g}}_2^{n+1}\big\rangle \\
&- \frac{\Delta t}{2\alpha}\big\langle \boldsymbol{g}_2^{n+1}, \tilde{\boldsymbol{g}}_2^{n+1}\big\rangle - \Delta t\big\langle \boldsymbol{h}_4^{n+1}, \tilde{\boldsymbol{g}}_2^{n+1}\big\rangle \\
&+ \Delta t\big\langle \boldsymbol{g}_1^{n+1}, \tilde{\boldsymbol{g}}_2^{n+1}\big\rangle - \frac{\Delta t\rho_s}{\alpha}(\boldsymbol{h}_1^{n+1}, \tilde{\boldsymbol{g}}_2^{n+1})_s\Bigg) \\
=& \sum_{n=0}^{M-1}\Bigg(-\frac{\rho_s}{\alpha}(\boldsymbol{e_q}^{n+1} - \boldsymbol{e_q}^n, \tilde{\boldsymbol{g}}_2^{n+1})_s - \frac{\Delta t}{\alpha}a_s(\boldsymbol{e}_\eta^{n+1/2}, \tilde{\boldsymbol{g}}_2^{n+1}) \\
&- \Delta t\big\langle \boldsymbol{e_q}^{n+1/2} - \boldsymbol{e_u}^n, \tilde{\boldsymbol{g}}_2^{n+1}\big\rangle - \frac{\Delta t}{2\alpha}\big\langle \boldsymbol{g}_2^{n+1}, \tilde{\boldsymbol{g}}_2^{n+1}\big\rangle
\end{aligned}$$

$$+\frac{\Delta t}{2}\langle \boldsymbol{g}_1^{n+1}, \tilde{\boldsymbol{g}}_2^{n+1}\rangle - \frac{\Delta t \rho_s}{\alpha}(\boldsymbol{h}_1^{n+1}, \tilde{\boldsymbol{g}}_2^{n+1})_s\Bigg)$$

For all but the term $-\frac{\rho_s}{\alpha}(\boldsymbol{e_q}^{n+1} - \boldsymbol{e_q}^{n}, \tilde{\boldsymbol{g}}_2^{n+1})_s$, we proceed as we have many times before.

$$\begin{aligned}
&\sum_{n=0}^{M-1}\Bigg(-\frac{\Delta t}{\alpha} a_s(\boldsymbol{e}_\eta^{n+1/2}, \tilde{\boldsymbol{g}}_2^{n+1}) - \Delta t\langle \boldsymbol{e_q}^{n+1/2} - \boldsymbol{e_u}^{n}, \tilde{\boldsymbol{g}}_2^{n+1}\rangle - \frac{\Delta t}{2\alpha}\langle \boldsymbol{g}_2^{n+1}, \tilde{\boldsymbol{g}}_2^{n+1}\rangle \\
&\qquad + \frac{\Delta t}{2}\langle \boldsymbol{g}_1^{n+1}, \tilde{\boldsymbol{g}}_2^{n+1}\rangle - \frac{\Delta t \rho_s}{\alpha}(\boldsymbol{h}_1^{n+1}, \tilde{\boldsymbol{g}}_2^{n+1})_s\Bigg) \\
&\leq \sum_{n=0}^{M-1}\Bigg(\frac{\Delta t}{64T}\|\boldsymbol{e}_\eta^{n+1}\|_S^2 + \frac{\Delta t\alpha}{16}\|\boldsymbol{e_q}^{n+1/2} - \boldsymbol{e_u}^{n}\|_{L^2(\Sigma)}^2\Bigg) \\
&\quad + C\Delta t\sum_{n=0}^{M-1}\Bigg(\frac{T}{\alpha^2}\|\tilde{\boldsymbol{g}}_2^{n+1}\|_S^2 + \big(1 + \frac{1}{\alpha}\big)\|\boldsymbol{g}_2^{n+1}\|_{L^2(\Sigma)}^2 + \|\boldsymbol{g}_1^{n+1}\|_{L^2(\Sigma)}^2 \\
&\qquad\qquad + \rho_s\|\boldsymbol{h}_1^{n+1}\|_{L^2(\Omega_s)}^2 + \frac{\rho_s}{\alpha^2}\|\tilde{\boldsymbol{g}}_2^{n+1}\|_{L^2(\Omega_s)}^2\Bigg) \\
&\quad \leq \sum_{n=0}^{M-1}\frac{\Delta t}{32T}\|\boldsymbol{e}_\eta^{n+1}\|_S^2 + \frac{1}{8}\sum_{n=0}^{M-1}\mathsf{S}^{n+1} \\
&\qquad + C\Delta t\sum_{n=0}^{M-1}\Bigg(\frac{T}{\alpha^2}\|\tilde{\boldsymbol{g}}_2^{n+1}\|_S^2 + \big(1 + \frac{1}{\alpha}\big)\|\boldsymbol{g}_2^{n+1}\|_{L^2(\Sigma)}^2 \\
&\qquad\qquad + \|\boldsymbol{g}_1^{n+1}\|_{L^2(\Sigma)}^2 + \rho_s\|\boldsymbol{h}_1^{n+1}\|_{L^2(\Omega_s)}^2 + \frac{\rho_s}{\alpha^2}\|\tilde{\boldsymbol{g}}_2^{n+1}\|_{L^2(\Omega_s)}^2\Bigg)
\end{aligned}$$

Note that here we used the fact that $|\boldsymbol{g}_2^{n+1}| \geq |\tilde{\boldsymbol{g}}_2^{n+1}|$ on Σ.

The term $\sum_{n=0}^{M-1} -\frac{\rho_s}{\alpha}(\boldsymbol{e_q}^{n+1} - \boldsymbol{e_q}^{n}, \tilde{\boldsymbol{g}}_2^{n+1})_s$ is now bounded in the same way as the term $\frac{1}{\alpha}\sum_{n=0}^{M-1}(U^{n+1} - U^{n}, \tilde{g}_2^{n+1})_f$ in Section 3.4.3. We therefore find (recalling that

$\boldsymbol{e_q}^0 = 0)$

$$
\begin{aligned}
&\sum_{n=0}^{M-1} -\frac{\rho_s}{\alpha}(\boldsymbol{e_q}^{n+1} - \boldsymbol{e_q}^{n}, \tilde{\boldsymbol{g}}_2^{n+1})_s \\
=&\sum_{n=0}^{M-1} -\frac{\rho_s}{\alpha}(\boldsymbol{e_q}^{n}, \tilde{\boldsymbol{g}}_2^{n} - \tilde{\boldsymbol{g}}_2^{n+1})_s - \frac{\rho_s}{\alpha}(\boldsymbol{e_q}^{M}, \tilde{\boldsymbol{g}}_2^{M})_s \\
=&\sum_{n=0}^{M-1} -\frac{\rho_s}{\alpha}(\boldsymbol{e_q}^{n}, (\Delta t)^2 \partial_{\Delta t}^2 \mathcal{L}_s^n)_s - \frac{\rho_s}{\alpha}(\boldsymbol{e_q}^{M}, \tilde{\boldsymbol{g}}_2^{M})_s \\
\leq&\frac{\Delta t \rho_s}{32T} \sum_{n=0}^{M-1} \|\boldsymbol{e_q}^n\|_{L^2(\Omega_s)}^2 + \frac{CT(\Delta t)^3 \rho_s}{\alpha^2} \sum_{n=0}^{M-1} \|\partial_{\Delta t}^2 \mathcal{L}_s^n\|_{L^2(\Omega_s)}^2 \\
&+ \frac{\rho_s}{32}\|\boldsymbol{e_q}^M\|_{L^2(\Omega_s)}^2 + \frac{C\rho_s}{\alpha^2}\|\tilde{\boldsymbol{g}}_2^M\|_{L^2(\Omega_s)}^2.
\end{aligned}
$$

We now combine everything, to find

$$
\frac{\Delta t}{\alpha} \sum_{n=0}^{M-1} \left\langle \boldsymbol{g}_2^{n+1}, \boldsymbol{e_\lambda}^n \right\rangle \leq \frac{1}{8} \max_{0 \leq m \leq M} \mathsf{Z}^m + \frac{1}{8} \sum_{n=0}^{M-1} \mathsf{S}^{n+1} + C \boldsymbol{\Psi}_2(M).
$$

To finish the proof, it remains to bound the term $\frac{\Delta t}{2} \sum_{n=0}^{M-1} \left\langle \boldsymbol{g}_1^{n+1}, \boldsymbol{e_\lambda}^n \right\rangle$. Recall that we are now considering $\boldsymbol{g}_1^{n+1} = \mathbf{q}^{n+1} - \mathbf{q}^n$ using (4.1.3a) so that we have a natural extension from Σ into Ω_s.

To do this, we again apply (4.3.1a) to write

$$
\begin{aligned}
\frac{\Delta t}{2}\left\langle \boldsymbol{g}_1^{n+1}, \boldsymbol{e_\lambda}^n \right\rangle =& -\frac{\rho_s}{2}(\boldsymbol{e_q}^{n+1} - \boldsymbol{e_q}^{n}, \boldsymbol{g}_1^{n+1})_s - \frac{\Delta t}{2} a_s(\boldsymbol{e}_\eta^{n+1/2}, \boldsymbol{g}_1^{n+1}) \\
&- \frac{\Delta t \alpha}{2}\left\langle \boldsymbol{e_q}^{n+1/2} - \boldsymbol{e_u}^n, \boldsymbol{g}_1^{n+1} \right\rangle + \frac{\Delta t \alpha}{2}\left\langle \boldsymbol{h}_3^{n+1}, \boldsymbol{g}_1^{n+1} \right\rangle \\
&- \frac{\Delta t}{4}\left\langle \boldsymbol{g}_2^{n+1}, \boldsymbol{g}_1^{n+1} \right\rangle - \frac{\Delta t \alpha}{2}\left\langle \boldsymbol{h}_4^{n+1}, \boldsymbol{g}_1^{n+1} \right\rangle \\
&+ \frac{\Delta t \alpha}{2}\left\langle \boldsymbol{g}_1^{n+1}, \boldsymbol{g}_1^{n+1} \right\rangle - \frac{\Delta t \rho_s}{2}(\boldsymbol{h}_1^{n+1}, \boldsymbol{g}_1^{n+1})_s.
\end{aligned}
$$

Thus, using the same steps as before, we find

$$
\begin{aligned}
&\sum_{n=0}^{M-1}\Bigg(-\frac{\Delta t}{2}a_s(\boldsymbol{e}_\eta^{n+1/2},\boldsymbol{g}_1^{n+1}) - \frac{\Delta t\alpha}{2}\big\langle {\boldsymbol{e}_{\boldsymbol{q}}}^{n+1/2} - {\boldsymbol{e}_{\boldsymbol{u}}}^{n}, \boldsymbol{g}_1^{n+1}\big\rangle \\
&\qquad + \frac{\Delta t\alpha}{2}\big\langle \boldsymbol{h}_3^{n+1},\boldsymbol{g}_1^{n+1}\big\rangle - \frac{\Delta t}{4}\big\langle \boldsymbol{g}_2^{n+1},\boldsymbol{g}_1^{n+1}\big\rangle - \frac{\Delta t\alpha}{2}\big\langle \boldsymbol{h}_4^{n+1},\boldsymbol{g}_1^{n+1}\big\rangle \\
&\qquad + \frac{\Delta t\alpha}{2}\big\langle \boldsymbol{g}_1^{n+1},\boldsymbol{g}_1^{n+1}\big\rangle - \frac{\Delta t\rho_s}{2}(\boldsymbol{h}_1^{n+1},\boldsymbol{g}_1^{n+1})_s\Bigg) \\
&= \sum_{n=0}^{M-1}\Bigg(-\frac{\Delta t}{2}a_s(\boldsymbol{e}_\eta^{n+1/2},\boldsymbol{g}_1^{n+1}) - \frac{\Delta t\alpha}{2}\big\langle {\boldsymbol{e}_{\boldsymbol{q}}}^{n+1/2} - {\boldsymbol{e}_{\boldsymbol{u}}}^{n}, \boldsymbol{g}_1^{n+1}\big\rangle \\
&\qquad - \frac{\Delta t}{4}\big\langle \boldsymbol{g}_2^{n+1},\boldsymbol{g}_1\big\rangle + \frac{\Delta t\alpha}{4}\|\boldsymbol{g}_1^{n+1}\|^2_{L^2(\Sigma)} - \frac{\Delta t\rho_s}{2}(\boldsymbol{h}_1^{n+1},\boldsymbol{g}_1^{n+1})_s\Bigg) \\
&\le \sum_{n=0}^{M-1}\Bigg(\frac{\Delta t}{64T}\|\boldsymbol{e}_\eta^{n+1}\|^2_S + \frac{\Delta t\alpha}{16}\|{\boldsymbol{e}_{\boldsymbol{q}}}^{n+1/2} - {\boldsymbol{e}_{\boldsymbol{u}}}^{n}\|^2_{L^2(\Sigma)}\Bigg) \\
&\quad + C\Delta t\sum_{n=0}^{M-1}\Bigg(T\|\boldsymbol{g}_1^{n+1}\|^2_S + \big(1+\alpha\big)\|\boldsymbol{g}_1^{n+1}\|^2_{L^2(\Sigma)} + \|\boldsymbol{g}_2^{n+1}\|^2_{L^2(\Sigma)} \\
&\qquad\qquad + \rho_s\|\boldsymbol{h}_1^{n+1}\|^2_{L^2(\Omega_s)} + \rho_s\|\boldsymbol{g}_1^{n+1}\|^2_{L^2(\Omega_s)}\Bigg) \\
&\quad \le \sum_{n=0}^{M-1}\frac{\Delta t}{32T}\|\boldsymbol{e}_\eta^{n+1}\|^2_S + \frac{1}{8}\sum_{n=0}^{M-1}\mathsf{S}^{n+1} + C\Delta t\sum_{n=0}^{M-1}\Bigg(T\|\boldsymbol{g}_1^{n+1}\|^2_S + \big(1+\alpha\big)\|\boldsymbol{g}_1^{n+1}\|^2_{L^2(\Sigma)} \\
&\qquad\qquad\qquad + \|\boldsymbol{g}_2^{n+1}\|^2_{L^2(\Sigma)} + \rho_s\|\boldsymbol{h}_1^{n+1}\|^2_{L^2(\Omega_s)} + \rho_s\|\boldsymbol{g}_1^{n+1}\|^2_{L^2(\Omega_s)}\Bigg).
\end{aligned}
$$

As above, we use the same summation by parts technique to find

$$
\begin{aligned}
\sum_{n=0}^{M-1} -\frac{\rho_s}{2}({\boldsymbol{e}_{\boldsymbol{q}}}^{n+1} - {\boldsymbol{e}_{\boldsymbol{q}}}^{n},\boldsymbol{g}_1^{n+1})_s \le{}& \frac{\Delta t\rho_s}{32T}\sum_{n=0}^{M-1}\|{\boldsymbol{e}_{\boldsymbol{q}}}^{n}\|^2_{L^2(\Omega_s)} + CT(\Delta t)^3\rho_s\sum_{n=0}^{M-1}\|\partial^2_{\Delta t}\mathsf{q}^n\|^2_{L^2(\Omega_s)} \\
&+ \frac{\rho_s}{32}\|{\boldsymbol{e}_{\boldsymbol{q}}}^{M}\|^2_{L^2(\Omega_s)} + C\rho_s\|\boldsymbol{g}_1^M\|^2_{L^2(\Omega_s)}.
\end{aligned}
$$

Thus we arrive at

$$\frac{\Delta t}{2}\sum_{n=0}^{M-1}\left\langle \boldsymbol{g}_1^{n+1}, \boldsymbol{e_\lambda}^n\right\rangle \leq \frac{1}{8}\max_{0\leq m\leq M}\mathsf{Z}^m + \frac{1}{8}\sum_{n=0}^{M-1}\mathsf{S}^{n+1} + C\boldsymbol{\Psi}_1(M).$$

Combining the two parts completes the proof. □

Combining this result with Lemmas 4.3.1 and 4.3.2, we have

$$\frac{1}{2}\max_{1\leq M\leq N}\mathsf{Z}^M + \frac{1}{2}\sum_{n=0}^{N-1}\mathsf{S}^{n+1} \leq + C\max_{0\leq M\leq N}\big(\mathbf{D}(M) + \boldsymbol{\Psi}(M)\big), \tag{4.3.10}$$

where we have again used the fact that these estimates are true for all $0 \leq M \leq N$.

4.3.5 Step 3: Main Result

It now remains for us to bound $\mathbf{D}(M)$ and $\boldsymbol{\Psi}(M)$ in terms of the exact solutions. As before, these catch-all terms are made up of residuals and discretization errors, and they may be bounded in the exact same way as the corresponding terms in Section 3.4.4. However, many of these terms will also contain the physical parameters μ, L_1, and L_2. Therefore it is at this stage that we will be able to see how these terms will impact the convergence of the Robin-Robin method. Thus we will take extra care in the following analysis to keep track of these values.

As before, we will make heavy use of the bounds derived in Lemma 3.4.7. However, we will also need the following additional estimate to address the norm $\|\cdot\|_S$.

Lemma 4.3.7. *Let $\boldsymbol{v}$ be a vector-valued function in a domain Y. Define* $\|\cdot\|_S^2 =$

$2L_1\|\varepsilon(\cdot)\|^2_{L^2(Y)} + L_2\|\mathrm{div}\cdot\|^2_{L^2(Y)}$. *It follows*

$$\|\boldsymbol{v}^{n+1} - \boldsymbol{v}^n\|^2_S \leq C\Delta t(L_1 + L_2)\int_{t_n}^{t_{n+1}} \|\partial_t \boldsymbol{v}(\cdot, s)\|^2_{H^1(Y)} ds, \tag{4.3.11a}$$

$$\|\partial_{\Delta t}\boldsymbol{v}^{n+1} - \partial_t \boldsymbol{v}^{n+1/2}\|^2_S \leq C(\Delta t)^3(L_1 + L_2)\int_{t_n}^{t_{n+1}} \|\partial_t^3 \boldsymbol{v}(\cdot, s)\|^2_{H^1(Y)} ds. \tag{4.3.11b}$$

Proof. The proof follows from (3.4.11b), (3.4.11d), and the definition of $\varepsilon(\cdot)$. $\square$

We may now prove the following bounds.

Lemma 4.3.8. *For all* $1 \leq M \leq N$, *it holds*

$$\begin{aligned}
\mathbf{D}(M) \leq & CT(\Delta t)^4\Big(\rho_s\|\partial_t^3 \mathsf{q}\|^2_{L^2(0,T;L^2(\Omega_s))} + (L_1 + L_2)\|\partial_t^3 \mathsf{e}\|^2_{L^2(0,T;H^1(\Omega_s))}\Big) \\
& + C(\Delta t)^2\Big(T\rho_f\|\partial_t^2 \mathsf{u}\|^2_{L^2(0,T;L^2(\Omega_f))} + \Big(\alpha + \frac{\alpha^2}{\mu} + \mu + \frac{\mu^2}{\alpha}\Big)\|\partial_t \mathsf{u}\|^2_{L^2(0,T;H^1(\Sigma))} \\
& + \Big(\frac{1}{\alpha} + \frac{1}{\mu}\Big)\|\partial_t \mathsf{p}\|^2_{L^2(0,T;L^2(\Sigma))}\Big),
\end{aligned}$$

$$\begin{aligned}
\boldsymbol{\Psi}_1(M) \leq & C(\Delta t)^4\rho_s\|\partial_t^3 \mathsf{q}\|^2_{L^2(0,T;L^2(\Omega_s))} + C(\Delta t)^2\Big(T\rho_s\|\partial_t^2 \mathsf{q}\|^2_{L^2(0,T;L^2(\Omega_s))} \\
& + \rho_s T\|\partial_t \mathsf{q}\|^2_{L^\infty(0,T;L^2(\Omega_s))} + (\rho_s + T(L_1 + L_2))\|\partial_t \mathsf{q}\|^2_{L^2(0,T;H^1(\Omega_s))} \\
& + (1 + \alpha)\|\partial_t \mathsf{u}\|^2_{L^2(0,T;L^2(\Sigma))} + \mu^2\|\partial_t \mathsf{u}\|^2_{L^2(0,T;H^1(\Sigma)} \\
& + \|\partial_t \mathsf{p}\|^2_{L^2(0,T;L^2(\Sigma))}\Big),
\end{aligned}$$

$$\begin{aligned}
\boldsymbol{\Psi}_2(M) \leq & (\Delta t)^4\rho_s\|\partial_t^3 \mathsf{q}\|^2_{L^2(0,T;L^2(\Omega_s))} + C(\Delta t)^2\Big(\frac{\rho_s}{\alpha^2}(L_1^2 + L_2^2)\|\partial_t \mathsf{e}\|^2_{L^\infty(0,T;H^1(\Omega_s))} \\
& + \frac{(1+T)\rho_s}{\alpha^2}(L_1^2 + L_2^2)\|\partial_t^2 \mathsf{e}\|^2_{L^2(0,T;H^1(\Omega_s))} + \frac{T(L_1 + L_2)^3}{\alpha^2}\|\partial_t \mathsf{e}\|^2_{L^2(0,T;H^2(\Omega_s))} \\
& + \frac{(L_1 + L_2)^3}{\alpha^2}\Big(1 + \log\frac{1}{\Delta t}\Big)\Big(\|\partial_t \varepsilon(\mathsf{e})\|^2_{L^2(0,T;L^\infty(\Omega_s))} \\
& + \|\partial_t \mathrm{div}\,\mathsf{e}\|^2_{L^2(0,T;L^\infty(\Omega_s))}\Big) + \big(1 + \mu^2\big(1 + \frac{1}{\alpha}\big)\big)\|\partial_t \mathsf{u}\|^2_{L^2(0,T;H^1(\Sigma))} \\
& + \big(1 + \frac{1}{\alpha}\big)\|\partial_t \mathsf{p}\|^2_{L^2(0,T;L^2(\Sigma))} + \frac{\mu^2 T}{\alpha}\|\partial_t \varepsilon(\mathsf{u})\|^2_{L^2(0,T;L^\infty(\Sigma))}
\end{aligned}$$

$$+\frac{T}{\alpha}\|\partial_t \mathsf{p}\|^2_{L^2(0,T;L^\infty(\Sigma))}\Bigg).$$

Proof. Most of these bounds follow immediately from Lemmas 3.4.7 and 4.3.7 and the methods of the proof of Lemma 3.4.8. However, we must treat a few terms with extra care to make sure that we account for all physical parameters. For maximum clarity, we will list the bounds for every term appearing in $\mathbf{D}(M)$ and $\mathbf{\Psi}(M)$.

To begin, we note that $\boldsymbol{g}_3^{n+1}$ and $\boldsymbol{g}_4^{n+1}$ are functions of $\boldsymbol{g}_1^{n+1}$ and $\boldsymbol{g}_2^{n+1}$. Thus we have

$$\begin{aligned}
\|\boldsymbol{g}_3^{n+1}\|^2_{L^2(\Sigma)} \leq & C\alpha^2\|\boldsymbol{g}_1^{n+1}\|^2_{L^2(\Sigma)} + C\|\boldsymbol{g}_2^{n+1}\|^2_{L^2(\Sigma)},\\
\|\boldsymbol{g}_4^{n+1}\|^2_{L^2(\Sigma)} \leq & C\alpha^2\|\boldsymbol{g}_1^{n+1}\|^2_{L^2(\Sigma)} + C\|\boldsymbol{g}_2^{n+1}\|^2_{L^2(\Sigma)}.
\end{aligned}$$

Recall also that whenever $\boldsymbol{g}_1^{n+1}$ is evaluated on Ω_s, it is considered $\boldsymbol{g}_1^{n+1} = \mathbf{q}^{n+1} - \mathbf{q}^n$, whereas on Σ we consider $\boldsymbol{g}_1^{n+1} = \mathbf{u}^{n+1} - \mathbf{u}^n$.

We will first address the terms that do not involve $\tilde{\phi}$. The following bounds all follow immediately from (3.4.11b) in Lemma 3.4.7.

$$\begin{aligned}
\|\boldsymbol{g}_1^{n+1}\|^2_{L^2(\Sigma)} \leq & C\Delta t\int_{t_n}^{t_{n+1}} \|\partial_t \mathbf{u}(\cdot,s)\|^2_{L^2(\Sigma)}ds,\\
\|\boldsymbol{g}_2^{n+1}\|_{L^2(\Sigma)} \leq & C\mu^2\|\varepsilon(\mathbf{u}^{n+1}-\mathbf{u}^n)\|^2_{L^2(\Sigma)} + \|\mathsf{p}^{n+1}-\mathsf{p}^n\|^2_{L^2(\Sigma)}\\
\leq & C\Delta t\mu^2\int_{t_n}^{t_{n+1}} \|\partial_t \mathbf{u}(\cdot,s)\|^2_{H^1(\Sigma)}ds + C\Delta t\int_{t_n}^{t_{n+1}} \|\partial_t \mathsf{p}(\cdot,s)\|^2_{L^2(\Sigma)}ds,\\
\|\boldsymbol{g}_1^{n+1}\|^2_{L^2(\Omega_s)} \leq & C\Delta t\int_{t_n}^{t_{n+1}} \|\partial_t \mathbf{q}^{n+1}(\cdot,s)\|^2_{L^2(\Omega_s)}ds,\\
\|\boldsymbol{g}_2^{n+1}\|^2_{L^\infty(\Sigma)} \leq & C\mu^2\|\varepsilon(\mathbf{u}^{n+1}-\mathbf{u}^n)\|^2_{L^\infty(\Sigma)} + \|\mathsf{p}^{n+1}-\mathsf{p}^n\|^2_{L^\infty(\Sigma)}\\
\leq & c\mu^2\Delta t\int_{t_n}^{t_{n+1}} \|\partial_t \epsilon(\mathbf{u}(\cdot,s))\|^2_{L^\infty(\Sigma)}ds + C\Delta t\int_{t_n}^{t_{n+1}} \|\partial_t \mathsf{p}(\cdot,s)\|^2_{L^\infty(\Sigma)}ds.
\end{aligned}$$

From (4.3.11a) and (4.3.11b) of Lemma 4.3.7, we have

$$\begin{aligned}
\|\boldsymbol{g}_1^{n+1}\|_S^2 \leq & C\Delta t \int_{t_n}^{t_{n+1}} \|\partial_t \mathbf{q}(\cdot,s)\|_{H^1(\Omega_s)}^2 ds, \\
\|\boldsymbol{h}_3^{n+1}\|_S^2 \leq & C(\Delta t)^3 (L_1+L_2) \int_{t_n}^{t_{n+1}} \|\partial_t^3 \mathbf{e}(\cdot,s)\|_{H^1(\Omega_s)}^2 ds.
\end{aligned}$$

Next, from (3.4.11c) and (3.4.11d), it follows

$$\begin{aligned}
\|\boldsymbol{h}_2^{n+1}\|_{L^2(\Omega_f)}^2 \leq & C\Delta t \int_{t_n}^{t_{n+1}} \|\partial_t^2 \mathbf{u}(\cdot,s)\|_{L^2(\Omega_f)}^2 ds, \\
\|\boldsymbol{h}_1^{n+1}\|_{L^2(\Omega_s)}^2 \leq & C(\Delta t)^3 \int_{t_n}^{t_{n+1}} \|\partial_t^3 \mathbf{q}(\cdot,s)\|_{L^2(\Omega_s)}^2 ds.
\end{aligned}$$

Using (3.4.11b) followed by (3.4.11a), we determine,

$$\begin{aligned}
\|\boldsymbol{g}_1^{M}\|_{L^2(\Omega_s)}^2 \leq & C\Delta t \int_{t_{M-1}}^{t_M} \|\partial_t \mathbf{q}(\cdot,s)\|_{L^2(\Omega_s)}^2 ds \\
\leq & C(\Delta t)^2 \|\partial_t \mathbf{q}\|_{L^\infty(0,T;L^2(\Omega_s))}^2.
\end{aligned}$$

Finally, from (3.4.11e), we have

$$\|\partial_{\Delta t}^2 \mathbf{q}^n\|_{L^2(\Omega_s)}^2 \leq \frac{C}{\Delta t} \int_{t_n-1}^{t_{n+1}} \|\partial_t^2 \mathbf{q}(\cdot,s)\|_{L^2(\Omega_s)}^2 ds.$$

We may now deal with the terms involving $\tilde{\phi}$. To do so, we recall the boundedness of $\tilde{\boldsymbol{n}}_s$ and $\tilde{\phi}$ from Assumptions 4.3.3 and 4.3.4. It therefore follows from (3.4.11b)

$$\begin{aligned}
\|\tilde{\boldsymbol{g}}_2^{n+1}\|_{L^2(\Omega_s)}^2 \leq & C\|\tilde{\phi}\|_{L^\infty(\Omega_s)}^2 \|\tilde{\boldsymbol{n}}_s\|_{L^\infty(\Omega_s)}^2 \|\sigma_s(\mathbf{e}^{n+1}-\mathbf{e}^n)\|_{L^2(\Omega_s)}^2 \\
\leq & C\|\sigma_s(\mathbf{e}^{n+1}-\mathbf{e}^n)\|_{L^2(\Omega_s)}^2
\end{aligned}$$

$$
\begin{aligned}
&= C\|2L_1\epsilon(\mathbf{e}^{n+1}-\mathbf{e}^n) + L_2\mathrm{div}\,(\mathbf{e}^{n+1}-\mathbf{e}^n)\boldsymbol{I}\|^2_{L^2(\Omega_s)} \\
&\leq C(L_1^2+L_2^2)\|\mathbf{e}^{n+1}-\mathbf{e}^n\|^2_{H^1(\Omega_s)} \\
&\leq C(L_1^2+L_2^2)\Delta t \int_{t_n}^{t_{n+1}} \|\partial_t \mathbf{e}(\cdot,s)\|^2_{H^1(\Omega_s)} ds.
\end{aligned}
$$

Furthermore, using the same combination for (3.4.11b) and (3.4.11a) used for the $\boldsymbol{g}_1^M$ term above, we have

$$
\begin{aligned}
\|\tilde{\boldsymbol{g}}_2^M\|^2_{L^2(\Omega_s)} &\leq C\|\tilde{\phi}\|^2_{L^\infty(\Omega_s)}\|\tilde{\boldsymbol{n}}_s\|^2_{L^\infty(\Omega_s)}\|\sigma_s(\mathbf{e}^M-\mathbf{e}^{M-1})\|^2_{L^2(\Omega_s)} \\
&\leq C(L_1^2+L_2^2)\|\mathbf{e}^M-\mathbf{e}^{M-1}\|^2_{H^1(\Omega_s)} \\
&\leq C(L_1^2+L_2^2)(\Delta t)^2\|\partial_t\mathbf{e}\|^2_{L^\infty(0,T;H^1(\Omega_s))},
\end{aligned}
$$

and from (3.4.11e) it follows

$$
\begin{aligned}
\|\partial^2_{\Delta t}\mathcal{L}_s^n\|^2_{L^2(\Omega_s)} &\leq C\|\tilde{\phi}\|^2_{L^\infty(\Omega_s)}\|\tilde{\boldsymbol{n}}_s\|^2_{L^\infty(\Omega_s)}\|\partial^2_{\Delta t}\sigma_s(\mathbf{e}^n)\|^2_{L^2(\Omega_s)} \\
&\leq C(L_1^2+L_2^2)\|\partial^2_{\Delta t}\mathbf{e}^n\|^2_{H^1(\Omega_s)} \\
&\leq \frac{C(L_1^2+L_2^2)}{\Delta t}\int_{t_{n-1}}^{t_{n+1}} \|\partial_t^2\mathbf{e}(\cdot,s)\|^2_{H^1(\Omega_s)} ds.
\end{aligned}
$$

Finally, we must address the term $\|\tilde{\boldsymbol{g}}_2^{n+1}\|^2_S$. We do this by recalling the definition of $\|\cdot\|_S$, applying the product rule, and making use of Assumptions 4.3.3 and 4.3.4. Thus we have

$$
\begin{aligned}
\|\tilde{\boldsymbol{g}}_2^{n+1}\|_S &\leq 2L_1\|\varepsilon(\tilde{\boldsymbol{g}}_2^{n+1})\|^2_{L^2(\Omega_s)} + L_1\|\mathrm{div}\,\tilde{\boldsymbol{g}}_2^{n+1}\|^2_{L^2(\Omega_s)} \\
&\leq C(L_1+L_2)\|\nabla\tilde{\boldsymbol{g}}_2^{n+1}\|^2_{L^2(\Omega_s)} \\
&\leq C(L_1+L_2)\Bigg(\|\nabla\tilde{\phi}\|^2_{L^2(\Omega_s)}\|\sigma_s(\mathbf{e}^{n+1}-\mathbf{e}^n)\|^2_{L^\infty(\Omega_s)}
\end{aligned}
$$

$$
\begin{aligned}
&+ \|\nabla \tilde{\boldsymbol{n}}_s\|^2_{L^\infty(\Omega_s)} \|\sigma_s(\mathbf{e}^{n+1} - \mathbf{e}^n)\|^2_{L^2(\Omega_s)} + \|(L_1 + L_2) D^2(\mathbf{e}^{n+1} - \mathbf{e}^n)\|^2_{L^2(\Omega_s)} \Bigg) \\
\leq & C(L_1 + L_2) \Bigg(\big(1 + \log \frac{1}{\Delta t}\big) \Big(L_1^2 \|\varepsilon(\mathbf{e}^{n+1} - \mathbf{e}^n)\|^2_{L^\infty(\Omega_s)} \\
&+ L_2^2 \|\mathrm{div}\,(\mathbf{e}^{n+1} - \mathbf{e}^n)\|^2_{L^\infty(\Omega_s)} \Big) + L_1^2 \|\varepsilon(\mathbf{e}^{n+1} - \mathbf{e}^n)\|^2_{L^2(\Omega_s)} \\
&+ L_2^2 \|\mathrm{div}\,(\mathbf{e}^{n+1} - \mathbf{e}^n)\|^2_{L^2(\Omega_s)} + (L_1 + L_2)^2 \|D^2(\mathbf{e}^{n+1} - \mathbf{e}^n)\|^2_{L^2(\Omega_s)} \Bigg) \\
\leq & C(L_1 + L_2)^3 \Bigg(\big(1 + \log \frac{1}{\Delta t}\big) \Big(\|\varepsilon(\mathbf{e}^{n+1} - \mathbf{e}^n)\|^2_{L^\infty(\Omega_s)} \\
&+ \|\mathrm{div}\,(\mathbf{e}^{n+1} - \mathbf{e}^n)\|^2_{L^\infty(\Omega_s)} \Big) + \|\mathbf{e}^{n+1} - \mathbf{e}^n\|^2_{H^2(\Omega_s)} \Bigg). \qquad (4.3.12)
\end{aligned}
$$

where, as before, $D^2\mathbf{e}$ denotes the Hessian of $\mathbf{e}$.

Consequently, we have

$$
\begin{aligned}
\|\tilde{\boldsymbol{g}}_2^{n+1}\|_S \leq & C(L_1 + L_2)^3 \Bigg(\big(1 + \log \frac{1}{\Delta t}\big) \Big(\int_{t_n}^{t_{n+1}} \|\epsilon(\partial_t \mathbf{e}(\cdot, s))\|^2_{L^\infty(\Omega_s)} ds \\
&+ \int_{t_n}^{t_{n+1}} \|\mathrm{div}\,(\partial_t \mathbf{e}(\cdot, s))\|^2_{L^\infty(\Omega_s)} ds \Big) + \int_{t_n}^{t_{n+1}} \|\partial_t \mathbf{e}(\cdot, s)\|^2_{H^2(\Omega_s)} ds \Bigg)
\end{aligned}
$$

The proof is then completed by summing the terms and incorporating the coefficients. □

We may now present the main–and final–result of the error analysis. Note that we choose o now combine the terms $\partial_t \mathbf{q}$ and $\partial_t^2 \mathbf{e}$ whenever possible.

Theorem 4.3.9. *Under Assumptions 4.3.3 and 4.3.4, and assuming that the solution is smooth enough so that* $\mathbf{Y}$ *defined below and* $\|\partial_t \varepsilon(\mathbf{e})\|^2_{L^2(0,T;L^\infty(\Omega_s))}$ *and*

$\|\partial_t \mathrm{div}\,\mathbf{e}\|^2_{L^2(0,T;L^\infty(\Omega_s))}$ *are bounded, we have*

$$\max_{1\le M\le N} \mathsf{Z}^M + \sum_{n=0}^{N-1} \mathsf{S}^{n+1} \le C(\Delta t)^2 \Bigg(\mathbf{Y} + \frac{T(L_1+L_2)^3}{\alpha^2}\big(1+\log\frac{1}{\Delta t}\big)\Big(\|\partial_t \varepsilon(\mathbf{e})\|^2_{L^2(0,T;L^\infty(\Omega_s))} + \|\partial_t \mathrm{div}\,\mathbf{e}\|^2_{L^2(0,T;L^\infty(\Omega_s))}\Big)\Bigg),$$

where

$$\begin{aligned}
\mathbf{Y} :=&(\Delta t)^2\Big((1+T)\rho_s\|\partial_t^3\mathbf{q}\|^2_{L^2(0,T;L^2(\Omega_s))} + T(L_1+L_2)\|\partial_t^3\mathbf{e}\|^2_{L^2(0,T;H^1(\Omega_s))}\Big)\\
&+ T\rho_f\|\partial_t^2\mathbf{u}\|^2_{L^2(0,T;L^2(\Omega_f))} + \Big(1+\alpha+\frac{\alpha^2}{\mu}+\mu+\mu^2+\frac{\mu^2}{\alpha}\Big)\|\partial_t\mathbf{u}\|^2_{L^2(0,T;H^1(\Sigma))}\\
&+ \Big(1+\frac{1}{\alpha}+\frac{1}{\mu}\Big)\|\partial_t \mathsf{p}\|^2_{L^2(0,T;L^2(\Sigma))} + T\rho_s\|\partial_t^2\mathbf{q}\|^2_{L^2(0,T;L^2(\Omega_s))}\\
&+ \rho_s T\|\partial_t\mathbf{q}\|^2_{L^\infty(0,T;L^2(\Omega_s))} + \frac{\rho_s}{\alpha^2}(L_1^2+L_2^2)\|\partial_t\mathbf{e}\|^2_{L^\infty(0,T;H^1(\Omega_s)}\\
&+ \Big(\rho_s + T(L_1+L_2) + (L_1^2+L_2^2)\frac{\rho_s(1+T)}{\alpha^2}\Big)\|\partial_t^2\mathbf{e}\|^2_{L^2(0,T;H^1(\Omega_s))}\\
&+ \frac{\mu^2 T}{\alpha}\|\partial_t\varepsilon(\mathbf{u})\|^2_{L^2(0,T;L^\infty(\Sigma))} + \frac{T}{\alpha}\|\partial_t\mathsf{p}\|^2_{L^2(0,T;L^\infty(\Sigma))}\\
&+ \frac{T(L_1+L_2)^3}{\alpha^2}\|\partial_t\mathbf{e}\|^2_{L^2(0,T;H^2(\Omega_s))}
\end{aligned}$$

4.4 Final Discussion

4.4.1 Parameter sensitivity

In 4.3.5, we took special care to account for all physical parameters in the error analysis, namely the viscosity, μ, the densities, ρ_s and ρ_f, the Lamé parameters, L_1 and L_2, and the Robin parameter α. As we will see in the numerical experiments below, when all physical parameters are set to 1, the method displays the predicted, nearly optimal convergence. However, early numerical experiments for the Robin-Robin method presented sub-optimal ($\mathcal{O}(\sqrt{\Delta t})$) convergence behavior (see e.g. [17, 18, 14]).

On the surface, this seems to contradict the theoretical results. However, we note that the physical parameters in these early experiments were chosen to match values that would appear in blood flow simulations. As mentioned previously, this necessarily required Lamé parameters on the order of 10^6. The densities, on the other hand, were on the order of 10^3 (assuming the units are kg/m^3), and the viscosity was on the order of 10^{-1} (see [46, 17, 18, 14]). It could be, therefore, that the Robin-Robin scheme is highly sensitive to the values of the physical parameters, causing the discrepancy in results.

We know from our error analysis that the Robin-Robin method is nearly first order, but perhaps the splitting method introduces some oscillation between which term or terms dominate the error for larger values of Δt. Perhaps then having large values of the parameters prolongs this oscillation, delaying the asymptotic convergence of the system.

This, however, is just speculation without much evidence to back it up. With just the a priori estimates for the Robin-Robin coupling, we will not be able to rigorously understand the importance of this alphabet soup of parameters, but it is certainly worth investigating. Therefore, we have run numerical models of the Stokes-Elastic problem with Robin-Robin coupling and compared it to the constructed solution (4.4.4) given below.

In the experimental results that follow, we set the interface to be the straight line $y = 0.75$, and the domain Ω is the unit square $[0, 1] \times [0, 1]$. For all cases, we set

ρ_f and ρ_s to be 1 and vary the values of α, μ, and L_1. Note that we set $\mu = L_1$ to more easily construct a solution to the forced version of (4.1.1)-(4.1.3), given by

$$\rho_f \partial_t \mathbf{u} - \operatorname{div} \sigma_f(\mathbf{u}, \mathsf{p}) = \mathbf{f}_1 \quad \text{in } (0,T) \times \Omega_f, \tag{4.4.1a}$$

$$\operatorname{div} \mathbf{u} = g_f \quad \text{in } (0,T) \times \Omega_f, \tag{4.4.1b}$$

$$\mathbf{u} = 0 \quad \text{on } (0,T) \times \Sigma_f, \tag{4.4.1c}$$

$$\rho_s \partial_t \mathbf{q} - \operatorname{div} \sigma_s(\mathbf{e}) = \mathbf{f}_2 \quad \text{in } (0,T) \times \Omega_s, \tag{4.4.2a}$$

$$\boldsymbol{q} - \partial_t \mathbf{e} = 0 \quad \text{in } (0,T) \times \Omega_s, \tag{4.4.2b}$$

$$\mathbf{e} = 0 \quad \text{on } (0,T) \times \Sigma_s, \tag{4.4.2c}$$

$$\mathbf{u} = \mathbf{q} \quad \text{on } (0,T) \times \Sigma, \tag{4.4.3a}$$

$$\sigma_f(\mathbf{u}, \mathsf{p}) \boldsymbol{n}_f + \sigma_s(\mathbf{e}) \boldsymbol{n}_s = 0 \quad \text{on } (0,T) \times \Sigma. \tag{4.4.3b}$$

Consequently, we compare the approximate result provided by the Robin-Robin method to the constructed solution (see also [13])

$$\mathbf{u} = 10^{-3} e^t \begin{pmatrix} 2x(1-x)y(1-y) \\ x(1-x)(1-y) \end{pmatrix}, \tag{4.4.4a}$$

$$\mathsf{p} = -10^{-3} e^t L_2 (2(1-2x)y(1-y) + x(1-x)(1-2y)), \tag{4.4.4b}$$

$$\mathbf{e} = 10^{-3} e^t \begin{pmatrix} 2x(1-x)y(1-y) \\ x(1-x)(1-y) \end{pmatrix}, \tag{4.4.4c}$$

$$\mathbf{f}_1 = \mathbf{f}_2 = 10^{-3}e^t \begin{pmatrix} 2x(1-x)y(1-y) + 4(2\mu + L_2)y(1-y) \\ x(1-x)y(1-y) + 2(2\mu + L_2)x(1-x) \end{pmatrix} + 10^{-3}e^t \begin{pmatrix} 4\mu x(1-x) - (\mu + L_2)(1-2x)(1-2y) \\ 2\mu y(1-y) - 2(\mu + L_2)(1-2x)(1-2y) \end{pmatrix}. \tag{4.4.4d}$$

We run the model on the time interval $[0, 0.5]$ with $\Delta t = h \in \{(\frac{1}{2})^i\}_{i=2}^{7}$. We use linear finite elements for all terms (on a uniform mesh) for the spacial discretization, and add the term $h^2(\nabla p^{n+1}, \nabla\theta)_f$ to the divergence equation to stabilize the method in lieu of an inf-sup stable choice of elements [9]. The results for the fully discrete counterpart[1] of the error term $\|\boldsymbol{e_q}^N\|_{L^2(\Omega_s)}$ are shown in Figure 4.1.

[1]Using the notation of Chapter 5, we are measuring $\|\mathbf{q}^N - \boldsymbol{q}_h^N\|_{L^2(\Omega_s)}$.

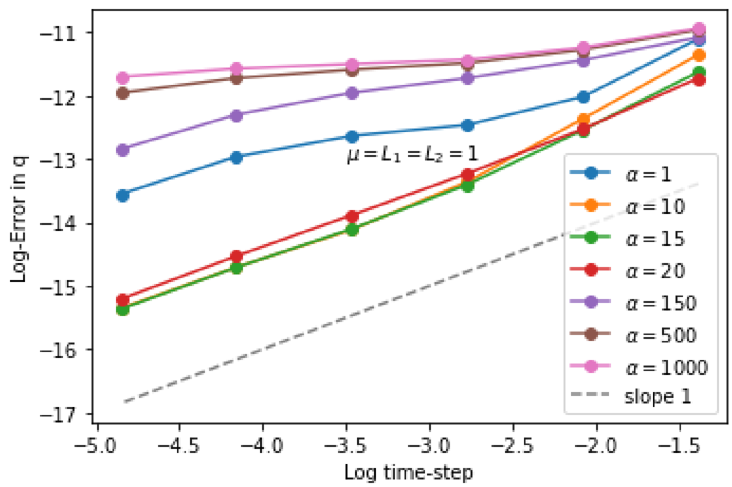

(a)

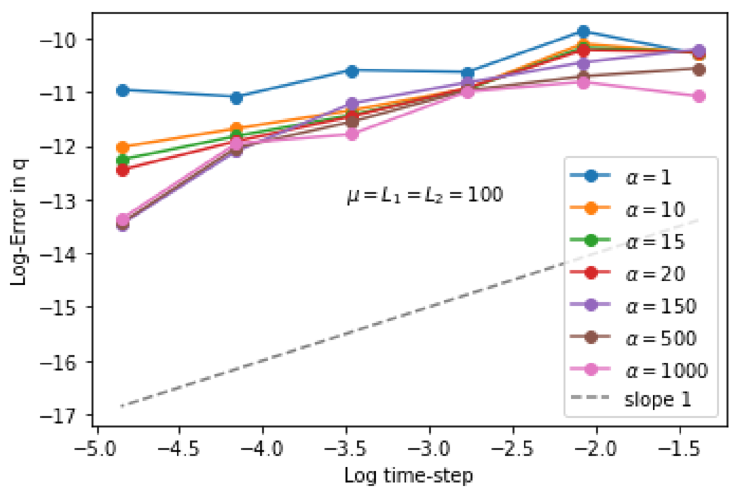

(b)

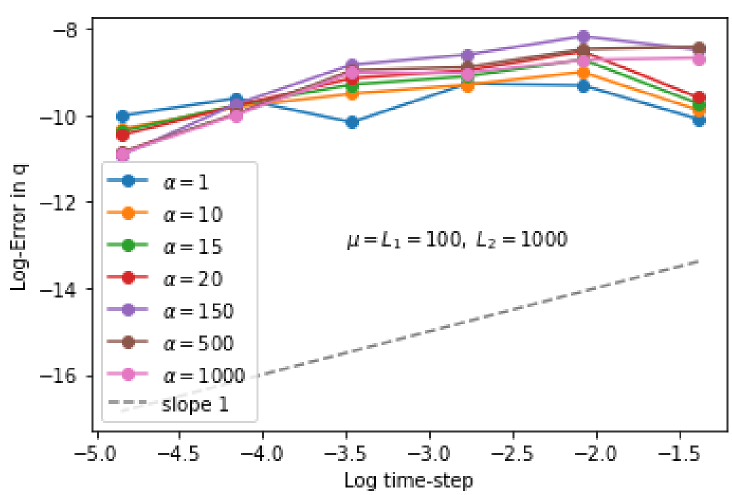

(c)

Figure 4.1: Numerical experiments demonstrating the effect of parameters on convergence of the Robin-Robin method.

In Figure 4.1, we plot the (log-log) convergence of the term $\|\mathbf{q} - \boldsymbol{q}\|_{L^2(\Omega_s)}$ (at the final time T) with respect to Δt. for increasing values of μ, L_1, and L_2. For each case, we run the method for 7 values of α in order to investigate how the Robin parameter may influence the sensitivity of the method to the physical parameters. These results are further summarized in Table 4.1-4.3, where we have provided the rates of convergence for four relevant values of α.

From 4.1a and Table 4.1, we observe that the Robin-Robin method is nearly first order for almost all values of α when the physical parameters are all set to 1, particularly in the limit as Δt gets small (or $\log \Delta t \to -\infty$). This is especially true for $\alpha = 15, 20$, whereas for larger values of α, it appears that this convergence behavior is more delayed. Thus, when all parameters are 1, it appears that a smaller value of α is preferable, but the scheme will still demonstrate nearly optimal convergence within a reasonable Δt.

From Figure 4.1b and Table 4.2, we see that increasing the values of the parameters by a factor of 100 significantly delays the asymptotic convergence until $\alpha = 150, 500$. At this point, the method performs noticeably better until $\alpha = 1000$. Thus, it seems that α must be larger than the previous case in order to compensate for the larger values of μ, L_1, and L_2, but not *too* large, relative to the physical parameters. We see this suggested even more when we move to $L_2 = 1000$, as shown in Figure 4.1c and Table 4.3. Here again we require large values of α in order to observe nearly optimal convergence. However, now it seems that $\alpha = 1000$ permits reasonably good convergence even for larger Δt.

Rates for $\mu = L_1 = L_2 = 1$				
Δt	$\alpha = 1$	$\alpha = 10$	$\alpha = 150$	$\alpha = 1000$
$(\frac{1}{2})^2$	–	–	–	–
$(\frac{1}{2})^3$	1.32	1.46	0.52	0.44
$(\frac{1}{2})^4$	0.64	1.43	0.41	0.27
$(\frac{1}{2})^5$	0.25	1.09	0.33	0.10
$(\frac{1}{2})^6$	0.47	0.85	0.50	0.10
$(\frac{1}{2})^7$	0.85	0.94	0.78	0.19

Table 4.1: Convergence rates for select values of α when $\mu = L_1 = L_2 = 1$.

Rates for $\mu = L_1 = L_2 = 100$				
Δt	$\alpha = 1$	$\alpha = 10$	$\alpha = 150$	$\alpha = 1000$
$(\frac{1}{2})^2$	–	–	–	–
$(\frac{1}{2})^3$	-0.61	-0.25	0.36	-0.39
$(\frac{1}{2})^4$	1.01	1.2	0.54	0.27
$(\frac{1}{2})^5$	-0.05	0.58	0.56	1.14
$(\frac{1}{2})^6$	0.72	0.49	1.28	0.25
$(\frac{1}{2})^7$	-0.18	0.50	1.97	2.04

Table 4.2: Convergence rates for select values of α when $\mu = L_1 = L_2 = 100$.

Rates for $\mu = L_1 = 100$ and $L_2 = 1000$				
Δt	$\alpha = 1$	$\alpha = 10$	$\alpha = 150$	$\alpha = 1000$
$(\frac{1}{2})^2$	–	–	–	–
$(\frac{1}{2})^3$	-1.13	-1.27	-0.45	0.07
$(\frac{1}{2})^4$	-0.05	0.42	0.61	0.44
$(\frac{1}{2})^5$	1.29	0.30	0.34	-0.01
$(\frac{1}{2})^6$	-0.80	0.45	1.31	1.41
$(\frac{1}{2})^7$	0.59	0.73	1.72	1.29

Table 4.3: Convergence rates for select values of α when $\mu = L_1 = 100$ and $L_2 = 1000$.

4.4.2 Concluding remarks

In this chapter, we extended the Robin-Robin splitting method introduced in Chapter 3 to the fluid-structure interaction problem in a time semi-discrete framework. We showed that the nearly optimal accuracy observed in the parabolic-parabolic and parabolic-hyperbolic systems is preserved in the FSI system, provided we accommodate the additional pressure term appropriately in the analysis.

Although the error estimate indicates nearly optimal convergence, we note that this behavior may be obscured or delayed depending on the values of the system's parameters. However, to the best of our knowledge, this splitting method is the first loose coupling for the FSI system developed with provable unconditional stability and nearly first-order accuracy.

So far, we have restricted our analysis to the semi-discrete case, choosing to discretize only in time, and leaving space continuous. We have done so because the main goal of this work is to develop splitting methods to efficiently march an approximate solution forward in time. However, this means that we have not yet explored how the splitting method or the analytical tools we have developed may translate when we consider a fully discrete framework.

In the next chapter, we will see extend the Robin-Robin method to this fully discrete formulation using linear finite elements (although there are certainly other appropriate discretization methods). As we will see, adding this layer of discretization to the problem adds significant complexity, and even more care must be taken, particularly with terms at the interface.

4.5 Numerical Experiements

4.6 Numerical Experiments for Stokes-Elastic

In this section we discuss numerical experiments. We take $\Omega = [0,1]^2$ and $\Omega_f = [0,1] \times [0,3/4]$ and $\Omega_s = [0,1] \times [3/4,1]$ and of course $\Sigma = \overline{\Omega_f} \cap \overline{\Omega_s}$. For our experiments, we set $h = \Delta t$ and run each simulation to $T = 0.25$. For a full description of the method used in the numerical experiments below, see the fully discrete formulation in Chapter 5.

Furthermore, we also set all constants (ρ_s, ρ_f, μ, L_1, and L_2) equal to 1. We then take the exact solution given by (4.4.4), and note that this will lead to forcing terms. In particular, the divergence free condition is not preserved. In other words, our solution satisfies (4.4.1)-(4.4.3).

The forcing terms are given by

$$\begin{aligned}
\boldsymbol{f}_1(t,x) =& \boldsymbol{f}_2(t,x) = (10^{-3})e^t \begin{pmatrix} 2x_1(1-x_1)x_2(1-x_2) + 12x_2(1-x_2) \\ x_1(1-x_1)x_2(1-x_2) + 6x_1(1-x_1) \end{pmatrix} \\
&\qquad + (10^{-3})e^t \begin{pmatrix} 4x_1(1-x_1) - 2(1-2x_1)(1-2x_2) \\ 2x_2(1-x_2) - 4(1-2x_1)(1-2x_2) \end{pmatrix}, \\
g_f(t,x) =& (10^{-3})e^t(2(1-2x_1)x_2(1-x_2) + x_1(1-x_1)(1-2x_2)).
\end{aligned}$$

We also use the following notation:

$$e_u := \|\boldsymbol{e_u}^N\|_{L^2(\Omega_f)} \qquad\qquad e_q := \|\boldsymbol{e_q}^N\|_{L^2(\Omega_s)}$$

$$e_{\epsilon(u)} := (\Delta t \sum_{n=0}^{N-1} (\|\epsilon(\boldsymbol{e_u}^{n+1})\|^2_{L^2(\Omega_f)})^{1/2} \qquad e_S := \|\boldsymbol{e}^N_\eta\|_S$$

$$e_\lambda := \Delta t^{1/2} \|\boldsymbol{e_\lambda}^N\|_{L^2(\Sigma)} \qquad e_{u-\Sigma} := \Delta t^{1/2} \|\boldsymbol{e_u}^N\|_{L^2(\Sigma)}$$

$$e_{resid} := (\Delta t \sum_{n=1}^{N} \|\boldsymbol{e_q}^{n+1/2} - \boldsymbol{e_u}^n\|^2_{L^2(\Sigma)})^{1/2} \quad e_{u-step} := (\|\boldsymbol{e_u}^{n+1} - \boldsymbol{e_u}^n\|^2_{L^2(\Omega_f)})^{1/2}$$

$$e_{\nabla p} := (\sum_{n=1}^{N} \Delta t h^2 \|\nabla e_p^{n+1}\|^2_{L^2(\Omega_f)})^{1/2}$$

As we see from Tables 4.4-4.6, the test problem with the appropriate parameters displayse nearly optimal convergence in all terms, although convergence is notably slower in the term e_S.

Rates									
Δt	e_u	e_q	e_λ	$e_{\epsilon(u)}$	e_S	$e_{u-\Sigma}$	e_{resid}	e_{u-step}	$e_{\nabla p}$
$(\frac{1}{2})^2$	–	–	–	–	–	–	–	–	–
$(\frac{1}{2})^3$	0.65	1.11	0.90	0.92	0.38	1.47	0.57	1.09	1.48
$(\frac{1}{2})^4$	1.26	0.58	0.96	1.14	0.47	1.84	0.43	1.53	1.55
$(\frac{1}{2})^5$	1.41	0.75	1.08	1.27	0.59	1.66	0.58	1.70	1.59
$(\frac{1}{2})^6$	1.33	0.96	1.12	1.32	0.73	1.51	0.77	1.76	1.57
$(\frac{1}{2})^7$	1.14	1.04	1.09	1.24	0.83	1.46	0.88	1.72	1.54
$(\frac{1}{2})^8$	1.03	1.03	1.06	1.12	0.88	1.46	0.94	1.63	1.51
$(\frac{1}{2})^9$	1.00	1.01	1.04	1.02	0.91	1.46	0.97	1.55	1.49

Table 4.4: Convergence rates for the FSI system.

Errors						
Δt	e_u	e_q	e_λ	$e_{\epsilon(u)}$	e_S	$e_{u-\Sigma}$
$(\frac{1}{2})^2$	1.42e-05	1.98e-05	5.30e-05	4.12e-05	2.24e-05	1.58e-05
$(\frac{1}{2})^3$	9.08e-06	9.14e-06	2.84e-05	2.19e-05	1.72e-05	5.71e-06
$(\frac{1}{2})^4$	3.80e-06	6.11e-06	1.46e-05	9.91e-06	1.24e-05	1.59e-06
$(\frac{1}{2})^5$	1.43e-06	3.64e-06	6.93e-06	4.11e-06	8.24e-06	5.04e-07
$(\frac{1}{2})^6$	5.72e-07	1.87e-06	3.19e-06	1.65e-06	4.97e-06	1.77e-07
$(\frac{1}{2})^7$	2.59e-07	9.11e-07	1.50e-06	6.98e-07	2.80e-06	6.45e-08
$(\frac{1}{2})^8$	1.27e-07	4.47e-07	7.20e-07	3.22e-07	1.52e-06	2.35e-08
$(\frac{1}{2})^9$	6.36e-08	2.22e-07	3.51e-07	1.59e-07	8.07e-07	8.53e-09

Table 4.5: Errors for the FSI system, part 1.

Errors (continued)			
Δt	e_{resid}	e_{u-step}	$e_{\nabla p}$
$(\frac{1}{2})^2$	1.45e-05	1.91e-05	1.38e-04
$(\frac{1}{2})^3$	9.78e-06	8.97e-06	4.99e-05
$(\frac{1}{2})^4$	7.24e-06	3.10e-06	1.71e-05
$(\frac{1}{2})^5$	4.86e-06	9.57e-07	5.66e-06
$(\frac{1}{2})^6$	2.85e-06	2.83e-07	1.90e-06
$(\frac{1}{2})^7$	1.55e-06	8.60e-08	6.57e-07
$(\frac{1}{2})^8$	8.07e-07	2.78e-08	2.30e-07
$(\frac{1}{2})^9$	4.13e-07	9.51e-09	8.19e-08

Table 4.6: Errors for the FSI system, part 2.

Chapter Five

Robin-Robin coupling for fluid-structure interaction, Part II: the fully discrete framework

5.1 Robin-Robin coupling for fluid-structure interaction, fully discrete formulation

In this chapter, we present and analyze the Robin-Robin splitting method in a fully discrete framework. Much of this analysis will follow the structure and methods of the previous chapter, but we will need to take special care when applying the spacial discretization, particularly when addressing the function $\tilde{\phi}$ (see 4.3.4).

This chapter is organized as follows. We first introduce the fully-discrete Robin-Robin method for the FSI system. We make a particular point to describe the Lagrange multiplier method/discrete lifting operator argument that has been referenced in the previous chapters. We then comment on the stability of the method before proceeding to the error analysis.

5.1.1 The fully-discrete Robin-Robin method for FSI

The goal of this chapter is to present and analyze a fully discrete approximation for the FSI system (4.1.1)-(4.1.3) using the Robin-Robin splitting method. As such, we begin by applying a spacial discretization to the time-semi-discrete Robin-Robin method for FSI (4.1.6). To keep the analysis simple, we will assume Ω is the union of two *polygonal* domains, Ω_f (the fluid domain), and Ω_s (the solid domain), with matching interface $\Sigma = \partial\Omega_f \cap \partial\Omega_s$, as shown in Figure **??**. Furthermore we will restrict ourselves to linear Lagrange elements, so that $\partial\Omega$ matches with the edges of elements that contain boundary nodes.

Let $\mathcal{T}_h^i$ be a simplicial triangulation of Ω_i where $i = s, f$, and assume that the

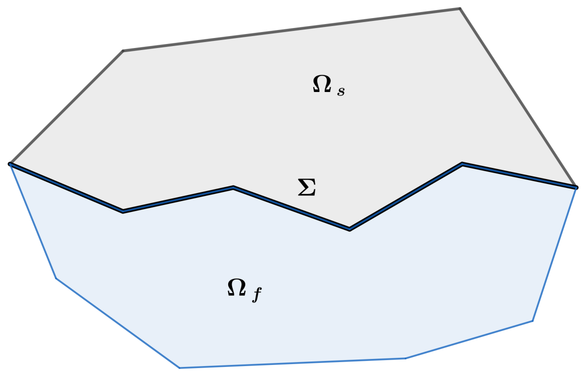

Figure 5.1: An example of a polygonal domain as described above.

meshes are quasi-uniform and shape regular [8] (in fact, our numerical experiments for the FSI problem have been restricted to uniform meshes). We further assume that the meshes on Ω_f and Ω_s match on the interface Σ for reasons that will be made clear below.

Let $\mathcal{P}^1(K)$ be the space of linear functions defined on the element $K \in \mathcal{T}_h^i$ and $\boldsymbol{\mathcal{P}}^1(K) = [\mathcal{P}^1(K)]^2$. We may then define the finite element spaces:

$$\begin{aligned}
\boldsymbol{V}_h^s &:= \{\boldsymbol{v} \in \boldsymbol{V}^s : \boldsymbol{v}|_K \in \boldsymbol{\mathcal{P}}^1(K), \forall K \in \mathcal{T}_h^s\}, \\
\boldsymbol{V}_h^f &:= \{\boldsymbol{v} \in \boldsymbol{V}^f : \boldsymbol{v}|_K \in \boldsymbol{\mathcal{P}}^1(K), \forall K \in \mathcal{T}_h^f\}, \\
\boldsymbol{V}_h^g &:= \{ \text{ trace space of } \boldsymbol{V}_h^f \text{ on } \Sigma\}, \\
M_h^f &:= \{v \in M^f : v|_K \in \mathcal{P}^1(K), \forall K \in \mathcal{T}_h^f\}.
\end{aligned}$$

Note that because the meshes match at Σ, we could alternatively write

$$\boldsymbol{V}_h^g := \{ \text{ trace space of } \boldsymbol{V}_h^s \text{ on } \Sigma\}.$$

As $\boldsymbol{V}_h^f$ and M_h^f do not form an inf-sup stable pair, we include the penalty term $h^2(\nabla p_h^{n+1}, \nabla\theta_h)_f$ to the divergence-free condition in our fluid bilinear form as in [9].

Thus, our fluid and solid bilinear forms for the fully discrete problem are now

$$
\begin{aligned}
a_{f,h}\big((\boldsymbol{u}_h, p_h), (\boldsymbol{v}_h, \theta_h)\big) :=& a_f\big((\boldsymbol{u}_h, p_h), (\boldsymbol{v}_h, \theta_h)\big) + h^2(\nabla p_h, \nabla \theta_h)_f,\\
a_{s,h}\big(\boldsymbol{\eta}_h, \boldsymbol{\xi}_h\big) :=& a_s\big(\boldsymbol{\eta}_h, \boldsymbol{\xi}_h\big),
\end{aligned}
$$

where $a_s(\cdot,\cdot)$ and $a_f(\cdot,\cdot)$ are defined in 4.1.1.

Finally, with the finite element formulation that follows, we see the motivation for representing our normal derivative/fluid stress term as λ in the previous two chapters. Specifically, as stated in 3.2.1 and 4.1.2, the Robin interface conditions (4.1.5) will require piece-wise linear terms–in this case the fluid and solid velocities–which must be continuous across element boundaries, to be equal to linear combinations of the stress terms. These stresses, however, depend on spatial derivatives of the velocities and are therefore not required to be continuous across element boundaries. Consequently, we must enforce continuity across element boundaries in our fluid stress term by introducing a fluid-sided discrete lifting operator $\mathcal{L}_h : \boldsymbol{V}_h^g \rightarrow \boldsymbol{V}_h^f$, such that $\mathcal{L}_h \boldsymbol{\mu}_h$ vanishes on nodes outside of Σ, and $(\mathfrak{L}_h \boldsymbol{\mu}_h)|_\Sigma = \boldsymbol{\mu}_h$, for all $\boldsymbol{\mu}_h \in \boldsymbol{V}_h^g$. We then use this lifting operator to define $\boldsymbol{\lambda}_h^{n+1}$ such that the resulting method is written as follows.

Find $\boldsymbol{q}_h^{n+1}, \boldsymbol{\eta}_h^{n+1} \in \boldsymbol{V}_h^s$, $\boldsymbol{u}_h^{n+1} \in \boldsymbol{V}_h^f$, $\boldsymbol{\lambda}_h^{n+1} \in \boldsymbol{V}_h^g$, and $p_h \in M_h^f$ such that such that

$$
\rho_s(\partial_{\Delta t}\boldsymbol{q}_h^{n+1}, \boldsymbol{\xi}_h)_s + a_s(\boldsymbol{\eta}_h^{n+1/2}, \boldsymbol{\xi}_h) + \alpha\big\langle(\partial_{\Delta t}\boldsymbol{\eta}_h^{n+1} - \boldsymbol{u}_h^n), \boldsymbol{\xi}_h\big\rangle + \big\langle\boldsymbol{\lambda}_h^n, \boldsymbol{\xi}_h\big\rangle = 0 \quad \forall \boldsymbol{\xi}_h \in \boldsymbol{V}_h^s, \tag{5.1.1a}
$$

$$
(\boldsymbol{q}_h^{n+1/2}, \boldsymbol{\tau}_h)_s - (\partial_{\Delta t}\boldsymbol{\eta}_h^{n+1}, \boldsymbol{\tau}_h)_s = 0 \quad \forall \boldsymbol{\tau}_h \in \boldsymbol{V}_h^s. \tag{5.1.1b}
$$

$$\rho_f(\partial_{\Delta t}\boldsymbol{u}_h^{n+1},\boldsymbol{v}_h)_f + 2\mu(\varepsilon(\boldsymbol{u}_h^{n+1}),\varepsilon(\boldsymbol{v}_h))_f - (p_h^{n+1},\operatorname{div}\boldsymbol{v}_h)_f \tag{5.1.2a}$$

$$-\alpha\big\langle \boldsymbol{u}_h^{n+1} - \boldsymbol{q}_h^{n+1/2},\boldsymbol{v}_h\big\rangle - \big\langle \boldsymbol{\lambda}_h^n,\boldsymbol{v}_h\big\rangle = 0 \quad \forall \boldsymbol{v}_h \in \boldsymbol{V}_h^f, \tag{5.1.2b}$$

$$(\operatorname{div}\boldsymbol{u}_h^{n+1},\theta_h)_f + h^2(\nabla p_h^{n+1},\nabla\theta_h)_f = 0 \quad \forall \theta \in M_h^f, \tag{5.1.2c}$$

$$\big\langle \boldsymbol{\lambda}_h^{n+1},\boldsymbol{\mu}_h\big\rangle = \rho_f(\partial_{\Delta t}\boldsymbol{u}_h^{n+1},\mathfrak{L}_h\boldsymbol{\mu}_h)_f + a_{f,h}\big((\boldsymbol{u}_h^{n+1},p_h^{n+1}),(\mathfrak{L}_h\boldsymbol{\mu}_h,0)\big) \quad \forall \boldsymbol{\mu}_h \in \boldsymbol{V}_h^g. \tag{5.1.3}$$

Thus $\boldsymbol{\lambda}_h$ is a variationally consistent representation of the fluid stress on the interface (see [38] and [18], Algorithm 3).

Using (4.1.6c) and (4.1.6d), we may then simplify (5.1.3) to

$$\big\langle \boldsymbol{\lambda}_h^{n+1},\boldsymbol{\mu}_h\big\rangle = \alpha\big\langle \boldsymbol{q}_h^{n+1/2} - \boldsymbol{u}_h^{n+1},\boldsymbol{\mu}_h\big\rangle + \big\langle \boldsymbol{\lambda}_h^n,\boldsymbol{\mu}_h\big\rangle$$

for all $\boldsymbol{\mu}_h \in \boldsymbol{V}_h^g$, allowing us to cast our scheme as a Lagrange multiplier method, as seen below.

Thus the fully discrete Robin-Robin method that we will work with is as follows: find $\boldsymbol{q}_h^{n+1},\boldsymbol{\eta}_h^{n+1} \in \boldsymbol{V}_h^s$, $\boldsymbol{u}_h^{n+1} \in \boldsymbol{V}_h^f$, $p_h \in M_h^f$, and $\boldsymbol{\lambda}_h^{n+1} \in \boldsymbol{V}_h^g$ such that such that

$$\rho_s(\partial_{\Delta t}\boldsymbol{q}_h^{n+1},\boldsymbol{\xi}_h)_s + a_s(\boldsymbol{\eta}_h^{n+1/2},\boldsymbol{\xi}_h) + \alpha\big\langle(\partial_{\Delta t}\boldsymbol{\eta}_h^{n+1} - \boldsymbol{u}_h^n),\boldsymbol{\xi}_h\big\rangle + \big\langle \boldsymbol{\lambda}_h^n,\boldsymbol{\xi}_h\big\rangle = 0 \quad \forall \boldsymbol{\xi}_h \in \boldsymbol{V}_h^s, \tag{5.1.4a}$$

$$(\boldsymbol{q}_h^{n+1/2},\boldsymbol{\tau}_h)_s - (\partial_{\Delta t}\boldsymbol{\eta}_h^{n+1},\boldsymbol{\tau}_h)_s = 0 \quad \forall \phi_h \in \boldsymbol{V}_h^s. \tag{5.1.4b}$$

$$\rho_f(\partial_{\Delta t}\boldsymbol{u}_h^{n+1},\boldsymbol{v}_h)_f + 2\mu(\varepsilon(\boldsymbol{u}_h^{n+1}),\varepsilon(\boldsymbol{v}_h))_f - (p_h^{n+1},\operatorname{div}\boldsymbol{v}_h)_f - \langle\boldsymbol{\lambda}_h^{n+1},\boldsymbol{v}_h\rangle = 0 \quad \forall\boldsymbol{v}_h\in\boldsymbol{V}_h^f \tag{5.1.5a}$$

$$(\operatorname{div}\boldsymbol{u}_h^{n+1},\theta_h)_f + h^2(\nabla p_h^{n+1},\nabla\theta_h)_f = 0 \quad \forall\theta\in M_h^f \tag{5.1.5b}$$

$$\alpha\langle\boldsymbol{u}_h^{n+1}-\boldsymbol{q}_h^{n+1/2},\boldsymbol{\mu}_h\rangle + \langle\boldsymbol{\lambda}_h^{n+1}-\boldsymbol{\lambda}_h^{n},\boldsymbol{\mu}_h\rangle = 0 \quad \forall\boldsymbol{\mu}_h\in\boldsymbol{V}_h^g. \tag{5.1.5c}$$

As before, we have identities analogous to (3.2.3) and (3.2.5) as well as (4.1.7) and (4.1.8). Thus, using the same approach as in previous chapters, we find

$$\boldsymbol{q}_h^{n+1/2} = \partial_{\Delta t}\boldsymbol{\eta}_h^{n+1} \quad \text{on } \Omega_s, \tag{5.1.6}$$

and

$$\boldsymbol{\lambda}_h^{n+1} = \alpha(\boldsymbol{q}_h^{n+1/2}-\boldsymbol{u}_h^{n+1}) + \boldsymbol{\lambda}_h^{n} \quad \text{on } \Sigma, \tag{5.1.7}$$

for $n \geq 1$.

5.1.2 Stability

We will not provide a proof of stability for the fully discrete method as it is essentially identical to the proof of Lemma 4.2.1. The only notable difference is the presence of the term

$$h^2(\nabla p^{n+1},\nabla\theta)_f.$$

This term, however, is immediately addressed when we set $\theta = p$, as in the proof of Lemma 4.2.1. The result is an additional term in $\mathbf{S}^{n+1}$, as seen below. As this term only appears on the left-hand side, it does not change the stability result or the remainder of the proof in any meaningful way. As such, we state the following without proof.

Lemma 5.1.1. *Let*

$$\begin{aligned}
\mathcal{S}_h^n =& \|\boldsymbol{\eta}_h^n\|_S^2 + \rho_s\|\boldsymbol{q}_h^n\|_{L^2(\Omega_s)}^2 + \rho_f\|\boldsymbol{u}_h^n\|_{L^2(\Omega_f)}^2 + \Delta t(\alpha\|\boldsymbol{u}_h^n\|_{L^2(\Sigma)}^2 + \frac{1}{\alpha}\|\boldsymbol{\lambda}_h^n\|_{L^2(\Sigma)}^2),\\
\mathcal{Z}_h^n =& \rho_f\|\boldsymbol{u}_h^n - \boldsymbol{u}_h^{n-1}\|_{L^2(\Omega_f)}^2 + 2\alpha\Delta t\|\partial_{\Delta t}\boldsymbol{\eta}_h^n - \boldsymbol{u}_h^{n-1}\|_{L^2(\Sigma)}^2 + 4\mu\Delta t\|\varepsilon(\boldsymbol{u}_h^{n+1})\|_{L^2(\Omega_f)}^2\\
&+ 2h^2\Delta t\|\nabla p_h^n\|_{L^2(\Omega_s)}^2.
\end{aligned}$$

Then it holds,

$$\mathcal{S}_h^M + \sum_{m=1}^{M}\mathcal{Z}_h^m = \mathcal{S}_h^0 \qquad \textit{for } 1 \leq M \leq N.$$

5.2 Error Analysis

Similar to the previous chapters, the main result of this chapter is the a priori error estimate of the Robin-Robin splitting method in the fully discrete framework. As before, we will approach this result in three parts. We will first bound all but one term that must be treated with special care. We will then bound this isolated term before proceeding to the complete error result.

5.2.1 Time-semi-discrete vs. fully discrete: linear interpolants and L^2-projections

We already have the error estimate for the time-discrete formulation from Chapter 4. Thus, the main challenge of this chapter will be to incorporate the spatial error arising from the finite element approximation. To do so, we define the following discrete errors:

$$\begin{aligned} \boldsymbol{e}_{\eta,h}^{n} &:= \boldsymbol{\eta}_h^n - R_h^s \mathbf{e}^n, & \boldsymbol{e}_{\boldsymbol{q},h}^{n} &:= \boldsymbol{q}_h^n - R_h^s \mathbf{q}^n, \\ \boldsymbol{e}_{\boldsymbol{u},h}^{n} &:= \boldsymbol{u}_h^n - R_h^f(\mathbf{u}^n), & \boldsymbol{e}_{\boldsymbol{\lambda},h}^{n} &:= \boldsymbol{\lambda}_h^n - \mathbb{P}_h \mathbf{l}^n, \\ e_{p,h}^{n} &:= p_h^n - S_h(\mathsf{p}^n), \end{aligned}$$

where R_h^i, $i = s, f$ are the Scott-Zhang interpolants (as defined in 2.2.1, (2.2.11)) projecting onto our finite element spaces V_h^s and V_h^f, and S_h is the Scott-Zhang interpolant into M_h^f modified by a global constant so the average on Ω_f is zero. For projecting into V_h^g, we use $\mathbb{P}_h$, the L^2 orthogonal projection from V^g to V_h^g defined in Definition 2.2.8.

Recall from 2.2.1 that there is flexiblity in defining the Scott-Zhang interpolant. Thus we may choose the degrees of freedom on the boundary to honor the fact that the fluid and solid meshes match on Σ. In other words, we may choose the degrees of freedom so that we will have $R_h^s \boldsymbol{v} = R_h^f \boldsymbol{w}$ on Σ if $\boldsymbol{v} \in [H^1(\Omega_s)]^2$ and $\boldsymbol{w} \in [H^1(\Omega_f)]^2$ and $\boldsymbol{v} = \boldsymbol{w}$ on Σ.

Clearly, the ultimate goal of our error analysis is to provide an error estimate for the terms

$$\begin{aligned} \boldsymbol{e}_{\eta}^{n} :=& \boldsymbol{\eta}_h^n - \mathbf{e}^n, \quad \boldsymbol{e_q}^n := \boldsymbol{q}_h^n - \mathbf{q}^n, \\ \boldsymbol{e_u}^n :=& \boldsymbol{u}_h^n - \mathbf{u}^n, \quad \boldsymbol{e_\lambda}^n := \boldsymbol{\lambda}_h^n - \mathbf{l}^n, \\ e_p^n :=& p_h^n - \mathsf{p}^n, \end{aligned}$$

which measure the error between the fully discrete approximation and the exact solution. These error terms can subsequently be rewritten

$$\begin{aligned} \boldsymbol{e}_{\eta}^{n} :=& \boldsymbol{e}_{\eta,h}^{\ n} + (R_h^s \mathbf{e}^n - \mathbf{e}^n), \quad \boldsymbol{e_q}^n := \boldsymbol{e_q}_{,h}^{\ n} + (R_h^s \mathbf{q}^n - \mathbf{q}^n), \\ \boldsymbol{e_u}^n :=& \boldsymbol{e_u}_{,h}^{\ n} + (R_h^f \mathbf{u}^n - \mathbf{u}^n), \quad \boldsymbol{e_\lambda}^n := \boldsymbol{e_\lambda}_{,h}^{\ n} + (\mathbb{P}_h \mathbf{l}^n - \mathbf{l}^n), \\ e_p^n :=& e_{p,h}^n + (S_h \mathsf{p}^n - \mathsf{p}^n). \end{aligned}$$

In the analysis that follows, we will obtain an error bound for the discrete terms $\boldsymbol{e}_{\eta,h}^{\ n}$, $\boldsymbol{e_q}_{,h}^{\ n}$, $\boldsymbol{e_u}_{,h}^{\ n}$, $\boldsymbol{e_\lambda}_{,h}^{\ n}$, and $e_{p,h}^n$, rather than the full errors $\boldsymbol{e}_{\eta}^{n}$, $\boldsymbol{e_q}^n$, $\boldsymbol{e_u}^n$, $\boldsymbol{e_\lambda}^n$, and e_p^n. We do so because we already have optimal bounds for the interpolation error of the Scott-Zhang interpolants from Lemma 2.2.14, so the results in this chapter yield error bounds for $\boldsymbol{e}_{\eta}^{n}$, $\boldsymbol{e_q}^n$, $\boldsymbol{e_u}^n$, and e_p^n by triangle inequality.

Unfortunately, this cannot be guaranteed for the term $\boldsymbol{e_\lambda}^n$ because we cannot guarantee a good error bound for the L^2 orthogonal projection defined on a boundary. Thus, the analysis below only guarantees a bound for $\boldsymbol{e_\lambda}_{,h}^{\ n}$, not $\boldsymbol{e_\lambda}^n$, and we cannot verify whether or not $\boldsymbol{\lambda}_h^n$ is a good approximation. However, this does not necessarily mean that we have a problem, as we recall that $\mathbf{l}^n = \sigma_f(\mathbf{u}^n, \mathsf{p}^n)\boldsymbol{n}_f$. Therefore, if $\boldsymbol{u}_h^n$ and p_h^n are good approximations of $\mathbf{u}^n$ and p^n (which is guaranteed by the error bounds), then we will have a good approximation for $\mathbf{l}^n$ without $\boldsymbol{\lambda}_h^n$.

5.2.2 The error equations

To formulate the error equations, we begin by first establishing the consistency of the interpolated and projected terms. We do so by plugging these terms into (5.1.4)-(5.1.5). Obviously, the interpolants will not satisfy these equations, but we use this step to write two expressions to describe how inconsistent the interpolants are in terms of quantities that we can bound in terms of the solutions to (4.1.4). As such, we have the following result.

Lemma 5.2.1. *The following identities hold for all $\boldsymbol{\xi}_h \in \boldsymbol{V}_h^s$, $\boldsymbol{v}_h \in \boldsymbol{V}_h^f$, and $\boldsymbol{\mu}_h \in \boldsymbol{V}_h^g$.*

$$\begin{aligned}\rho_s(\partial_{\Delta t} R_h^s \mathbf{q}^{n+1}, \boldsymbol{\xi}_h)_s + a_s(R_h^s \mathbf{e}^{n+1/2}, \boldsymbol{\xi}_h) + \alpha\big\langle(\partial_{\Delta t} R_h^s \mathbf{e}^{n+1} - R_h^f \mathbf{u}^n), \boldsymbol{\xi}_h\big\rangle + \big\langle \mathbb{P}_h \mathbf{l}^n, \boldsymbol{\xi}_h\big\rangle \\ = T_1(\boldsymbol{\xi}_h) + \frac{1}{2} T_2(\boldsymbol{\xi}_h) + V_1(\boldsymbol{\xi}_h) - S_2(\boldsymbol{\xi}_h) + S_3(\boldsymbol{\xi}_h),\end{aligned} \tag{5.2.1}$$

$$(R_h^s \mathbf{q}^{n+1/2} - \partial_{\Delta t} R_h^s \mathbf{e}^{n+1}, \boldsymbol{\tau}_h)_s = (\boldsymbol{h}_{3,h}^{n+1}, \boldsymbol{\tau}_h)_s, \tag{5.2.2}$$

$$\begin{aligned}\rho_f(\partial_{\Delta t} R_h^f \mathbf{u}^{n+1}, \boldsymbol{v}_h)_f + 2\mu(\varepsilon(R_h^f \mathbf{u}^{n+1}), \varepsilon(\boldsymbol{v}_h))_f - (S_h \mathsf{p}^{n+1}, \operatorname{div} \boldsymbol{v}_h)_f - \big\langle \mathbb{P}_h \mathbf{l}^{n+1}, \boldsymbol{v}_h\big\rangle \\ = S_1(\boldsymbol{v}_h) + V_2(\boldsymbol{v}_h),\end{aligned} \tag{5.2.3}$$

$$(\operatorname{div} R_h^f \mathbf{u}^{n+1}, \theta_h)_f + h^2(\nabla S_h \mathsf{p}^{n+1}, \nabla \theta_h)_f = V_3(\theta_h) + V_4(\theta_h), \tag{5.2.4}$$

$$\begin{aligned}\alpha\big\langle R_h^f \mathbf{u}^{n+1} - \partial_{\Delta t} R_h^s \mathbf{e}^{n+1}, \boldsymbol{\mu}_h\big\rangle = \big\langle \mathbf{l}^n - \mathbf{l}^{n+1}, \boldsymbol{\mu}_h\big\rangle + \alpha\big\langle \boldsymbol{h}_{4,h}^{n+1}, \boldsymbol{\mu}_h\big\rangle \\ + \big\langle \boldsymbol{g}_2^{n+1}, \boldsymbol{\mu}_h\big\rangle,\end{aligned} \tag{5.2.5}$$

where

$$\begin{aligned}\boldsymbol{g}_{1,h}^{n+1} &:= R_h^f \mathbf{u}^{n+1} - R_h^f \mathbf{u}^n, \\ \boldsymbol{g}_2^{n+1} &:= \mathbf{l}^{n+1} - \mathbf{l}^n,\end{aligned}$$

$$\begin{aligned}
\boldsymbol{h}_{3,h}^{n+1} :=& R_h^s \mathbf{q}^{n+1/2} - \partial_{\Delta t} R_h^s \mathbf{e}^{n+1}, \\
\boldsymbol{h}_{4,h}^{n+1} :=& R_h^s \partial_t \mathbf{e}^{n+1} - \partial_{\Delta t} R_h^s \mathbf{e}^{n+1}, \\
T_1(\boldsymbol{\xi}_h) :=& \rho_s(\partial_{\Delta t} R_h^s \mathbf{q}^{n+1} - \partial_t \mathbf{q}^{n+1/2}, \boldsymbol{\xi}_h)_s, \\
T_2(\boldsymbol{\xi}_h) :=& \langle \mathbf{l}^n - \mathbf{l}^{n+1}, \boldsymbol{\xi}_h \rangle, \\
S_1(\boldsymbol{v}_h) :=& \rho_f(\partial_{\Delta t} R_h^f \mathbf{u}^{n+1} - \partial_t \mathbf{u}^{n+1}, \boldsymbol{v}_h)_f, \\
S_2(\boldsymbol{\mu}_h) :=& \alpha \langle R_h^f \mathbf{u}^{n+1} - \partial_{\Delta t} R_h^s \mathbf{e}^{n+1}, \boldsymbol{\mu}_h \rangle, \\
S_3(\boldsymbol{\mu}_h) :=& \alpha \langle R_h^f \mathbf{u}^{n+1} - R_h^f \mathbf{u}^{n}, \boldsymbol{\mu}_h \rangle, \\
V_1(\boldsymbol{\xi}_h) :=& a_s(R_h^s \mathbf{e}^{n+1/2} - \mathbf{e}^{n+1/2}, \boldsymbol{\xi}_h)_s, \\
V_2(\boldsymbol{v}_h) :=& 2\mu(\varepsilon(R_h^f \mathbf{u}^{n+1} - \mathbf{u}^{n+1}), \varepsilon(\boldsymbol{v}_h))_f - (S_h \mathsf{p}^{n+1} - \mathsf{p}^{n+1}, \operatorname{div} \boldsymbol{v}_h)_f, \\
V_3(\theta_h) :=& (\operatorname{div}(R_h^f \mathbf{u}^{n+1} - \mathbf{u}^{n+1}), \theta_h)_f, \\
V_4(\theta_h) :=& h^2(\nabla S_h \mathsf{p}^{n+1}, \nabla \theta_h)_f.
\end{aligned}$$

Note that, as in previous chapters, we use the average of the exact equation (4.1.4a) at times t_n and t_{n+1}. Furthermore, the quantities $\boldsymbol{g}_{1,h}^{n+1}$, $\boldsymbol{h}_{3,h}^{n+1}$, and $\boldsymbol{h}_{4,h}^{n+1}$ are the interpolated versions of $\boldsymbol{g}_1^{n+1}$, $\boldsymbol{h}_3^{n+1}$, and $\boldsymbol{h}_4^{n+1}$ defined in Chapter 4. The quantity $\boldsymbol{g}_2^{n+1}$, on the other hand, is the same as it was in Chapter 4. As we will see, this quantity occurs as a result of (2.2.2).

Proof. The proof for (5.2.2) is trivial, so we will only prove (5.2.1), (5.2.3), (5.2.4), and (5.2.5).

Let $\mathbb{L}_1$ denote the left-hand side of (5.2.1). Then using (4.1.4a) and (2.2.2), we have

$$\mathbb{L}_1 = \rho_s(\partial_{\Delta t} R_h^s \mathbf{q}^{n+1} - \partial_t \mathbf{q}^{n+1/2}, \boldsymbol{\xi}_h)_s + \rho_s(\partial_t \mathbf{q}^{n+1/2}, \boldsymbol{\xi}_h)_s + a_s(R_h^s \mathbf{e}^{n+1/2}, \boldsymbol{\xi}_h)$$

$$
\begin{aligned}
&+ \alpha\big\langle(\partial_{\Delta t} R_h^s \mathbf{e}^{n+1} - R_h^f \mathbf{u}^{n+1}), \boldsymbol{\xi}_h\big\rangle + S_3(\boldsymbol{\xi}_h) + \big\langle \mathbb{P}_h \mathbf{l}^n, \boldsymbol{\xi}_h\big\rangle \\
=& T_1(\boldsymbol{\xi}_h) - a_s(\mathbf{e}^{n+1/2}, \boldsymbol{\xi}_h) + a_s(R_h^s \mathbf{e}^{n+1/2}, \boldsymbol{\xi}_h) + \big\langle \mathbf{l}^n - \mathbf{l}^{n+1/2}, \boldsymbol{\xi}_h\big\rangle \\
&- S_2(\boldsymbol{\xi}_h) + S_3(\boldsymbol{\xi}_h) \\
=& T_1(\boldsymbol{\xi}_h) + V_1(\boldsymbol{\xi}_h) + \frac{1}{2} T_2(\boldsymbol{\xi}_h) - S_2(\boldsymbol{\xi}_h) + S_3(\boldsymbol{\xi}_h).
\end{aligned}
$$

Similarly, let $\mathbb{L}_2$ denote the left hand side of (5.2.3). Then using (4.1.4c), we have

$$
\begin{aligned}
\mathbb{L}_2 =& \rho_f(\partial_{\Delta t} R_h^f \mathbf{u}^{n+1} - \partial_t \mathbf{u}^{n+1}, \boldsymbol{v}_h)_f + \rho_f(\partial_t \mathbf{u}^{n+1}, \boldsymbol{v}_h)_f \\
&+ 2\mu(\varepsilon(R_h^f \mathbf{u}^{n+1}), \varepsilon(\boldsymbol{v}_h))_f - (S_h \mathsf{p}^{n+1}, \operatorname{div} \boldsymbol{v}_h)_f - \big\langle \mathbb{P}_h \mathbf{l}^{n+1}, \boldsymbol{v}_h\big\rangle \\
=& S_1(\boldsymbol{v}_h) - 2\mu(\varepsilon(\mathbf{u}^{n+1}), \varepsilon(\boldsymbol{v}_h))_f + (\mathsf{p}^{n+1}, \operatorname{div} \boldsymbol{v}_h)_f + \big\langle \mathbf{l}^{n+1}, \boldsymbol{v}_h\big\rangle \\
&+ 2\mu(\varepsilon(R_h^f \mathbf{u}^{n+1}), \varepsilon(\boldsymbol{v}_h))_f - (S_h \mathsf{p}^{n+1}, \operatorname{div} \boldsymbol{v}_h)_f - \big\langle \mathbf{l}^{n+1}, \boldsymbol{v}_h\big\rangle \\
=& S_1(\boldsymbol{v}_h) + V_2(\boldsymbol{v}_h).
\end{aligned}
$$

Next, recall that $\operatorname{div} \boldsymbol{u}^n = 0$ for all $n \geq 1$. Therefore, we let $\mathbb{L}_3$ denote the left hand side of (5.2.4). Then using (4.1.4c) with $\boldsymbol{v} = 0$, we have

$$
\begin{aligned}
\mathbb{L}_3 =& (\operatorname{div} R_h^f \mathbf{u}^{n+1}, \theta_h)_f + h^2(\nabla S_h \mathsf{p}^{n+1}, \nabla \theta_h)_f \\
=& (\operatorname{div} R_h^f \mathbf{u}^{n+1} - \operatorname{div} \mathbf{u}^{n+1}, \theta_h)_f + h^2(\nabla S_h \mathsf{p}^{n+1}, \nabla \theta_h)_f \\
=& V_3(\theta_h) + V_4(\theta_h).
\end{aligned}
$$

Finally, (5.2.5) is very straightforward. Recall that $R_h^s = R_h^f$ on Σ. Therefore, since $\partial_t \mathbf{e}^{n+1} = \mathbf{u}^{n+1}$ on Σ, it follows that,

$$
R_h^f \mathbf{u}^{n+1} - \partial_{\Delta t} R_h^s \mathbf{e}^{n+1} - \boldsymbol{h}_{4,h}^{n+1} = R_h^f \mathbf{u}^{n+1} - R_h^s \partial_t \mathbf{e}^{n+1} = 0,
$$

on Σ. The rest follows immediately once we apply the properties of the L^2-projection.

$\square$

We may now subtract the results of Lemma 5.2.1 from (5.1.4)-(5.1.5), to obtain our error equations. They hold for all $\boldsymbol{\xi}_h, \boldsymbol{\tau}_h \in \boldsymbol{V}_h^s$, $\boldsymbol{v}_h \in \boldsymbol{V}_h^f$, and $\theta_h \in M_h^f$.

$$\rho_s(\partial_{\Delta t}\boldsymbol{e}_{\boldsymbol{q},h}^{n+1}, \boldsymbol{\xi}_h)_s + a_s(\boldsymbol{e}_{\eta,h}^{n+1/2}, \boldsymbol{\xi}_h) + \alpha\big\langle(\partial_{\Delta t}\boldsymbol{e}_{\eta,h}^{n+1} - \boldsymbol{e}_{\boldsymbol{u},h}^{n}), \boldsymbol{\xi}_h\big\rangle + \big\langle \boldsymbol{e}_{\boldsymbol{\lambda},h}^{n}, \boldsymbol{\xi}_h\big\rangle$$
$$= -T_1(\boldsymbol{\xi}_h) - \frac{1}{2}T_2(\boldsymbol{\xi}_h) - V_1(\boldsymbol{\xi}_h) + S_2(\boldsymbol{\xi}_h) - S_3(\boldsymbol{\xi}_h), \tag{5.2.6a}$$
$$(\boldsymbol{e}_{\boldsymbol{q},h}^{n+1/2} - \partial_{\Delta t}\boldsymbol{e}_{\eta,h}^{n+1}, \boldsymbol{\tau}_h)_s = (-\boldsymbol{h}_{3,h}^{n+1}, \boldsymbol{\tau}_h)_s, \tag{5.2.6b}$$

$$\rho_f(\partial_{\Delta t}\boldsymbol{e}_{\boldsymbol{u},h}^{n+1}, \boldsymbol{v}_h)_f + 2\mu(\varepsilon(\boldsymbol{e}_{\boldsymbol{u},h}^{n+1}), \varepsilon(\boldsymbol{v}_h))_f - (e_{p,h}^{n+1}, \operatorname{div}\boldsymbol{v}_h)_f - \big\langle \boldsymbol{e}_{\boldsymbol{\lambda},h}^{n+1}, \boldsymbol{v}_h\big\rangle$$
$$= -S_1(\boldsymbol{v}_h) - V_2(\boldsymbol{v}_h), \tag{5.2.7a}$$
$$(\operatorname{div}\boldsymbol{e}_{\boldsymbol{u},h}^{n+1}, \theta_h)_f + h^2(\nabla e_{p,h}^{n+1}, \nabla\theta_h)_f = -V_3(\theta_h) - V_4(\theta_h), \tag{5.2.7b}$$
$$\big\langle \boldsymbol{e}_{\boldsymbol{\lambda},h}^{n+1} - \boldsymbol{e}_{\boldsymbol{\lambda},h}^{n}, \boldsymbol{\mu}_h\big\rangle - \alpha\big\langle(\partial_{\Delta t}\boldsymbol{e}_{\eta,h}^{n+1} - \boldsymbol{e}_{\boldsymbol{u},h}^{n+1}), \boldsymbol{\mu}_h\big\rangle = \alpha\big\langle \boldsymbol{h}_{4,h}^{n+1}, \boldsymbol{\mu}_h\big\rangle + \big\langle \boldsymbol{g}_2^{n+1}, \boldsymbol{\mu}_h\big\rangle. \tag{5.2.7c}$$

Note that the terms $\big\langle \boldsymbol{e}_{\boldsymbol{\lambda},h}^{n}, \boldsymbol{\xi}_h\big\rangle$ and $\big\langle \boldsymbol{e}_{\boldsymbol{\lambda},h}^{n+1}, \boldsymbol{v}_h\big\rangle$ are equivalent to $\big\langle \boldsymbol{e}_{\boldsymbol{\lambda}}{}^{n}, \boldsymbol{\xi}_h\big\rangle$ and $\big\langle \boldsymbol{e}_{\boldsymbol{\lambda}}{}^{n+1}, \boldsymbol{v}_h\big\rangle$, respectively, but we leave them as is for clarity.

As in the previous chapters, we will more often use the strong counterparts of (5.2.6b) and (5.2.7c):

$$\boldsymbol{e}_{\boldsymbol{\lambda},h}^{n+1} - \boldsymbol{e}_{\boldsymbol{\lambda},h}^{n} = \alpha(\partial_{\Delta t}\boldsymbol{e}_{\eta,h}^{n+1} - \boldsymbol{e}_{\boldsymbol{u},h}^{n+1}) + \alpha\boldsymbol{h}_{4,h}^{n+1} + \mathbb{P}_h\boldsymbol{g}_2^{n+1}, \quad \text{on } \Sigma, \tag{5.2.8a}$$

$$\boldsymbol{e}_{\boldsymbol{q},h}^{n+1/2} = \partial_{\Delta t}\boldsymbol{e}_{\eta,h}^{n+1} - \boldsymbol{h}_{3,h}^{n+1}, \quad \text{on } \Omega_s. \tag{5.2.8b}$$

Combined, these further yield

$$\alpha(\boldsymbol{e}_{\boldsymbol{u},h}^{n+1} - \boldsymbol{e}_{\boldsymbol{q},h}^{n+1/2}) = \boldsymbol{e}_{\boldsymbol{\lambda},h}^{n} - \boldsymbol{e}_{\boldsymbol{\lambda},h}^{n+1} + \boldsymbol{g}_{3,h}^{n+1} \tag{5.2.9}$$

where

$$\boldsymbol{g}_{3,h}^{n+1} := \frac{\alpha}{2}\boldsymbol{g}_{1,h}^{n+1} + \mathbb{P}_h \boldsymbol{g}_2^{n+1}.$$

Indeed, that if we restrict to the interface, we may use (4.1.3) and the fact that $R_h^s = R_h^f$ on Σ to determine

$$\begin{aligned}
\boldsymbol{g}_{3,h}^{n+1}|_{\Sigma} =& \frac{\alpha}{2}(R_h^s \partial_t \mathbf{e}^{n+1} - R_h^s \partial_t \mathbf{e}^{n}) + \boldsymbol{g}_2^{n+1} \\
=& \alpha(R_h^s \partial_t \mathbf{e}^{n+1} - R_h^s \mathbf{q}^{n+1/2}) + \boldsymbol{g}_2^{n+1} \\
=& \alpha(R_h^s \partial_t \mathbf{e}^{n+1} - \partial_{\Delta t} R_h^s \mathbf{e}^{n+1} + \partial_{\Delta t} R_h^s \mathbf{e}^{n+1} - R_h^s \mathbf{q}^{n+1/2}) + \boldsymbol{g}_2^{n+1} \\
=& \alpha(\boldsymbol{h}_{4,h}^{n+1} - \boldsymbol{h}_{3,h}) + \boldsymbol{g}_2^{n+1}.
\end{aligned}$$

Finally, we define the following quantities to construct our error estimate. Note that we use more terms than in previous chapters in order to break the analysis up into clearer steps.

$$\begin{aligned}
\mathcal{S}_h^n :=& \|\boldsymbol{e}_{\eta,h}^{n}\|_S^2 + \rho_s \|\boldsymbol{e}_{\boldsymbol{q},h}^{n}\|_{L^2(\Omega_s)}^2 + \rho_f \|\boldsymbol{e}_{\boldsymbol{u},h}^{n}\|_{L^2(\Omega_f)}^2, \\
\mathcal{E}_h^n :=& \Delta t \alpha \|\boldsymbol{e}_{\boldsymbol{u},h}^{n}\|_{L^2(\Sigma)}^2 + \frac{\Delta t}{\alpha}\|\boldsymbol{e}_{\boldsymbol{\lambda},h}^{n}\|_{L^2(\Sigma)}^2, \\
\mathcal{W}_h^n :=& \rho_f \|\boldsymbol{e}_{\boldsymbol{u},h}^{n} - \boldsymbol{e}_{\boldsymbol{u},h}^{n-1}\|_{L^2(\Omega_f)}^2 + 4\mu\Delta t \|\varepsilon(\boldsymbol{e}_{\boldsymbol{u},h}^{n})\|_{L^2(\Omega_f)}^2 + 2\Delta t h^2 \|\nabla e_{p,h}^n\|_{L^2(\Omega_s)}^2, \\
\mathcal{Z}_h^n :=& \Delta t \alpha \|\boldsymbol{e}_{\boldsymbol{q},h}^{n-1/2} - \boldsymbol{e}_{\boldsymbol{u},h}^{n-1}\|_{L^2(\Sigma)}^2.
\end{aligned}$$

5.2.3 Step 1: Preliminary Estimates

We begin, as always, with a preliminary bound. The proof will proceed similarly to the previous chapters, but there will now be more terms to manage with care.

Lemma 5.2.2. *It holds,*

$$\begin{aligned}
&\frac{1}{2}\mathcal{S}_h^{n+1} + \frac{1}{2}\mathcal{E}_h^{n+1} + \frac{1}{2}\mathcal{W}_h^{n+1} + \frac{1}{2}\mathcal{Z}_h^{n+1} \\
&= \frac{1}{2}\mathcal{S}_h^{n} + \frac{1}{2}\mathcal{E}_h^{n} + \Delta t \sum_{i=1}^{9} K_i^{n+1} + \frac{\Delta t}{2\alpha}\|\boldsymbol{g}_{3,h}^{n+1}\|^2_{L^2(\Sigma)} + \frac{\Delta t}{\alpha}\langle \boldsymbol{e}_{\boldsymbol{\lambda},h}^{n}, \boldsymbol{g}_{3,h}^{n+1}\rangle,
\end{aligned} \tag{5.2.10}$$

where

$$\begin{aligned}
K_1^{n+1} &:= -T_1(\boldsymbol{e}_{\boldsymbol{q},h}^{n+1/2}), & K_2^{n+1} &:= \frac{1}{2}T_2(\boldsymbol{e}_{\boldsymbol{q},h}^{n+1/2}), & K_3^{n+1} &:= -S_3(\boldsymbol{e}_{\boldsymbol{q},h}^{n+1/2}), \\
K_4^{n+1} &:= -S_1(\boldsymbol{e}_{\boldsymbol{u},h}^{n+1}), & K_5^{n+1} &:= a_s(\boldsymbol{e}_{\eta,h}^{n+1/2}, \boldsymbol{h}_{3,h}^{n+1}), & K_6^{n+1} &:= -V_3(e_{p,h}^{n+1}), \\
K_7^{n+1} &:= -V_4(e_{p,h}^{n+1}), & K_8^{n+1} &:= -V_1(\boldsymbol{e}_{\boldsymbol{q},h}^{n+1/2}), & K_9^{n+1} &:= -V_2(\boldsymbol{e}_{\boldsymbol{u},h}^{n+1}).
\end{aligned}$$

Proof. To begin, we let $\boldsymbol{\xi}_h = \Delta t \boldsymbol{e}_{\boldsymbol{q},h}^{n+1/2}$ in (5.2.6a) to obtain

$$\begin{aligned}
&\frac{1}{2}\|\boldsymbol{e}_{\eta,h}^{n+1}\|_S^2 + \frac{\rho_s}{2}\|\boldsymbol{e}_{\boldsymbol{q},h}^{n+1}\|^2_{L^2(\Omega_s)} \\
=&\frac{1}{2}\|\boldsymbol{e}_{\eta,h}^{n}\|_S^2 + \frac{\rho_s}{2}\|\boldsymbol{e}_{\boldsymbol{q},h}^{n}\|^2_{L^2(\Omega_s)} + \Delta t\, a_s(\boldsymbol{e}_{\eta,h}^{n+1/2}, \boldsymbol{h}_{3,h}^{n+1}) - \Delta t T_1(\boldsymbol{e}_{\boldsymbol{q},h}^{n+1/2}) \\
&- \frac{\Delta t}{2}T_2(\boldsymbol{e}_{\boldsymbol{q},h}^{n+1/2}) - \Delta t V_1(\boldsymbol{e}_{\boldsymbol{q},h}^{n+1/2}) + \Delta t S_2(\boldsymbol{e}_{\boldsymbol{q},h}^{n+1/2}) - \Delta t S_3(\boldsymbol{e}_{\boldsymbol{q},h}^{n+1/2}) + J_1,
\end{aligned} \tag{5.2.11}$$

where

$$J_1 := -\alpha\Delta t\big\langle(\partial_{\Delta t}\boldsymbol{e}_{\eta,h}^{n+1} - \boldsymbol{e}_{\boldsymbol{u},h}^{n}), \boldsymbol{e}_{\boldsymbol{q},h}^{n+1/2}\big\rangle - \Delta t\big\langle \boldsymbol{e}_{\boldsymbol{\lambda},h}^{n}, \boldsymbol{e}_{\boldsymbol{q},h}^{n+1/2}\big\rangle.$$

Note that here we used (5.2.8b) to write

$$a_s(\boldsymbol{e}_{\eta h}^{\,n+1/2}, \boldsymbol{e}_{\boldsymbol{q} h}^{\,n+1/2}) = \frac{1}{2\Delta t}\|\boldsymbol{e}_{\eta,h}^{\,n+1}\|_S^2 - \frac{1}{2\Delta t}\|\boldsymbol{e}_{\eta,h}^{\,n}\|_S^2 - a_s(\boldsymbol{e}_{\eta,h}^{\,n+1/2}, \boldsymbol{h}_{3,h}^{n+1}).$$

We may then simplify J_1 by using (5.2.8a), to find

$$\begin{aligned}
J_1 = &-\alpha\Delta t\big\langle(\partial_{\Delta t}\boldsymbol{e}_{\eta,h}^{\,n+1} - \boldsymbol{e}_{\boldsymbol{u},h}^{\,n+1}), \boldsymbol{e}_{\boldsymbol{q},h}^{\,n+1/2}\big\rangle + \Delta t\big\langle\boldsymbol{e}_{\boldsymbol{\lambda},h}^{\,n+1} - \boldsymbol{e}_{\boldsymbol{\lambda},h}^{\,n}, \boldsymbol{e}_{\boldsymbol{q},h}^{\,n+1/2}\big\rangle \\
&-\alpha\Delta t\big\langle\boldsymbol{e}_{\boldsymbol{u},h}^{\,n+1} - \boldsymbol{e}_{\boldsymbol{u},h}^{\,n}, \boldsymbol{e}_{\boldsymbol{q},h}^{\,n+1/2}\big\rangle - \Delta t\big\langle\boldsymbol{e}_{\boldsymbol{\lambda},h}^{\,n+1}, \boldsymbol{e}_{\boldsymbol{q},h}^{\,n+1/2}\big\rangle \\
=&\Delta t\big\langle\alpha\boldsymbol{h}_{4,h}^{n+1} + \boldsymbol{g}_2^{n+1}, \boldsymbol{e}_{\boldsymbol{q},h}^{\,n+1/2}\big\rangle - \alpha\Delta t\big\langle\boldsymbol{e}_{\boldsymbol{u},h}^{\,n+1} - \boldsymbol{e}_{\boldsymbol{u},h}^{\,n}, \boldsymbol{e}_{\boldsymbol{q},h}^{\,n+1/2}\big\rangle - \Delta t\big\langle\boldsymbol{e}_{\boldsymbol{\lambda},h}^{\,n+1}, \boldsymbol{e}_{\boldsymbol{q},h}^{\,n+1/2}\big\rangle.
\end{aligned}$$

Therefore, if we plug this in to (5.2.11) we have

$$\begin{aligned}
&\frac{1}{2}\|\boldsymbol{e}_{\eta,h}^{\,n+1}\|_S^2 + \frac{\rho_s}{2}\|\boldsymbol{e}_{\boldsymbol{q},h}^{\,n+1}\|_{L^2(\Omega_s)}^2 \\
=&\frac{1}{2}\|\boldsymbol{e}_{\eta,h}^{\,n}\|_S^2 + \frac{\rho_s}{2}\|\boldsymbol{e}_{\boldsymbol{q},h}^{\,n}\|_{L^2(\Omega_s)}^2 + \Delta t a_s(\boldsymbol{e}_{\eta,h}^{\,n+1/2}, \boldsymbol{h}_{3,h}^{n+1}) - \Delta t T_1(\boldsymbol{e}_{\boldsymbol{q},h}^{\,n+1/2}) \\
&-\frac{\Delta t}{2}T_2(\boldsymbol{e}_{\boldsymbol{q},h}^{\,n+1/2}) - \Delta t V_1(\boldsymbol{e}_{\boldsymbol{q}}^{\,n+1/2}) + \Delta t S_2(\boldsymbol{e}_{\boldsymbol{q},h}^{\,n+1/2}) - \Delta t S_3(\boldsymbol{e}_{\boldsymbol{q},h}^{\,n+1/2})\big\rangle \\
&+\Delta t\big\langle\alpha\boldsymbol{h}_{4,h}^{n+1} + \boldsymbol{g}_2^{n+1}, \boldsymbol{e}_{\boldsymbol{q},h}^{\,n+1/2}\big\rangle - \alpha\Delta t\big\langle\boldsymbol{e}_{\boldsymbol{u},h}^{\,n+1} - \boldsymbol{e}_{\boldsymbol{u},h}^{\,n}, \boldsymbol{e}_{\boldsymbol{q},h}^{\,n+1/2}\big\rangle - \Delta t\big\langle\boldsymbol{e}_{\boldsymbol{\lambda},h}^{\,n+1}, \boldsymbol{e}_{\boldsymbol{q},h}^{\,n+1/2}\big\rangle.
\end{aligned} \tag{5.2.12}$$

If we now set $\boldsymbol{v}_h = \boldsymbol{e}_{\boldsymbol{u},h}^{\,n+1}$ in (5.2.7a) and $\theta_h = e_{p,h}^{n+1}$ in (5.2.7b) we get

$$\frac{\rho_f}{2}\|\boldsymbol{e}_{\boldsymbol{u},h}^{\,n+1}\|_{L^2(\Omega_f)}^2 + \frac{\rho_f}{2}\|\boldsymbol{e}_{\boldsymbol{u},h}^{\,n+1} - \boldsymbol{e}_{\boldsymbol{u},h}^{\,n}\|_{L^2(\Omega_f)}^2 \tag{5.2.13}$$

$$+\Delta t 2\mu\|\varepsilon(\boldsymbol{e}_{\boldsymbol{u},h}^{\,n+1})\|_{L^2(\Omega_f)}^2 + \Delta t h^2\|\nabla e_{p,h}^{n+1}\|_{L^2(\Omega_s)}^2$$

$$=\frac{1}{2}\|\boldsymbol{e}_{\boldsymbol{u},h}^{\,n}\|_{L^2(\Omega_f)}^2 + \Delta t\big\langle\boldsymbol{e}_{\boldsymbol{\lambda},h}^{\,n+1}, \boldsymbol{e}_{\boldsymbol{u},h}^{\,n+1}\big\rangle \tag{5.2.14}$$

$$-\Delta t S_1(\boldsymbol{e}_{\boldsymbol{u},h}^{\,n+1}) - \Delta t V_2(\boldsymbol{e}_{\boldsymbol{u},h}^{\,n+1}) - \Delta t V_3(e_{p,h}^{n+1}) - \Delta t V_4(e_{p,h}^{n+1}). \tag{5.2.15}$$

We now note that

$$\Delta t S_2(\boldsymbol{e}_{\boldsymbol{q},h}^{n+1/2}) - \frac{\Delta t}{2} T_2(\boldsymbol{e}_{\boldsymbol{q},h}^{n+1/2}) + \Delta t \big\langle \alpha \boldsymbol{h}_{4,h}^{n+1} + \boldsymbol{g}_2^{n+1}, \boldsymbol{e}_{\boldsymbol{q},h}^{n+1/2} \big\rangle = \frac{\Delta t}{2} T_2(\boldsymbol{e}_{\boldsymbol{q},h}^{n+1/2}).$$

With this in mind, we add (5.2.12) and (5.2.15), to write the following

$$\frac{1}{2}\mathcal{S}_h^{n+1} + \frac{1}{2}\mathcal{W}_h^{n+1} = \frac{1}{2}\mathcal{S}_h^{n} + \Delta t (K_1^{n+1} + \cdots + K_9^{n+1}) + J_2, \tag{5.2.16}$$

where

$$J_2 := -\alpha \Delta t \big\langle \boldsymbol{e}_{\boldsymbol{u},h}^{n+1} - \boldsymbol{e}_{\boldsymbol{u},h}^{n}, \boldsymbol{e}_{\boldsymbol{q},h}^{n+1/2} \big\rangle - \Delta t \big\langle \boldsymbol{e}_{\boldsymbol{\lambda},h}^{n+1}, \boldsymbol{e}_{\boldsymbol{q},h}^{n+1/2} \big\rangle + \Delta t \big\langle \boldsymbol{e}_{\boldsymbol{\lambda},h}^{n+1}, \boldsymbol{e}_{\boldsymbol{u},h}^{n+1} \big\rangle.$$

Then (5.2.9) gives

$$\begin{aligned} J_2 =& -\alpha \Delta t \big\langle \boldsymbol{e}_{\boldsymbol{u},h}^{n+1} - \boldsymbol{e}_{\boldsymbol{u},h}^{n}, \boldsymbol{e}_{\boldsymbol{q},h}^{n+1/2} \big\rangle + \Delta t \big\langle \boldsymbol{e}_{\boldsymbol{\lambda},h}^{n+1}, \boldsymbol{e}_{\boldsymbol{u},h}^{n+1} - \boldsymbol{e}_{\boldsymbol{q},h}^{n+1/2} \big\rangle \\ =& \alpha \Delta t \big\langle \boldsymbol{e}_{\boldsymbol{u},h}^{n} - \boldsymbol{e}_{\boldsymbol{u},h}^{n+1}, \boldsymbol{e}_{\boldsymbol{q},h}^{n+1/2} \big\rangle + \frac{\Delta t}{\alpha} \big\langle \boldsymbol{e}_{\boldsymbol{\lambda},h}^{n} - \boldsymbol{e}_{\boldsymbol{\lambda},h}^{n+1}, \boldsymbol{e}_{\boldsymbol{\lambda},h}^{n+1} \big\rangle \\ & + \frac{\Delta t}{\alpha} \big\langle \boldsymbol{e}_{\boldsymbol{\lambda},h}^{n+1}, \boldsymbol{g}_{3,h}^{n+1} \big\rangle. \end{aligned}$$

We can then use the identity (2.1.2) to get

$$\begin{aligned} \alpha \Delta t \big\langle \boldsymbol{e}_{\boldsymbol{u},h}^{n} - \boldsymbol{e}_{\boldsymbol{u},h}^{n+1}, \boldsymbol{e}_{\boldsymbol{q},h}^{n+1/2} \big\rangle =& \frac{\alpha \Delta t}{2} (\|\boldsymbol{e}_{\boldsymbol{u},h}^{n}\|_{L^2(\Sigma)}^2 - \|\boldsymbol{e}_{\boldsymbol{u},h}^{n+1}\|_{L^2(\Sigma)}^2 - \|\boldsymbol{e}_{\boldsymbol{q},h}^{n+1/2} - \boldsymbol{e}_{\boldsymbol{u},h}^{n}\|_{L^2(\Sigma)}^2 \\ & + \|\boldsymbol{e}_{\boldsymbol{q},h}^{n+1/2} - \boldsymbol{e}_{\boldsymbol{u},h}^{n+1}\|_{L^2(\Sigma)}^2) \\ \frac{\Delta t}{\alpha} \big\langle \boldsymbol{e}_{\boldsymbol{\lambda},h}^{n+1}, \boldsymbol{e}_{\boldsymbol{\lambda},h}^{n} - \boldsymbol{e}_{\boldsymbol{\lambda},h}^{n+1} \big\rangle =& \frac{\Delta t}{2\alpha} (\|\boldsymbol{e}_{\boldsymbol{\lambda} h}^{n}\|_{L^2(\Sigma)}^2 - \|\boldsymbol{e}_{\boldsymbol{\lambda},h}^{n+1}\|_{L^2(\Sigma)}^2 - \|\boldsymbol{e}_{\boldsymbol{\lambda},h}^{n+1} - \boldsymbol{e}_{\boldsymbol{\lambda},h}^{n}\|_{L^2(\Sigma)}^2). \end{aligned}$$

Following the method of the previous chapters, we note from (5.2.9) that we have

$$
\begin{aligned}
-\frac{1}{2\alpha}\|\boldsymbol{e}_{\boldsymbol{\lambda},h}^{n+1}-\boldsymbol{e}_{\boldsymbol{\lambda},h}^{n}\|_{L^2(\Sigma)}^2 =& \frac{-\alpha}{2}\|\boldsymbol{e}_{\boldsymbol{q},h}^{n+1/2}-\boldsymbol{e}_{\boldsymbol{u},h}^{n+1}\|_{L^2(\Sigma)}^2+\frac{1}{2\alpha}\|\boldsymbol{g}_{3,h}^{n+1}\|_{L^2(\Sigma)}^2\\
&+\frac{1}{\alpha}\left\langle \boldsymbol{e}_{\boldsymbol{\lambda},h}^{n}-\boldsymbol{e}_{\boldsymbol{\lambda},h}^{n+1},\boldsymbol{g}_{3,h}^{n+1}\right\rangle.
\end{aligned}
$$

Therefore, combining the above equations we have

$$
\begin{aligned}
J_2 =& \frac{\alpha\Delta t}{2}(\|\boldsymbol{e}_{\boldsymbol{u},h}^{n}\|_{L^2(\Sigma)}^2-\|\boldsymbol{e}_{\boldsymbol{u},h}^{n+1}\|_{L^2(\Sigma)}^2-\|\boldsymbol{e}_{\boldsymbol{q},h}^{n+1/2}-\boldsymbol{e}_{\boldsymbol{u},h}^{n}\|_{L^2(\Sigma)}^2)\\
&+\frac{\Delta t}{2\alpha}(\|\boldsymbol{e}_{\boldsymbol{\lambda},h}^{n}\|_{L^2(\Sigma)}^2-\|\boldsymbol{e}_{\boldsymbol{\lambda},h}^{n+1}\|_{L^2(\Sigma)}^2)+\frac{\Delta t}{2\alpha}\|\boldsymbol{g}_{3,h}^{n+1}\|_{L^2(\Sigma)}^2+\frac{\Delta t}{\alpha}\left\langle \boldsymbol{e}_{\boldsymbol{\lambda},h}^{n},\boldsymbol{g}_{3,h}^{n+1}\right\rangle.
\end{aligned}
$$

Substituting this into (5.2.16) we arrive at our result.

□

5.2.3.1 Estimate for $\sum_{i=1}^{9} K_i^{n+1}$

We have now isolated the problem term $\left\langle \boldsymbol{e}_{\boldsymbol{\lambda},h}^{n+1},\boldsymbol{g}_{3,h}^{n+1}\right\rangle$ as in previous chapters. However, similar to before, we will pause to bound the terms K_i^{n+1} before proceeding.

This step will be analogous to bounding the terms F^{n+1} and $\mathbf{F}^{n+1}$ in Chapters 3 and 4, but now the terms K_i^{n+1} also contain information about the *consistency error* incurred by projecting into the discrete spaces, in addition to the temporal and splitting errors encoded in F^{n+1} and $\mathbf{F}^{n+1}$. As such, $\sum_{i=1}^{9} K_i^{n+1}$ is more complicated, so we will not be able to mirror the previous proofs as much as before.

Lemma 5.2.3. *It holds*

$$\Delta t \sum_{n=0}^{M-1} \sum_{i=1}^{9} K_i^{n+1} \leq \frac{1}{8} \max_{0\leq m\leq M} \Big(\mathcal{S}_h^m + \mathcal{E}_h^m \Big) + \frac{1}{8} \sum_{n=0}^{M-1} \Big(\mathcal{W}_h^{n+1} + \mathcal{Z}_h^{n+1} \Big) + C\mathbf{D}_h(M), \tag{5.2.17}$$

where

$$\begin{aligned} \mathbf{D}_h(M) :=& \Delta t \sum_{n=0}^{M-1} \Bigg(\mu \|\varepsilon(R_h^f \mathbf{u}^{n+1} - \mathbf{u}^{n+1})\|^2_{L^2(\Omega_f)} + \frac{1}{\mu}\|S_h \mathsf{p}^{n+1} - \mathsf{p}^{n+1}\|^2_{L^2(\Omega_f)} \\ &+ (1+T)\|\boldsymbol{h}_{3,h}^{n+1}\|^2_S + (1+T)\|(R_h^s - I)\partial_{\Delta t}\mathbf{e}^{n+1}\|^2_S + h^2\|\mathbf{u}^{n+1}\|^2_{H^3(\Omega_f)} \\ &+ (\alpha + \frac{\alpha^2}{\mu})\|\boldsymbol{g}_{1,h}^{n+1}\|^2_{L^2(\Sigma)} + (1 + \frac{1}{\alpha} + \frac{1}{\mu})\|\mathbf{l}^{n+1} - \mathbf{l}^n\|^2_{L^2(\Sigma)} \\ &+ T\rho_s\|\partial_{\Delta t} R_h^s \mathbf{q}^{n+1} - \partial_t \mathbf{q}^{n+1/2}\|^2_{L^2(\Omega_s)} + \rho_f T \|\partial_{\Delta t} R_h^f \mathbf{u}^{n+1} - \partial_t \mathbf{u}^{n+1}\|^2_{L^2(\Omega_f)} \\ &+ h^2 \|\nabla S_h \mathsf{p}^{n+1}\|^2_{L^2(\Omega_f)} \Bigg) + \|(R_h^s - I)\mathbf{e}^M\|^2_S. \end{aligned}$$

Proof. We will proceed by bounding the individual K_i^{n+1}. For $i \in \{1,4,5,7\}$, the bounds follow from Cauchy-Schwarz and Young's inequalities using the methods established in the previous chapters. Thus we have for $0 \leq M \leq N$

$$\begin{aligned} \Delta t \sum_{n=0}^{M-1} K_1^{n+1} \leq& \frac{\rho_s}{8} \max_{0\leq m\leq M} \|\boldsymbol{e}_{\boldsymbol{q},h}^{\;m}\|^2_{L^2(\Omega_s)} + CT\Delta t \rho_s \sum_{n=0}^{M-1} \|\partial_{\Delta t} R_h^s \mathbf{q}^{n+1} - \partial_t \mathbf{q}^{n+1/2}\|^2_{L^2(\Omega_s)}, \\ \Delta t \sum_{n=0}^{M-1} K_4^{n+1} \leq& \frac{\rho_f}{8} \max_{0\leq m\leq M} \|\boldsymbol{e}_{\boldsymbol{u},h}^{\;m}\|^2_{L^2(\Omega_f)} + C\rho_f \Delta t T \sum_{n=0}^{M-1} \|\partial_{\Delta t} R_h^f \mathbf{u}^{n+1} - \partial_t \mathbf{u}^{n+1}\|^2_{L^2(\Omega_f)}, \\ \Delta t \sum_{n=0}^{M-1} K_5^{n+1} \leq& \frac{1}{16} \max_{0\leq m\leq M} \|\boldsymbol{e}_{\eta,h}^{\;m}\|^2_S + CT\Delta t \sum_{n=0}^{M-1} \|\boldsymbol{h}_{3,h}^{n+1}\|^2_S, \\ \Delta t \sum_{n=0}^{M-1} K_7^{n+1} \leq& \frac{\Delta t h^2}{4} \sum_{n=0}^{M-1} \|\nabla e_{p,h}^{n+1}\|^2_{L^2(\Omega_f)} + C\Delta t h^2 \sum_{n=0}^{M-1} \|\nabla S_h \mathsf{p}^{n+1}\|^2_{L^2(\Omega_f)}. \end{aligned}$$

To bound K_2^{n+1} we write

$$\Delta t K_2^{n+1} = -\frac{\Delta t}{2}(T_2(\boldsymbol{e}_{\boldsymbol{q},h}^{n+1/2} - \boldsymbol{e}_{\boldsymbol{u},h}^{n}) - T_2(\boldsymbol{e}_{\boldsymbol{u},h}^{n})).$$

Therefore, using the Cauchy-Schwarz inequality, the trace inequality, and Korn's inequality we have

$$\begin{aligned}\Delta t K_2^{n+1} \leq & \frac{\Delta t}{2}\|\mathbf{l}^{n+1} - \mathbf{l}^n\|_{L^2(\Sigma)}(\|\boldsymbol{e}_{\boldsymbol{q},h}^{n+1/2} - \boldsymbol{e}_{\boldsymbol{u},h}^{n}\|_{L^2(\Sigma)} + \|\boldsymbol{e}_{\boldsymbol{u},h}^{n}\|_{L^2(\Sigma)}) \\ \leq & \frac{\Delta t}{2}\|\mathbf{l}^{n+1} - \mathbf{l}^n\|_{L^2(\Sigma)}(\|\boldsymbol{e}_{\boldsymbol{q},h}^{n+1/2} - \boldsymbol{e}_{\boldsymbol{u},h}^{n}\|_{L^2(\Sigma)} + C_{tr}\|\varepsilon(\boldsymbol{e}_{\boldsymbol{u},h}^{n})\|_{L^2(\Omega_f)}).\end{aligned}$$

Hence, we see that

$$\begin{aligned}\Delta t \sum_{n=0}^{M-1} K_2^{n+1} \leq & \frac{\Delta t \mu}{12}\sum_{n=0}^{M-1}\|\varepsilon(\boldsymbol{e}_{\boldsymbol{u},h}^{n+1})\|_{L^2(\Omega_f)}^2 + \frac{\Delta t \alpha}{24}\sum_{n=0}^{M-1}\|\boldsymbol{e}_{\boldsymbol{q},h}^{n+1/2} - \boldsymbol{e}_{\boldsymbol{u},h}^{n}\|_{L^2(\Sigma)}^2 \\ & + C\Delta t(\frac{1}{\alpha} + \frac{1}{\mu})\sum_{n=0}^{M-1}\|\mathbf{l}^{n+1} - \mathbf{l}^n\|_{L^2(\Sigma)}^2.\end{aligned}$$

Using

$$S_3(\boldsymbol{\mu}_h) = \alpha\big\langle \boldsymbol{g}_{1,h}^{n+1}, \boldsymbol{\mu}_h\big\rangle,$$

we similarly have

$$\Delta t K_3^{n+1} \leq \Delta t \alpha \|\boldsymbol{g}_{1,h}^{n+1}\|_{L^2(\Sigma)}\big(\|\boldsymbol{e}_{\boldsymbol{q},h}^{n+1/2} - \boldsymbol{e}_{\boldsymbol{u},h}^{n}\|_{L^2(\Sigma)} + \|\boldsymbol{e}_{\boldsymbol{u},h}^{n}\|_{L^2(\Sigma)}\big),$$

so that

$$\begin{aligned}\Delta t \sum_{n=0}^{M-1} K_3^{n+1} \leq & \frac{\Delta t \mu}{12}\sum_{n=0}^{M-1}\|\varepsilon(\boldsymbol{e}_{\boldsymbol{u},h}^{n+1})\|_{L^2(\Omega_f)}^2 + \frac{\Delta t \alpha}{24}\sum_{n=0}^{M-1}\|\boldsymbol{e}_{\boldsymbol{q},h}^{n+1/2} - \boldsymbol{e}_{\boldsymbol{u},h}^{n}\|_{L^2(\Sigma)}^2 \\ & + C\Delta t(\alpha + \frac{\alpha^2}{\mu})\sum_{n=0}^{M-1}\|\boldsymbol{g}_{1,h}^{n+1}\|_{L^2(\Sigma)}^2.\end{aligned}$$

To estimate K_6^{n+1}, we perform integration by parts and proceed as before. Thus,

$$\begin{aligned}
\Delta t K_6^{n+1} &= \Delta t(\operatorname{div}(R_h^f \mathbf{u}^{n+1} - \mathbf{u}^{n+1}), e_{p,h}^{n+1})_f \\
&= -\Delta t(R_h^f \mathbf{u}^{n+1} - \mathbf{u}^{n+1}, \nabla e_{p,h}^{n+1})_f + \Delta t\big\langle (R_h^f \mathbf{u}^{n+1} - \mathbf{u}^{n+1}) \cdot \boldsymbol{n}, e_{p,h}^{n+1} \big\rangle \\
&\leq \Delta t \|R_h^f \mathbf{u}^{n+1} - \mathbf{u}^{n+1}\|_{L^2(\Omega_f)} \|\nabla e_{p,h}^{n+1}\|_{L^2(\Omega_f)} + \Delta t \|R_h^f \mathbf{u}^{n+1} - \mathbf{u}^{n+1}\|_{L^2(\Sigma)} \|e_{p,h}^{n+1}\|_{L^2(\Sigma)} \\
&\leq C\Delta t h^2 \|\mathbf{u}^{n+1}\|_{H^2(\Omega_f)} \|\nabla e_{p,h}^{n+1}\|_{L^2(\Omega_f)} + C\Delta t h^2 \|\mathbf{u}^{n+1}\|_{H^3(\Omega_f)} \|\nabla e_{p,h}^{n+1}\|_{L^2(\Omega_f)},
\end{aligned}$$

where the last step follows from applying (2.2.9c) on $e_{p,h}^{n+1}$. We also used the variation of Poincare's inequality from Proposition 2.1.10 because M_h^f satisfies the necessary conditions. Thus, applying this result along with Young's inequality, we have

$$\Delta t \sum_{n=0}^{M-1} K_6^{n+1} \leq \frac{\Delta t h^2}{4} \sum_{n=0}^{M-1} \|\nabla e_{p,h}^{n+1}\|_{L^2(\Omega_f)}^2 + C\Delta t h^2 \sum_{n=0}^{M-1} \|\mathbf{u}^{n+1}\|_{H^3(\Omega_f)}^2.$$

To bound K_8^{n+1}, we apply (5.2.8b) to obtain

$$\Delta t K_8^{n+1} = -\,\Delta t a_s((R_h^s - I)\mathbf{e}^{n+1/2}, \partial_{\Delta t} \boldsymbol{e}_{\eta,h}^{\;n+1}) + \Delta t a_s((R_h^s - I)\mathbf{e}^{n+1/2}, \boldsymbol{h}_{3,h}^{n+1}).$$

Then, one can verify the following discrete integration by parts

$$-\Delta t a_s((R_h^s - I)\mathbf{e}^{n+1/2}, \partial_{\Delta t} \boldsymbol{e}_{\eta,h}^{\;n+1}) = B^{n+1} + \Delta t a_s((R_h^s - I)\partial_{\Delta t} \mathbf{e}^{n+1}, \boldsymbol{e}_{\eta,h}^{\;n+1/2}).$$

where

$$B^{n+1} := a_s((R_h^s - I)\mathbf{e}^n, \boldsymbol{e}_{\eta,h}^{\;n}) - a_s((R_h^s - I)\mathbf{e}^{n+1}, \boldsymbol{e}_{\eta,h}^{\;n+1}).$$

Thus, we have

$$\Delta t K_8^{n+1} = B^{n+1} + \Delta t a_s((R_h^s - I)\partial_{\Delta t} \mathbf{e}^{n+1}, \boldsymbol{e}_{\eta,h}^{\;n+1/2}) + \Delta t a_s((R_h^s - I)\mathbf{e}^{n+1/2}, \boldsymbol{h}_{3,h}^{n+1}),$$

from which it follows

$$\Delta t \sum_{n=0}^{M-1} K_8^{n+1} \leq \frac{1}{32} \max_{0\leq m\leq M} \|\boldsymbol{e}_{\eta,h}^m\|_S^2 + C\Delta t \sum_{n=0}^{M-1} \|\boldsymbol{h}_{3,h}^{n+1}\|_S^2 + C\Delta t(1+T) \sum_{n=0}^{M-1} \|(R_h^2 - I)\partial_{\Delta t}\mathbf{e}^{n+1}\|_S^2 + \sum_{n=0}^{M-1} B^{n+1}.$$

For the term $\sum_{n=0}^{M-1} B^{n+1}$, we have a telescoping sum, so that

$$\sum_{m=1}^{M} B^m = a_s((R_h^s - I)\mathbf{e}^0, \boldsymbol{e}_{\eta,h}^0) - a_s((R_h^s - I)\mathbf{e}^M, \boldsymbol{e}_{\eta,h}^M).$$

We may then bound this term in the usual method to find

$$\begin{aligned}\sum_{m=1}^{M} B^m \leq& \frac{1}{64}(\|\boldsymbol{e}_{\eta,h}^M\|_S^2 + \|\boldsymbol{e}_{\eta,h}^0\|_S^2) + C(\|(R_h - I)\mathbf{e}^M\|_S^2 + \|(R_h - I)\mathbf{e}^0\|_S^2) \\ \leq& \frac{1}{32} \max_{0\leq m\leq M} \|\boldsymbol{e}_{\eta,h}^m\|_S^2 + C(\|(R_h - I)\mathbf{e}^M\|_S^2 + \|(R_h - I)\mathbf{e}^0\|_S^2)\end{aligned}$$

Consequently,

$$\begin{aligned}\Delta t \sum_{n=0}^{M-1} K_8^{n+1} \leq& \frac{1}{16} \max_{0\leq m\leq M} \|\boldsymbol{e}_{\eta,h}^m\|_S^2 + C\Delta t \sum_{n=0}^{M-1} \|\boldsymbol{h}_{3,h}^{n+1}\|_S^2 \\ &+ C\Delta t(1+T) \sum_{n=0}^{M-1} \|(R_h^s - I)\partial_{\Delta t}\mathbf{e}^{n+1}\|_S^2 \\ &+ C(\|(R_h^s - I)\mathbf{e}^M\|_S^2 + \|(R_h^s - I)\mathbf{e}^0\|_S^2).\end{aligned}$$

Finally, for K_9, we note that $|\operatorname{div}\boldsymbol{v}| \leq C|\varepsilon(v)|$. Thus we can show

$$\Delta t \sum_{n=0}^{M-1} K_9^{n+1} \leq \frac{\Delta t \mu}{4} \sum_{n=0}^{M-1} \|\varepsilon(\boldsymbol{e}_{\boldsymbol{u},h}^{n+1})\|^2_{L^2(\Omega_f)} + C\Delta t \mu \sum_{n=0}^{M-1} \|\varepsilon(R_h^f \mathbf{u}^{n+1} - \mathbf{u}^{n+1})\|^2_{L^2(\Omega_f)} + C\frac{\Delta t}{\mu} \sum_{n=0}^{M-1} \|S_h \mathsf{p}^{n+1} - \mathsf{p}^{n+1}\|^2_{L^2(\Omega_f)}.$$

Finally, we address the term $\frac{\Delta t}{2\alpha}\|\boldsymbol{g}_{3,h}^{n+1}\|^2_{L^2(\Sigma)}$.

To do so, we just recognize that $\boldsymbol{g}_{3,h}^{n+1} = \frac{\alpha}{2}\boldsymbol{g}_{1,h}^{n+1} + \boldsymbol{g}_2^{n+1}$. Thus,

$$\frac{\Delta t}{2\alpha} \sum_{n=0}^{M-1} \|\boldsymbol{g}_{3,h}^{n+1}\|^2_{L^2(\Sigma)} \leq C\Delta t \sum_{n=0}^{M-1} \left(\alpha \|\boldsymbol{g}_{1,h}^{n+1}\|^2_{L^2(\Sigma)} + \frac{1}{\alpha}\|\boldsymbol{g}_2^{n+1}\|^2_{L^2(\Sigma)} \right).$$

To complete the proof, we combine the terms above, keeping in mind that

$$\|\boldsymbol{g}_2^{n+1}\|^2_{L^2(\Sigma)} = \|\mathbf{l}^{n+1} - \mathbf{l}^n\|^2_{L^2(\Sigma)}.$$

□

5.2.4 Step 2: Estimate for $\frac{\Delta t}{\alpha}\langle \boldsymbol{g}_{3,h}^{n+1}, \boldsymbol{e}_{\boldsymbol{\lambda},h}^{n} \rangle$

We now turn our attention, once again, to bounding the isolated term. In this case, our isolated term

$$\frac{\Delta t}{\alpha}\langle \boldsymbol{g}_{3,h}^{n+1}, \boldsymbol{e}_{\boldsymbol{\lambda},h}^{n} \rangle,$$

is precisely the fully discrete counterpart to the isolated term bounded in Chapter 4. Consequently, we will find that we may use the method from Chapter 4 to bound this isolated term, with some important modifications.

Recall that the key to bounding the isolated terms in the previous chapters was to assume the existence of a function (ϕ or $\tilde{\phi}$) that serves as a pseudo-lifting operator from the interface Σ into an interior domain. In the case of the semi-discrete FSI problem in Chapter 4, this function $\tilde{\phi}$ was necessarily in the space $\boldsymbol{V}^s$ so that the extended function $\tilde{\boldsymbol{g}}_2^{n+1}$ could satisfy the error equation (4.3.1a). This will not work for the fully discrete case, however, because the fully discrete error equation (5.2.6a) is only satisfied for $\boldsymbol{\xi}_h \in \boldsymbol{V}_h^s \subset \boldsymbol{V}^s$, and $\tilde{\boldsymbol{g}}_2^{n+1}$ is not guaranteed to be in $\boldsymbol{V}_h^s$. Indeed, we can see that the example ϕ constructed in 3.5.2 would allow $\tilde{\boldsymbol{g}}_2^{n+1}$ be in $\boldsymbol{V}^s$ but not $\boldsymbol{V}_h^s$ because it is not a piece-wise linear.

In order to circumvent this issue, we choose to interpolate into the finite dimensional subspace $\boldsymbol{V}_h^s$ in such a way that we retain the critical characteristics provided by multiplying by $\tilde{\phi}$. Crucially, we need the interpolated function to not interfere with conditions (iii) and (iv) of Assumption 4.3.4. Thus, we require an interpolant that will allow us flexibility when choosing the degrees of freedom. Specifically, we would like the interpolated function on the interface Σ to not depend on the rest of the domain. Thus, we choose our interpolant to be R_h^s, the Scott-Zhang interpolant used in Ω_s (see (2.2.11)) so that we may interpolate nodes on $\partial\Omega_s$ along element edges that match $\partial\Omega_s$, rather than the entire element.

By only interpolating along edges in this way, we can be sure that the interpolated function is zero along $\partial\Omega_s \setminus \Sigma$ (a property introduced by $\tilde{\phi}$, as we recall from Chapter 4). Consequently, any stability and error results from Chapter 2 for the Scott Zhang interpolant that hold on the boundary of Ω_s will reduce to results only on Σ, as we will see below.

We may now proceed almost exactly as in Chapter 4, and define our extended version of $\boldsymbol{g}_2^{n+1}$. We define $\tilde{\boldsymbol{n}}_s \in \boldsymbol{W}^{1,\infty}(\Omega_s)^2$ as in Assumption 4.3.3 and $\tilde{\phi}$ as in

Assumption 4.3.4. We then recall that $\mathbf{l}_s^{n+1} = -\sigma_s(\mathbf{e}^{n+1})\boldsymbol{n}_s$ such that in Chapter 4 we defined on Ω_s

$$\begin{aligned}
\tilde{\mathbf{l}}_s(x,t) :=& \sigma_s(\mathbf{e}(x,t))\tilde{\boldsymbol{n}}_s, \\
\mathcal{L}_s :=& \tilde{\phi}\tilde{\mathbf{l}}_s(x,t), \\
\tilde{\boldsymbol{g}}_2^{n+1} :=& -(\mathcal{L}_s^{n+1} - \mathcal{L}_s^n).
\end{aligned}$$

To extend this to $\boldsymbol{V}_h^s$, we then define

$$\begin{aligned}
\mathcal{L}_{s,h} :=& R_h^s\big(\tilde{\phi}\tilde{\mathbf{l}}_s(x,t)\big), \\
\tilde{\boldsymbol{g}}_{2,h}^{n+1} :=& -(\mathcal{L}_{s,h}^{n+1} - \mathcal{L}_{s,h}^n) = R_h^s\tilde{\boldsymbol{g}}_2^{n+1}.
\end{aligned}$$

Thus, $\tilde{\boldsymbol{g}}_{2,h}^{n+1} \in \boldsymbol{V}_h^s$, as R_h^s retains the boundary behavior of $\tilde{\boldsymbol{g}}_2$ by only interpolating along the edges, as explained above. Furthermore, as mentioned before, this means that the stability and error results given by (2.2.7) and (2.2.9) will reduce to results only on Σ for $\tilde{\boldsymbol{g}}_{2,h}^{n+1}$.

We also have a result analogous to Lemma 4.3.5.

Lemma 5.2.4. *Under Assumptions 4.3.3 and 4.3.4 we have*

$$\|\tilde{\boldsymbol{g}}_{2,h}^{n+1} - \boldsymbol{g}_2^{n+1}\|_{L^2(\Sigma)}^2 \leq C\Delta t\|\boldsymbol{g}_2^{n+1}\|_{L^\infty(\Sigma)}^2 + Ch^2\|\boldsymbol{g}_2^{n+1}\|_{H^1(\Sigma)}^2. \tag{5.2.18}$$

Proof. To prove this, we write

$$\begin{aligned}
\|\tilde{\boldsymbol{g}}_{2,h}^{n+1} - \boldsymbol{g}_2^{n+1}\|_{L^2(\Sigma)}^2 =& \|R_h^s(\tilde{\boldsymbol{g}}_2^{n+1} - \boldsymbol{g}_2^{n+1}) + (R_h^s - I)\boldsymbol{g}_2^{n+1}\|_{L^2(\Sigma)}^2 \\
\leq& C\big(\|R_h^s(\tilde{\boldsymbol{g}}_2^{n+1} - \boldsymbol{g}_2^{n+1})\|_{L^2(\Sigma)}^2 + \|(R_h^s - I)\boldsymbol{g}_2^{n+1}\|_{L^2(\Sigma)}.
\end{aligned}$$

From Lemmas 2.2.12 and 4.3.5, we have

$$\begin{aligned}\|R_h^s(\tilde{\boldsymbol{g}}_2^{n+1} - \boldsymbol{g}_2^{n+1})\|^2_{L^2(\Sigma)} \leq & \|\tilde{\boldsymbol{g}}_2^{n+1} - \boldsymbol{g}_2^{n+1}\|^2_{L^2(\Sigma)} \\ \leq & C\Delta t \|\boldsymbol{g}_2^{n+1}\|^2_{L^\infty(\Sigma)},\end{aligned}$$

and from Lemma 2.2.14, we have

$$\|(R_h^s - I)\boldsymbol{g}_2^{n+1}\|^2_{L^2(\Sigma)} \leq Ch^2 \|\boldsymbol{g}_2^{n+1}\|^2_{H^1(\Sigma)}.$$

Combining these results completes the proof. □

We may now state the error bound.

Lemma 5.2.5. *Under Assumptions 4.3.3 and 4.3.4 we have*

$$\frac{\Delta t}{\alpha} \sum_{n=0}^{M-1} \left\langle \boldsymbol{g}_{3,h}^{n+1}, \boldsymbol{e}_{\boldsymbol{\lambda},h}^{n} \right\rangle \leq \frac{1}{8} \max_{0 \leq m \leq M} (\mathcal{S}_h^m + \mathcal{E}_h^m) + \frac{1}{8} \sum_{n=0}^{M-1} \mathcal{Z}_h^{n+1} + C\boldsymbol{\Psi}_h(M),$$

where

$$\begin{aligned}\boldsymbol{\Psi}_h(M) := & \boldsymbol{\Psi}_{1,h}(M) + \boldsymbol{\Psi}_{2,h}(M) \\ \boldsymbol{\Psi}_1(M) := & T(\Delta t)^3 \rho_s \sum_{n=0}^{M-1} \|\partial^2_{\Delta t} R_h^s \mathbf{q}^n\|^2_{L^2(\Omega_s)} + \rho_s \|\boldsymbol{g}_{1,h}^M\|^2_{L^2(\Omega_s)} \\ & + \Delta t \sum_{n=0}^{M-1} \Bigg((1+T)\|\boldsymbol{g}_{1,h}^{n+1}\|^2_S + \big(1+\alpha\big)\|\boldsymbol{g}_{1,h}^{n+1}\|^2_{L^2(\Sigma)} + \|\mathbf{l}^{n+1} - \mathbf{l}^n\|^2_{L^2(\Sigma)} \\ & \qquad + \rho_s \|\partial_{\Delta t} R_h^s \mathbf{q}^{n+1} - \partial_t \mathbf{q}^{n+1/2}\|^2_{L^2(\Omega_s)} + \rho_s \|\boldsymbol{g}_{1,h}^{n+1}\|^2_{L^2(\Omega_s)} \\ & \qquad + \|(R_h^s - I)\mathbf{e}^{n+1/2}\|^2_S + \alpha \|R_h^f \mathbf{u}^{n+1} - \partial_{\Delta t} R_h^s \mathbf{e}^{n+1}\|^2_{L^2(\Sigma)} \\ & \qquad + \alpha \|\boldsymbol{h}_{3,h}^{n+1}\|^2_{L^2(\Sigma)} \Bigg),\end{aligned}$$

$$
\begin{aligned}
\boldsymbol{\Psi}_2(M) :=& \frac{T(\Delta t)^3\rho_s}{\alpha^2}\sum_{n=0}^{M-1}\|\partial_{\Delta t}^2\mathcal{L}_{s,h}^n\|_{L^2(\Omega_s)}^2 + \frac{\rho_s}{\alpha^2}\|\tilde{\boldsymbol{g}}_{2,h}^M\|_{L^2(\Omega_s)}^2 + \frac{Th^2}{\alpha}\sum_{n=0}^{M-1}\|\boldsymbol{g}_2^{n+1}\|_{H^1(\Sigma)}^2 \\
&+ \Delta t\sum_{n=0}^{M-1}\Bigg(\frac{1+T}{\alpha^2}\|\tilde{\boldsymbol{g}}_{2,h}^{n+1}\|_S^2 + \big(1+\frac{1}{\alpha}\big)\|\mathbf{l}^{n+1}-\mathbf{l}^n\|_{L^2(\Sigma)}^2 \\
&\qquad + \|\boldsymbol{g}_{1,h}^{n+1}\|_{L^2(\Sigma)}^2 + \rho_s\|\partial_{\Delta t}R_h^s\mathbf{q}^{n+1} - \partial_t\mathbf{q}^{n+1/2}\|_{L^2(\Omega_s)}^2 + \frac{\rho_s}{\alpha^2}\|\tilde{\boldsymbol{g}}_{2,h}^{n+1}\|_{L^2(\Omega_s)}^2 \\
&\qquad + \|(R_h^s - I)\mathbf{e}^{n+1/2}\|_S^2 + \|R_h^f\mathbf{u}^{n+1} - \partial_{\Delta t}R_h^s\mathbf{e}^{n+1}\|_{L^2(\Sigma)}^2 \\
&\qquad + \|\boldsymbol{h}_{3,h}^{n+1}\|_{L^2(\Sigma)}^2 + \frac{T}{\alpha}\|\boldsymbol{g}_2^{n+1}\|_{L^\infty(\Sigma)}^2\Bigg)
\end{aligned}
$$

Proof. The proof of this result follows the proof of Lemma 4.3.6. We begin by splitting up the term $\boldsymbol{g}_{3,h}^{n+1}$ to write

$$
\frac{\Delta t}{\alpha}\sum_{n=0}^{M-1}\big\langle \boldsymbol{g}_{3,h}^{n+1}, \boldsymbol{e}_{\boldsymbol{\lambda},h}^n\big\rangle = \frac{\Delta t}{\alpha}\sum_{n=0}^{M-1}\big\langle \boldsymbol{g}_2^{n+1}, \boldsymbol{e}_{\boldsymbol{\lambda},h}^n\big\rangle + \frac{\Delta t}{2}\sum_{n=0}^{M-1}\big\langle \boldsymbol{g}_{1,h}^{n+1}, \boldsymbol{e}_{\boldsymbol{\lambda},h}^n\big\rangle. \tag{5.2.19}
$$

Following the proof of Lemma 4.3.6, we may bound the first term. To start, we write

$$
\frac{\Delta t}{\alpha}\sum_{n=0}^{M-1}\big\langle \boldsymbol{g}_2^{n+1}, \boldsymbol{e}_{\boldsymbol{\lambda},h}^n\big\rangle = \frac{\Delta t}{\alpha}\sum_{n=0}^{M-1}\big\langle \boldsymbol{g}_2^{n+1} - \tilde{\boldsymbol{g}}_{2,h}^{n+1}, \boldsymbol{e}_{\boldsymbol{\lambda},h}^n\big\rangle + \frac{\Delta t}{\alpha}\sum_{n=0}^{M-1}\big\langle \tilde{\boldsymbol{g}}_{2,h}^{n+1}, \boldsymbol{e}_{\boldsymbol{\lambda},h}^n\big\rangle.
$$

Then, using (5.2.18), we bound the first term above.

$$
\begin{aligned}
\frac{\Delta t}{\alpha}\sum_{n=0}^{M-1}\big\langle \boldsymbol{g}_2^{n+1} - \tilde{\boldsymbol{g}}_{2,h}^{n+1}, \boldsymbol{e}_{\boldsymbol{\lambda},h}^n\big\rangle \leq& \frac{CT}{\alpha}\sum_{n=0}^{M-1}\|\boldsymbol{g}_2^{n+1} - \tilde{\boldsymbol{g}}_{2,h}^{n+1}\|_{L^2(\Sigma)}^2 + \frac{(\Delta t)^2}{32T\alpha}\sum_{n=0}^{M-1}\|\boldsymbol{e}_{\boldsymbol{\lambda},h}^n\|_{L^2(\Sigma)}^2 \\
\leq& \frac{CT\Delta t}{\alpha}\sum_{n=0}^{M-1}\|\boldsymbol{g}_2^{n+1}\|_{L^\infty(\Sigma)}^2 + \frac{CTh^2}{\alpha}\sum_{n=0}^{M-1}\|\boldsymbol{g}_2^{n+1}\|_{H^1(\Sigma)}^2 \\
&+ \frac{(\Delta t)^2}{32T\alpha}\sum_{n=0}^{M-1}\|\boldsymbol{e}_{\boldsymbol{\lambda},h}^n\|_{L^2(\Sigma)}^2 \\
\leq& \frac{CT\Delta t}{\alpha}\sum_{n=0}^{M-1}\|\boldsymbol{g}_2^{n+1}\|_{L^\infty(\Sigma)}^2 + \frac{CTh^2}{\alpha}\sum_{n=0}^{M-1}\|\boldsymbol{g}_2^{n+1}\|_{H^1(\Sigma)}^2 \\
&+ \frac{1}{8}\max_{0\leq m\leq M}\mathcal{E}_h^m
\end{aligned}
$$

To bound the second term $\frac{\Delta t}{\alpha}\sum_{n=0}^{M-1}\langle \tilde{\boldsymbol{g}}_{2,h}^{n+1}, \boldsymbol{e}_{\boldsymbol{\lambda},h}^{\ n}\rangle$, we use (5.2.6a) to move as many terms as possible from the interface Σ into Ω_s. Note that we may do this only because $\tilde{\boldsymbol{g}}_{2,h} \in \boldsymbol{V}_h^s$. Note that we also apply (5.2.8b) in order to replace $\partial_{\Delta t}\boldsymbol{e}_{\eta,h}^{\ n+1}$ with $\boldsymbol{e}_{\boldsymbol{q},h}^{\ n+1/2} + \boldsymbol{h}_{3,h}^{n+1}$.

Thus we have

$$\begin{aligned}
\frac{\Delta t}{\alpha}\sum_{n=0}^{M-1}\langle \tilde{\boldsymbol{g}}_{2,h}^{n+1}, \boldsymbol{e}_{\boldsymbol{\lambda},h}^{\ n}\rangle = \sum_{n=0}^{M-1}\Bigg(& -\frac{\rho_s}{\alpha}(\boldsymbol{e}_{\boldsymbol{q},h}^{\ n+1} - \boldsymbol{e}_{\boldsymbol{q},h}^{\ n}, \tilde{\boldsymbol{g}}_{2,h}^{n+1})_s - \frac{\Delta t}{\alpha}a_s(\boldsymbol{e}_{\eta,h}^{\ n+1/2}, \tilde{\boldsymbol{g}}_{2,h}^{n+1}) \\
& - \Delta t\langle \boldsymbol{e}_{\boldsymbol{q},h}^{\ n+1/2} - \boldsymbol{e}_{\boldsymbol{u},h}^{\ n}, \tilde{\boldsymbol{g}}_{2,h}^{n+1}\rangle + \frac{\Delta t}{\alpha}\Big(- T_1(\tilde{\boldsymbol{g}}_{2,h}^{n+1}) \\
& - \frac{1}{2}T_2(\tilde{\boldsymbol{g}}_{2,h}^{n+1}) - V_1(\tilde{\boldsymbol{g}}_{2,h}^{n+1}) + S_2(\tilde{\boldsymbol{g}}_{2,h}^{n+1}) \\
& - S_3(\tilde{\boldsymbol{g}}_{2,h}^{n+1}) - \alpha\langle \boldsymbol{h}_{3,h}^{n+1}, \tilde{\boldsymbol{g}}_{2,h}^{n+1}\rangle\Big)\Bigg).
\end{aligned}$$

Following 4.3.4, we bound all but the term $\frac{-\rho_s}{\alpha}(\boldsymbol{e}_{\boldsymbol{q},h}^{\ n+1} - \boldsymbol{e}_{\boldsymbol{q},h}^{\ n}, \tilde{\boldsymbol{g}}_{2,h}^{n+1})_s$.

$$\begin{aligned}
&\sum_{n=0}^{M-1}\Bigg(-\frac{\Delta t}{\alpha}a_s(\boldsymbol{e}_{\eta,h}^{\ n+1/2}, \tilde{\boldsymbol{g}}_{2,h}^{n+1}) - \Delta t\langle \boldsymbol{e}_{\boldsymbol{q},h}^{\ n+1/2} - \boldsymbol{e}_{\boldsymbol{u},h}^{\ n}, \tilde{\boldsymbol{g}}_{2,h}^{n+1}\rangle + \frac{\Delta t}{\alpha}\Big(- T_1(\tilde{\boldsymbol{g}}_{2,h}^{n+1}) \\
&\qquad - \frac{1}{2}T_2(\tilde{\boldsymbol{g}}_{2,h}^{n+1}) - V_1(\tilde{\boldsymbol{g}}_{2,h}^{n+1}) + S_2(\tilde{\boldsymbol{g}}_{2,h}^{n+1}) - S_3(\tilde{\boldsymbol{g}}_{2,h}^{n+1}) - \alpha\langle \boldsymbol{h}_{3,h}^{n+1}, \tilde{\boldsymbol{g}}_{2,h}^{n+1}\rangle\Big)\Bigg) \\
&\leq \sum_{n=0}^{M-1}\left(\frac{\Delta t}{32T}\|\boldsymbol{e}_{\eta,h}^{\ n+1}\|_S^2 + \frac{\Delta t\alpha}{16}\|\boldsymbol{e}_{\boldsymbol{q},h}^{\ n+1/2} - \boldsymbol{e}_{\boldsymbol{u},h}^{\ n}\|_{L^2(\Sigma)}^2\right) \\
&\quad + C\Delta t\sum_{n=0}^{M-1}\Bigg(\frac{1+T}{\alpha^2}\|\tilde{\boldsymbol{g}}_{2,h}^{n+1}\|_S^2 + (1+\frac{1}{\alpha})\|\mathbf{l}^{n+1} - \mathbf{l}^n\|_{L^2(\Sigma)}^2 + \|\boldsymbol{g}_{1,h}^{n+1}\|_{L^2(\Sigma)}^2 \\
&\qquad + \rho_s\|\partial_{\Delta t}R_h^s\mathbf{q}^{n+1} - \partial_t\mathbf{q}^{n+1/2}\|_{L^2(\Omega_s)}^2 + \frac{\rho_s}{\alpha^2}\|\tilde{\boldsymbol{g}}_{2,h}^{n+1}\|_{L^2(\Omega_s)}^2 \\
&\qquad + \|(R_h^s - I)\mathbf{e}^{n+1/2}\|_S^2 + \|R_h^f\mathbf{u}^{n+1} - \partial_{\Delta t}R_h^s\mathbf{e}^{n+1}\|_{L^2(\Sigma)}^2 \\
&\qquad + \|\boldsymbol{h}_{3,h}^{n+1}\|_{L^2(\Sigma)}^2\Bigg)
\end{aligned}$$

$$
\begin{aligned}
&\le \sum_{n=0}^{M-1} \frac{\Delta t}{32T}\|\boldsymbol{e}_\eta^{n+1}\|_S^2 + \frac{1}{16}\sum_{n=0}^{M-1} \mathcal{Z}_h^{n+1} \\
&\qquad + C\Delta t \sum_{n=0}^{M-1}\Bigg(\frac{1+T}{\alpha^2}\|\tilde{\boldsymbol{g}}_{2,h}^{n+1}\|_S^2 + \big(1+\frac{1}{\alpha}\big)\|\mathbf{l}^{n+1}-\mathbf{l}^n\|_{L^2(\Sigma)}^2 \\
&\qquad\qquad + \|\boldsymbol{g}_{1,h}^{n+1}\|_{L^2(\Sigma)}^2 + \rho_s\|\partial_{\Delta t} R_h^s \mathbf{q}^{n+1} - \partial_t \mathbf{q}^{n+1/2}\|_{L^2(\Omega_s)}^2 \\
&\qquad\qquad + \frac{\rho_s}{\alpha^2}\|\tilde{\boldsymbol{g}}_{2,h}^{n+1}\|_{L^2(\Omega_s)}^2 + \|(R_h^s - I)\mathbf{e}^{n+1/2}\|_S^2 \\
&\qquad\qquad + \|R_h^f \mathbf{u}^{n+1} - \partial_{\Delta t} R_h^s \mathbf{e}^{n+1}\|_{L^2(\Sigma)}^2 + \|\boldsymbol{h}_{3,h}^{n+1}\|_{L^2(\Sigma)}^2 \Bigg),
\end{aligned}
$$

where we used Lemma 2.2.12 to bound

$$
\|\tilde{\boldsymbol{g}}_{2,h}^{n+1}\|_{L^2(\Sigma)}^2 = \|R_h^s \tilde{\boldsymbol{g}}_2^{n+1}\|_{L^2(\Sigma)}^2 \le C\|\tilde{\boldsymbol{g}}_2^{n+1}\|_{L^2(\Sigma)}^2 \le C\|\boldsymbol{g}_2^{n+1}\|_{L^2(\Sigma)}^2.
$$

We also used the facts $S_3(\boldsymbol{\mu}_h) = \alpha\big\langle \boldsymbol{g}_{1,h}^{n+1}, \boldsymbol{\mu}_h\big\rangle$ and $\|\boldsymbol{g}_2^{n+1}\|_{L^2(\Sigma)}^2 = \|\mathbf{l}^{n+1}-\mathbf{l}^n\|_{L^2(\Sigma)}^2$.

For the term $\sum_{n=0}^{M-1} -\frac{\rho_s}{\alpha}(\boldsymbol{e}_{\boldsymbol{q},h}^{n+1} - \boldsymbol{e}_{\boldsymbol{q},h}^{n}, \tilde{\boldsymbol{g}}_{2,h}^{n+1})_s$, we again use summation by parts. Thus

$$
\begin{aligned}
\sum_{n=0}^{M-1} -\frac{\rho_s}{\alpha}(\boldsymbol{e}_{\boldsymbol{q},h}^{n+1} - \boldsymbol{e}_{\boldsymbol{q},h}^{n}, \tilde{\boldsymbol{g}}_{2,h}^{n+1})_s \le& \frac{\Delta t \rho_s}{32T}\sum_{n=0}^{M-1}\|\boldsymbol{e}_{\boldsymbol{q},h}^{n}\|_{L^2(\Omega_s)}^2 + \frac{CT(\Delta t)^3\rho_s}{\alpha^2}\sum_{n=0}^{M-1}\|\partial_{\Delta t}^2 \mathcal{L}_{s,h}^n\|_{L^2(\Omega_s)}^2 \\
&+ \frac{\rho_s}{32}\|\boldsymbol{e}_{\boldsymbol{q},h}^{M}\|_{L^2(\Omega_s)}^2 + \frac{C\rho_s}{\alpha^2}\|\tilde{\boldsymbol{g}}_{2,h}^{M}\|_{L^2(\Omega_s)}^2.
\end{aligned}
$$

Consequently, we have

$$
\frac{\Delta t}{\alpha}\sum_{n=0}^{M-1}\big\langle \tilde{\boldsymbol{g}}_{2,h}^{n+1}, \boldsymbol{e}_{\boldsymbol{\lambda},h}^{n}\big\rangle \le \frac{1}{16}\max_{0\le m\le M}\mathcal{S}_h^m + \frac{1}{8}\max_{0\le m\le M}\mathcal{E}_h^m + \frac{1}{16}\sum_{n=0}^{M-1}\mathcal{Z}_h^{n+1} + C\boldsymbol{\Psi}_{2,h}(M).
$$

We follow the same method to bound $\frac{\Delta t}{\alpha}\sum_{n=0}^{M-1}\big\langle \boldsymbol{g}_{1,h}^{n+1}, \boldsymbol{e}_{\boldsymbol{\lambda},h}^{n}\big\rangle$. However, in this case we do not need to extend the $\boldsymbol{g}_{1,h}^{n+1}$ into Ω_s in a fancy way. Instead, we know

$\boldsymbol{g}_{1,h}^{n+1} = R_h^s \mathbf{q}^{n+1} - R_h^s \mathbf{q}^n$ on Σ by (4.1.3a) and our definition of R_h^s, R_h^f. Thus we may use the fact that $R_h^s \mathbf{q} \in \boldsymbol{V}_h^s$ to extend $\boldsymbol{g}_{1,h}^{n+1}$ naturally into Ω_s, just as we did for $\boldsymbol{g}_1^{n+1}$ in Chapter 4. Thus we begin with

$$\frac{\Delta t}{\alpha}\sum_{n=0}^{M-1}\left\langle \boldsymbol{g}_{1,h}^{n+1}, \boldsymbol{e}_{\boldsymbol{\lambda},h}^{\,n}\right\rangle = \sum_{n=0}^{M-1}\Bigg(-\frac{\rho_s}{\alpha}(\boldsymbol{e}_{\boldsymbol{q},h}^{\,n+1} - \boldsymbol{e}_{\boldsymbol{q},h}^{\,n}, \boldsymbol{g}_{1,h}^{n+1})_s - \frac{\Delta t}{\alpha} a_s(\boldsymbol{e}_{\eta,h}^{\,n+1/2}, \boldsymbol{g}_{1,h}^{n+1}) \\ - \Delta t\left\langle \boldsymbol{e}_{\boldsymbol{q},h}^{\,n+1/2} - \boldsymbol{e}_{\boldsymbol{u},h}^{\,n}, \boldsymbol{g}_{1,h}^{n+1}\right\rangle + \frac{\Delta t}{\alpha}\Bigg(-T_1(\boldsymbol{g}_{1,h}^{n+1}) \\ - \frac{1}{2}T_2(\boldsymbol{g}_{1,h}^{n+1}) - V_1(\boldsymbol{g}_{1,h}^{n+1}) + S_2(\boldsymbol{g}_{1,h}^{n+1}) \\ - S_3(\boldsymbol{g}_{1,h}^{n+1}) - \alpha\left\langle \boldsymbol{h}_{3,h}^{n+1}, \boldsymbol{g}_{1,h}^{n+1}\right\rangle \Bigg)\Bigg),$$

and proceed with the steps above to determine

$$\sum_{n=0}^{M-1}\Bigg(-\frac{\Delta t}{2} a_s(\boldsymbol{e}_{\eta,h}^{\,n+1/2}, \boldsymbol{g}_{1,h}^{n+1}) \\ - \frac{\alpha\Delta t}{2}\left\langle \boldsymbol{e}_{\boldsymbol{q},h}^{\,n+1/2} - \boldsymbol{e}_{\boldsymbol{u},h}^{\,n}, \boldsymbol{g}_{1,h}^{n+1}\right\rangle + \frac{\Delta t}{2}\Bigg(-T_1(\boldsymbol{g}_{1,h}^{n+1}) \\ - \frac{1}{2}T_2(\boldsymbol{g}_{1,h}^{n+1}) - V_1(\boldsymbol{g}_{1,h}^{n+1}) + S_2(\boldsymbol{g}_{1,h}^{n+1}) \\ - S_3(\boldsymbol{g}_{1,h}^{n+1}) - \alpha\left\langle \boldsymbol{h}_{3,h}^{n+1}, \boldsymbol{g}_{1,h}^{n+1}\right\rangle \Bigg)\Bigg) \\ \le \sum_{n=0}^{M-1}\frac{\Delta t}{32T}\|\boldsymbol{e}_{\eta}^{n+1}\|_S^2 + \frac{1}{16}\sum_{n=0}^{M-1}\mathcal{Z}_h^{n+1} \\ + C\Delta t\sum_{n=0}^{M-1}\Bigg((1+T)\|\boldsymbol{g}_{1,h}^{n+1}\|_S^2 + \big(1+\alpha\big)\|\boldsymbol{g}_{1,h}^{n+1}\|_{L^2(\Sigma)}^2 \\ + \rho_s\|\partial_{\Delta t}R_h^s\mathbf{q}^{n+1} - \partial_t\mathbf{q}^{n+1/2}\|_{L^2(\Omega_s)}^2 + \rho_s\|\boldsymbol{g}_{1,h}^{n+1}\|_{L^2(\Omega_s)}^2 + \|\mathbf{l}^{n+1} - \mathbf{l}^n\|_{L^2(\Sigma)}^2 \\ + \|(R_h^s - I)\mathbf{e}^{n+1/2}\|_S^2 + \alpha\|R_h^f\mathbf{u}^{n+1} - \partial_{\Delta t}R_h^s\mathbf{e}^{n+1}\|_{L^2(\Sigma)}^2 + \alpha\|\boldsymbol{h}_{3,h}^{n+1}\|_{L^2(\Sigma)}^2\Bigg),$$

and

$$\sum_{n=0}^{M-1} -\frac{\rho_s}{2}(\boldsymbol{e}_{\boldsymbol{q},h}^{\,n+1} - \boldsymbol{e}_{\boldsymbol{q},h}^{\,n}, \boldsymbol{g}_{1,h}^{n+1})_s \le \frac{\Delta t\rho_s}{32T}\sum_{n=0}^{M-1}\|\boldsymbol{e}_{\boldsymbol{q},h}^{\,n}\|_{L^2(\Omega_s)}^2 + CT(\Delta t)^3\rho_s\sum_{n=0}^{M-1}\|\partial_{\Delta t}^2R_h^s\mathbf{q}^n\|_{L^2(\Omega_s)}^2$$

$$+\frac{\rho_s}{32}\|\boldsymbol{e_{q}}_{,h}^M\|^2_{L^2(\Omega_s)} + C\rho_s\|\boldsymbol{g}^M_{1,h}\|^2_{L^2(\Omega_s)}.$$

Thus we have

$$\frac{\Delta t}{\alpha}\sum_{n=0}^{M-1}\langle \boldsymbol{g}^{n+1}_{1,h}, \boldsymbol{e_{\lambda}}_{,h}^n\rangle \leq \frac{1}{16}\max_{0\leq m\leq M}\mathcal{S}^m_h + \frac{1}{16}\sum_{n=0}^{M-1}\mathcal{Z}^{n+1}_h + C\boldsymbol{\Psi}_{1,h}(M).$$

Combining these bounds completes the proof. □

The results of Lemmas 5.2.2, 5.2.3, and 5.2.4 combine to provide a penultimate error estimate

$$\frac{1}{4}\max_{0\leq M\leq N}(\mathcal{S}^M_h + \mathcal{E}^M_h) + \frac{1}{4}\sum_{n=0}^{N-1}(\mathcal{Z}^{n+1}_h + \mathcal{W}^{n+1}_h) \leq C\max_{0\leq M\leq N}(\mathbf{D}_h(M) + \boldsymbol{\Psi}_h(M)). \quad (5.2.20)$$

5.2.5 Step 3: Main Result

As always, it now remains for us to bound the collected errors contained in $\mathbf{D}_h(m)$ and $\boldsymbol{\Psi}_h(m)$. To do so, we will rely heavily on the work previously done in 4.3.5. We may do this because the error terms in $\mathbf{D}_h(m)$ and $\boldsymbol{\Psi}_h(m)$ loosely fall into one of two categories: terms such as $\boldsymbol{g}^{n+1}_{1,h}$ are just versions of the the splitting errors defined in Chapter 4 projected into the finite element space. Thus, they are bounded in norm by the terms in Chapter 4 according to (2.2.12), as we will show. Terms such as $R^f_h\mathbf{u}^{n+1} - \mathbf{u}^{n+1}$, on the other hand, are interpolation errors that we will bound according to the properties of the interpolant.

We will also employ the following result which will allow us to avoid factors like

$\Delta t h^2$.

Lemma 5.2.6. *Let X be a Sobolev space with $w \in X$. Then it follows*

$$\|w^{n+1}\|_X^2 \leq C\left(\Delta t\|\partial_t w\|^2_{L^2(t_n,t_{n+1};X)} + \frac{1}{\Delta t}\|w\|^2_{L^2(t_n,t_{n+1};X)}\right).$$

Proof. We first define

$$\bar{w}^{n+1}(x) := \frac{1}{\Delta t}\int_{t_n}^{t_{n+1}} w(x,s)\,ds.$$

Then it is straightforward to show

$$w^{n+1} - \bar{w}^{n+1} = \frac{1}{\Delta t}\int_{t_n}^{t_{n+1}} (s-t_n)\partial_t w(\cdot,s)ds.$$

Consequently, we have

$$\begin{aligned}\|w^{n+1}\|_X^2 =& \|w^{n+1} - \bar{w}^{n+1} + \bar{w}^{n+1}\|_X^2 \\ \leq& C\big(\|w^{n+1} - \bar{w}^{n+1}\|_X^2 + \|\bar{w}^{n+1}\|_X^2\big).\end{aligned}$$

The result follows from applying (3.4.12).

□

Some quantities, however, will represent errors that result from *both* the interpolation and the time discretization. For these terms, we will refer to the following lemma.

Lemma 5.2.7. *The following inequalities hold*

$$\begin{aligned}
\|\partial_{\Delta t} R_h^s \mathbf{q}^{n+1} - \partial_t \mathbf{q}^{n+1/2}\|^2_{L^2(\Omega_s)} \leq & C\bigg(\frac{h^4}{\Delta t}\|\partial_t \mathbf{q}\|^2_{L^2(t_n,t_{n+1};H^2(\Omega_s))} \\
& + \Delta t^3 \|\partial_t^3 \mathbf{q}\|^2_{L^2(t_n,t_{n+1};L^2(\Omega_s))}\bigg), \qquad (5.2.21a) \\
\|\partial_{\Delta t} R_h^f \mathbf{u}^{n+1} - \partial_t \mathbf{u}^{n+1}\|^2_{L^2(\Omega_f)} \leq & C\bigg(\frac{h^4}{\Delta t}\|\partial_t \mathbf{u}\|^2_{L^2(t_n,t_{n+1};H^2(\Omega_f))} \\
& + \Delta t \|\partial_t^2 \mathbf{u}\|^2_{L^2(t_n,t_{n+1};L^2(\Omega_f))}\bigg), \qquad (5.2.21b) \\
\|\nabla(R_h^s - I)\partial_{\Delta t}\mathbf{e}^{n+1}\|^2_{L^2(\Omega_s)} \leq & C\frac{h^2}{\Delta t}\|\partial_t \mathbf{e}\|^2_{L^2(t_n,t_{n+1};H^2(\Omega_s))}, \qquad (5.2.21c) \\
\|S_h \mathsf{p}^{n+1} - \mathsf{p}^{n+1}\|^2_{L^2(\Omega_f)} \leq & C\bigg(\Delta t h^4 \|\partial_t \mathsf{p}\|^2_{L^2(t_n,t_{n+1};H^2(\Omega_f))} \\
& + \frac{h^4}{\Delta t}\|\mathsf{p}\|^2_{L^2(t_n,t_{n+1};H^2(\Omega_f))}\bigg), \qquad (5.2.21d) \\
\|\varepsilon(R_h^f \boldsymbol{u}^{n+1} - \boldsymbol{u}^{n+1})\|^2_{L^2(\Omega_f)} \leq & C\bigg(\Delta t h^2 \|\partial_t \mathbf{u}\|^2_{L^2(t_n,t_{n+1};H^2(\Omega_f))} \\
& + \frac{h^2}{\Delta t}\|\mathbf{u}\|^2_{L^2(t_n,t_{n+1};H^2(\Omega_f))}\bigg). \qquad (5.2.21e)
\end{aligned}$$

Proof. To prove (5.2.21a), we write

$$\partial_{\Delta t} R_h^s \mathbf{q}^{n+1} - \partial_t \mathbf{q}^{n+1/2} = (R_h^s - I)\partial_{\Delta t}\mathbf{q}^{n+1} + (\partial_{\Delta t}\mathbf{q}^{n+1} - \partial_t \mathbf{q}^{n+1/2})$$

and

$$\partial_{\Delta t}\boldsymbol{q}^{n+1} = \frac{1}{\Delta t}\int_{t_n}^{t_{n+1}} (\partial_t \mathbf{q})(\cdot, s)ds. \qquad (5.2.22)$$

Hence,

$$(R_h^s - I)\partial_{\Delta t}\mathbf{q}^{n+1} = \frac{1}{\Delta t}\int_{t_n}^{t_{n+1}} (R_h^s - I)(\partial_t \mathbf{q})(\cdot, s)ds.$$

It therefore follows from (3.4.12) and Lemma 2.2.14 that

$$\|(R_h^s - I)\partial_{\Delta t}\mathbf{q}^{n+1}\|^2_{L^2(\Omega_s)} \leq \frac{1}{\Delta t}\int_{t_n}^{t_{n+1}} \|(R_h^s - I)(\partial_t \mathbf{q})(\cdot, s)\|^2_{L^2(\Omega_s)} ds$$

$$\leq \frac{Ch^4}{\Delta t} \int_{t_n}^{t_{n+1}} \|\partial_t \mathbf{q}(\cdot, s)\|^2_{H^2(\Omega_s)} ds. \tag{5.2.23}$$

To estimate $\partial_{\Delta t}\mathbf{q}^{n+1} - \partial_t \mathbf{q}^{n+1/2}$, we use Lemma 3.4.7. Therefore,

$$\|\partial_{\Delta t}\boldsymbol{q}^{n+1} - \partial_t \boldsymbol{q}^{n+1/2}\|^2_{L^2(\Omega_s)} \leq C\Delta t^3 \int_{t_n}^{t_{n+1}} \|\partial_t^3 \boldsymbol{q}(\cdot, s)\|^2_{L^2(\Omega_s)} ds. \tag{5.2.24}$$

To get the bound (5.2.21b) we write

$$\partial_{\Delta t} R_h^f \mathbf{u}^{n+1} - \partial_t \mathbf{u}^{n+1} = (R_h^f - I)\partial_{\Delta t}\mathbf{u}^{n+1} + \partial_{\Delta t}\mathbf{u}^{n+1} - \partial_t \mathbf{u}^{n+1}.$$

Similar to the bound (5.2.23), we can show that

$$\|(R_h^f - I)\partial_{\Delta t}\mathbf{u}^{n+1}\|^2_{L^2(\Omega_f)} \leq \frac{Ch^4}{\Delta t}\Big(\int_{t_n}^{t_{n+1}} \|\partial_t \mathbf{u}(\cdot, s)\|^2_{H^2(\Omega_f)}\Big).$$

Furthermore, applying Lemma 3.4.7 and Hölder's inequality, we establish

$$\|\partial_{\Delta t}\mathbf{u}^{n+1} - \partial_t \mathbf{u}^{n+1}\|^2_{L^2(\Omega_f)} \leq \frac{\Delta t}{3} \int_{t_n}^{t_{n+1}} \|\partial_t^2 \mathbf{u}(\cdot, s)\|^2_{L^2(\Omega_f)} ds.$$

Combining the above two inequalites gives (5.2.21b).

For (5.2.21c) we use (3.4.12) and Lemma 2.2.14, to get

$$\|\nabla(R_h^s - I)\partial_{\Delta t}\boldsymbol{\eta}^{n+1/2}\|^2_{L^2(\Omega_s)} \leq C\frac{h^2}{\Delta t}\|\partial_t \boldsymbol{\eta}\|^2_{L^2(t_n, t_{n+1}; H^2(\Omega_s))}.$$

The proofs for (5.2.21d) and (5.2.21e) follow the same method, so we will only show the work for (5.2.21d).

Thus, for (5.2.21d), we recall from Lemma 2.2.14 that

$$\|S_h\mathsf{p}^{n+1} - \mathsf{p}^{n+1}\|^2_{L^2(\Omega_f)} \leq Ch^4\|\mathsf{p}^{n+1}\|^2_{H^2(\Omega_f)}.$$

The result then follows from Lemma 5.2.6.

□

Consequently, we will prove the following bound.

Lemma 5.2.8. *Under Assumptions 4.3.3 and 4.3.4 and assuming $h \leq C\Delta t$, we have that, for all $1 \leq M \leq N$, it holds*

$$\begin{aligned}\mathbf{D}_h(M) + \mathbf{\Psi}_h(M) \leq & C(\Delta t)^2\Bigg(\frac{(1+T)(L_1+L_2)^3}{\alpha^2}\Bigg(\big(1+\log\frac{1}{\Delta t}\big)\|\partial_t\varepsilon(\mathbf{e})\|^2_{L^2(0,T;L^\infty(\Omega_s))} \\ & + \|\partial_t \mathrm{div}\,\mathbf{e}\|^2_{L^2(0,T;L^\infty(\Omega_s))}\Bigg) + C\big(\mathbf{Y}_{1,h} + \mathbf{Y}_{2,h} + \mathbf{Y}_{3,h}\big),\end{aligned}$$

where

$$\begin{aligned}\mathbf{Y}_{1,h} :=& h^2\Bigg((1+h^2)\rho_s(1+T)\|\partial_t\mathbf{q}\|^2_{L^2(0,T;H^2(\Omega_s))} + (1+h^2)\rho_f T\|\partial_t\mathbf{u}\|^2_{L^2(0,T;H^2(\Omega_f))} \\ & + (1+T)(L_1+L_2)\|\partial_t\mathbf{e}\|^2_{L^2(0,T;H^2(\Omega_s))} + \mu\|\mathbf{u}\|^2_{L^2(0,T;H^2(\Omega_f))} \\ & + \frac{h^2}{\mu}\|\mathsf{p}\|^2_{L^2(0,T;H^2(\Omega_f))} + (L_1+L_2)\|\mathbf{e}\|^2_{L^2(0,T;H^2(\Omega_s))} \\ & + (L_1+L_2)\|\mathbf{e}\|^2_{L^\infty(0,T;H^2(\Omega_s))}\Bigg) \\ & + (\Delta t)^2\Bigg((\Delta t)^2\rho_s(1+T)\|\partial_t^3\mathbf{q}\|^2_{L^2(0,T;L^2(\Omega_s))} + \rho_f T\|\partial_t^2\mathbf{u}\|^2_{L^2(0,T;L^2(\Omega_f))} \\ & + \frac{h^4}{\mu}\|\partial_t\mathsf{p}\|^2_{L^2(0,T;H^2(\Omega_f))} + h^2(L_1+L_2)\|\partial_t\mathbf{e}\|^2_{L^2(0,T;H^2(\Omega_s))} \\ & + h^2\mu\|\partial_t\mathbf{u}\|^2_{L^2(0,T;H^2(\Omega_f))}\Bigg) \\ \mathbf{Y}_{2,h} :=& (\Delta t)^2\Bigg((\Delta t)^2(1+T)(L_1+L_2)\|\partial_t^3\mathbf{q}\|^2_{L^2(0,T;H^1(\Omega_S))} + h^2\|\partial_t\mathbf{u}\|^2_{L^2(0,T;H^3(\Omega_f))}\end{aligned}$$

$$
\begin{aligned}
&+ (1 + \alpha + \frac{\alpha^2}{\mu} + \mu + \mu^2 + \frac{(1+T)\mu^2}{\alpha})\|\partial_t \mathbf{u}\|^2_{L^2(0,T;H^2(\Sigma))} \\
&+ (1+\alpha)\|\partial_t^2 \mathbf{e}\|^2_{L^2(0,T;L^2(\Sigma))} + (1 + \frac{1+T}{\alpha} + \frac{1}{\mu})\|\partial_t \mathsf{p}\|^2_{L^2(0,T;H^1(\Sigma))} \\
&+ (\Delta t)^2 (1+\alpha)\|\partial_t^3 \mathbf{q}\|^2_{L^2(0,T;L^2(\Sigma))} + T\rho_s \|\partial_t^2 \mathbf{q}\|^2_{L^2(0,T;L^2(\Omega_s))} \\
&+ ((1+T)(L_1+L_2) + \rho_s)\|\partial_t \mathbf{q}\|^2_{L^2(0,T;H^1(\Omega_s))} + \frac{\mu^2 T}{\alpha}\|\varepsilon(\partial_t \mathbf{u})\|^2_{L^2(0,T;L^\infty(\Sigma))} \\
&+ \frac{T}{\alpha}\|\partial_t \mathsf{p}\|^2_{L^2(0,T;L^\infty(\Sigma))} + \rho_s \|\partial_t \mathbf{q}\|^2_{L^\infty(0,T;L^2(\Omega_s))} + h^2 \|\partial_t \mathsf{p}\|^2_{L^2(0,T;H^1(\Omega_f))} \Bigg) \\
&+ h^2 \Bigg(\|\mathbf{u}\|^2_{L^2(0,T;H^3(\Omega_f))} + \|\nabla \mathsf{p}\|^2_{L^2(0,T;L^2(\Omega_f))} \Bigg) + h^4 \Bigg(\frac{T\mu^2}{\alpha}\|\partial_t \mathbf{u}\|^2_{L^2(0,T;H^2(\Sigma))} \\
&+ \frac{T}{\alpha}\|\partial_t \mathsf{p}\|^2_{L^2(0,T;H^1(\Sigma))} \Bigg)
\end{aligned}
$$

$$
\begin{aligned}
\mathbf{Y}_{3,h} :=& (\Delta t)^2 \Bigg(\frac{(1+T)(L_1+L_2)^3 + \rho_s(L_1^2+L_2^2)}{\alpha^2}\|\partial_t \mathbf{e}\|^2_{L^2(0,T;H^2(\Omega_s))} \\
&+ \frac{\rho_s T(L_1^2+L_2^2)}{\alpha^2}\|\partial_t^2 \mathbf{e}\|^2_{L^2(0,T;H^2(\Omega_s))} + \frac{\rho_s(L_1^2+L_2^2)}{\alpha^2}\|\partial_t \mathbf{e}\|^2_{L^\infty(0,T;H^1(\Omega_s))} \Bigg).
\end{aligned}
$$

Proof. Since so many of the error terms may be bounded using results from previous chapters, we bound the sum of $\mathbf{D}_h(m)$ and $\mathbf{\Psi}_h(m)$ instead of the two terms individually. Thus, to begin, we write

$$
\mathbf{D}_h(M) + \mathbf{\Psi}_h(M) := \boldsymbol{H}_h + \boldsymbol{L}_h + \boldsymbol{I}_h,
$$

where

$$
\begin{aligned}
\boldsymbol{H}_h :=& \Delta t \sum_{n=0}^{M-1} \Bigg((1+T)\rho_s \|\partial_{\Delta t} R_h^s \mathbf{q}^{n+1} - \partial_t \mathbf{q}^{n+1/2}\|^2_{L^2(\Omega_s)} \\
&+ T\rho_f \|\partial_{\Delta t} R_h^f \mathbf{u}^{n+1} - \partial_t \mathbf{u}^{n+1}\|^2_{L^2(\Omega_f)} + (1+T)\|(R_h^s - I)\partial_{\Delta t}\mathbf{e}^{n+1}\|^2_S \\
&+ \mu \|\varepsilon(R_h^f \mathbf{u}^{n+1} - \mathbf{u}^{n+1})\|^2_{L^2(\Omega_f)} + \frac{1}{\mu}\|S_h \mathsf{p}^{n+1} - \mathsf{p}^{n+1}\|^2_{L^2(\Omega_f)} \\
&+ \|(R_h^s - I)\mathbf{e}^{n+1/2}\|^2_S \Bigg) + \|(R_h^s - I)\mathbf{e}^M\|^2_S + \|(R_h - I)\mathbf{e}^0\|^2_S
\end{aligned}
$$

$$
\begin{aligned}
\boldsymbol{L}_h := & \Delta t \sum_{n=0}^{M-1} \Bigg((1+T)\|\boldsymbol{h}_{3,h}\|_S^2 + h^2\|\mathbf{u}^{n+1}\|^2_{H^3(\Omega_f)} + h^2\|\nabla S_h \mathsf{p}^{n+1}\|^2_{L^2(\Omega_f)} \\
& + (1+\alpha+\frac{\alpha^2}{\mu})\|\boldsymbol{g}_{1,h}^{n+1}\|^2_{L^2(\Sigma)} + (1+\alpha)\|R_h^f \mathbf{u}^{n+1} - \partial_{\Delta t} R_h^s \mathbf{e}^{n+1}\|^2_{L^2(\Sigma)} \\
& + (1+\frac{1}{\alpha}+\frac{1}{\mu})\|\mathbf{l}^{n+1} - \mathbf{l}^n\|^2_{L^2(\Sigma)} + (1+\alpha)\|\boldsymbol{h}_{3,h}^{n+1}\|^2_{L^2(\Sigma)} \\
& + T(\Delta t)^2 \rho_s \|\partial^2_{\Delta t} R_h^s \mathbf{q}^n\|^2_{L^2(\Omega_s)} + (1+T)\|\boldsymbol{g}_{1,h}^{n+1}\|_S^2 \\
& + \rho_s \|\boldsymbol{g}_{1,h}^{n+1}\|^2_{L^2(\Omega_s)} + \frac{T}{\alpha}\|\boldsymbol{g}_{2,h}^{n+1}\|^2_{L^\infty(\Sigma)} \Bigg) + \rho_s\|\boldsymbol{g}_{1,h}^M\|^2_{L^2(\Omega_s)} \\
& + \frac{Th^2}{\alpha}\sum_{n=0}^{M-1}\|\boldsymbol{g}_2^{n+1}\|^2_{H^1(\Sigma)} \\
\boldsymbol{I}_h := & \Delta t \sum_{n=0}^{M-1} \Bigg(\frac{\rho_s}{\alpha^2}\|\tilde{\boldsymbol{g}}_{2,h}^{n+1}\|^2_{L^2(\Omega_s)} \\
& + \frac{1+T}{\alpha^2}\|\tilde{\boldsymbol{g}}_{2,h}^{n+1}\|_S^2 + \frac{T(\Delta t)^2\rho_s}{\alpha^2}\|\partial^2_{\Delta t}\mathcal{L}^n_{s,h}\|^2_{L^2(\Omega_s)} \Bigg) + \frac{\rho_s}{\alpha^2}\|\tilde{\boldsymbol{g}}_{2,h}^M\|^2_{L^2(\Omega_s)}.
\end{aligned}
$$

Above, we can consider $\boldsymbol{H}_h$ to consist of the error terms resulting from either the interpolation or a combination of the interpolation and the time discretization. Most of these terms may be bounded by directly applying Lemma 2.2.14, and the results of Lemma 5.2.7. For the terms involving the norm $\|\cdot\|_S$, however, we work more carefully, in order to keep track of the physical parameters as we did in the previous chapter. Thus we have,

$$
\begin{aligned}
\|(R_h^s - I)\mathbf{e}\|_S^2 := & 2L_1\|\varepsilon(R_h^s\mathbf{e} - \mathbf{e})\|^2_{L^2(\Omega_s)} + L_2\|\mathrm{div}\,(R_h^s\mathbf{e} - \mathbf{e})\|^2_{L^2(\Omega_s)} \\
\leq & C(L_1+L_2)\|(R_h^s - I)\mathbf{e}\|^2_{H^1(\Omega_s)} \\
\leq & C(L_1+L_2)h^2\|\mathbf{e}\|^2_{H^2(\Omega_s)},
\end{aligned}
$$

where the last step follows from Lemma 2.2.14.

Then, using Lemma 5.2.6 and results from previous chapters, it follows

$$\begin{aligned}\|(R_h^s - I)\mathbf{e}^{n+1/2}\|_S^2 \leq & C(L_1+L_2)\bigg(\Delta t h^2 \|\partial_t \mathbf{e}\|^2_{L^2(t_n-1,t_{n+1};H^2(\Omega_s))} \\ & + \frac{h^2}{\Delta t}\|\mathbf{e}\|^2_{L^2(t_n-1,t_{n+1};H^2(\Omega_s))}\bigg), \\ \|(R_h^s - I)\mathbf{e}^M\|_S^2 + \|(R_h^s - I)\mathbf{e}^0\|_S^2 \leq & C(L_1+L_2)\Delta t h^2 \|\partial_t \mathbf{e}\|^2_{L^\infty(0,T;H^2(\Omega_s))}.\end{aligned}$$

We may also use identities(3.4.12) and (5.2.22) to establish

$$\|(R_h^s - I)\partial_{\Delta t}\mathbf{e}^{n+1}\|_S^2 \leq C(L_1+L_2)\frac{h^2}{\Delta t}\int_{t_n}^{t_{n+1}} \|\partial_t \mathbf{e}(\cdot,s)\|^2_{H^2(\Omega_s)} ds.$$

Consequently, we have

$$\begin{aligned}\boldsymbol{H}_h \leq & Ch^2\bigg((1+h^2)\rho_s(1+T)\|\partial_t \mathbf{q}\|^2_{L^2(0,T;H^2(\Omega_s))} + (1+h^2)\rho_f T\|\partial_t \mathbf{u}\|^2_{L^2(0,T;H^2(\Omega_f))} \\ & + (1+T)(L_1+L_2)\|\partial_t \mathbf{e}\|^2_{L^2(0,T;H^2(\Omega_s))} + \mu\|\mathbf{u}\|^2_{L^2(0,T;H^2(\Omega_f))} \\ & + \frac{h^2}{\mu}\|\mathsf{p}\|^2_{L^2(0,T;H^2(\Omega_f))} + (L_1+L_2)\|\mathbf{e}\|^2_{L^2(0,T;H^2(\Omega_s)} \\ & + (L_1+L_2)\|\mathbf{e}\|^2_{L^\infty(0,T;H^2(\Omega_s))}\bigg) \\ & + C(\Delta t)^2\bigg((\Delta t)^2\rho_s(1+T)\|\partial_t^3 \mathbf{q}\|^2_{L^2(0,T;L^2(\Omega_s))} + \rho_f T\|\partial_t^2 \mathbf{u}\|^2_{L^2(0,T;L^2(\Omega_f))} \\ & + \frac{h^4}{\mu}\|\partial_t \mathsf{p}\|^2_{L^2(0,T;H^2(\Omega_f))} + h^2(L_1+L_2)\|\partial_t \mathbf{e}\|^2_{L^2(0,T;H^2(\Omega_s))} \\ & + h^2\mu\|\partial_t \mathbf{u}\|^2_{L^2(0,T;H^2(\Omega_f))}\bigg) \\ =: & C\mathbf{Y}_{1,h}.\end{aligned}$$

For $\boldsymbol{L}_h$, we first rewrite the terms in the $\|\cdot\|_S$ norm.

$$\begin{aligned}\|\boldsymbol{h}_{3,h}^{n+1}\|_S^2 =& 2L_1\|\epsilon(\boldsymbol{h}_{3,h}^{n+1}\|_{L^2(\Omega_s)}^2 + L_2\|\operatorname{div}\boldsymbol{h}_{3,h}^{n+1}\|_{L^2(\Omega_s)}^2\\ \leq C(L_1+L_2)\|\boldsymbol{h}_{3,h}^{n+1}\|_{H^1(\Omega_s)}^2,\end{aligned}$$

and

$$\begin{aligned}\|\boldsymbol{g}_{1,h}^{n+1}\|_S^2 =& 2L_1\|\epsilon(\boldsymbol{g}_{1,h}^{n+1}\|_{L^2(\Omega_s)}^2 + L_2\|\operatorname{div}\boldsymbol{g}_{1,h}^{n+1}\|_{L^2(\Omega_s)}^2\\ \leq C(L_1+L_2)\|\boldsymbol{g}_{1,h}^{n+1}\|_{H^1(\Omega_s)}^2,\end{aligned}$$

Thus, we may use (2.2.12) to write

$$\begin{aligned}\boldsymbol{L}_h \leq & C\Delta t\sum_{n=0}^{M-1}\Bigg((1+T)(L_1+L_2)\|\boldsymbol{h}_3\|_{H^1(\Omega_s)}^2 + h^2\|\mathbf{u}^{n+1}\|_{H^3(\Omega_f)}^2\\ &+(1+\alpha+\frac{\alpha^2}{\mu})\|\boldsymbol{g}_1^{n+1}\|_{L^2(\Sigma)}^2 + h^2\|\nabla\mathsf{p}^{n+1}\|_{L^2(\Omega_f)}^2\\ &+(1+\alpha)\|\partial_t\mathbf{e}^{n+1}-\partial_{\Delta t}\mathbf{e}^{n+1}\|_{L^2(\Sigma)}^2 + (1+\frac{1}{\alpha}+\frac{1}{\mu})\|\boldsymbol{g}_2^{n+1}\|_{L^2(\Sigma)}^2\\ &+(1+\alpha)\|\boldsymbol{h}_3^{n+1}\|_{L^2(\Sigma)}^2 + T(\Delta t)^2\rho_s\|\partial_{\Delta t}^2\mathbf{q}^n\|_{L^2(\Omega_s)}^2\\ &+(1+T)(L_1+L_2)\|\boldsymbol{g}_1^{n+1}\|_{H^1(\Omega_s)}^2 + \rho_s\|\boldsymbol{g}_1^{n+1}\|_{L^2(\Omega_s)}^2 + \frac{T}{\alpha}\|\boldsymbol{g}_2^{n+1}\|_{L^\infty(\Sigma)}^2\Bigg)\\ &+\rho_s\|\boldsymbol{g}_1^M\|_{L^2(\Omega_s)}^2 + \frac{Th^2}{\alpha}\sum_{n=0}^{M-1}\|\boldsymbol{g}_2^{n+1}\|_{H^1(\Sigma)}^2,\end{aligned}$$

where we use (4.1.3a) to replace $\mathbf{u}$ with $\partial_t\mathbf{e}$ on the interface.

We may then use (3.4.12) and the results from the previous two chapters–namely Lemma 3.4.7–to bound all of the terms in $\boldsymbol{L}_h$. We therefore determine

$$\boldsymbol{L}_h \leq C(\Delta t)^2\Bigg((\Delta t)^2(1+T)(L_1+L_2)\|\partial_t^3\mathbf{q}\|_{L^2(0,T;H^1(\Omega_S))}^2 + h^2\|\partial_t\mathbf{u}\|_{L^2(0,T;H^3(\Omega_f))}^2$$

$$+ (1 + \alpha + \frac{\alpha^2}{\mu} + \mu + \mu^2 + \frac{\mu^2}{\alpha})\|\partial_t \mathbf{u}\|^2_{L^2(0,T;H^1(\Sigma))}$$
$$+ (1 + \alpha)\|\partial_t^2 \mathbf{e}\|^2_{L^2(0,T;L^2(\Sigma))} + (1 + \frac{1}{\alpha} + \frac{1}{\mu})\|\partial_t \mathsf{p}\|^2_{L^2(0,T;L^2(\Sigma))}$$
$$+ (\Delta t)^2(1 + \alpha)\|\partial_t^3 \mathbf{q}\|^2_{L^2(0,T;L^2(\Sigma))} + T\rho_s\|\partial_t^2 \mathbf{q}\|^2_{L^2(0,T;L^2(\Omega_s))}$$
$$+ ((1 + T)(L_1 + L_2) + \rho_s)\|\partial_t \mathbf{q}\|^2_{L^2(0,T;H^1(\Omega_s))} + \frac{\mu^2 T}{\alpha}\|\varepsilon(\partial_t \mathbf{u})\|^2_{L^2(0,T;L^\infty(\Sigma))}$$
$$+ \frac{T}{\alpha}\|\partial_t \mathsf{p}\|^2_{L^2(0,T;L^\infty(\Sigma))} + \rho_s\|\partial_t \mathbf{q}\|^2_{L^\infty(0,T;L^2(\Omega_s))} + h^2\|\partial_t \mathsf{p}\|^2_{L^2(0,T;H^1(\Omega_f))}\Bigg)$$
$$+ Ch^2\left(\|\mathbf{u}\|^2_{L^2(0,T;H^3(\Omega_f))} + \|\nabla \mathsf{p}\|^2_{L^2(0,T;L^2(\Omega_f))}\right)$$
$$+ \frac{CTh^2\Delta t}{\alpha}\mu^2\|\partial_t \mathbf{u}\|^2_{L^2(0,T;H^2(\Sigma))} + \frac{CTh^2\Delta t}{\alpha}\|\partial_t \mathsf{p}\|^2_{L^2(0,T;H^1(\Sigma))}.$$

For the coefficient in front of the last two terms, $\frac{CTh^2\Delta t}{\alpha}$, we may avoid the term $h^2\Delta t$ by using Young's inequality to determine

$$\frac{CTh^2\Delta t}{\alpha} \leq \frac{CT(h^4 + (\Delta t)^2)}{\alpha}.$$

Applying this to the result above yields $C\mathbf{Y}_{2,h}$.

Finally, we consider $\boldsymbol{I}_h$. Recall that we have

$$\mathcal{L}_{s,h} = R_h^s \mathcal{L}_s = R_h^s(\tilde{\phi}\tilde{\mathbf{l}}_s),$$

where $\mathcal{L}_s$ and $\tilde{\mathbf{l}}_s$ are as defined in 4.3.4.

Thus, from (2.2.12), we may write

$$\boldsymbol{I}_h \leq C\Delta t \sum_{n=0}^{M-1} \Bigg(\frac{\rho_s}{\alpha^2}\|\tilde{\phi}(\tilde{\mathbf{l}}_s^{n+1} - \tilde{\mathbf{l}}_s^n)\|^2_{L^2(\Omega_s)}$$
$$+ \frac{1+T}{\alpha^2}\|R_h^s\big(\tilde{\phi}(\tilde{\mathbf{l}}_s^{n+1} - \tilde{\mathbf{l}}_s^n)\big)\|^2_S + \frac{T(\Delta t)^2\rho_s}{\alpha^2}\|\partial^2_{\Delta t}(\tilde{\phi}(\tilde{\mathbf{l}}_s^n))\|^2_{H^1(\Omega_s)}\Bigg)$$

$$+\frac{\rho_s}{\alpha^2}\|\tilde{\phi}(\tilde{\mathbf{l}}_s^M-\tilde{\mathbf{l}}_s^{M-1})\|^2_{L^2(\Omega_s)}.$$

From Assumption 4.3.3 and condition (i) of Assumption 4.3.4, we know that $\tilde{\boldsymbol{n}}_s$ is bounded, and $0 \leq \tilde{\phi} \leq 1$. Thus,

$$\begin{aligned}
\|\tilde{\phi}(\tilde{\mathbf{l}}_s^{n+1}-\tilde{\mathbf{l}}_s^{n})\|^2_{L^2(\Omega_s)} \leq& C\|\sigma_s(\mathbf{e}^{n+1}-\mathbf{e}^n)\|^2_{L^2(\Omega_s)} \leq C(L_1^2+L_2^2)\|\mathbf{e}^{n+1}-\mathbf{e}^n\|^2_{H^1(\Omega_s)},\\
\|\partial^2_{\Delta t}(\tilde{\phi}(\tilde{\mathbf{l}}_s^{n}))\|^2_{L^2(\Omega_s)} \leq& C\|\partial^2_{\Delta t}\sigma_s(\mathbf{e}^n)\|^2_{H^1(\Omega_s)} \leq C(L_1^2+L_2^2)\|\partial^2_{\Delta t}\mathbf{e}^n\|^2_{H21(\Omega_s)}.
\end{aligned}$$

Applying the results of Lemma 3.4.7, we have

$$\begin{aligned}
\boldsymbol{I}_h \leq& C\Delta t\sum_{n=0}^{M-1}\frac{1+T}{\alpha^2}\|R_h^s\big(\tilde{\phi}(\tilde{\mathbf{l}}_s^{n+1}-\tilde{\mathbf{l}}_s^{n})\big)\|^2_S + C(\Delta t)^2\Bigg(\frac{\rho_s(L_1^2+L_2^2)}{\alpha^2}\|\partial_t\mathbf{e}\|^2_{L^2(0,T;H^1(\Omega_s))}\\
&+\frac{\rho_s T(L_1^2+L_2^2)}{\alpha^2}\|\partial_t^2\mathbf{e}\|^2_{L^2(0,T;H^1(\Omega_s))}+\frac{\rho_s(L_1^2+L_2^2)}{\alpha^2}\|\partial_t\mathbf{e}\|^2_{L^\infty(0,T;H^1(\Omega_s))}\Bigg).
\end{aligned}$$

For the term in the $\|\cdot\|_S$-norm, we follow the method of 4.3.5 and begin by applying Lemma 2.2.12, followed by the product rule.

$$\begin{aligned}
\|R_h^s\big(\tilde{\phi}(\tilde{\mathbf{l}}_s^{n+1}-\tilde{\mathbf{l}}_s^{n})\big)\|^2_S =& 2L_1\|\epsilon\big(R_h^s\big(\tilde{\phi}(\tilde{\mathbf{l}}_s^{n+1}-\tilde{\mathbf{l}}_s^{n})\big)\big)\|^2_{L^2(\Omega_s)}+L_1\|\operatorname{div}R_h^s\big(\tilde{\phi}(\tilde{\mathbf{l}}_s^{n+1}-\tilde{\mathbf{l}}_s^{n})\big)\|^2_{L^2(\Omega_s)}\\
\leq& C(L_1+L_2)\|\nabla R_h^s\big(\tilde{\phi}(\tilde{\mathbf{l}}_s^{n+1}-\tilde{\mathbf{l}}_s^{n})\big)\|^2_{L^2(\Omega_s)}\\
\leq&(L_1+L_2)\|\nabla\tilde{\phi}(\tilde{\mathbf{l}}_s^{n+1}-\tilde{\mathbf{l}}_s^{n})\|^2_{L^2(\Omega_s)}\\
\leq& C(L_1+L_2)\Bigg(\|\nabla\tilde{\phi}\|^2_{L^2(\Omega_s)}\|\tilde{\mathbf{l}}_s^{n+1}-\tilde{\mathbf{l}}_s^{n}\|^2_{L^\infty(\Omega_s)}\\
&+\|\tilde{\phi}\|^2_{L^\infty(\Omega_s)}\|\nabla(\tilde{\mathbf{l}}_s^{n+1}-\tilde{\mathbf{l}}_s^{n})\|^2_{L^2(\Omega_s)}\Bigg)\\
\leq& C(L_1+L_2)\Bigg((1+\log\frac{1}{\Delta t})\|\tilde{\mathbf{l}}_s^{n+1}-\tilde{\mathbf{l}}_s^{n}\|^2_{L^\infty(\Omega_s)}
\end{aligned}$$

$$+ \|\nabla(\tilde{\mathbf{l}}_s^{n+1} - \tilde{\mathbf{l}}_s^n)\|^2_{L^2(\Omega_s)}\Bigg).$$

Thus, recalling the definition of $\tilde{\mathbf{l}}_s$ and $\mathbf{l}_s$ and using product rule once more, we have

$$\begin{aligned}
\|R_h^s\big(\tilde{\phi}(\tilde{\mathbf{l}}_s^{n+1} - \tilde{\mathbf{l}}_s^n)\big)\|_S \leq & C(L_1+L_2)\Bigg((1+\log\frac{1}{\Delta t})\|\sigma_s(\mathbf{e}^{n+1}-\mathbf{e}^n)\|^2_{L^\infty(\Omega_s)} \\
& + \|\nabla\tilde{\boldsymbol{n}}_s\|^2_{L^\infty(\Omega_s)}\|\sigma_s(\mathbf{e}^{n+1}-\mathbf{e}^n)\|^2_{L^2(\Omega_s)} \\
& + \|(L_1+L_2)D^2(\mathbf{e}^{n+1}-\mathbf{e}^n)\|^2_{L^2(\Omega_s)}\Bigg) \\
\leq & C(L_1+L_2)\Bigg(\big(1+\log\frac{1}{\Delta t}\big)\Big(L_1^2\|\varepsilon(\mathbf{e}^{n+1}-\mathbf{e}^n)\|^2_{L^\infty(\Omega_s)} \\
& + L_2^2\|\mathrm{div}\,(\mathbf{e}^{n+1}-\mathbf{e}^n)\|^2_{L^\infty(\Omega_s)}\Big) \\
& + L_1^2\|\varepsilon(\mathbf{e}^{n+1}-\mathbf{e}^n)\|^2_{L^2(\Omega_s)} + L_2^2\|\mathrm{div}\,(\mathbf{e}^{n+1}-\mathbf{e}^n)\|^2_{L^2(\Omega_s)} \\
& + (L_1+L_2)^2\|D^2(\mathbf{e}^{n+1}-\mathbf{e}^n)\|^2_{L^2(\Omega_s)}\Bigg) \\
\leq & C(L_1+L_2)^3\Bigg(\big(1+\log\frac{1}{\Delta t}\big)\Big(\|\varepsilon(\mathbf{e}^{n+1}-\mathbf{e}^n)\|^2_{L^\infty(\Omega_s)} \\
& + \|\mathrm{div}\,(\mathbf{e}^{n+1}-\mathbf{e}^n)\|^2_{L^\infty(\Omega_s)}\Big) + \|\mathbf{e}^{n+1}-\mathbf{e}^n\|^2_{H^2(\Omega_s)}\Bigg) \\
\leq & C\Delta t(L_1+L_2)^3\Bigg(\big(1+\log\frac{1}{\Delta t}\big)\Big(\|\partial_t\varepsilon(\mathbf{e})\|^2_{L^2(0,T;L^\infty(\Omega_s))} \\
& + \|\partial_t\mathrm{div}\,\mathbf{e}\|^2_{L^2(0,T;L^\infty(\Omega_s))}\Big) + \|\partial_t\mathbf{e}\|^2_{L^2(0,T;H^2(\Omega_s))}\Bigg).
\end{aligned}$$

where, as before, $D^2\mathbf{e}$ denotes the Hessian of $\mathbf{e}$.

Putting everything together, the bound for $\boldsymbol{I}_h$ becomes

$$\begin{aligned}\boldsymbol{I}_h \leq & C(\Delta t)^2\Bigg(\frac{(1+T)(L_1+L_2)^3}{\alpha^2}\Big(\big(1+\log\frac{1}{\Delta t}\big)\|\partial_t\varepsilon(\mathbf{e})\|^2_{L^2(0,T;L^\infty(\Omega_s))}\\ &+\|\partial_t \mathrm{div}\,\mathbf{e}\|^2_{L^2(0,T;L^\infty(\Omega_s))}\Big)\\ &+\frac{(1+T)(L_1+L_2)^3+\rho_s(L_1^2+L_2^2)}{\alpha^2}\|\partial_t\mathbf{e}\|^2_{L^2(0,T;H^2(\Omega_s))}\\ &+\frac{\rho_s T(L_1^2+L_2^2)}{\alpha^2}\|\partial_t^2\mathbf{e}\|^2_{L^2(0,T;H^2(\Omega_s))}+\frac{\rho_s(L_1^2+L_2^2)}{\alpha^2}\|\partial_t\mathbf{e}\|^2_{L^\infty(0,T;H^1(\Omega_s))}\Bigg)\\ =& C(\Delta t)^2\frac{(1+T)(L_1+L_2)^3}{\alpha^2}\Big(\big(1+\log\frac{1}{\Delta t}\big)\|\partial_t\varepsilon(\mathbf{e})\|^2_{L^2(0,T;L^\infty(\Omega_s))}\\ &+\|\partial_t \mathrm{div}\,\mathbf{e}\|^2_{L^2(0,T;L^\infty(\Omega_s))}\Big)+C\mathbf{Y}_{3,h}.\end{aligned}$$

□

From here, we may combine this result with (5.2.20) to present the final result.

Theorem 5.2.9. *Under Assumptions 4.3.3 and 4.3.4, and assuming that $h \leq C\Delta t$ and the solution is smooth enough so that $\mathbf{Y}_h$ defined below, $\|\partial_t\varepsilon(\mathbf{e})\|^2_{L^2(0,T;L^\infty(\Omega_s))}$, and $\|\partial_t \mathrm{div}\,\mathbf{e}\|^2_{L^2(0,T;L^\infty(\Omega_s))}$ are bounded, we have*

$$\begin{aligned}&\max_{0\leq M\leq N}(\mathcal{S}_h^M+\mathcal{E}_h^M)+\sum_{n=0}^{N-1}(\mathcal{Z}_h^{n+1}+\mathcal{W}_h^{n+1})\\ &\qquad\leq C(\Delta t)^2\Bigg(\frac{(1+T)(L_1+L_2)^3}{\alpha^2}\Big(\big(1+\log\frac{1}{\Delta t}\big)\|\partial_t\varepsilon(\mathbf{e})\|^2_{L^2(0,T;L^\infty(\Omega_s))}\\ &\qquad\qquad+\|\partial_t \mathrm{div}\,\mathbf{e}\|^2_{L^2(0,T;L^\infty(\Omega_s))}\Big)+\mathbf{Y}_h\Bigg),\end{aligned}$$

where

$$\mathbf{Y}_h := \mathbf{Y}_{1,h}+\mathbf{Y}_{2,h}+\mathbf{Y}_{3,h},$$

are as defined in Lemma 5.2.8.

5.3 Final Discussion

5.3.1 A comment about the numerical experiments

The fully discrete method developed in this chapter is not exactly the method used in the numerical experiments in Chapter 4. The major difference is that in the numerical experiments, we approach the method purely as a Lagrange multiplier method, and treat $\boldsymbol{\lambda}_h$ as test function in its own finite element space. Critically, we do not impose boundary conditions for $\boldsymbol{\lambda}_h$ at the endpoints of Σ.

In the method in this chapter, on the other hand, we associate $\boldsymbol{\lambda}_h$ as an element of the trace space of $\boldsymbol{V}_h^f$ using a discrete lifting operator argument. Consequently, $\boldsymbol{\lambda}_h$ inherits the boundary conditions in $\boldsymbol{V}_h^f$ at the endpoints of Σ which suggests that $\boldsymbol{\lambda}_h$ must be zero at the endpoints.

However, the reader will be relieved to know that the method described here in this chapter is neither worse nor better than the method used in the numerical experiments![1] When using the Lagrange multiplier method, we have

$$\alpha(\boldsymbol{u}_h^{n+1} - \partial_{\Delta t}\boldsymbol{\eta}_h^{n+1/2}) = \boldsymbol{\lambda}_h^n - \boldsymbol{\lambda}_h^{n+1} \quad \text{on } \Sigma.$$

Thus, given that $\boldsymbol{u}_h$ and $\boldsymbol{\eta}_h$ are both zero at the endpoints of Σ, we have

$$\boldsymbol{\lambda}_h^n - \boldsymbol{\lambda}_h^{n+1} = 0 \quad \forall n \in \{0, \ldots, N\},$$

at the endpoints of Σ. In other words, $\boldsymbol{\lambda}_h$ will be constant at the endpoints!

[1] So it's nothing to panic about...

Additionally, when $\boldsymbol{\lambda}_h$ is used to approximate the fluid stress on Σ in the discrete Robin-Robin method described in this chapter, the term appears in an inner product with a function in $\boldsymbol{V}_h^f$, which will *also* be zero at the endpoints of Σ. Consequently, one could say that the discrete Robin-Robin method does not notice the endpoint behavior of $\boldsymbol{\lambda}_h^{n+1}$, as we never actually use V_h^g to approximate the fluid stress on Σ.

Furthermore, the analysis of these two methods are the same since the Scott-Zhang interpolant R_h^g can be modified to accommodate the boundary conditions of $\boldsymbol{V}_h^g$. Therefore, choosing between the lifting operator method and the Lagrange multiplier method for numerical experiments is simply a matter of preference.[2]

5.3.2 Concluding remarks

In this chapter, we extended the FSI results on the time semi-discrete system in Chapter 4 to the fully discrete system. We showed that the nearly optimal convergence in time (and optimal convergence in space) holds when linear Lagrange finite elements are applied to the spacial variables, provided $h \leq C\Delta t$.

More specifically, the final error estimate (Theorem 5.2.9) yields an upper bound of

$$C(\Delta t)^2\Bigg(\frac{T(L_1+L_2)^3}{\alpha^2}\Bigg(\Big(1+\log\frac{1}{\Delta t}\Big)\|\partial_t\varepsilon(\mathbf{e})\|^2_{L^2(0,T;L^\infty(\Omega_s))} \\ + \|\partial_t \operatorname{div}\mathbf{e}\|^2_{L^2(0,T;L^\infty(\Omega_s))}\Bigg) + \mathbf{Y}_{1,h} + \mathbf{Y}_{2,h} + \mathbf{Y}_{3,h}\Bigg).$$

Disregarding the parameters ρ_S, ρ_f, μ, L_1, L_2, and α for the moment, we may deduce

[2] The lifting operator approach also allows you to avoid an additional finite element space, which some people find very convenient.

from Lemma 5.2.8

$$\begin{aligned}
\mathbf{Y}_{1,h} =& \mathcal{O}(h^2 + (\Delta t)^2) \\
\mathbf{Y}_{2,h} =& \mathcal{O}(h^2 + (\Delta t)^2) \\
\mathbf{Y}_{3,h} =& \mathcal{O}((\Delta t)^2).
\end{aligned}$$

Consequently, taking the square root results in optimal orders of convergence for the term $\mathcal{Y}_h$. It is therefore clear that the error estimate for the FSI system is determined by the logarithmic term that is $\mathcal{O}((\Delta t)^2\left(1 + \log\frac{1}{\Delta t}\right)$. To the best of our knowledge, there is no other explicit coupling for FSI with superior *and provable* error estimates.

However, we saw in 4.4.1 that this is clearly not the whole story when it comes to the convergence of the Robin-Robin method, and the parameters cannot be disregarded. Furthermore, although nearly optimal convergence is the best we know of for rigorously proven convergence results, higher order methods would certainly be desirable. Thus, there is still interesting work to be done with the Robin-Robin method, and we will dedicate the next and final chapter of this thesis to exploring these future paths.

Chapter Six

Conclusion

6.1 Summary of results

In this thesis, we explored the application of the Robin-Robin method for explicit couplings. We applied the method to four cases: the parabolic-parabolic coupled problem, the parabolic-hyperbolic coupled problem, the semi-discrete FSI problem, and the fully discrete FSI problem.

In each of these cases, the Robin-Robin method was proven to be stable with nearly optimal convergence. Critically, we believe this work provides the first rigorous analysis of such results for an explicit coupling of the FSI problem. Previously, the provable convergence results we are aware of were $\mathcal{O}(\sqrt{\Delta t})$ at best. Our method is unconditionally stable with no restrictions on the parameters. Consequently, we believe these results represent a significant step forward in the development of robust explicit couplings for the FSI problem. In the remainder of this thesis, we will explore the possible extensions to the results presented here, and the projects we hope to pursue in the future.

6.2 Future work

6.2.1 Parameter sensitivity questions

Recall from 4.4.1 that the values of the physical parameters had a significant impact on the convergence of the Robin-Robin method for FSI. Indeed, when all parameters were set to 1, the method displayed nearly first order convergence after one or two refinements of the time step. However, when μ, L_1, and L_2 were increased by factors of 100 and 1000, we immediately saw what appears to be a significant delay in the convergence.

Unfortunately, we cannot say for certain what causes the Robin-Robin method for FSI to be so sensitive to the values of the physical parameters. It could, perhaps, indicate that there is fluctuation among the terms that dominate the error, and this fluctuation is balanced out when the physical parameters are all equal to 1. In this case, it could be that larger values of μ, L_1, and L_2 throw off the balance for these fluctuations and delay the asymptotic convergence of the system. This, however, is purely conjecture.

As a future direction for this research, we propose an in-depth study of the effect of the physical parameters on the convergence. Initially, this would likely consist of a series of numerical experiments like those conducted in 4.4.1. In addition, it would be interesting to develop *a posteriori* error estimates for the FSI system with Robin-Robin coupling. Ideally, these would allow us to isolate terms in the method and determine their contribution to the error estimates.

6.2.1.1 Choice of α

We also observed in 4.4.1 that the value of the Robin parameter α appeared to have a significant impact on the convergence. Although this seems strongly correlated with the values of the physical parameters (recall from 4.4.1 that α appeared to somewhat counteract the negative effects of increasing μ, L_1, and L_2), it is also interesting to consider α on its own. This is because α is a parameter that is artificially introduced by the splitting method, so it does not immediately represent any physical property of the system.

However, α *is not dimensionless.* The Robin interface conditions relate the fluid and solid *stresses*, $\sigma_f(\mathbf{u}, \mathsf{p})$ and $\sigma_s(\mathbf{e})$, to the fluid and solid *velocities*, $\mathbf{u}$ and $\mathbf{q}$, at the interface. However, stress is measured in Pascals (Pa), or Newtons per square-meter (N/m^2), whereas velocity is in meters-per-second (m/s) [50]. Thus, in order for the Robin conditions to make physical sense, α must have units of measure to make the dimensional analysis balance out. In other words, we need

$$\alpha\left(\frac{m}{s}\right) = \frac{N}{m^2} = \frac{kg}{s^2 \cdot m},$$

where we are using α in this case to represent the *units of measure* for the parameter α.

Following the dimensional analysis, we find that α must have the units

$$\frac{kg}{s \cdot m^2},$$

which may potentially be interpreted as the units corresponding to *mass flow rate per unit area*. The *mass flow rate* (also referred to as *mass flux*) represents the mass of the fluid flowing per unit time (assuming the fluid has a constant density)[50]. Recall that the concept of *mass* is difficult to prescribe to a fluid because it flows and fills the space it occupies, so we use the mass flow rate to quantify the transfer of mass over time. Thus, this quantity shows up in the equations governing conservation of mass, which we know are broken when loose couplings are applied. Consequently, it is possible that choosing α to be related to this mass flow allows us to minimize the error by limiting how much mass is lost/gained.[1]

Note, however, that we do not have the exact units for the mass flow rate, as we

[1] In other words, perhaps α can limit how badly we break the law of conservation of mass.

have an additional $(1/m^2)$. More precisely, the units of measure for α indicate that it may be related to the quantity of mass flowing through a unit of area per a unit of time. This perhaps makes sense, as the Robin conditions are only applied at the interface, so it would be better to consider a localized mass flow rate instead of the traditional global quantity. Unfortunately, as this is a qualitative argument, we cannot take it much further without making unsubstantiated claims, but it does provide us with an interesting possible direction when considering the following question: *is there an optimal value for α?*

Clearly, an optimal choice for α will be the value that speeds up asymptotic convergence of the system as much as possible. In other words, it is the value that best counteracts the negative effects of large physical parameters. If α truly does correspond to a physical quantity related to the mass flow rate, then perhaps there is a way to relate this value to the values of the physical parameters. For example, L_1 and L_2 are measured in pascals (Pa), and μ is measured in $\frac{N \cdot s}{m^2}$, or pascal-seconds.[2] These units are all functions of kg (kilograms), m (meters), and s, so perhaps an optimal α may be written as a function of L_1, L_2, and μ.[3]

If we prefer to follow a less heuristic approach, however, perhaps the same a posteriori estimates mentioned above would prove useful in determining how to best choose α. Alternatively, one could employ techniques from machine learning or the optimal Schwarz methods mentioned in Chapter 1 (see e.g. [35, 41]).

[2]It is unclear if pascal-seconds is an actual unit of measure, but we will pretend it is for now.

[3]I would like to thank my high school chemistry and physics teachers for teaching me the power of persistence and following a dimensional analysis through until you can go no further.

6.2.2 Static interface vs. moving interface

As mentioned in 1.1.2.1, we have assumed that the structure in our FSI problem undergoes infinitesimal deformations. In other words, for all intents and purposes the interface is completely static. However, this is not realistic, as in many cases the structure can undergo significant deformation in response to the fluid. In the flight of a large aircraft, for example, the fluid (air) forces can deflect the tip of the wing up by 10 meters [45].

As a result, an interesting and important extension to the work in this thesis would be to extend the analysis of the Robin-Robin method to FSI problems with moving interfaces. Preliminary work on this problem, including a stability analysis, has been carried out in [48], however the extension of the convergence results remains elusive. The major challenge in this case appears to be the inclusion of a *third* coupling condition in the "moving interface" problem. Specifically, in addition to the traditional dynamic and kinematic coupling conditions (1.1.3), the moving domain problem has a *geometry condition* that forces the (moving) subdomains to remain flush.[4]

This new "domain updating" condition must be applied in such a way that it does not disrupt the loose/explicit coupling of the Robin-Robin method. In [48], it is applied as an intermediate step between the structure and fluid subproblems, using the newly computed solution to the structure at time step $n + 1$ to update the fluid domain. The numerical experiments carried out in [48] suggest that the Robin-Robin method for moving domains behaves comparably to the static interface system, thus it is very possible that this is sufficient, and the Robin-Robin approximation will

[4] This is similar to the kinematic coupling conditions, but it now applies directly to the domains, rather than the velocities.

remain consistent with the exact solution, but without a rigorous error analysis we can say nothing with certainty. As with any loose coupling, we are introducing a time delay by serializing the computation of the subsystem, and we know from the added-mass instability that this discrepancy should not be taken lightly. However, we believe that the results presented in this thesis will provide a valuable starting point for the moving domain analysis.

6.2.3 Second order and beyond!

Last but not least, the most immediate next step for the Robin-Robin method is perhaps to extend it to a second order method. We propose to begin with the simplified parabolic-parabolic coupling. There are many options to begin this extension. For example, we could apply a Crank-Nicholson time discretization in both subproblems, with an appropriate second order extrapolation in the Robin conditions on the terms occurring at time step n (i.e. replace l^n with $2\mathsf{l}^n = 2\mathsf{l}^n - \mathsf{l}^{n-1/2}$). However, this method may not be stable, so one or two correction steps would need to be applied to guarantee stability. Alternatively, BDF2 time stepping with correction steps could be investigated, or a two-stage Runge-Kutta method such as Heun's method.

Bibliography

[1] S. Badia, F. Nobile, and C. Vergara. Fluid–structure partitioned procedures based on robin transmission conditions. *Journal of Computational Physics*, 227(14):7027–7051, 2008.

[2] S. Badia, A. Quaini, and A. Quarteroni. Modular vs. non-modular preconditioners for fluid–structure systems with large added-mass effect. *Computer Methods in Applied Mechanics and Engineering*, 197(49-50):4216–4232, 2008.

[3] S. Badia, A. Quaini, and A. Quarteroni. Splitting methods based on algebraic factorization for fluid-structure interaction. *SIAM Journal on Scientific Computing*, 30(4):1778–1805, 2008.

[4] G. A. Baker. Error estimates for finite element methods for second order hyperbolic equations. *SIAM journal on numerical analysis*, 13(4):564–576, 1976.

[5] F. Ballarin. Multiphenics: Mathlab innovating with mathematics.

[6] J. W. Banks, W. D. Henshaw, and D. W. Schwendeman. An analysis of a new stable partitioned algorithm for FSI problems. Part I: Incompressible flow and elastic solids. *J. Comput. Phys.*, 269:108–137, 2014.

[7] C. Brennen. A review of added mass and fluid inertial forces, cr 82.010. 01 1982.

[8] S. Brenner and R. Scott. *The mathematical theory of finite element methods*, volume 15. Springer Science & Business Media, 2007.

[9] F. Brezzi and J. Pitkäranta. On the stabilization of finite element approximations of the Stokes equations. In *Efficient solutions of elliptic systems (Kiel, 1984)*, volume 10 of *Notes Numer. Fluid Mech.*, pages 11–19. Vieweg, 1984.

[10] M. Bukač. An extension of explicit coupling for fluid–structure interaction problems. *Mathematics*, 9(15):1747, 2021.

[11] M. Bukač, S. Čanić, R. Glowinski, B. Muha, and A. Quaini. A modular, operator-splitting scheme for fluid–structure interaction problems with thick structures. *International journal for numerical methods in fluids*, 74(8):577–604, 2014.

[12] M. Bukac and B. Muha. Stability and convergence analysis of the extensions of the kinematically coupled scheme for the fluid-structure interaction. *SIAM J. Numer. Anal.*, 54(5):3032–3061, 2016.

[13] M. Bukač, A. Seboldt, and C. Trenchea. Refactorization of cauchy's method: A second-order partitioned method for fluid–thick structure interaction problems. *Journal of Mathematical Fluid Mechanics*, 23(3):1–25, 2021.

[14] E. Burman, R. Durst, M. Fernandez, and J. Guzman. Fully discrete loosely coupled Robin-Robin scheme for incompressible fluid-structure interaction: stability and error analysis, 2020. arXiv: 2007.03846 (Submitted).

[15] E. Burman, R. Durst, M. A. Fernández, and J. Guzmán. Loosely coupled, non-iterative time-splitting scheme based on Robin-Robin coupling: unified analysis for parabolic/parabolic and parabolic/hyperbolic problems, 2021. arXiv:2110.08181 (Submitted).

[16] E. Burman, R. Durst, and J. Guzman. Stability and error analysis of a splitting method using Robin-Robin coupling applied to a fluid-structure interaction problem. *Numerical Methods for Partial Differential Equations*, 2021.

[17] E. Burman and M. A. Fernández. Stabilization of explicit coupling in fluid–structure interaction involving fluid incompressibility. *Computer Methods in Applied Mechanics and Engineering*, 198(5-8):766–784, 2009.

[18] E. Burman and M. A. Fernández. Explicit strategies for incompressible fluid-structure interaction problems: Nitsche type mortaring versus robin–robin coupling. *International Journal for Numerical Methods in Engineering*, 97(10):739–758, 2014.

[19] C. Canuto and A. Lo Giudice. A multi-timestep Robin-Robin domain decomposition method for time dependent advection-diffusion problems. *Applied Mathematics and Computation*, 363:124596, 2019.

[20] Y. Cao, M. Gunzberger, X. He, and X. Wang. Parallel, non-iterative, multi-physics domain decomposition methods for time-dependent Stokes-Darcy systems. *Mathematics of Computation*, 83(288):1617–1644, 2014.

[21] L. Carbone and R. d. Arcangelis. Chapman amp; Hall/CRC, Boca Raton, 2019.

[22] P. Causin, J.-F. Gerbeau, and F. Nobile. Added-mass effect in the design of partitioned algorithms for fluid–structure problems. *Computer methods in applied mechanics and engineering*, 194(42-44):4506–4527, 2005.

[23] A. J. Chorin. A numerical method for solving incompressible viscous flow problems. *Journal of Computational Physics*, (2):12–26, 1967.

[24] Q. Deng. Timely communicaton: An analysis for a nonoverlapping domain decomposition iterative procedure. *SIAM Journal on Scientific Computing*, 18(5):1517–1525, 1997.

[25] J. Douglas, P. Leme, J. Roberts, and J. Wang. A parallel iterative procedure applicable to the approximate solution of second order partial differential equations by mixed finite element methods. *Numerische Mathematik*, 65:95–108, 12 1993.

[26] A. Ern and J.-L. Guermond. *Theory and Practice of Finite Elements*, volume 159 of *Applied Mathematical Sciences*. Springer, New York, 2004.

[27] L. C. Evans. *Partial Differential Equations (Graduate Studies in Mathematics, V. 19) GSM/19*. American Mathematical Society, June 1998.

[28] M. Fernández, J. Mullaert, and M. Vidrascu. Explicit Robin-Neumann schemes for the coupling of incompressible fluids with thin-walled structures. *Comput. Methods Appl. Mech. Engrg.*, 267:566–593, 2013.

[29] M. Fernández, J. Mullaert, and M. Vidrascu. Generalized Robin-Neumann explicit coupling schemes for incompressible fluid-structure interaction: stability analysis and numerics. *Internat. J. Numer. Methods Engrg.*, 101(3):199–229, 2015.

[30] M. A. Fernández, J.-F. Gerbeau, and C. Grandmont. A projection semi-implicit scheme for the coupling of an elastic structure with an incompressible fluid. *International Journal for Numerical Methods in Engineering*, 69(4):794–821, 2007.

[31] M. A. Fernández, M. Landajuela, and M. Vidrascu. Fully decoupled time-marching schemes for incompressible fluid/thin-walled structure interaction. *J. Comput. Phys.*, 297:156–181, 2015.

[32] M. A. Fernández and J. Mullaert. Convergence and error analysis for a class of splitting schemes in incompressible fluid–structure interaction. *IMA Journal of Numerical Analysis*, 36(4):1748–1782, 2016.

[33] G. B. Folland. *Real analysis : modern techniques and their applications / Gerald B. Folland.* Wiley, New York, 1984.

[34] C. Förster, W. A. Wall, and E. Ramm. Artificial added mass instabilities in sequential staggered coupling of nonlinear structures and incompressible viscous flows. *Comput. Methods Appl. Mech. Engrg.*, 196(7):1278–1293, 2007.

[35] M. J. Gander. Optimized schwarz methods. *SIAM Journal on Numerical Analysis*, 44(2):699–731, 2006.

[36] L. Gerardo-Giorda, F. Nobile, and C. Vergara. Analysis and optimization of Robin-Robin partitioned procedures in fluid-structure interaction problems. *SIAM J. Numer. Anal.*, 48(6):2091–2116, 2010.

[37] P. Hansbo, J. Hermansson, and T. Svedberg. Nitsche's method combined with space-time finite elements for ALE fluid-structure interaction problems. *Comput. Methods Appl. Mech. Engrg.*, 193(39-41):4195–4206, 2004.

[38] P. Le Tallec and J. Mouro. Fluid structure interaction with large structural displacements. *Comput. Meth. Appl. Mech. Engrg.*, 190:3039–3067, 2001.

[39] P.-L. Lions. On the Schwarz alternating method. iii: a variant for nonoverlapping subdomains. In *Third international symposium on domain decomposition methods for partial differential equations*, volume 6, pages 202–223. SIAM Philadelphia, PA, 1990.

[40] F. Project. Fenics, 2003.

[41] L. Qin and X. Xu. Optimized schwarz methods with robin transmission conditions for parabolic problems. *SIAM Journal on Scientific Computing*, 31(1):608–623, 2008.

[42] A. Quaini and A. Quarteroni. A semi-implicit approach for fluid-structure interaction based on an algebraic fractional step method. *Mathematical models and methods in applied sciences*, 17(06):957–983, 2007.

[43] A. Quarteroni and A. Valli. *Domain decomposition methods for partial differential equations*. Number BOOK. Oxford University Press, 1999.

[44] P. Rå back, J. Ruokolainen, M. Lyly, and E. J arvinen. Fluid-structure interaction boundary conditions by artificial compressibility.

[45] T. Richter. *Fluid-structure interactions: models, analysis and finite elements*, volume 118. Springer, 2017.

[46] S. N. S, S. Saha, and A. Bhattacharjee. A 2d fsi mathematical model of blood flow to analyze the hyper-viscous effects in atherosclerotic covid patients. *Results in Engineering*, 12:100275, 2021.

[47] L. R. Scott and S. Zhang. Finite element interpolation of nonsmooth functions satisfying boundary conditions. *Mathematics of Computation*, 54(190):483–493, 1990.

[48] A. Seboldt and M. Bukač. A non-iterative domain decomposition method for the interaction between a fluid and a thick structure. *Numerical Methods for Partial Differential Equations*, 37(4):2803–2832, 2021.

[49] R. Temam. Sur l'approximation de la solution des équations de navier-stokes par la méthode des pas fractionnaires (ii). *Archive for Rational Mechanics and Analysis*, 33:377–385, 1969.

[50] D. Wiggert and M. Potter. *Schaum039;s Outline of Fluid Mechanics*. McGraw-Hill, 2007.